Universitetet i Stavanger

FACULTY OF SCIENCE AND TECHNOLOGY

MASTER'S THESIS

Study program/specialization: **Petroleum Engineering** **Drilling and Well Technology**	**Spring semester, 2019** **Open** /~~Confidential~~
Author: **Joakim Haram Svensson**	**Digital submission** …….. (signature of author)
Program coordinator: Jan Aage Aasen, University of Stavanger Supervisors: Jan Aage Aasen, University of Stavanger	
Title of master's thesis: **An experimental study of unsupported pipe buckling in live well intervention**	
Credits: **30 ECTS**	
Keywords: Experimental Buckling, Snubbing, Column buckling	Number of pages: 87 + supplemental material/other: 61 Stavanger, 06/19 date/year

Abstract

In this experimental study, unsupported pipe experiments are conducted. Information regarding intervention operation, focusing on snubbing operations in live well interventions and unsupported buckling during these operations, are described as well as the conducted experiments. The loads and forces acting on the pipes during these experiments are compared to the already known theoretical buckling load calculations. Determination of buckling loads, yield strength and Young's elasticity modulus has been conducted on short to intermediate columns for local buckling in this study. Equations used in the oil and gas industry today are used to show the experimental results, such as slenderness ratio, short column and intermediate column critical buckling loads. At last, the use of the two different slenderness ratio equations are investigated and compared with the experiment results. Indication from these results shows that the use of one of these two slenderness ratio equations, used in the oil and gas industry today, may not be applicable after all.

Acknowledgment

The author would like to thank the supervisor, Jan Aage Aasen, who provided this research idea, and all the support during this experimental study. He has been available and helpful throughout the research. Ideas and inspiration were provided along the way as well as suggestions to solutions of unforeseen issues that arrived along the way. Jan have been at great help and the author wish to give a huge thank for all the help and for all the information he has provided for this research.

Also thanks to the laboratory personnel, especially Caroline Einvik and Emil Surnevik Kristiansen with great support and help throughout this study. The preparation of several tools and new equipment used for the research and tests, and also the guiding on how to use machine to prepare tools needed for the experiments. Thanks to Kim Andre Nesse Vorland, who programmed the LabView program used to gather the data needed from the Enerpac, and also thanks for the effort and help to calibrate the transducer used to digitalize the pressure signal from the Enerpac machine.

At last, the author would give a thanks to the following people for helping with different issues that needed attention during the study. Jon Arne Evjenth, Sivert Bakken Drangeid, Jan Magne Nygård, Jørgen Grønsund and Johan Andreas Håland Thorkaas.

The research equipment was funded by The University of Stavanger (UiS), who provided all the pipes and economically support to weld the pipes used for the tensile testing.

Nomenclature

HWO = Hydraulic workover operation
HWU = Hydraulic workover unit
SR = Slenderness ratio
BL = Buckling load
RIH = Run in hole
POOH = Pull out of hole
WL = Wireline
WOB = Weight on bit
BOP = Blow out preventer
ENERPAC = Compression machine
INSTRON = Tensile testing machine
WH = Well head
F = Force [N]
F_y = Yield force [N]
F_b = Buckling force [N]
F_{cr} = Critical force [N]
P = Pressure [MPa]
P_y = Yield pressure [MPa]
P_{cr} = Critical pressure]MPa]
P_b =Buckling pressure [MPa]
σ = Sigma [MPa]
σ_y = Sigma Yield [MPa]
ID = Inner diameter [mm]
OD = Outer diameter [mm]
t = Wall thickness [mm]
A = Cross-sectional area [mm^2]
A_s = Cross-sectional area of steel [mm^2]
A_{s1} = Cross-sectional area of steel [mm^2]
S = Length of a part of the circular circumference
C_c =Column slenderness
r_g = Radius of gyration [mm]
I = Moment of inertia [mm^4]
M = Bending moment [Nm]
K = End constrain factor
R = (ID + t) / 2 [mm]
E = Young's modulus (Elasticity modulus) [MPa]
L_e = Effective length [mm]
$\lambda = \xi$ = Slenderness ratio
ε = Strain [mm/mm]
B_c =Bore cylinder
N = Number of active jack cylinder
DWT = Dead weight tester
r = radius [mm]
A_m = Milled area [mm^2]
α = Angle in degrees
BL = Buckling load [N] = F
API = American Petroleum Institute
OCTG = Oil Country Tubular Goods

Table of Contents

List of Figures

List of tables

1. Introduction

1.1 Project objectives and goals

This thesis study objective and goals are to investigate unsupported buckling for snubbing of pipe during live well interventions. The experiment conducted in this thesis will include compressive and tensile testing determine the buckling loads and pipe strength. Comprehensive testing will give information of the pipes experimented on and the results are compared with the equations used today given by Franklin and Abel's paper (Franklin & Abel, October, 1988) and Les Skinner's book (Skinner, 2019). The use of slenderness ratio determines the critical buckling loads. The slenderness ratios calculations listed in this study are still used today. In this study, several experiments are conducted to validate the use of critical snubbing calculations done for the pre-job calculations for conduct safer operations.
Several experiments on each pipe dimension are conducted to calculate the yield strength of the tubing by compression. The Young's modulus (elasticity modulus) is calculated through the tensile testing.

1.2 Objectives

Use several experiments to gain information of the pipes, and use calculations already used in the oil and gas business today. Compression and tensile testing of pipes to gather buckling and yield force. Preparations of these experiments need several tools and preparations in the workshop.

1.3 Method

Use tensile test machine, Instron, located in D-159, and Enerpac compression machine located at the workshop at Kjølv Egelands house at The University of Stavanger. Several pipes with different dimensions are used in these experiments – and with support of calculations to determine the different loads.

Enerpac compress is used to determine the yield and buckling force. Instron tensile test machine to validate the Enerpac results of the yield loads, and provide the Young's elasticity modulus for the calculations.

Several methods due to limitations of equipment have been tested in this research, but only the most accurate values have been enclosed.

The buckling experiments has been video recorded to better study the effect of the buckling load with different outer diameter, thickness and unsupported lengths.

1.4 Limitations of report and results

Instron dual floor frame tensile test machine has a maximum capacity of 250kN, while most of the tubing used in this study, has had a higher tensile strength. The maximum grip was also 34 mm OD, while the outer diameter of the three biggest pipe was larger. There have been several attempts to reach out to local workshops and companies who might have had bigger testing machines, but without any luck. Therefore, going forward a decision was made to make the area of the steel lower by cutting out steel, and then use the machine by modifying the input data. Due to low air suction in the workshop, welding was not allowed and the tubing was sent out to the local welder for preparations to the tensile test experiments.

2. Literature

2.1 Intervention and Workover operations

Intervention and workover are operations carried out in a well to enhance oil production, repair or to do maintenance. This can be performed in any stage of the production from a reservoir. This operation includes all types of maintenance downhole, such as pumping, replacement and maintenance of equipment in both dead wells and live wells. Several different methods are used for well interventions, such as help of a drilling rig, snubbing/ hydraulic workover unit (HWU), coiled tubing and wireline. Hydraulic workover operation (HWO) is often done to the whole completion, to change the reservoir condition. The benefit of using intervention where the pipe is pulled in to the well, is that circulations can be done from the bottom of the well. Such as artificial lift, wellbore cleanouts, acid treatments, remedial cementing and underbalanced drilling as some examples. Other operations for intervention may include hydrate removal, hydrate prevention, well stimulating (fracturing/acid treatment), mechanical repairs, wax deposit, reservoir production, drilling, logging, perforating or scale precipitation. The main goal is to ensure safe operations, as well as safe well conditions, enhance oil production and reduce the rate of decline. (Crumpton, 2018).

To ensure safe operations, determinations of the expected force and pressure's acting on the equipment is essential to prevent accidents. Calculations before these operations, such as snubbing and coiled tubing operations, are therefore important.

2.1.1 Coiled tubing

Coiled tubing can be used in a live well and is a commonly used well intervention technique. CT uses a long tubing that is spooled on to a reel. This reel is easily transportable and can be quickly applied. The setup consist of the coiled tubing reel, injector head, pressure control equipment, control cabin and power-pack (Crumpton, 2018). CT can be used instead of wireline in highly deviated wells. CT can perform well operations such as circulating, pumping, drilling, logging, perforating and production (shallow gas wells). For pumping, CT has been used since 1960, where some operations are nitrogen kickoffs, sand cleanouts and matrix acidizing. (Thomeer & Newman, 1991)

Due to the tubing is spooled on to the reel, the CT experience stresses when it's being unbends from the reel when RIH, and the bending back to the reel when POOH. These cyclones of bending back and forth,

limits the durability and material strength of the tubing. When these stresses occur, the tubing is bended above its yield force of the material, therefore these bending cycles is an important factor for calculations whether the tubing is safe for operation (Zheng & Adnan, 2004).

Coiled tubing normally buckle between the unsupported length between the bottom of the chains and the top of the stripper in the injector. Therefore in this unsupported length, buckle may occur if the compressive loads are high, (K. Newman & Aasen, 1998).

2.1.2 Wireline

Wireline uses a wire for well intervention operations, such as wireline and slickline. Slickline is normally used to retrieve and place tools, remove plugs and other operations where live data from the well is not needed. Wireline can transmit data from the well via its electrical cables and is therefore much more useful when information from the well is needed, such as during workover and where logging is needed, (Crumpton, 2018).

2.1.3 Hydraulic workover – Snubbing and Stripping

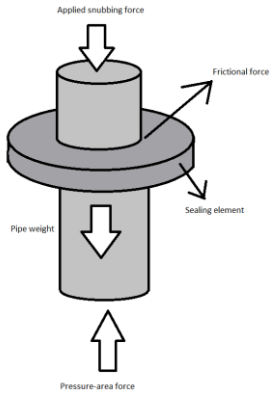

Figure 1 Snubbing forces

Snubbing is referred to the operation where the drill pipe or tubing is pulled in to a well against pressure. Pipe tripping and pipe stripping is definition for pull out of hole (POOH) and run in hole (RIH). The pipe can be pipe heavy or pipe light depending on pressure of the well. Pipe heavy is a definition where the tubing is heavier than the well pressure and needs to be restrained to not fall down into the well. Pipe light is when the pipe is lighter than the well pressure loads, and needs to be snubbed down in the well, (Crumpton, 2018).

Equipment is used to apply the forces needed to force the tubing downhole while supporting the tubing. The difference from coiled tubing operations is that the snubbing unit needs more space, therefore the rig-up is much larger and the pipes used needs more space as they are rigid. As an example, an 460K snubbing jack is used to deploy a 127 mm pipe into a wellbore with pressure. The maximum snub force

expected while snubbing the first joint when closed-end is equal to the wellhead pressure multiplied with the cross-sectional area of the closed pipe, (Aadnøy, 2010).

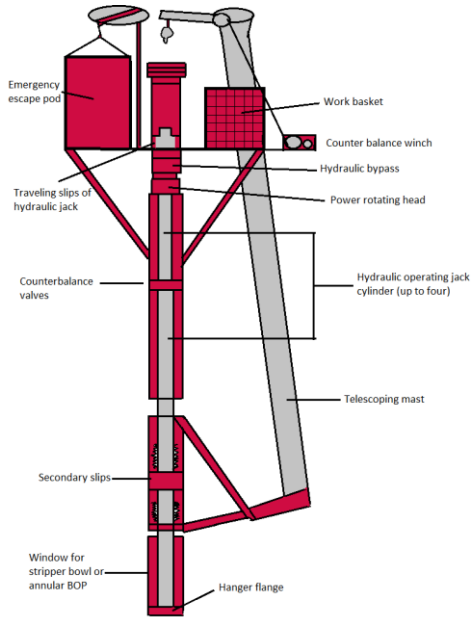

Figure 2 Snubbing Unit

A hydraulic workover unit (HWU) is the equipment that push and pull the pipe from the well. This is done without the drilling derrick. This units can therefore be used without the use of rig assisted snubbing units. The HWU is a powered jack that push and pull jointed pipes in and out of the well. This method can be used for recompletions, circulating, cleanouts, fishing and milling, reservoir stimulation, gravel pack operations and perforating. This unit can pull with greater force than CT, use heavy yield and greater wall thickness tubing. The equipment needed for HWO is a hydraulic jacking system, the workstring and bottom hole assembly, well control components and other normal ancillary equipment. See Figure 2 for a raw schematic.

Due to working with hydrocarbons under pressure, it's extremely important to predict the expected string loads and loads expected on the equipment when performing snubbing operations. Therefore, knowledge of expected pressure and forces acting on the workstring and equipment is extremely important, as well as the force needed to snub the pipe. It requires comprehensive analysis to calculate the expected loads to limit the workstring stress and avoid any types of failure to the pipe. Several unforeseen issues can occur while snubbing, such as hitting obstructions down hole, sudden increase of pressure, friction from fluid movement or high wall contact du to well deviation and helical buckling. A good safety factor is therefore needed to perform snubbing operations as safe as possible. Anti-buckling guides/ pipe guides are often used to prevent excessive bending and eliminate catastrophically failure (K. R. Newman, Overstreet, & Beynet, 2006).

Depends on the different snubbing job, but most snubbing services uses a good safety factor for routine jobs. If there is a chance for H_2S present, the safety factor may increase.

2.1.4 Buckling force

We derive the buckling into three categories, short column, intermediate column and long column buckling. Short column is referred to when the buckling only deforms the steel without bending. Intermediate column is the phase when bending occurs (local buckling) and deforms, and long column is referred to when we have major axis buckling.

Buckling occurs when the compressive forces applied to the workings string exceeds the buckling limit of the material used. This may lead to the workstring to bow in the unsupported length and displaced laterally. During HWO while snubbing pipe into a pressurized well, the buckle may occur just below the work basket, where the operating personnel is working, and then again puts them in great danger. The use of snubbing string with high yield strength, greater thickness and diameter can reduce the likelihood for buckling to occur. Larger diameters can be positive due to higher flow rates when doing clean outs. The collapse and burst loads can also be improved.

Buckling can also occur in the well, where the inner pipe has a compressive axial force and will typically buckle within the outer string. During well completion design, pipe buckling is an important analysis factor. Tubing buckling have two fundamental questions, what is the critical load, and what is the post-buckle configurations, (Mitchell, 2012). Post-buckling configurations is the way the tubing move when buckle, bending stresses, contact forces and axial-load distributions.

Insufficient lateral support can create helical buckling. Helical buckling can occur when snubbing a small OD tubing string in large OD BOP or riser. This contact between the pipe and wellbore, creating force on the wall of the hole. Helical buckling should be avoided for safety reasons, (Crumpton, 2018).

2.1.5 Strain hardening

From the experiments, results of strain hardening could be seen. This occurred especially for experiments where low unsupported lengths were used. Strain hardening is when the pipe is loaded to a force where plastic deformation occurs. This force is deforming the material crystal structure in a way that is strengthening the material. The strain hardening effect has significant influence on the ultimate bending capacity of steel pipes. Strain hardening causes higher bending yields than the assumed elastic-perfectly plastic material, (Xin, Yanfei, Tong, & Jing, 2009). As an example, we can look at the graph from 60,5mm x 3,7mm, with a length of 332 mm unsupported length compared to the 585 mm unsupported length. Here we can see the yield stress, and tensile stress measured is much greater, and the force increasing as the piston moves down. Clearly the tensile stress increases above the average strengths due to strain hardening.

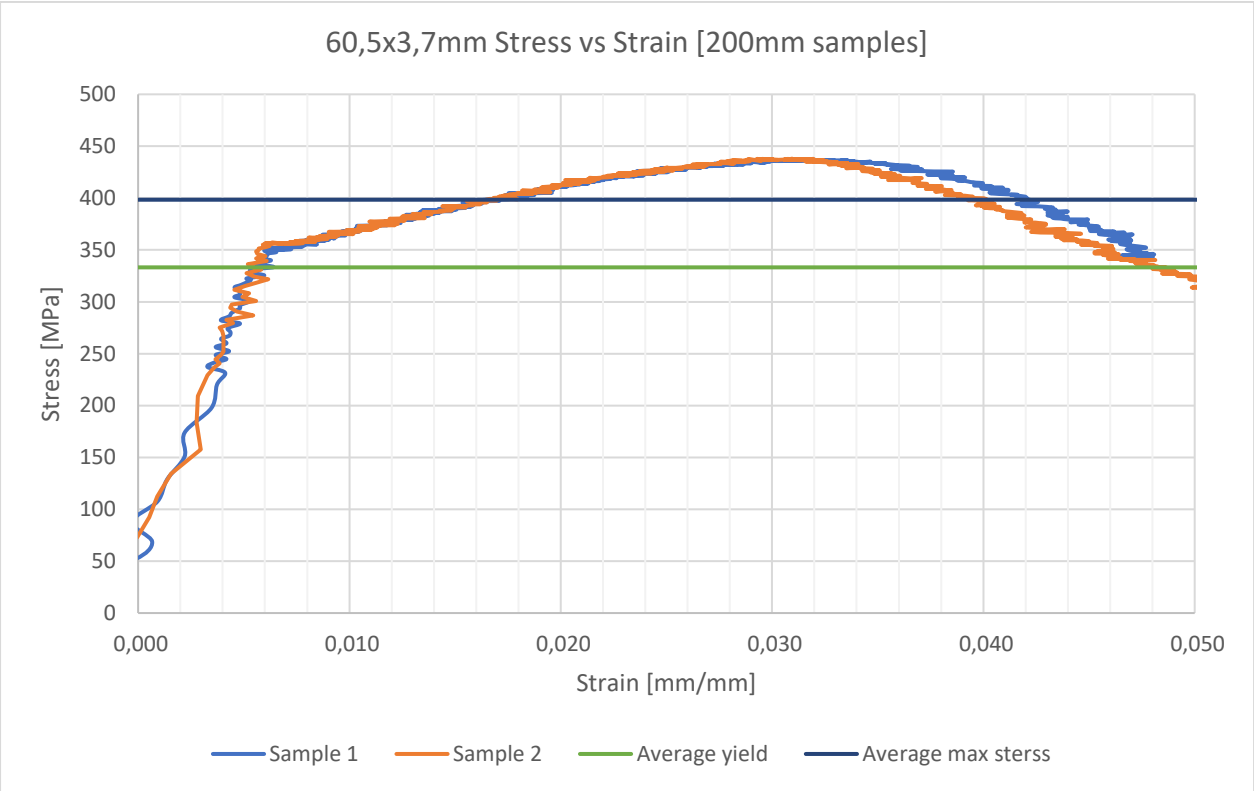

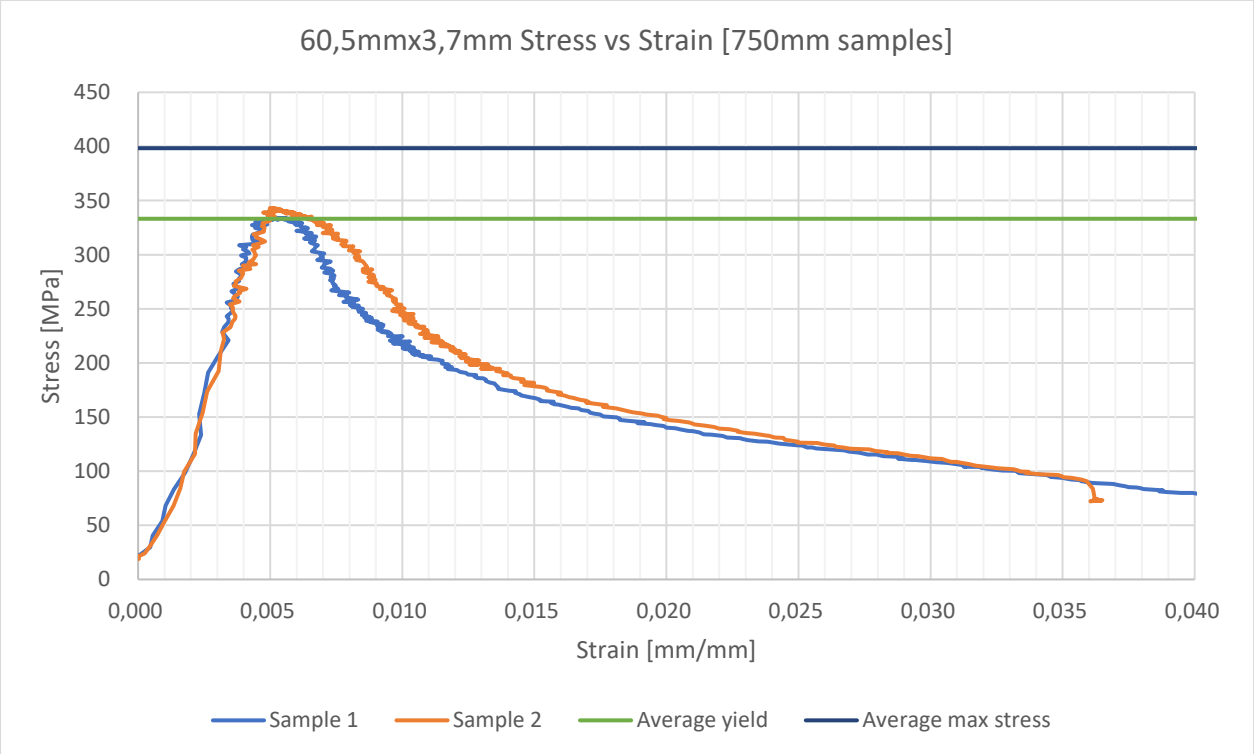

Figure 3 Strain hardening example from 60,5 mm x 3,7 mm, 332 mm vs 882 mm unsupported length

Figure 4 Video capture of strain hardening of 60,5 mm pipe with 332 mm unsupported length

2.1.6 Column Buckling

The Euler's buckling theory has its origin from Leonhard Euler in 1744, (Salmon, Johnson, & Malhas, 2009), and is used for long columns (major axis buckling). For basic column strength, three assumptions are made for buckling under axial loads to occur. The first assumption is that the material is uniform throughout the column and has equal compressive stress-strain properties. The second assumption is that there is no damage or initial stress in the material, and the thirds assumption is that the column has no bends and is straight. Compression of long columns is known to fail by elastic buckling, and that short columns may be loaded until the material yields, or even in to the strain-hardening range. Euler's elastic buckling is determining the strength for large slenderness ratios by the use of yield strength, $P_y = F_y A_s$. Euler's theory is that the bending moment, M_z, at any location of the member, z, that bends in axial direction, x, is given by

$$M_z = Py$$

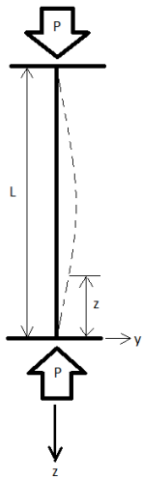

Figure 5 Compression force acting on a column to buckle

And the differential equation given by Salmon et al. (Salmon et al., 2009) gives,

$$\frac{d^2y}{dz^2} = -\frac{M_z}{EI}$$

And becomes

$$\frac{d^2y}{dz^2} + \frac{P}{EI}y = 0$$

Where
E = modulus of elasticity
I = Moment of inertia

Inserting $k^2 = P/EI$, the formula can be expressed as follows

$$y = A\,sin\,kz + B\,cos\,kz$$

When applying the boundary conditions for both ends, one can obtain condition for the end's.

y = 0, z = 0 and y = 0, z = L.

Obtains by this B = 0 for one end condition and $0 = A\,sin\,kL$ for the end.

This equation can be accomplished when there is no deflection (constant A = 0), or no applied load (kL = 0) or (kL = N π) when buckling occurs.

$$\frac{N\pi^2}{L} = \frac{P}{EI}$$

$$P = \frac{N^2\pi^2EI}{L^2}$$

L = effective length. When both ends are unrestrained, with pinned (pinned-pinned) or circular, means the column can buckle in any direction and where no rotational restraint exist, a single-curvature deflection will occur when N = 1.

Therefore, the critical Euler's buckling is given by

$$P_{cr} = \frac{\pi^2EI}{L^2}$$

Using $I = A_g r^2$ ones get

$$F_{Cr} = \frac{P_{Cr}}{A_g} = \frac{\pi^2E}{(L\,/\,r)^2}$$

The end constrains are an important factor for buckling calculation. This determines the effective length that is used in the calculations. Depending on the end points are restrained, unrestrained, one end restrained or partially restrained, the K – factor changes – and changes the effective length.

$$L_e = KL$$

We have the following end condition values (Skinner, 2019),

Table 1 K - values for various end condition (Skinner, 2019)

K values for various end conditions		
Top End Condition	**Bottom End Condition**	**k**
Rotation fixed Translation fixed	Rotation fixed Translation fixed	0,65
Rotation free Translation fixed	Rotation fixed Translation fixed	0,80
Rotation free Translation fixed	Rotation free Translation fixed	1,00
Rotation fixed Translation free	Rotation fixed Translation fixed	1,20
Rotation free Translation fixed	Rotation fixed Translation free	2,00
Rotation fixed Translation fixed	Rotation free Translation free	2,20

Local buckling (short to intermediate column) is defined by the slenderness ratio vs column slenderness ratio,

$$R = \frac{(ID + t)}{2}$$

$$C_C = \pi\sqrt{\frac{2E}{F_y}}$$

$$r = \sqrt{\frac{I}{A_s}}$$

$$I = \frac{\pi}{64}(OD^4 - ID^4)$$

$$SR1 = \frac{KL}{r}$$

$$SR2 = \sqrt{\left(\frac{R}{t}\right)} \times \left(4{,}8 + \frac{R}{225t}\right)$$

$$\text{Buckling load 1} = P_y A_s \left(1 - \frac{SR^2}{2C_c^2}\right)$$

$$\text{Buckling load 2} = A_s \left(\frac{286 \times 10^6}{SR^2}\right)$$

OD = Outside diameter, mm
ID = Inside diameter, mm
t =wall thickness, mm
I = Moment of inertia, mm^4
A_s = Area of steel, mm^2
E = Modulus if elasticity, GPa
F_y = Yield stress of pipe, kN
L = Maximum unsupported pipe length, mm^2
K = End constrain factor, in our case is equal to 1
C_c = Column slender ratio separating elastic and inelastic buckling.
SR = Slenderness ratio

There is local buckling if the effective slenderness ratio is less than Cc. Therefore, the column slender determines how much buckling resistance the pipe can handle before buckling. Slenderness ratio less than 80, does not apply to the Euler's classical elastic buckling equation (K. Newman & Aasen, 1998).
The biggest slenderness ratio of SR1 and SR2 should be used, (Skinner, 2019). If the column slenderness is greater than slenderness ration (SR1 or SR2), we have major axis buckling as described in figure 6 below, and the buckling load 2 formula above should be used. If we have local buckling, the buckling load 1 formula should be used.
For this study, the buckling load 1 is used. This is due to all the pipes in this research have slenderness ratio less than the column slenderness ratio C_c.

We also have Johnson's formula that is being used for short/intermediate column buckling (local buckling) calculations (DACC, 2015).

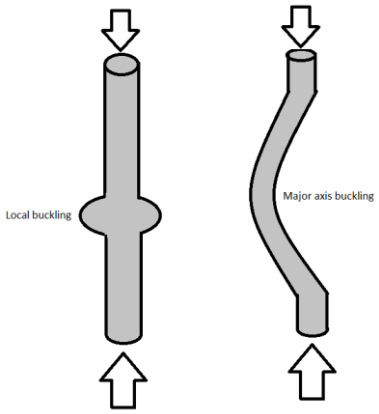

Figure 6 Local and Major Axis Buckling

These failure modes depend on where in the stress-strain relationship the deformation occurs. Generally, during snubbing , crushing failure occurs due to large diameter pipe with thin wall thickness. During snubbing, normally the value of k is equal is set to 1,0 (Skinner, 2019). Buckling may occur below the wellhead (WH), but during snubbing, the unsupported length between the slips (traveling or stationary) to the BOP, who is holding the well pressure, is where the critical weak point for buckling to occur during the operation.

From (K. Newman & Aasen, 1998) we have the following formulas,

r_g= radius of gyration

$$r_g = \sqrt{\frac{I}{A_s}} = \frac{1}{4}\sqrt{OD^2 - ID^2} = \frac{1}{2}\left(r_0^2 - r_i^2\right)$$

$$r_g = \frac{1}{2}\sqrt{r_0^2 + r_i^2}$$

Slenderness ratio

$$SR = \frac{L_e}{r_g}$$

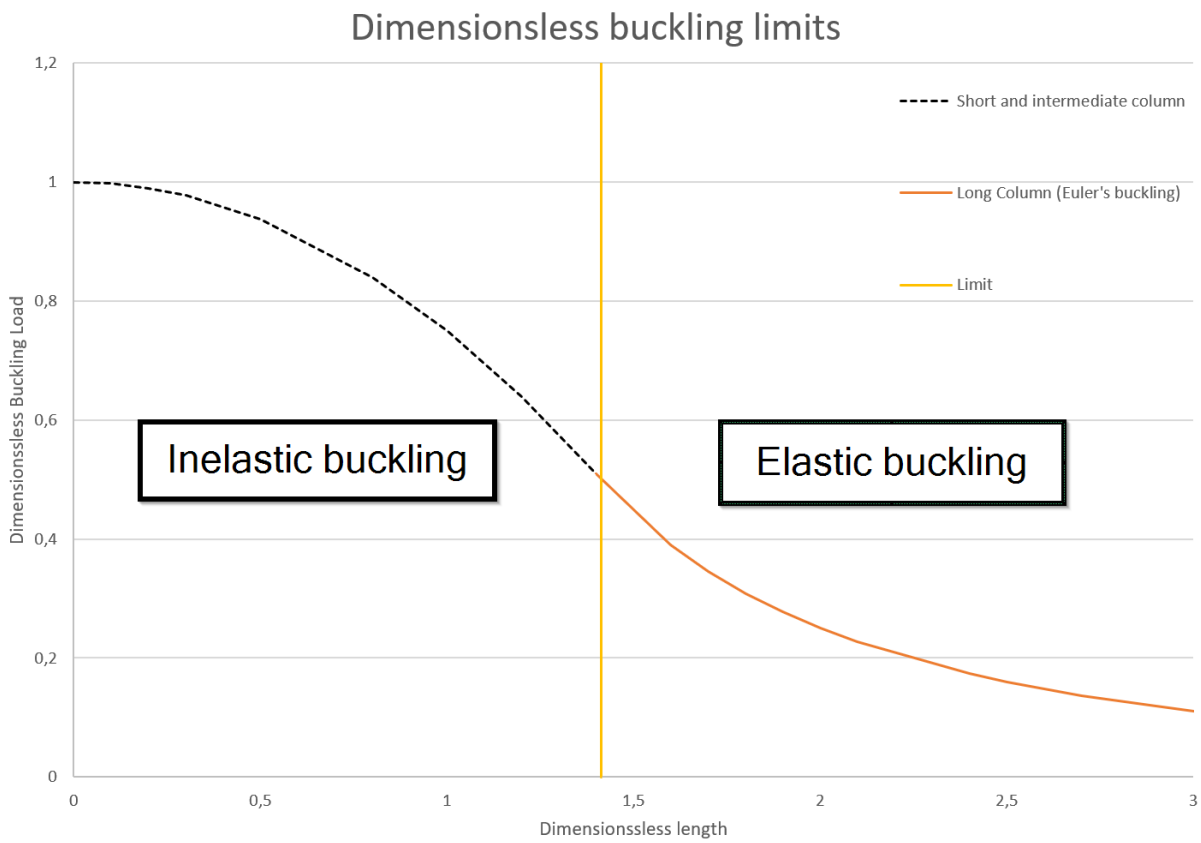

Figure 7 Inelastic and Elastic buckling graph

So, as we can see from Figure 7, the Euler's elastic buckling is for long columns is shown to the right. The short to intermediate column to the left where inelastic buckling occurs are experimented in this report.

2.1.7 Dimensionless force and length formula

From (Aasen & Skaugen, 2002), we have the following;

For short and intermediate columns, we have the formula,

$$y = 1 - \frac{x^2}{4} \text{ for } (x < \sqrt{2})$$

For long columns, using the Euler's critical buckler, we have

$$y = \frac{1}{x^2} \; for \; (x \geq \sqrt{2})$$

Critical buckling force, Gordon-Rankine;

$$F_{Cb} = yA_s\sigma_y$$

Dimensionless length

$$x = \sqrt{2}\frac{\lambda}{C_C}$$

Slenderness ratio

$$\lambda = \sqrt{\frac{As}{l}}L = \frac{L}{r_g}$$

Column constant

$$C_C = \pi\sqrt{\frac{2E}{\sigma_y}}$$

These formulas were used in the presentation of the results in the graphs presented in chapter 5. Results. The inelastic buckling formulas are gained from steel-structure (Salmon et al., 2009).

Also, calculation on hydraulic pressure needed to snub or strip a pipe depends on the number of active hydraulic jack cylinder, therefore the following formula is used depending on the operation.

Effective area of the jack;

For snubbing

$$A_{jack} = \frac{\pi\left(B_c^2 - D_p^2\right)N}{4}$$

For pulling

$$A_{jack} = \frac{\pi B_c^2 N}{4}$$

A_{jack} = Effective jack area, m^2
N = Number of active cylinders
B_c = Cylinder bore, m
D_p = Piston rod diameter, m^2

2.1.8 Slenderness ratio

The use of slenderness ratio is a part of determines the theoretically buckling loads. Slenderness ratio have its origin from structural engineering and is a part of the measurement of a column to buckle. It is defined as the effective length of a column divided by the minimum radius of gyration.

In the oil and gas business, the slenderness ratio is used in calculations to determine the critical buckling loads. If the slenderness ratio is greater than the pipe slenderness, (C_c), Euler's long column is used, and if the slenderness is less than the column slenderness, its local inelastic buckling.

In all application, the largest of the two slenderness ratio's listed below should be used (Franklin & Abel, October, 1988).

The slenderness ratio is defined as

$$\lambda = \frac{L_e}{r_{min}}$$

Where,

λ = Slenderness ratio
L_e = Effective length of the column
r_{min} = Minimum radius of gyration

$$r = \sqrt{\frac{I}{A_s}}$$

Where,

I = Moment of inertia
A_s = Cross-sectional area of steel

The general column slenderness ratio divides the distortion of a column into the elastic and inelastic regions of the stress-strain diagram and are given by,

$$C_C = \pi \sqrt{\frac{2E}{\sigma_y}}$$

Where Cc = column slenderness ratio, E = Young's modulus of elasticity and σ_y= yield stress. Young's modulus of elasticity is commonly used around 200 GPa, this is the average value for steel, (Skinner, 2019). The yield stress of the material is depending on the steel used (alloys) and is therefore varying depending on the material properties.

The two slenderness ratio's that needs to be calculated for critical buckling calculations are as listed below,

$$SR_1 = \frac{kL}{r_g}$$

$$SR_2 = \left(4.8 + \frac{R}{255t}\right)\sqrt{\frac{R}{t}}$$

The Gordon-Rankine's empirical formula, (K. Newman & Aasen, 1998) presented by Timoshenko are as listed below,

$$\frac{P_b}{P_y} = \frac{1}{(1 + \beta^2 SR^2)}$$

$$\frac{P_b}{P_y} = \frac{F_{Cr}}{\sigma_y A_s}$$

$$P_y = \sigma_y A$$

Where P_b = buckling force, P_y = yield force, F_{cr} = critical buckling force, A_s = cross-sectional area of steel. β is determined experimentally and includes the conversion of effective length causing effective length (L_e) to be equal to L. This calculation is used to calculate the buckling load for short columns, where C_c is less than 80 (K. Newman & Aasen, 1998).

2.1.9 Stress-Strain

Stress is defined as the force acting on the cross-sectional area, and strain is defined as deformation of the material, the formulas used is shown below,

$$\sigma = \frac{F}{A}$$

$$\sigma = E\varepsilon$$

$$\varepsilon = \frac{L - L_0}{L_0} = \frac{\Delta L}{L}$$

F = Force applied, N
A = Cross-sectional area, m^2
σ = Stress, MPa
E = Elasticity modulus, MPa
ε = Strain, measurement of deformation
L = Length, m
ΔL = Change in length, m

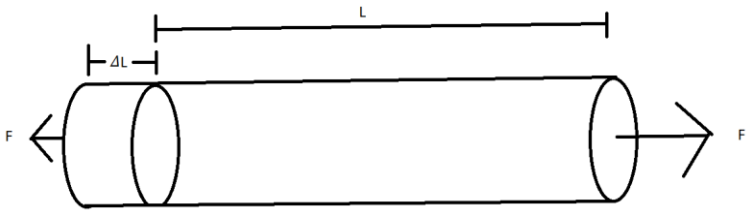

Figure 8 Tubing experiencing tensile strength

The relation between stress and strain is a stress-strain curve as shown below, where stress is on the y – axis, and strain is on the x- axis, the elasticity modulus is also shown in the graph.

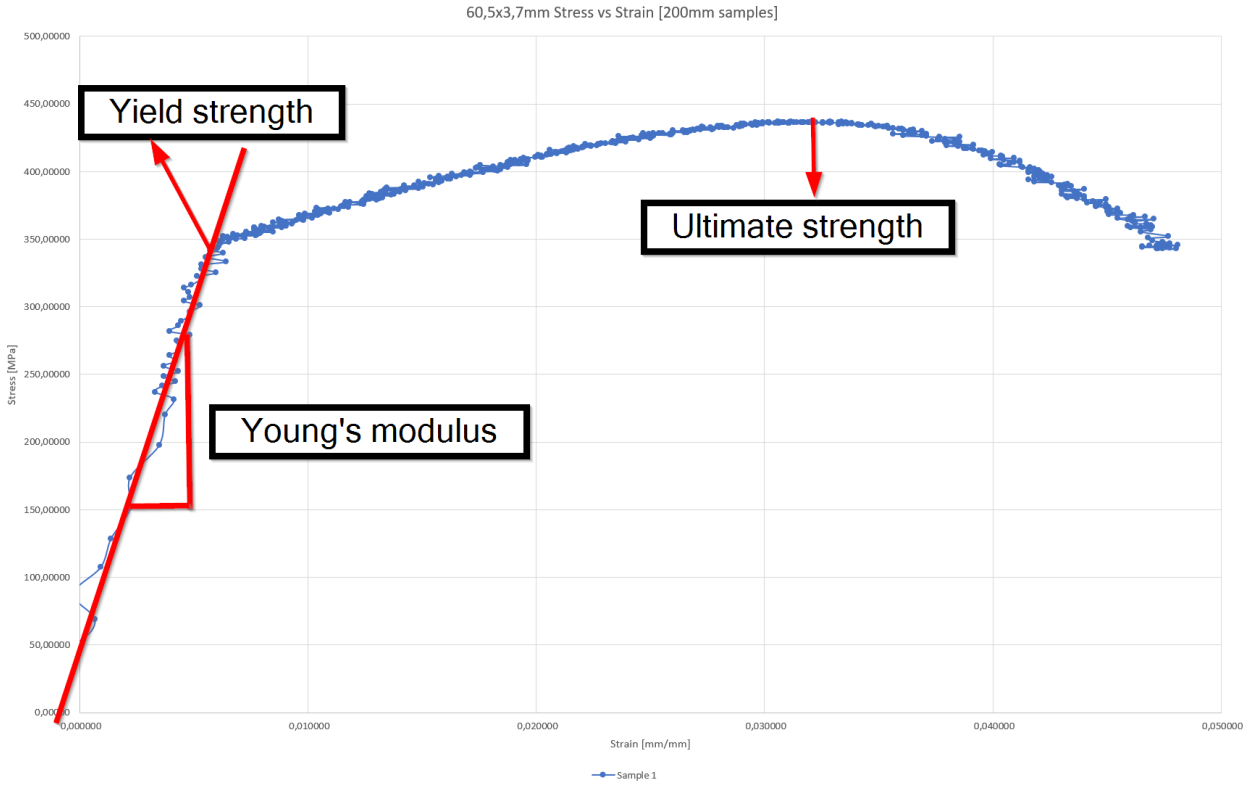

Figure 9 Stress vs Strain graph

3. Experimental preparations

For this research, axial load experiments on tubing is conducted. Compression and tensile strengths are measured and calculated. The use of several different pipe sizes with different strength and dimensions. The University of Stavanger provided these pipes for this experimental study, and the following lengths and dimensions are found in table 2 below.

Table 2 Available pipe lengths

Available pipe lengths	
OD x t	Length
26,9mm x 2,6mm	18 meters
33,7mm x 3,2mm	12 meters
48,3mm x 3,6mm	12 meters
60,3mm x 3,6 mm	6 meters
88,9mm x 3,2 mm	6 meters

During this research, several preparations were needed to perform these experiments and to gain accurate data. Setup of the compression machine, cutting of pipe, milling, welding, bushing preparations and other small adjustments needed before and during the experiments. All experiments and preparations were made in accordance to the University of Stavanger's HMS procedures.

The pipes gathered came with its own datasheets, (except the 33,7x3,2mm pipe), where the measured OD x t, tensile strength and yield data was as follow in the table.

Table 3 Pipe Datasheet

Pipe Datasheet			
OD x t	**Tensile [N/mm2]**	**Yield [N/mm^2]**	**Quality**
26,9mm x 2,6mm	413	322	S235JRH
33,7mm x 3,2mm	Unknown	Unknown	Unknown
48,3mm x 3,6mm	463	575	7T39715
60,3mm x 3,6 mm	373	272	S235JRH
88,9mm x 3,2 mm	425	373	S235JRH

However, the datasheet was only used as a pointer, and the values gathered from experiments are used in this research. Own measurements were taken from all off the pipes gathered. The results of these measurements were used in all the calculations from this experimental research.
In the table below, the results of these measurements are shown. Five measurements were taken from different places on each pipe to make sure it was as uniform as possible. Before the pipe was measured, the rust dust and other debris was removed and gently cleaned with sanding paper, so that the measurements were taken as accurate as possible in to the steel itself. The outer diameter and thickness was measured with an accurate caliper. The results are shown in the table below.

Table 4 OD x t measurements results

Datablad:	26,9x2,6mm pipe		33,7x3,2 pipe		48,3x3,6mm pipe		60,8x,3,6 pipe		88,9x3,2mm pipe	
Measured	OD [mm]	t [mm]	OD [mm]	t [mm]	OD [mm]	t [mm]	OD [mm]	t [mm]	OD [mm]	t [mm]
1	27,3	3,1	33,8	3,4	48,5	3,9	60,6	3,7	89,1	3,0
2	27,3	2,5	33,9	3,1	48,4	3,9	60,8	3,6	89,2	3,0
3	27,3	2,6	33,8	3,3	48,4	3,9	60,6	3,7	89,1	3,0
4	27,3	2,9	33,8	3,2	48,4	3,9	60,3	3,7	89,3	3,0
5	27,3	2,7	34,0	3,1	48,7	3,9	60,3	3,6	89,0	3,0
Average	**27,3**	**2,8**	**33,9**	**3,2**	**48,5**	**3,9**	**60,5**	**3,7**	**89,1**	**3,0**

The average values of all the measured OD and thickness was used. Many of the small pipe sizes used in snubbing operations are referred to by nominal size. However, the actual OD does not correspond to their actual OD, (Franklin & Abel, October, 1988).

Table 5 Tubing nominal size vs actual size

Actual size [mm]	Nominal [Inches]
27,3mm x 2,8 mm	3/4"
33,9 mm x 3,2 mm	1"
48,5 mm x 3,9 mm	1 1/2"
60,5 mm x 3,7 mm	2 3/8"
89,1 mm x 3,0 mm	3 1/2"

The tubing sizes gathered for these experiments can be compared to the following tubing standard given by Baker Hughe Engineering handbook, (Baker, 1995).

Table 6 Experimental tubing size compared to real tubing sizes

Gathered experimental size	Dimension data of tubing made to API Specification	Dimension data on selected heavy weight and non API tubing
27,3mm x 2,8 mm	26,7 mm x 2,87 mm	26,7 mm x 2,87 mm
33,9 mm x 3,2 mm	33,4 mm x 3,38 mm	33,4 mm x 3,38 mm
48,5 mm x 3,9 mm	48,3 mm x 3,17 mm	48,3 mm x 3,68 mm
60,5 mm x 3,7 mm	60,3 mm x 4,24 mm	60,3 mm x 4,83 mm
89,1 mm x 3,0 mm	88,9 mm x 5,49 mm	88,9 mm x 5,49 mm

As we can see, the tubing gathered for this study can be compared in sizes to tubing's being used today. In the table below, we can see the OD / t numerical value. This can be used to determine the buckling loads.

Table 7 (OD / t) for all pipes

Pipes	OD / t
27,3 mm x 2,8 mm	9,8
33,9mm x 3,2 mm	10,6
48,5 mm x 3,9 mm	12,4
60,5 mm x 3,7 mm	16,4
89,1 mm x 3,0 mm	29,7

3.1 Enerpac compression machine

Figure 10 Enerpac VLP setup

For the axial compression experiments, the Enerpac VLP series with 700 bars compression loads was used. For the rig-up of the equipment, two computer screens were used to show the force and length of the piston in real-time. This was logged on the computer with 60Hz (60 samples per seconds) and captured using to video-recorder devices. These video recording devices was attached to the Enerpac machine positioned with 90-degree angle to the compression area. This to be able to see both load, length of piston travelled and capture buckling in every direction. The setup is as shown in figure 10.

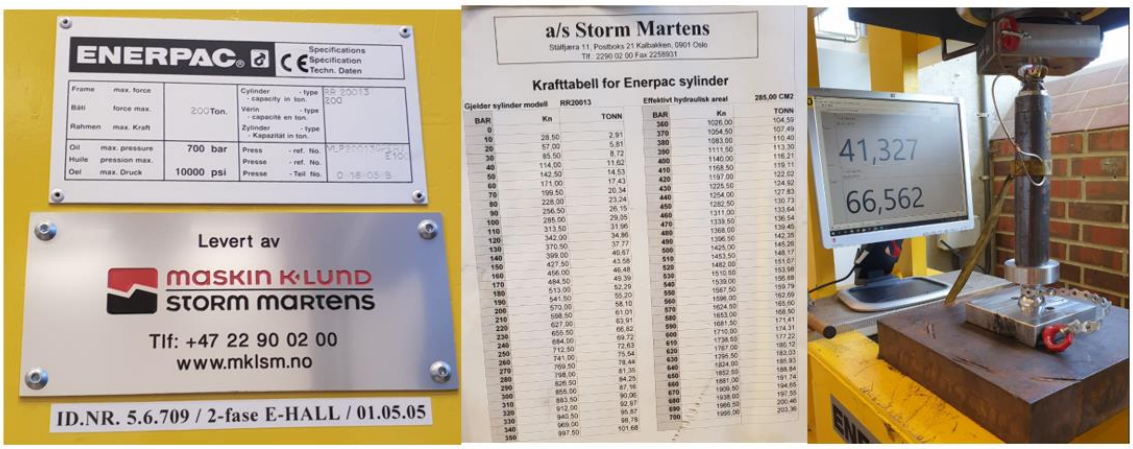

Figure 11 Enerpac information

The pressure injected into the cylinder bore diameter, as seen in below figure, was captured with the use of a transducer, that converts pressure into electrical signal and sent to the computer through a 250 Ohms resistor. This signal was calibrated to make sure it was as accurate as possible. Below a sketch of how a compression machine works. Conversion from bar to kN and tons are shown in the figure 11, this was just as an information to look at while performing the tests, and to be captured on the video for further investigation.

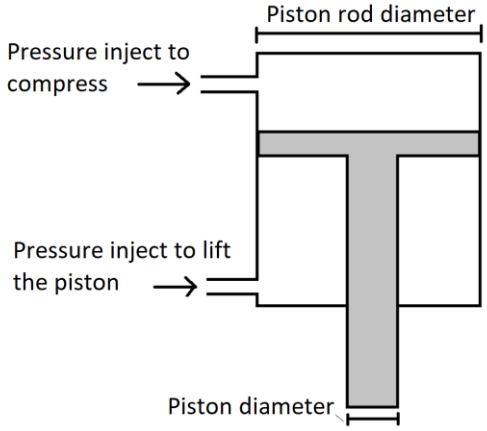

Figure 12 Enerpac explanation figure

This machine has several options regards to available heights. The table can be moved up and down, where there is 25 cm between each set point. This table was moved down two times to fit the increased pipe lengths used in the experiments. The pipes length used was 200 mm and all the way up to 750mm.

Figure 13 Enerpac different height levels

3.1.1 Calibration of the transducer and Enerpac

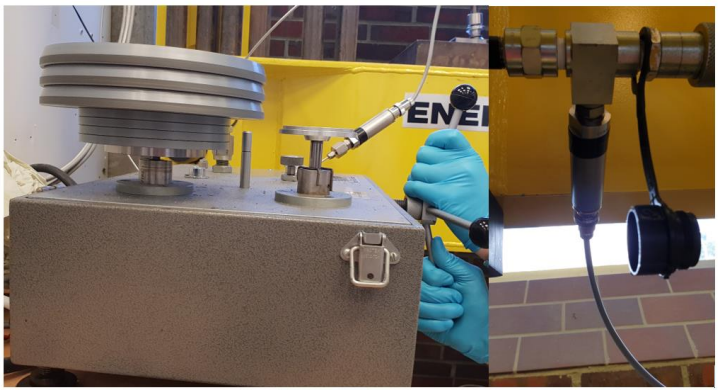

Figure 14 DWT to the left and a transducer to the right

The transducer used for these experiments was calibrated with a deadweight tester (DWT). These results were compared with the data gained by using the company Zwick's loadcell. Then the values gained from the DWT and Zwick was compared to get the calibration as accurate as possible. In the graph below, the results are compared, and the result's showed that the DWT calibration was accurate.

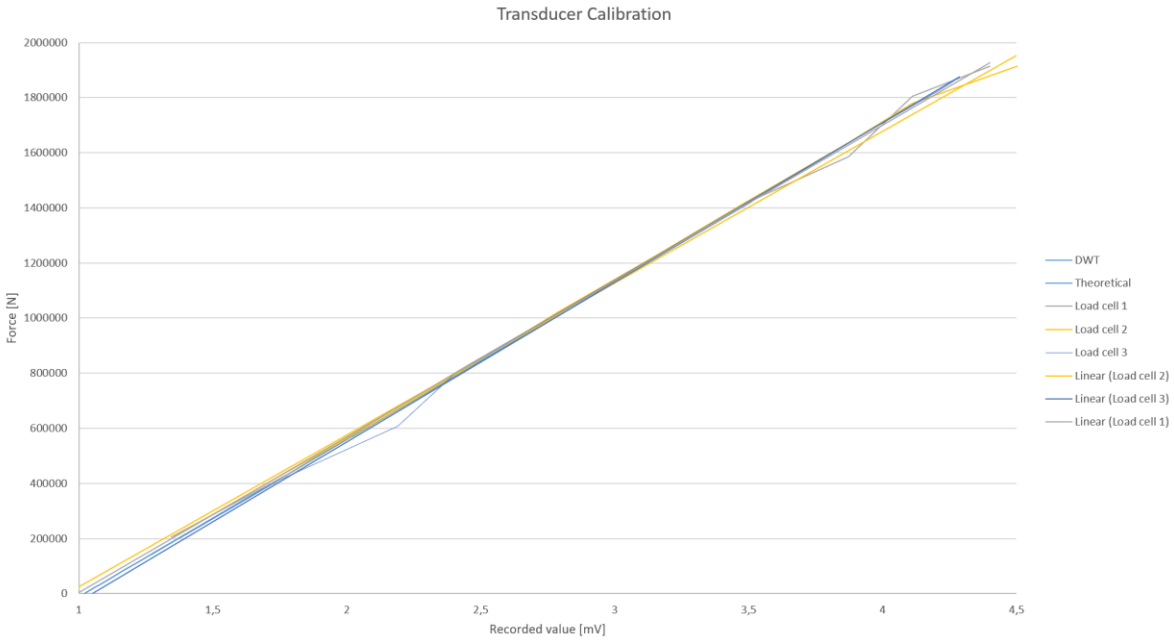

Figure 15 Transducer calibration

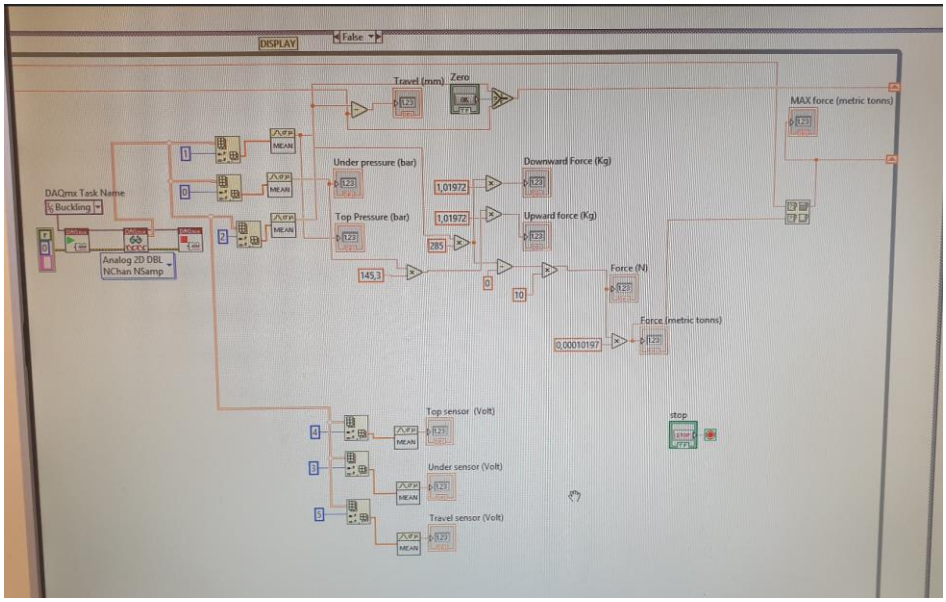

Figure 16 LabView program design

Transducer used in these experiments used a signal between 1-5mV. The calibrated linear graph was used as input for the program “LabView”. This program was used to show forces and travelled length in real time as well as saving the datapoints. The designer and programmer of this programming codes in LabView was Kim Andre Nesse Vorland.

The length of piston travelled was also accurately calibrated. This was provided by comparing the actual length the piston moved from top to bottom with the values gathered in LabView. This measurement had an accuracy of 0,2 mm.

3.2 Cutting machine

Figure 17 Rusch cutting Machine

Rusch circle saw was used to cut all the piping and bushing. This research needed the pipe and bushing to be as accurate as possible to the desired lengths. Rusch circle saw did not cut accurate enough. The solution was to use a milling machine after each pipe and bushing was cut to small pieces. Then they were milled to the desired lengths with a great accuracy. This reduced the error that could influence the results. Each pipe needed to have as accurate as possible angles to the cut, so when the compression tested was conducted, the angles of the cuts did not affect the buckling loads gathered.

The procedure was to cut the pipes with 3-5mm longer than it needed, so it could be milled down to exact lengths.

3.3 Milling machine

Figure 18 Milling machine

The milling machine was used to make the pipe cuts perpendicular to the pipe ss the Rusch circular saw not cut the pipes as accurate as needed. The accurate length needed was also done with this milling machine. Pipe length was measured correctly and cut to eliminating any imperfections. This was used on all pipes on every length to measure the exact length and get the cut as straight as possible. This operation was dependent on punctuality as there where several pipes that needed preparation.

Several bushing with different dimensions and purpose was made. Bushing was necessary to use to attach the pipes securely to the Enerpac machine. The circular end connection was used on the compression tests. These circular tow bars were gathered at Biltema shop and had a 19 mm screw treads that the bushing could be screw on to.

Figure 19 Circular tow bar from Biltema shop

These circular end attachments was use to let the pipe buckle freely in any direction. The treaded bushing screws was made on all bushing to the compression experiments.

Figure 20 Picture collage of operations performed from the milling machine

In the picture collage seen figure 20, some of the process of making these bushings from the shaft, as well on how to create the threaded screws.

3.4 Bushing preparation

Bushing was made for all the pipes. For the pipes with outer diameter greater than 60 mm, a 100 mm shaft was used, and a 60 mm shaft was used for diameters lower. For pipes that had a greater OD than 50 mm, a shoulder was necessary, due to the of the circular shaped tow bar shoulder only had a 50 mm diameter shoulder.

3.4.1 Bushing for compression test

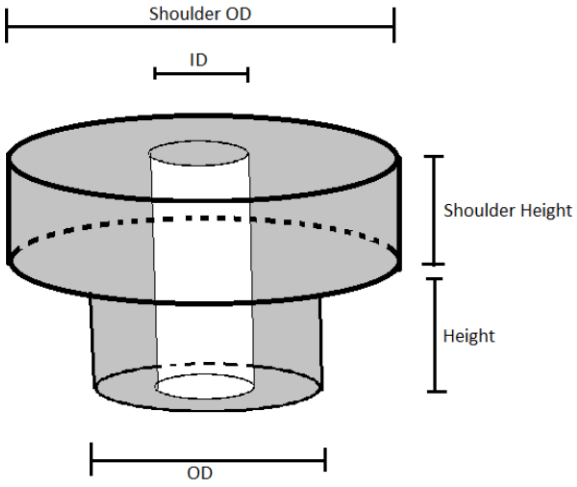

Figure 21 Bushing for compression testing

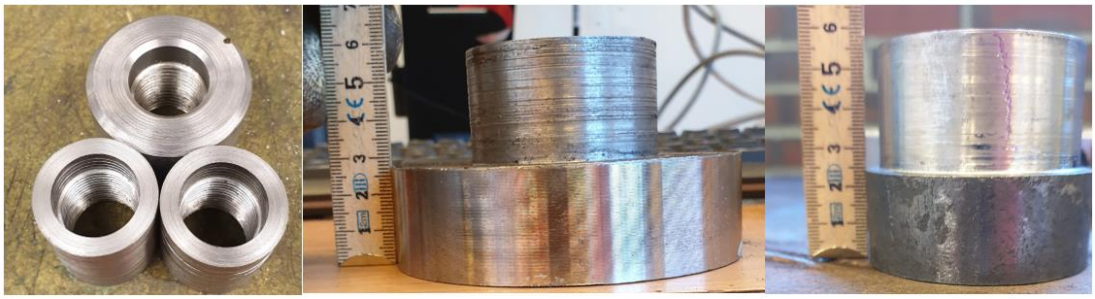

Figure 22 Bushing from compression testing examples

The bushing tool was used inside the pipe for both compression tests and the tensile tests. In below table, all dimensions for the bushing used in compression test are listed. These were made from the milling machine. Ten different bushing had to be made to all the five different pipe sizes. All of them had to be accurate measured and create screw treads to be able to screw on to the tow bar used as end constrain. This was a very time dependent task that several hours went by making them.

Table 8 Bushing dimensions compression testing

Bushing Dimensions		
27,3mm x 2,8 mm		
OD	21,7	mm
ID	19	mm
Height	30	mm
33,9mm x 3,2mm		
OD	27,5	mm
ID	19	mm
Height	30	mm
48,5mm x 3,9mm		
OD	40,7	mm
ID	19	mm
Height	30	mm
60,5mm x 3,7mm		
OD	53,1	mm
ID	19	mm
Height	30	mm
Shoulder OD	90	mm
Shoulder Height	25	mm
89,1mm x 3,0mm		
OD	83,1	mm
ID	19	mm
Height	30	mm
Shoulder OD	98	mm
Shoulder Height	25	mm

3.4.2 Bushing for tensile test

Since the maximum outer diameter to the tensile test machine was 34 mm, new grips needed to be made to attach the pipe firmly to the machine. These was milled out from 60 mm and 100 mm shaft.

These bushing needed to be welded on to the pipe. This without any distortions. Due to air vent restrictions as the workshop at the University in Stavanger, these bushings needed to be welded somewhere else. Smed T. Kristiansen AS welded was chosen to weld these bushing on to the pipes.

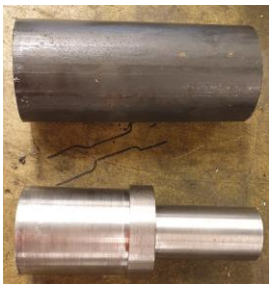

Figure 23 Bushing for tensile test example

In the picture below, an example of one of the bushing made for 48,5mm pipe is showed. The figure below, describes the different dimension listen in the table below.

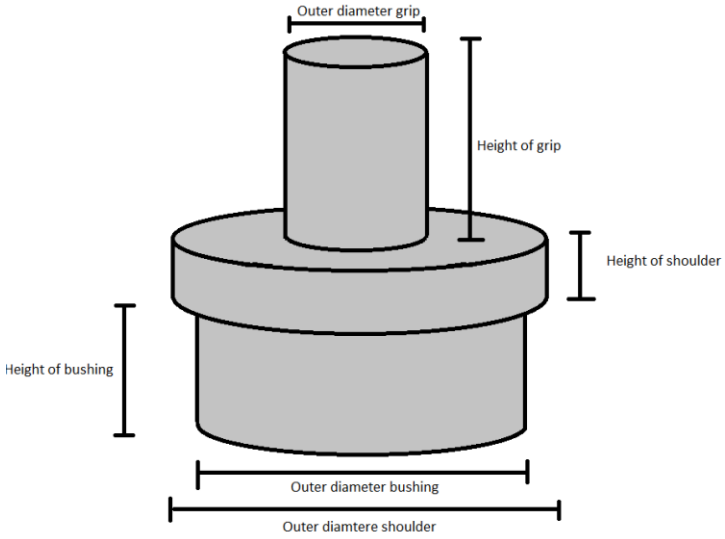

Figure 24 Bushing dimension figure for tensile test

The table below shows the dimensions of the bushing used to reduce the outer diameter and welded on to the pipes. The milling of these bushing took long time as twelve of the bushing had to be milled down from a 100 mm shaft, and the rest was milled out from 40 mm and 60 mm shafts. It was not possible to re-use the bushing as it had been welded on to the pipe.

Table 9 Tensile test bushing dimension

Tensile test bushing dimension		
48,5mm x 3,9mm		
OD grip	< 34	mm
Height of grip	60	mm
OD shoulder	44,6	mm
Height of shoulder	10	mm
OD bushing	40,7	mm
Height of bushing	60	mm
60,5mm x 3,7mm		
OD grip	< 34	mm
Height of grip	60	mm
OD shoulder	56,8	mm
Height of shoulder	10	mm
OD bushing	56,21	mm
Height of bushing	60	mm
89,1mm x 3,0mm		
OD grip	< 34	mm
Height of grip	60	mm
OD shoulder	86,1	mm
Height of shoulder	10	mm
OD bushing	83,1	mm
Height of bushing	60	mm

Two bushings of each dimension were needed, one in each end. In the picture below, the bushings is firmly welded on to the pipes, and is able to withstand the loads of the tensile test machine.

Figure 25 Welded bushing to pipes

Due to the limitations of the machine, we had to find new methods to find the elasticity modulus. Three attempts with different methods was used. The first was to mill out a small sample of the pipe and use this in a smaller tensile test machine. This result was not correct due to an extension meter needed and was not available, and the results therefore not reliable.

3.5 Pipe length with bushing determination

Figure 26 Tow bar height

The pipe length was cut to 200 mm, 250 mm, 300 mm, 500 mm and 750 mm. However, the bushing and circular tow bar added some extra length to the real unsupported lengths. In the calculations, the total free length of unsupported pipe was used. In the table below, the real unsupported length can be found. The measurements were taken from the middle of the circle on each end. This was done to get the worst-case scenarios of buckling.

Table 10 OD less than 50 mm unsupported lengths

OD less than 50 mm		
Pipe length	Real unsupported length	
200	284	mm
250	334	mm
300	384	mm
500	584	mm
750	834	mm

Table 11 OD greater than 50 mm unsupported lengths

OD greater than 50 mm		
Pipe length	Real unsupported length	
200	332	mm
250	382	mm
300	432	mm
500	632	mm
750	882	mm

3.6 Video recording setup

Video recording was set up for the compression experiments. Two cameras were placed in each direction of 90 degree to be able to capture deflection of the column as it buckled, and captured in any direction. Both cameras facing the computer screen, logged the force and extension together with the compressed pipe.
The cameras that was used was a GoPro 7 together with a Samsung S9 plus. Both cameras were set to linear view angle with 1440p, 60fps. All buckling experiments was recorded and edited with the video software DaVinci Resolve 16. The video was synchronized to show the exact same force and extension. In pictures below, several images captured from the video's is put in as examples. These are taken for each length of the 27,3 mm x 2,8 mm pipe ranging from 200 mm up to 750 mm.

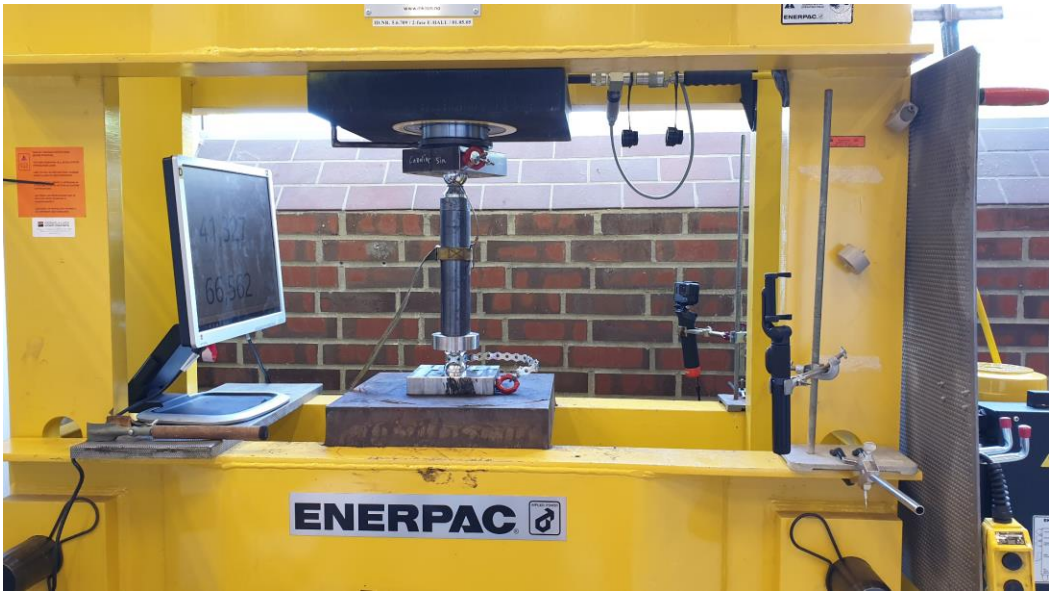

Figure 27 Enerpac video setup

Figure 28 Video captures from 27,3mm pipe, from 200 - 750 mm pipe size

3.7 Instron 5985 Dual Column Floor Frames Tensile test machine

Figure 29 Instron 5985 dual column floor frames tensile test machine

Instron 5985 dual column floor frames tensile test machine was used to gather information of the elasticity modulus (Young's modulus), yield strengths and tensile strengths of the pipes. This machine has the ability to perform several different tests such as compression, tensile, flex (bend), cyclic, creep and relaxion. January 2019 the machine was calibrated by the company Zwick. The software used to control, insert specimen data and calculating the results was BlueHill 3. In Appendix E, a small tutorial on how to operate the software in a step by step is shown in a procedure.

This machine was used for the tensile testing experiments. The limitations were max 250kN tensile strength and maximum outer diameter of 34 mm to attach the circular pipes. This was a big concern due to three of the pipes gathered for this research, had a higher yield force than the Instron 5985 could pull and also larger outer diameter than the grips.

Several local businesses were contacted to see if they had an available tensile test machine that could pull greater loads and larger circular attachment's, without any luck. Therefore, going forward a new method needed to be conducted to find the young's modulus and the yield stress.

The best working solution was to cut out steel from the three biggest pipes, reducing its cross-sectional area and therefore reducing its overall tensile strength. Calculations are showed in chapter 3.8.1 that was used to determine how to calculate a new tubing thickness to input in the software.

3.8 Tensile test experiments

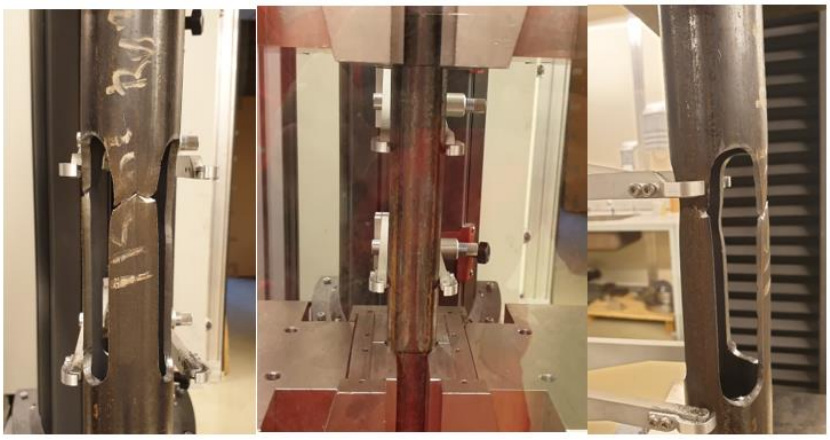

Figure 30 Tensile test experiments

The tensile strength experiments were one of the most important experiments. The goal was to collect as accurate values of the elasticity modulus (young's modulus) and the yield stress for each tubing. The tests were conducted in accordance to the ISO standard, ISO 6892-1 2016, to determine the yield loads, young's modulus and tensile strengths.

The 27,3mm x 2,8 mm pipe had four tensile tests runs where all was 30 cm long pipe specimens. The 33,9 mm x 3,2 mm pipes had three tests with the same length.

For the three other pipes, (48,5mm, 60,5mm and 89,1mm), there was an issue with the strength and the attachment of tubing's. Therefore, the best solution was to build bushing with 34 mm outer diameter to weld on to the tubing so the machine could grip the pipe from the bushing.

For the pipes expected to have a greater tensile load than the Instron machine was designed for. New method had to be investigated to find the best way for these experiments. Several methods were tried out in this investigation, but the one that was used was reduction of the cross-sectional area of the tubing. This would reduce its tensile strength in the test area and give the opportunity to use this machine.

Figure 31 Prepared bushing ready to be welded

3.8.1 Area reduction for tensile testing

Since the tensile test machine not was powerful enough to tensile test the three largest pipes, the pipe strength needed to be reduced. This was done by slicing the pipes to reduce its cross-sectional area around the testing area. This was done by experienced lab personnel, who did a great job slicing out these areas as accurate as possible. Three slices from 300 mm length pipes was preformed and all slices was 100 mm long. The width of these cuts was calculated as shown below. Below are the formulas used to calculate how much the cross-sectional area needed to be reduced.

$$A_s = \frac{\pi}{4}(OD^2 - ID^2)$$

$$ID = \sqrt{OD - \frac{4A}{\pi}}$$

$$t = \frac{OD - ID}{2}$$

Where,
A_s = Cross-sectional area of steel [mm^2]
ID = Inner diameter [mm]
OD = Outer diameter [mm]
t = thickness [mm]

The area cut out from 48,5mm, 60,5mm and 89,1mm tubing was calculated using the formulas below.

Circular segment

$$A = \left(\frac{\alpha}{360} - \frac{sin\,\alpha}{2\pi}\right)S$$

$$A_1 = \left(\frac{\alpha}{360} - \frac{sin\,\alpha}{2\pi}\right)S$$

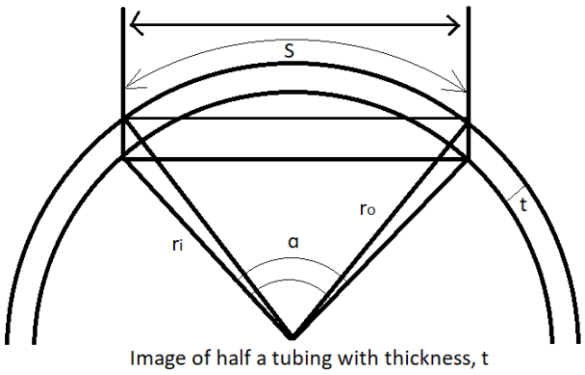

Figure 32 Image of a tubing with thickness, t and cut out area determination

$$A_m = d_m t$$

$$d_i = d_0 - 2t$$

$$A_{s_1} = \frac{\pi}{4}\left(d_0^2 - (d_0 - 2t)\right) - n d_m t$$

A_m = Milled area, m^2
d_o = Outer diameter
d_i = Inner diameter
n = number of cuts
A_{s1} = New area of steel, m^2

With the use of these formulas, the calculations were done to determine how much needed to be cut off, so the tubing was inside the limits of the machine. The table below descries the outcome of these calculations, and the new thickness needed to be input to the Bluehill 3 software in the computer. This tubing design has not been used in this software before, and modification was needed to get the correct values, so the method used in this study was to let the software think it was a smaller wall thickness tubing.

The table 9 shows the area that was cut out from the tubing's.

Table 12 Tubing cutting sizes for tensile testing

Pipe Slice	1	2	3	Total	
48,5x3,9mm	24	24	24	72	mm
60,5x3,7mm	30	30	30	90	mm
89,1x3,0mm	50	50	50	150	mm

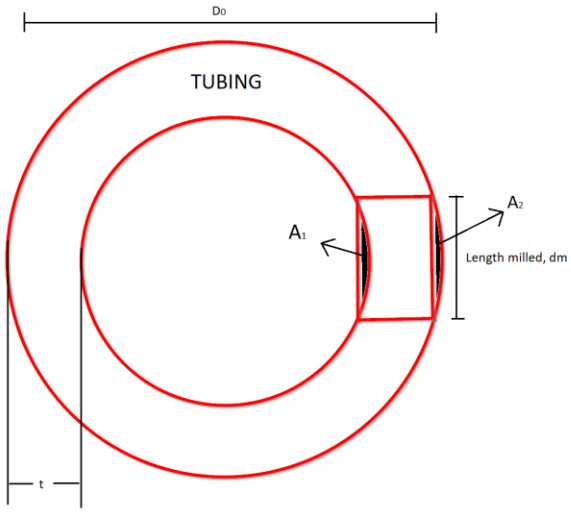

Figure 33 Tubing with assumed area A1 and A2

Assumptions was made that $A_1 = A_2$, meaning that the milled-out area on the outer circle is equal to the milled out inside circle. Calculations was done to determine how accurate these assumptions were. An example of the process is shown below. These calculations results show that the assumption can be used as it has less than 1 % wrong.

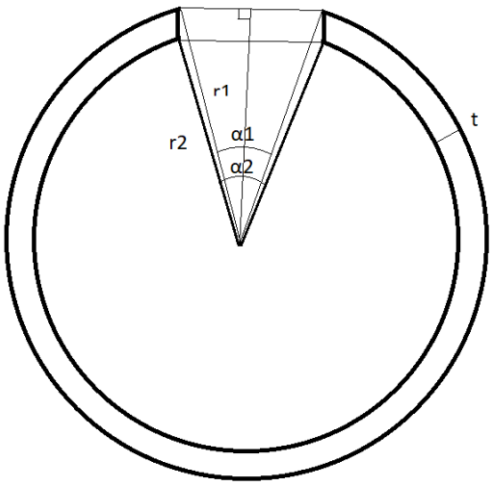

Figure 34 Tubing calculations figure for cut outs

Example of calculations for the 88,9mmx3,2mm tubing:

$r_1 = \frac{89,1}{2}$ = 44,55 mm

$r_2 = \frac{89,1-3,0}{2} = 43,35$mm

$$r = \frac{d}{2}$$

$$S = \frac{\alpha}{180}\pi r$$

$$sin(\alpha) = \frac{opposite}{hypotenuse}$$

Opposite = $\frac{50mm}{2}$ = 25 mm

Hypotenuse = r

$\alpha_1 = 34,13 \times 2 = 68,27$ degrees

$\alpha_2 = 35,21 \times 2 = 70,44$ degrees

S = length of the outer circle as shown in figure above,

S_1 = 53,0829mm
S_2 = 53,2949mm

$$A_1 = \left(\frac{\alpha}{360} - \frac{sin\,\alpha}{2\pi}\right) \cdot s$$

A_1 = 2,2185 mm^2

A_2 = 2,4350 mm^2

Milled out area assumption =

$A_{milled} = d_m$ x t = 50 mm * 3,0 mm = 150 mm

$A_{milled} + A_1 - A_2$ = 150 + 2,2185 - 2,4350 = 149,78 mm^2

Accuracy = $\frac{149,78}{150} \times 100\% = 99,85$ % Which is less than 1 % off.

Therefore, these calculations were done on all tubing's that needed to change the parameters to fit the limitations of the tensile test machine to validate its accuracy.

Table 13 Tensile test tubing calculations and calibration

Tensile test tubing pre-calibration																	
Pipe	OD [mm]	ID [mm]	t [mm]	Areal [mm^2]	P at Yield [N/mm^2]	Tensile strenght [N/mm^2]	Force Yield [kN]	Circumref-erence [mm]	Cutted out areas	Cutted area [mm]	Remaining CF [mm]	As [%]	New Area [mm^2]	New expected yield [kN]	New expected tensile [kN]	New ID [mm]	New thikness [mm]
48,5x3,9mm	48,5	40,7	3,9	546,449	463	575	253,0	152,4	3x24mm slisse	78	74,4	48,808 %	266,71	123,5	153,36	44,86	1,8186
60,5x3,7mm	60,5	53,1	3,7	660,237	272	373	179,6	190,1	3x30mm slisse	90	100,1	52,648 %	347,602	94,5	129,66	56,72	1,8878
89,1x3,0mm	89,1	83,1	3	811,473	373	425	302,7	279,9	3x50mm slisse	150	129,9	46,412 %	376,625	140,5	160,07	86,37	1,3664

Below picture, shows the outcome of the cut of 4 out of 6 tubing's that this technique was performed on. All pipes are 300 mm long and have 3 x 100 mm long cut outs. The width was changed on each pipe.

Figure 35 Pipe prepared for tensile test with cut out area for reduction of steel strength

4. Experimental results

4.1 Tensile test results

All lengths used for the tensile testing is 300 mm length. The three largest pipes needed to be modified before the test could be performed.

- 27,3mm x 2,8 mm pipe was tested four times.
- 33,9 mm 3,2 mm pipe was tester three times.
- 48,5 mm x 3,9 mm was tested one time – due to one miss-run.
- 60,5 mm x 3,9 mm was tested twice.
- 89,1 mm x 3,0 mm was tested twice.
-

The number of testes conducted on each pipe was limited due to limitation of pipe lengths, but also other limitation such as welding cost and time limitation (took long time to prepare these tests with bushing, cutting and welding).

Figure 36 Tensile test machine and prepared pipes for testing

4.1.1 27,3 mm x 2,8 mm tubing tensile test

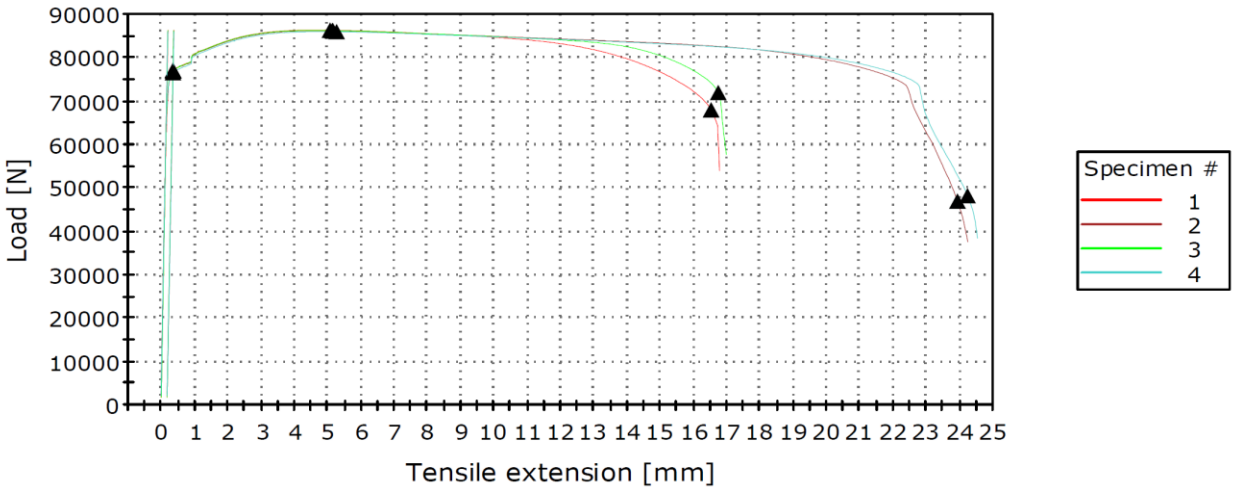

Figure 37 Tensile test graph, 27,3 mm x 2,8 mm pipe

This tubing size and strength was within the limits of the tensile test machine, and the ISO 6892-1 2016 standard was followed. The average values gained from these tests are shown in the table 14 below. The whole report from these tests can be found in Appendix F.

Table 14 Tensile test results, 27,3 mm x 2,8 mm

Pipe	27,3x2,8mm
Fy [kN]	76,91
Fmax [kN]	86,12
SigmaY [MPa]	356,85
SigmaMax [MPa]	399,60
E-modulus [GPa]	172,85

Figure 38 Tensile test picture of 27,3 mm x 2,8 mm pipe

4.1.2 33,9 mm x 3,2 mm tubing compression test

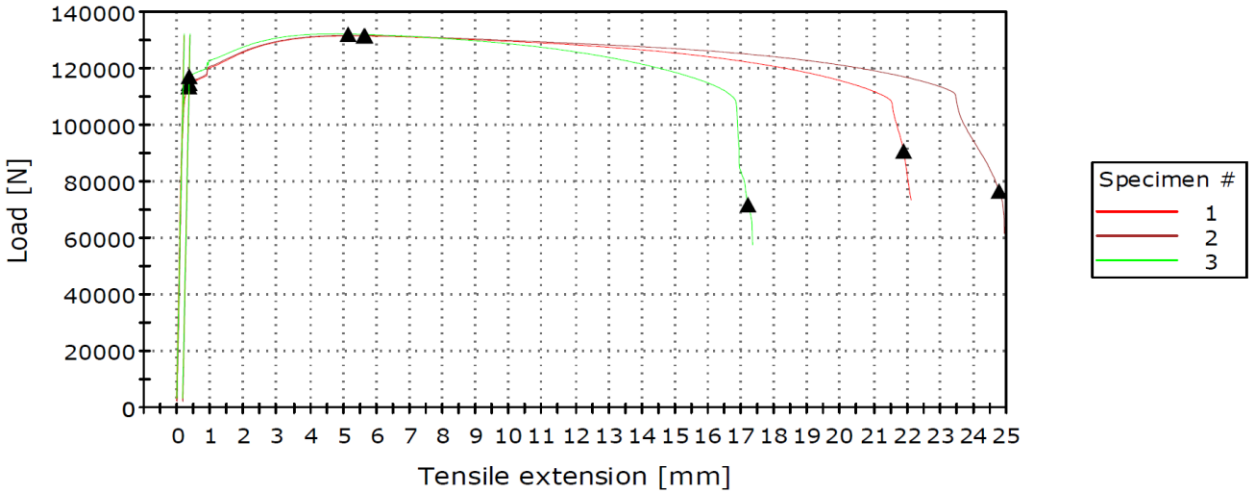

Figure 39 Tensile test graph, 33,9 mm x 3,2 mm pipe

Three pipe samples were tested with this pipe size. This tubing was also within the limits of the tensile test machine, and the ISO 6892-1 2016 standard was used. The average values are listed below. The whole report from these tests can be found in Appendix F.

Table 15 Tensile test results, 33,9 mm x 3,2 mm

Pipe	**33,9x3,2mm**
Fy [kN]	115,27
Fmax [kN]	131,77
SigmaY [MPa]	373,50
SigmaMax [MPa]	426,97
E-modulus [GPa]	170,13

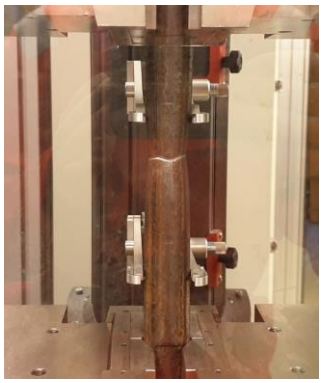

Figure 40 Tensile test picture of 33,9 mm x 3,2 mm pipe

4.1.3 48,5 mm x 3,9 mm tubing compression test

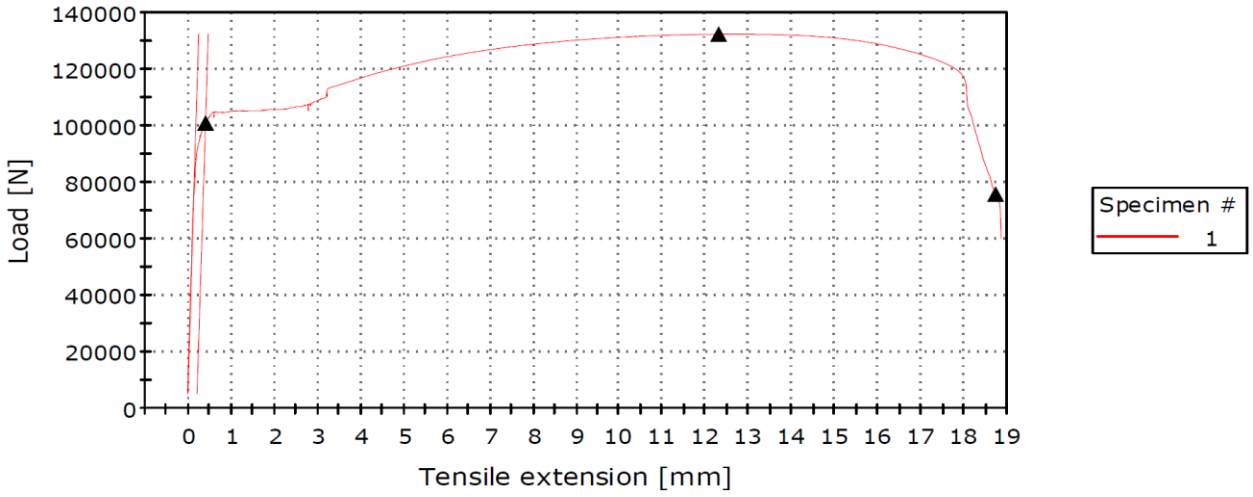

Figure 41 Tensile test graph, 48,5 mm x 3,9 mm pipe

Two tests was supposed to be tested on this pipe, but due to unforeseen issue during the experiment, only one of them was conducted as accordingly to the ISO 6892-1 2016 standard as possible. The result is shown in the graph in figure 41 above, and values in the table 16 below.

Table 16 Tensile test results, 48,5 mm x 3,9 mm

Pipe	**48,5x3,9mm**
Fy [kN]	201,80
Fmax [kN]	264,21
SigmaY [MPa]	369,30
SigmaMax [MPa]	483,50
E-modulus [GPa]	196,30

This test was conducted with the use of the method described earlier with welded ends for grip and cut out cross-sectional test area to reduce its overall strength to be able to use the Instron tensile test machine.

Figure 42 Tensile test picture of 48,5 mm x 3,9 mm pipe

4.1.4 60,5 mm x 3,7 mm tubing compression test

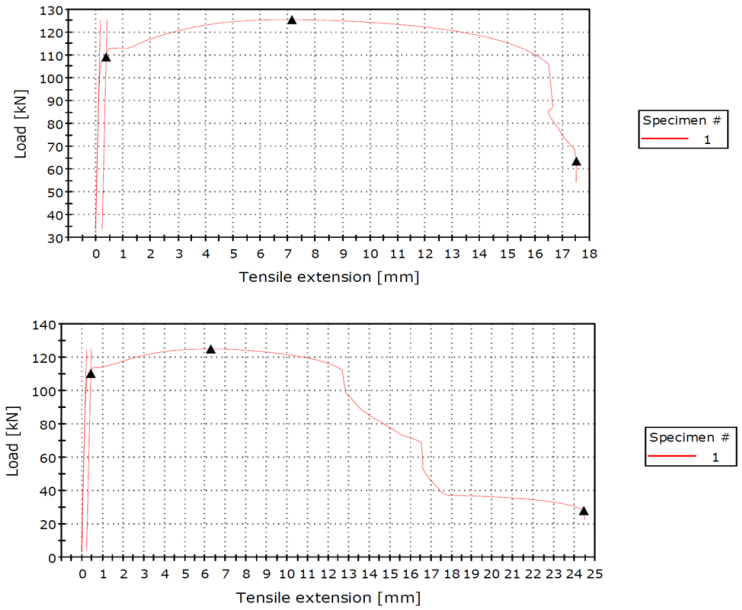

Figure 43 Tensile test graphs for both tests on 60,5 mm x 3,7 mm pipe

These pipe has also reduced cross-sectional area to reduce its overall strength. The average results are shown in the table 17 below.

Table 17 Tensile test result, 60,5 mm x 3,7 mm

Pipe	60,5x3,9mm
Fy [kN]	208,57
Fmax [kN]	237,95
SigmaY [MPa]	315,90
SigmaMax [MPa]	360,40
E-modulus [GPa]	175,50

Figure 44 Tensile test of 60,5 mm x 3,7 mm pipe

4.1.5 89,1 mm x 3,0 mm tubing compression test

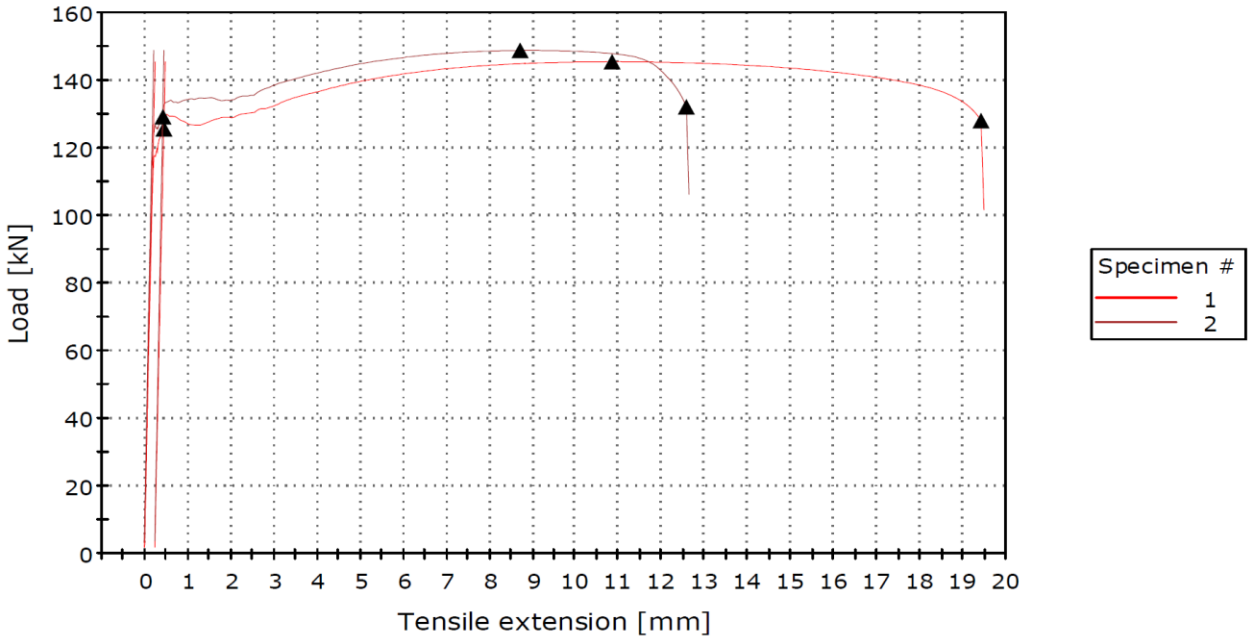

Figure 45 Tensile test graph, 89,1 mm x 3,0 mm pipe

The results from this test are shown in the table below. As we can see, the young's modulus is around 200 GPa, where steel normally is, but due to the method used to gather the date, this may not be accurate.

Table 18 Tensile test result, 89,1 mm x 3,0 mm pipe

Pipe	**89,1 x 3,0 mm**
Fy [kN]	274,60
Fmax [kN]	158,48
SigmaY [Mpa]	338,40
SigmaMax [Mpa]	195,30
E-modulus [Gpa]	198,65

Figure 46 Tensile test of 89,1 mm x 3,0 mm

4.2 Compression test results from Enerpac

Analysis of the video's compared with the data recorded during the compressive test's, the results shows that the compression experiment can be divided into three periods.

1. The measured force is increasing with a linear curve, without any deformations in the steel.
2. Period two shows that the force is stabilizing on the max load, with deformation to the steel, but not the end points. They remain stable.
3. Period three is bending the steel, and the end points is rotating.

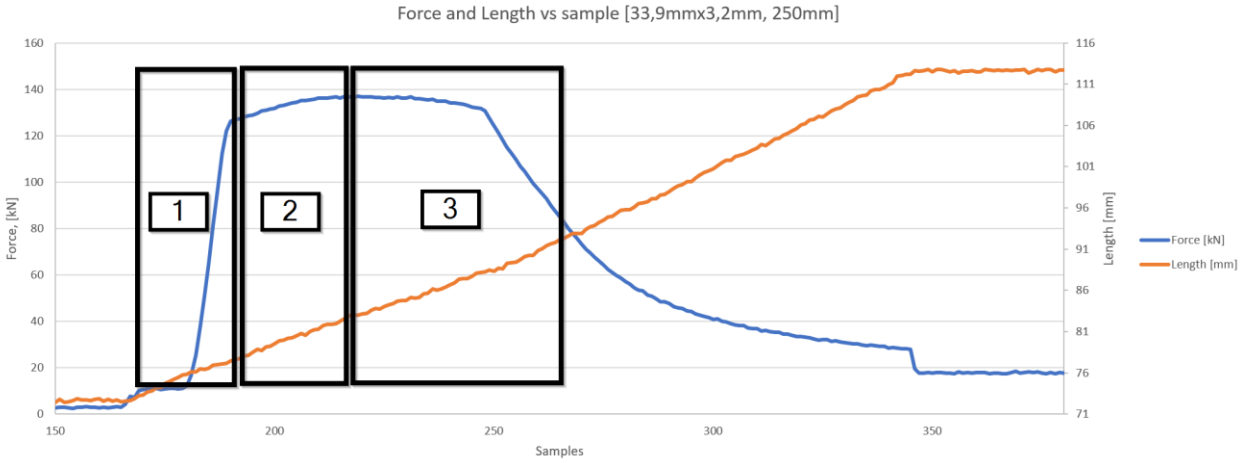

Figure 47 Force and Length vs sample showing three periods during compression

The graph above has three black squares that indicates the tree periods on the graph. The three figures below show captures from the videos at these periods. This graph is taken from the experiment on 33,7 mm x 3,2 mm pipe experiment number 3.

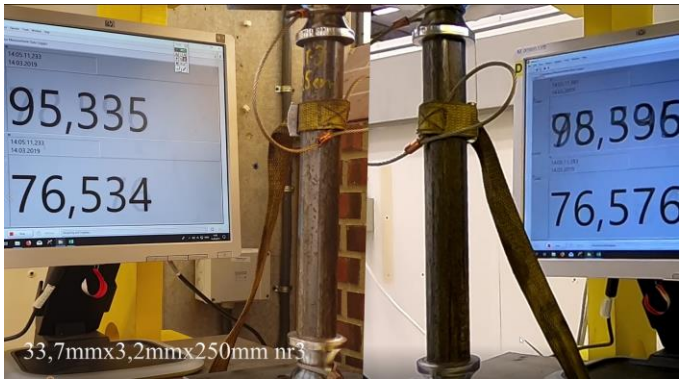

Figure 48 Period one from video

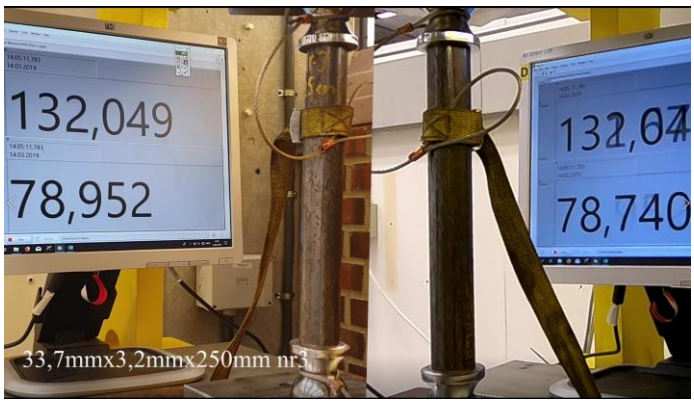

Figure 49 Period two from video

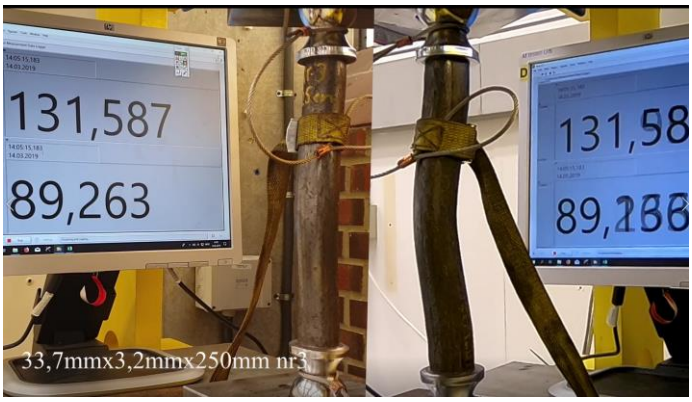

Figure 50 Period three from video

In this study, the columns are as described, divided into three. Short, intermediate and long column. This study are focusing on short and intermediate column lengths. From the results for low unsupported length where the bending not occurred, we can clearly see strain hardening. This is referred to as the short column while when the bending is occurred, as seen in figure 50, its referred to as intermediate column.

From what the results gained from this study, the determination of the different values for yield force was for some pipes challenge to determine. The way to determine these values was to make a trendline from the linear part of the force vs sample graph and find the point where it yield's from this trendline. Figure 51 below shows the method.

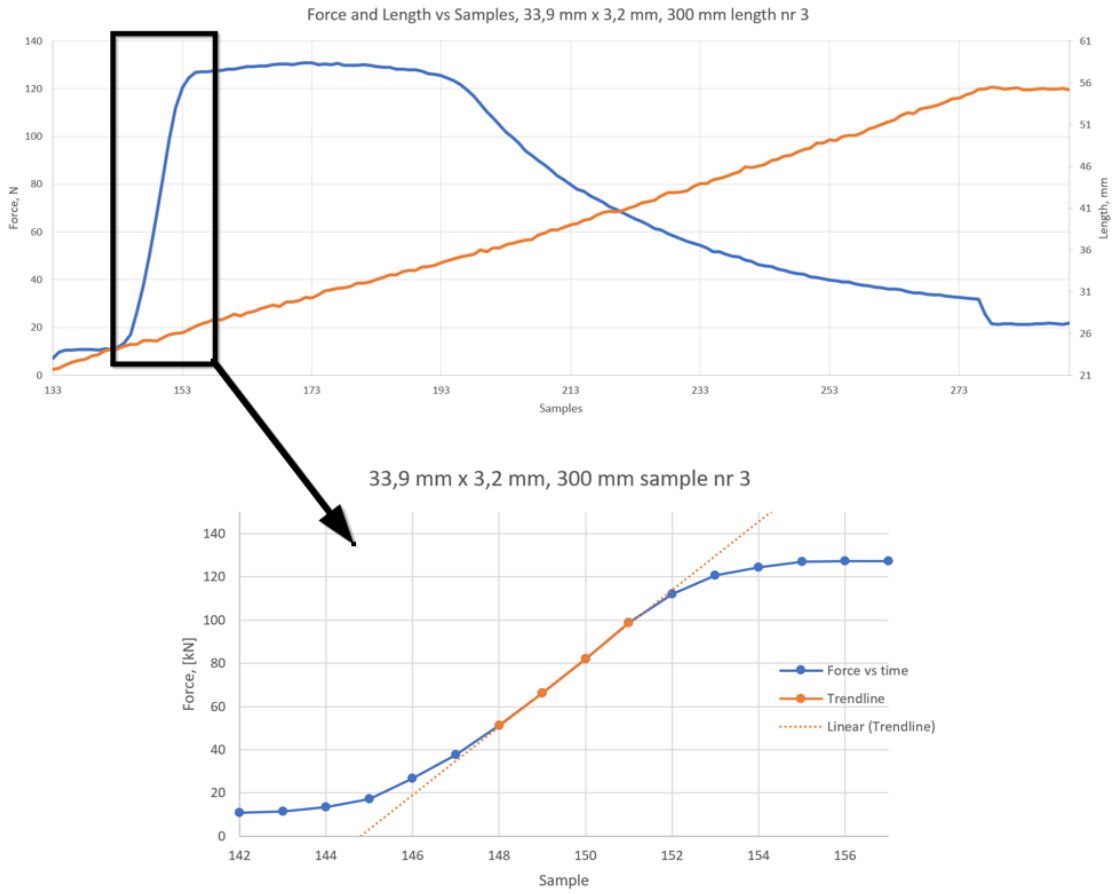

Figure 51 Determination of yield force

In every compressive experiment, the tubing was faced in a way that the "welding seam" was placed towards the computer screen in the back, so that every buckling direction could be compared to the welding seam. During these experiments, the pipe buckled occurred in every direction, and that the welding seam therefore had a minor impact on the buckling direction.

Based on these results, the buckling limit and yield force of each pipe could be determined.

Below are the results from the Enerpac compression testes. For every pipe size, the Stress-Strain graph is provided for each result chapter. These results were used to determine the yield point and ultimate strength. In Appendix A, all results in detail is provided. In the table below, we can see all the values gained from the experiments.

Table 19 Average values from all experimental results

Pipes	E-Modulus [Mpa=N/mm^2]	Area [mm^2]	Sigma Yield [N/mm^2]	I [mm^4]	OD [mm]	ID [mm]	t [mm]	K	Radius of gyration, r	R	Cc
27,3X2,8mm	172850	215,51	358,18	16381,43	27,3	21,7	2,8	1	8,72	9,45	97,60
33,9X3,2mm	170133	308,63	369,46	36755,14	33,9	27,5	3,2	1	10,91	15,35	95,34
48,5X3,9mm	196300	546,45	405,71	136910,65	48,5	40,7	3,9	1	15,83	22,30	97,73
60,5X3,7mm	175500	660,24	333,06	267390,25	60,5	53,1	3,7	1	20,12	28,40	101,99
89,1X3,0mm	198650	811,47	377,51	752865,73	89,1	83,1	3,0	1	30,46	43,05	101,97

As we can see from Table 19, we have chosen pipes that have two groups of column slenderness (not intentionally). The column slenderness ratio ranging from 95 – 102 and is determined by Young's modulus and yield stress.

$$C_C = \pi \sqrt{\frac{2E}{\sigma_y}}$$

Table 20 All slenderness ratio results from experiments

27,3x2,8mm pipe dimension						
Slenderness Ratio						
Pipe length [mm]	**284**	**334**	**384**	**584**	**834**	**SR2**
1	32,57	38,31	44,04	66,98	95,66	8,84

33,9x3,2mm pipe dimensions						
Slenderness Ratio						
Pipe length [mm]	**284**	**334**	**384**	**584**	**834**	SR2
1	26,02	30,61	35,19	53,51	76,42	10,55

48,5mmx3,9mm pipe dimensions						
Slenderness Ratio						
Pipe length [mm]	**284**	**334**	**384**	**584**	**834**	**SR2**
1	17,94	21,10	24,26	36,90	52,69	11,53

60,5mmx3,7mmmm pipe dimensions						
Slenderness Ratio						
Pipe length [mm]	**332**	**382**	**432**	**632**	**882**	**SR2**
1	16,50	18,98	21,47	31,40	43,83	13,38

89,1mmx3,0mm pipe Dimensions						
Slenderness Ratio						
Pipe length [mm]	**332**	**382**	**432**	**632**	**882**	**SR2**
1	10,90	12,54	14,18	20,75	28,96	18,40

Table 21 Slenderness ratio 1 = Slenderness ratio 2

Slenderness ratio 1 = Slenderness ratio 2					
Pipe OD x t	**27,3 x 2,8**	**33,9 x 3,2**	**48,5 x 3,9**	**60,5 x 3,7**	**89,1 x 3,0**
Length [mm]	77,09	115,17	182,52	269,3	560,33

From table 20, we can see all the slenderness ratio 1 for each unsupported length compared to the SR2, and in table 21, we can see the length where slenderness ratio 1 is equal to slenderness ratio 2 for each pipe size.

4.2.1 27,3 mm x 2,8 mm tubing compression test

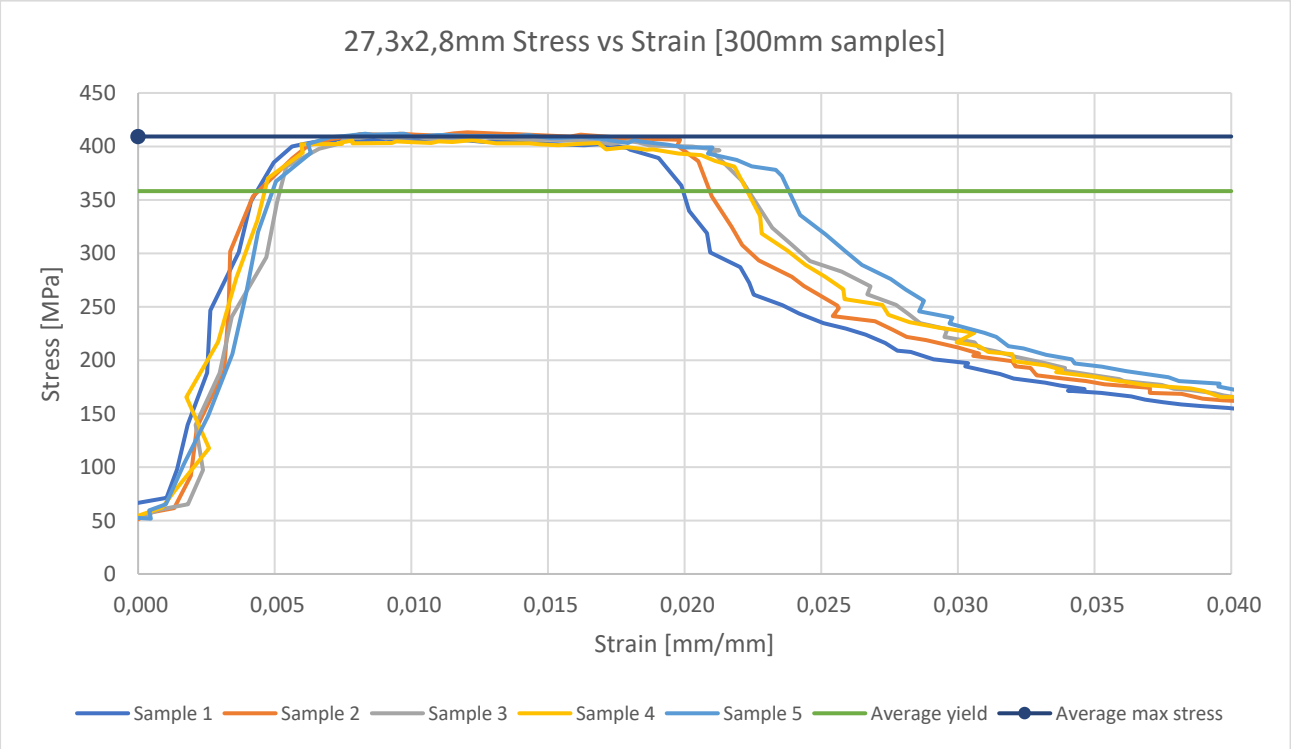

Figure 52, 27,3 mm x 2,8 mm Stress-Strain with unsupported length of 384 mm

An example of stress-strain graph gained from the 334 mm unsupported length, where five different pipe samples with the same length was compressed. As we can see from the graph, there is a great consistency. The average ultimate strength from all the different lengths are shown as the dark blue line, and as well as the average yield stress from all compression test is showed as the green line. All results from all the 16 compression experiments conducted on this pipe is shown in the table 22 below, where the total average values is found in the table.

The ultimate tensile strength is varying with different unsupported lengths. This is due to strain hardening. As we can see below, between the largest unsupported length (834mm) and the smallest (284 mm), we can

see the difference in ultimate strength. Also, two images from these experiments are shown for these two lengths captured from the video recordings.

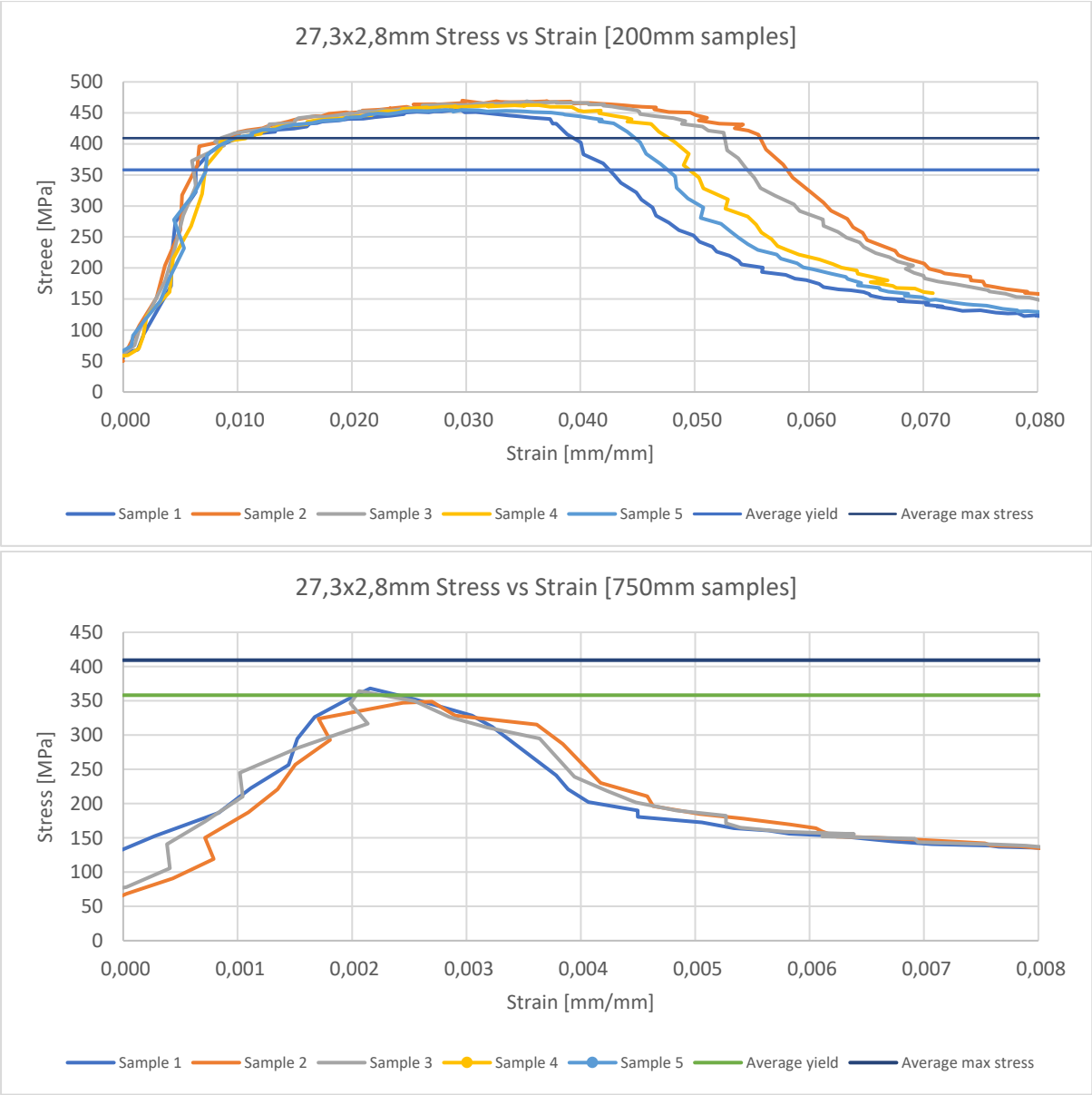

Figure 53, 27,3 mm x 2,8 mm graphs comparison for smallest to longest unsupported lengths

The smallest unsupported lengths (284 mm) is showing strain hardening, increasing the ultimate strength of the material, and the largest unsupported length (834 mm) is not reaching the same ultimate tensile strength, and start bending at yield point. For the smallest length, the pipe is yielding creating strain hardening until it reaches its ultimate strength, then the pipe starts to bend, and end constrains starts to rotate.

Figure 54 Capture from video; 27,3 mm x 2,8 mm graph comparison of smallest to longest unsupported lengths

Results given from these experiments are shown in the table below. As we can see from the results, the buckling force is some greater than the yield force for the smaller lengths, but closer to yield point when smaller unsupported lengths. Also, the column to the right is showing when the end constrains starts to rotate. These starts rotating when the maximum force is applied.

Table 22 All compression result 27,3 mm x 2,8 mm pipe

27,3x2,8x200mm experiments						
Sample	**Yield [kN]**	**Mpa**	**Max Force [kN]**	**Max Stress [Mpa]**	**Pb video [kN]**	**Pb video [kN] End rotation**
nr1	77,67	360,40	98,02	454,81		98,02
nr2	78,87	365,98	101,25	469,83	89,40	101,25
nr3	80,35	372,85	101,07	468,97	89,97	101,07
nr4	78,32	363,40	99,68	462,53	78,32	99,68
nr5	76,47	354,83	98,02	454,81	76,47	98,02
Average	78,34	363,49	99,61	462,19	83,54	99,61

27,3x2,8x250mm experiments						
Sample	**Yield [kN]**	**Mpa**	**Max Force [kN]**	**Max Stress [Mpa]**	**Pb video [kN]**	**Pb video [kN] End rotation**
nr1	82,67	383,57	92,38	428,63	82,67	92,38
nr2	80,55	373,77	91,82	426,06	80,35	91,82
nr3	77,95	361,69	91,27	423,48	77,95	91,27
nr4	81,93	380,14	92,65	429,92	81,93	92,65
nr5	80,45	373,28	92,84	430,78	85,07	92,84
Average	80,71	374,49	92,19	427,77	81,59	92,19

27,3x2,8x300mm Experiments						
Sample	**Yield [kN]**	**Mpa**	**Max Force [kN]**	**Max Stress [Mpa]**	**Pb video [kN]**	**Pb video [kN] End rotation**
nr1	82,94	384,86	87,75	407,18	82,94	87,75
nr2	76,10	353,11	89,05	413,18	83,78	89,05
nr3	79,80	370,27	88,31	409,75	82,11	88,31
nr4	82,11	381,00	87,47	405,89	79,80	87,47
nr5	79,15	367,27	88,77	411,90	84,89	88,77
Average	80,02	371,30	88,27	409,58	82,70	88,27

27,3x2,8x500mm Experiments						
Sample	**Yield [kN]**	**Mpa**	**Max Force [kN]**	**Max Stress [Mpa]**	**Pb video [kN]**	**Pb video [kN] End rotation**
nr1	72,90	338,26	82,57	383,15	73,00	82,57
nr2	75,63	350,93	82,30	381,86	66,85	82,30
nr3	77,39	359,10	85,07	394,73	60,38	85,07
Average	75,31	349,43	83,31	386,58	66,74	83,31

27,3x2,8x750mm Experiments						
Sample	**Yield [kN]**	**Mpa**	**Max Force [kN]**	**Max Stress [Mpa]**	**Pb video [kN]**	**Pb video [kN] End rotation**
nr1	70,36	326,48	79,34	368,13	55,29	79,34
nr2	69,81	323,92	75,17	348,82	55,38	75,17
nr3	74,61	346,20	78,50	364,26	52,80	78,50
Average	71,59	332,20	77,67	360,40	54,49	77,67

27,3mmx2,8xmm Averages						
Sample	**Yield [kN]**	**Mpa**	**Max Force [kN]**	**Max Stress [Mpa]**	**Pb video [kN]**	**Pb video [kN] End rotation**
Total average	77,19	358,18	88,21	409,30	73,81	88,21

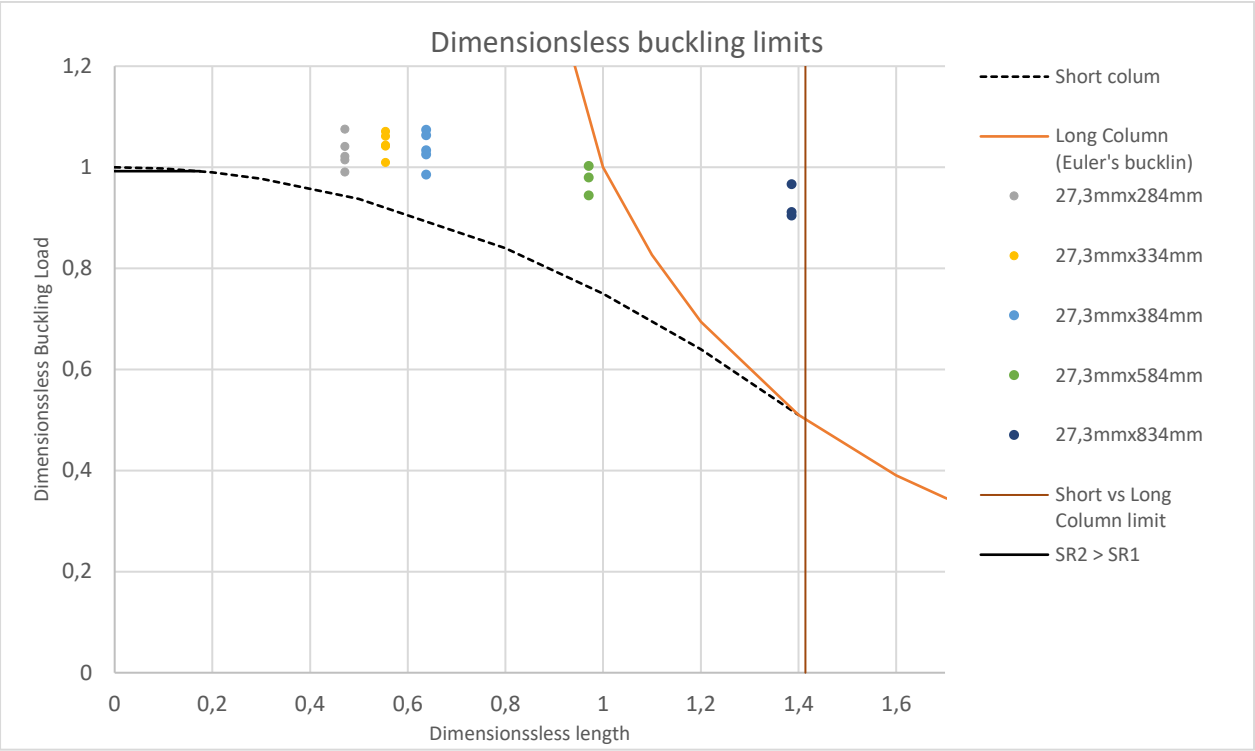

Figure 55, 27,3 mm x 2,8 mm Dimensionless buckling load vs length

In graph above, showing dimensionless buckling vs dimensionless length (Chapter 2.1.8), we can see that the dimensionless buckling load are greater than the Franklin/Abel short column critical buckling loads. Each experiment (five for each lengths) is shown. To the right of the limit is the Euler's long column theoretical critical buckling. Slenderness ratio 2 greater than slenderness ratio 1 are indicated as a straight line in the graph above. As we can see, the real critical buckling load are generally higher than the theoretically critically buckling loads.

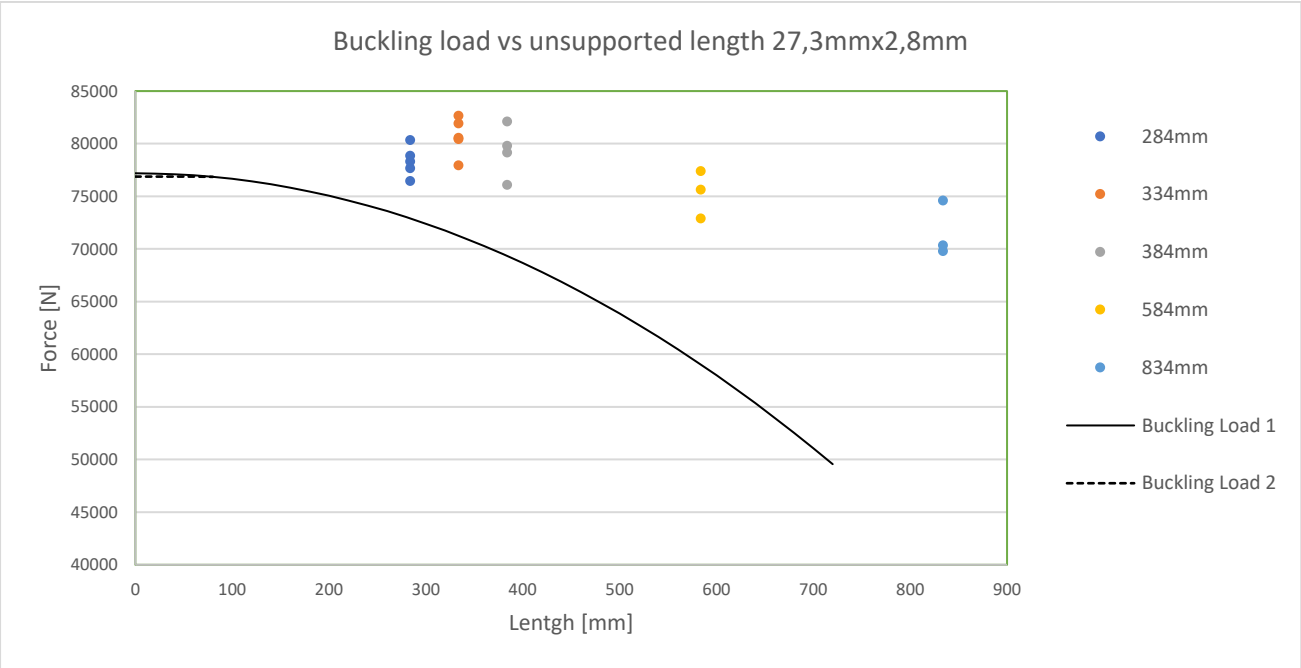

Figure 56, 27,3 mm x 2,8 mm Buckling Load vs Unsupported lengths

Above graph represents the theoretical buckling load for slenderness ratio 1, show an Buckling Load 1, and the buckling load for slenderness ratio 2, shown as Buckling Load 2. (Note that buckling load 1 and buckling load 2 is equal to buckling load 1 from Chapter 2.1.6. As we can see, the real values are greater than the theoretical. The dimensions are force [N] on y-axis and unsupported lengths [mm] on x- axis. The different dots represents the different unsupported lengths, where the results is showing the buckling force. The axis is zoomed in to see the different buckling loads for each experiment.

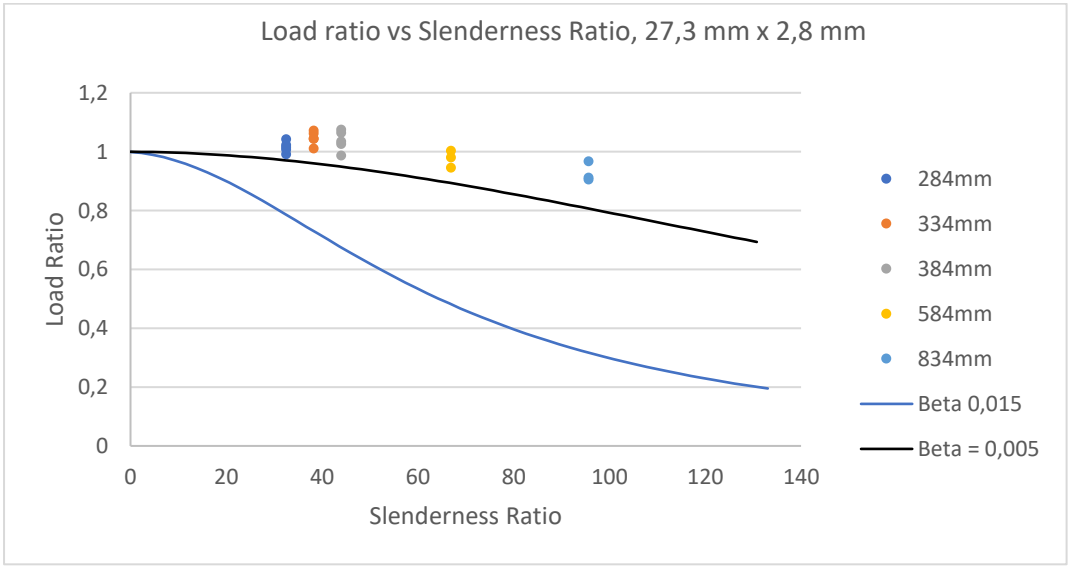

Figure 57 Load ratio vs Slenderness ratio 27,3mm x 2,8 mm

From Newman and Aasen, we have the illustrated overview of the load ratio vs the slenderness ratio (Chapter 2.1.8). Where the beta value in the Gordon-Rankine formula is chosen as to be 0,005, for comparison, the beta value for a straight pipe is shown as 0,015.

4.2.2 33,9 mm x 3,2 mm tubing compression test

Stress-Strain curve is shown in the graph below. Same results as in 27,3mmx2,8mm pipe, where great consistency is shown on all experiments.

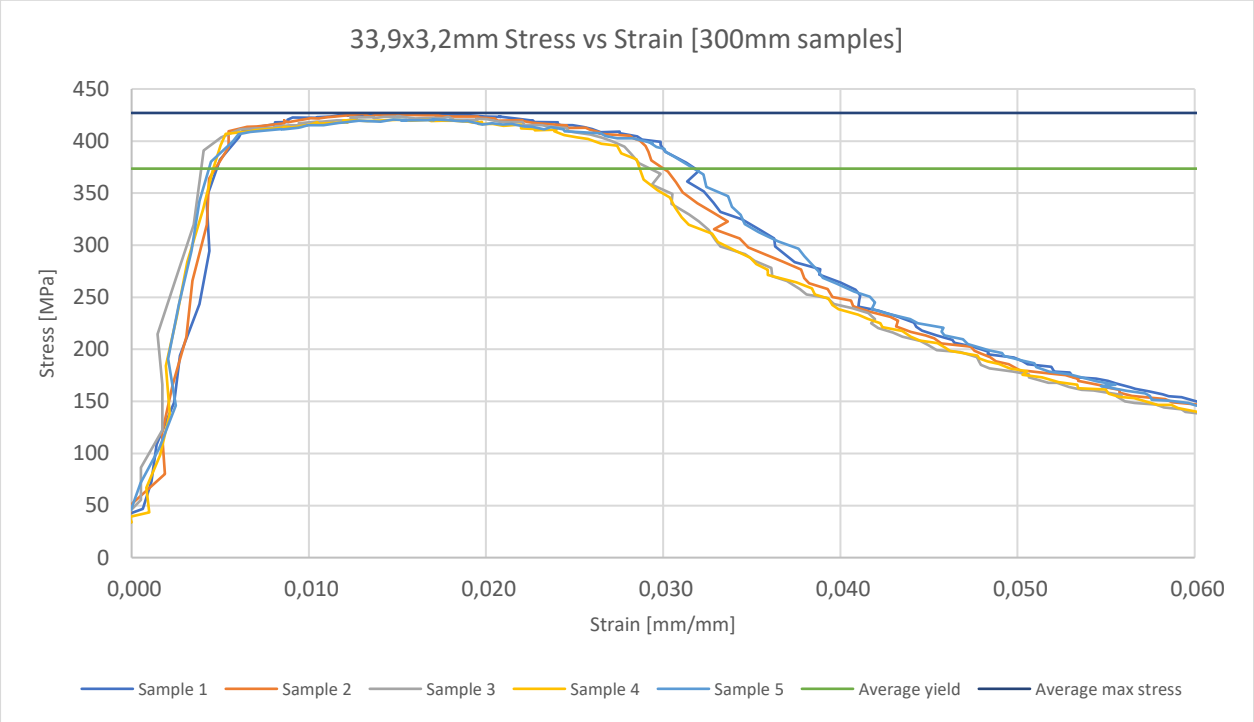

Figure 58, 33,9 mm x 3,2 mm Stress-Strain with unsupported length of 384 mm

The above line (dark blue) is showing the max tensile strength, and the below (green) line is showing the average yield for all samples. Again, we see the effect of strain hardening between the largest and smallest unsupported lengths below. In the Figure 48 below, we can see the deformation of a 250 mm pipe after its been applied compressive loads and a pipe that has not been compressed as a comparison.

Figure 59 Picture of 33,9mm x 3,2mm pipe after the compression test

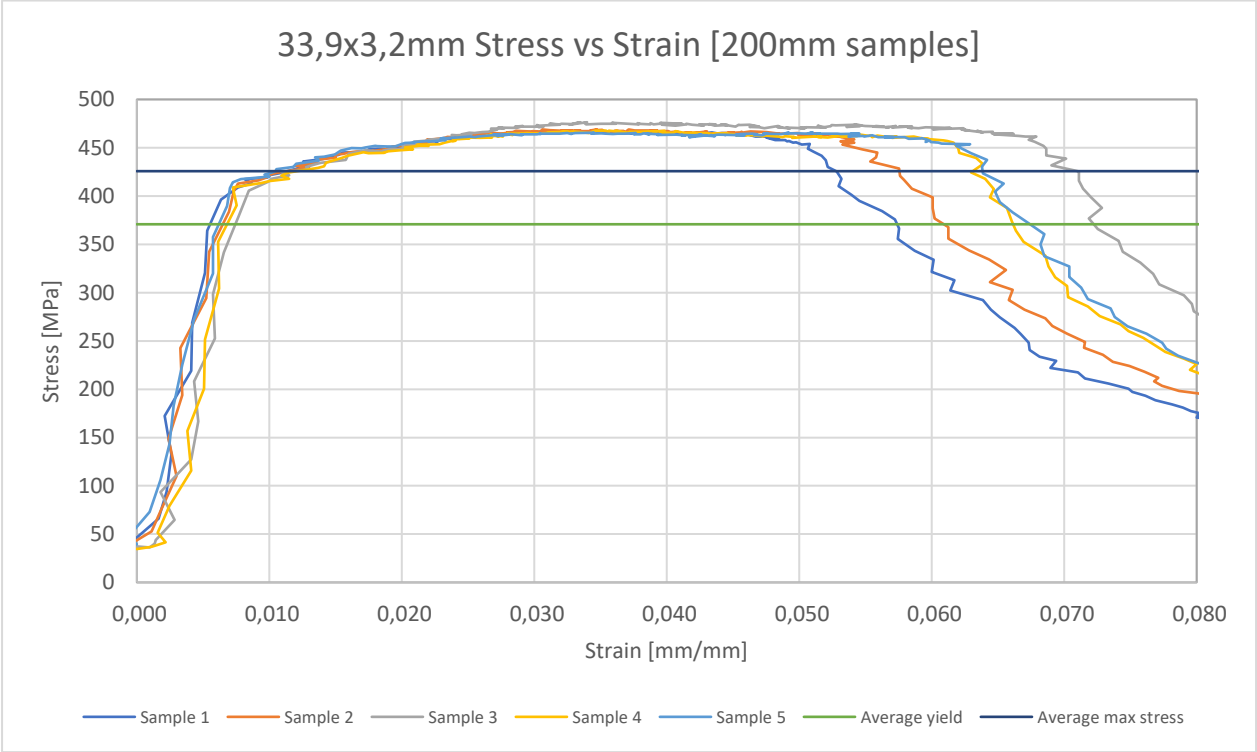

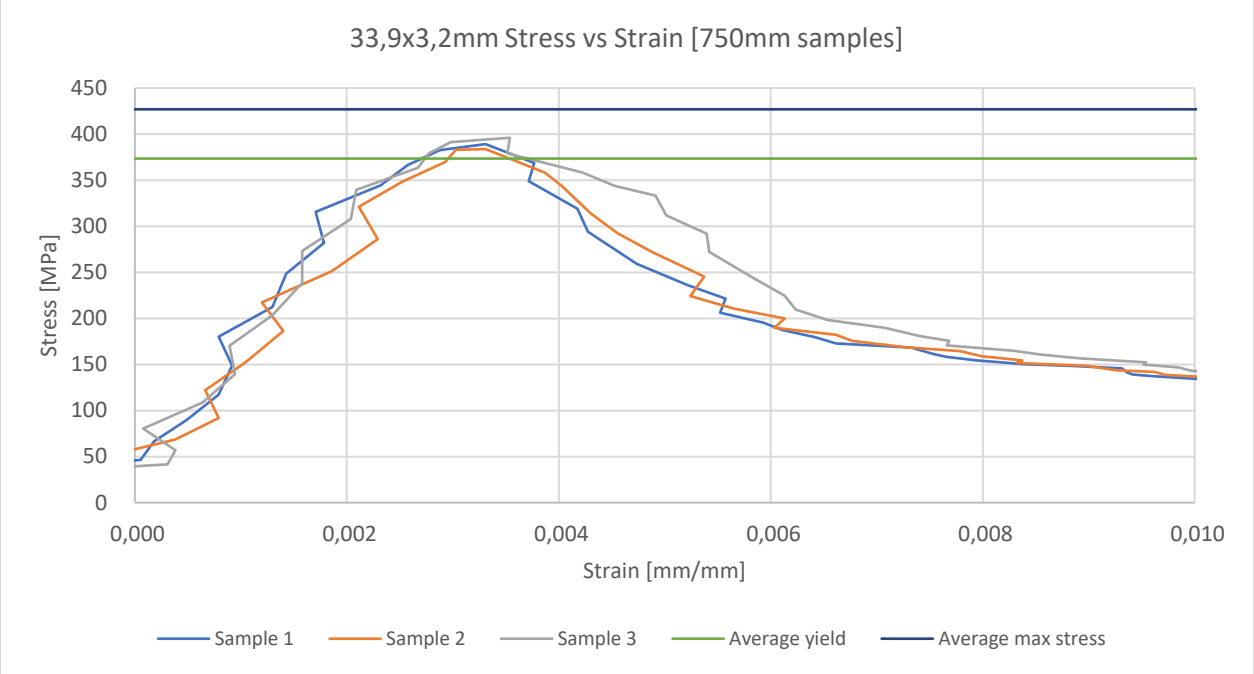

Figure 60, 33,9 mm x 3,2 mm graphs comparison for smallest to longest unsupported lengths

The same effect of unsupported length and strain hardening is present in these results. Below captures is from the video captured for the compressive test of the smallest and longest unsupported lengths.

Figure 61 Capture from video; 33,9 mm x 3,2 mm graph comparison of smallest to longest unsupported lengths

In below table, all the results are present from the 33,9 mm x 3,2 mm pipes for all lengths.

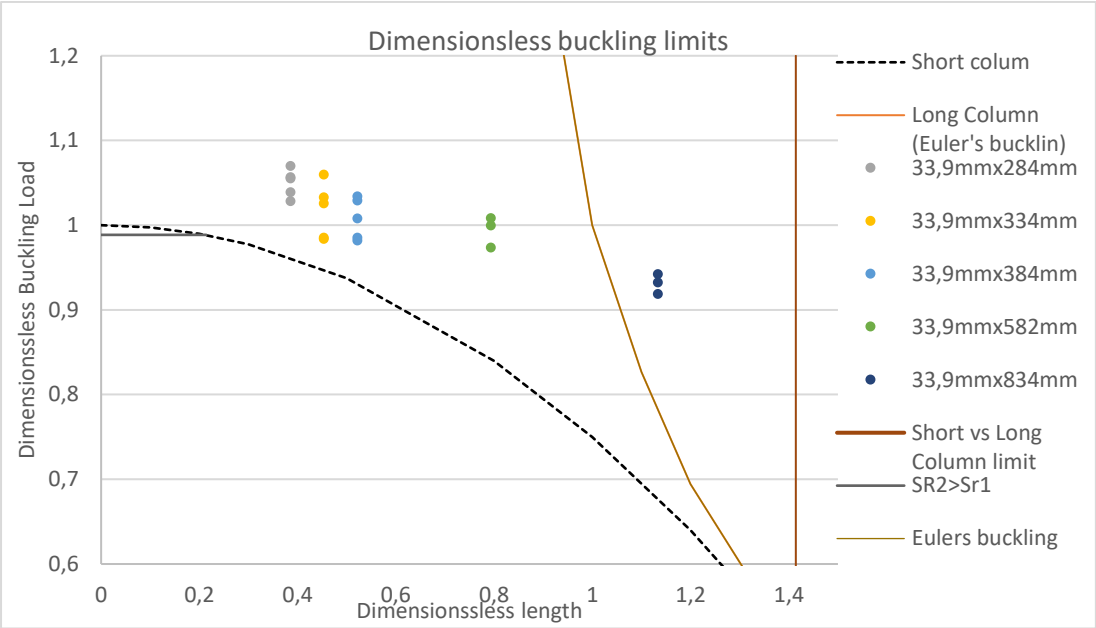

Figure 62, 33,9 mm x 3,2 mm Dimensionless buckling load vs length

Results from 33,9 mm x 3,2 mm pipe in graph above, showing dimensionless buckling vs dimensionless length, we can see that the dimensionless buckling load again are greater than the theoretically short column critical buckling loads.

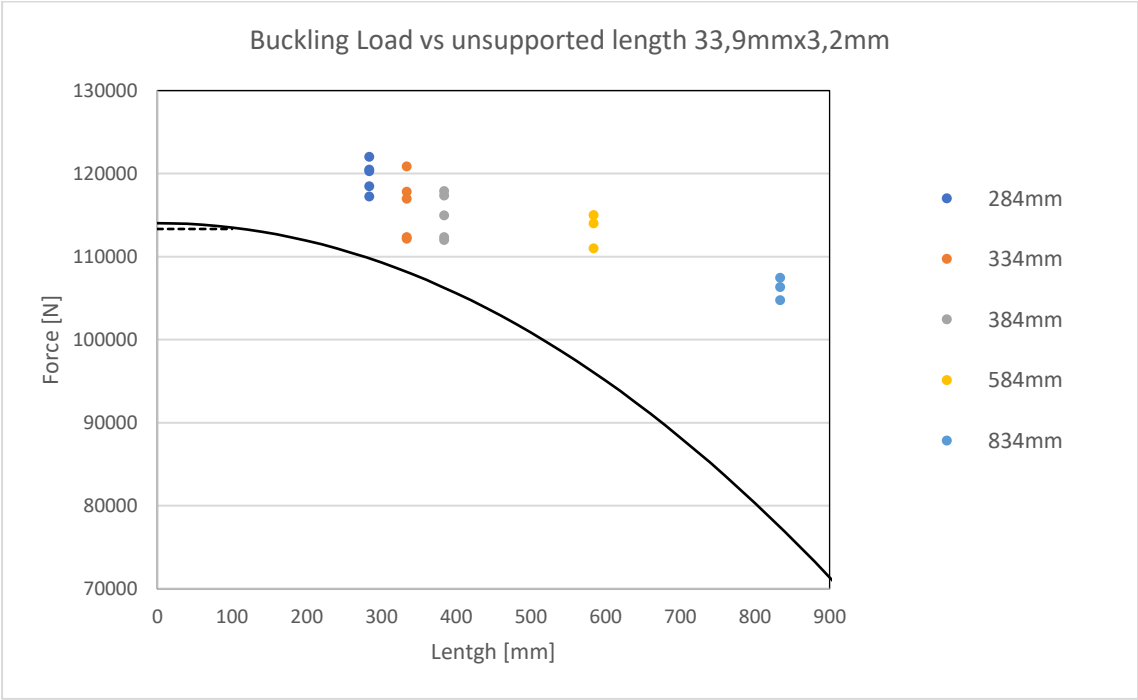

Figure 63, 33,9 mm x 3,2 mm Buckling Load vs Unsupported lengths

Again, the buckling load 1 is for SR1 and Buckling load to for SR2. The result again shows that the real buckling loads are greater than the theoretically critically buckling loads.

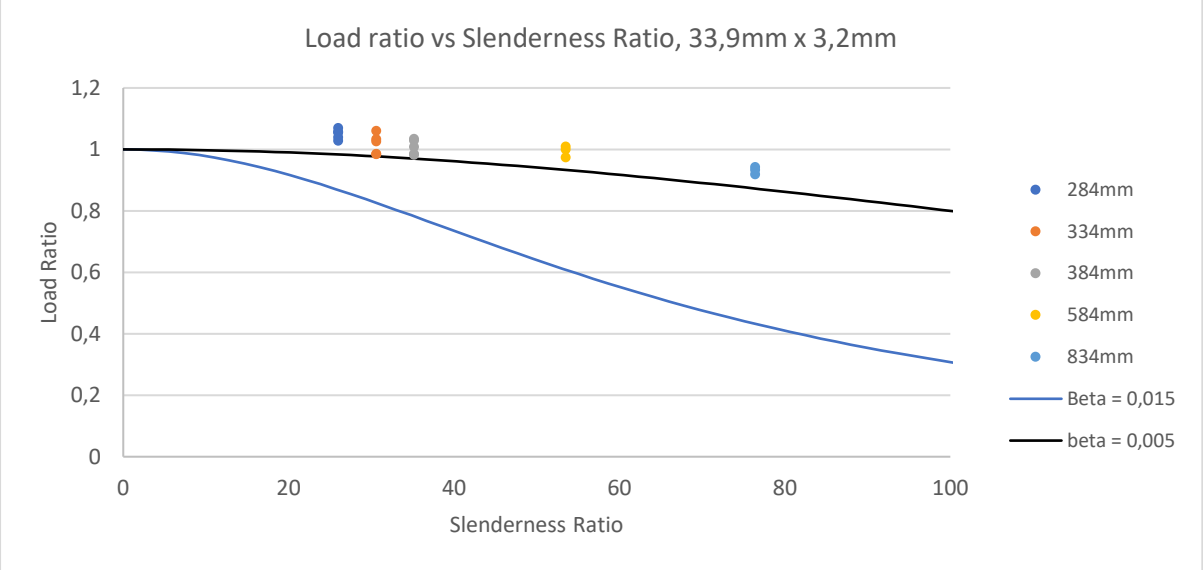

Figure 64 Load ratio vs Slenderness ratio 33,9 mm x 3,2 mm

From Newman and Aasen, we have the illustrated overview of the load ratio vs the slenderness ratio. Where the beta value in Gordon-Rankine formula is chosen experimentally to be 0,005. The value of a straight pipe is 0,015.

All results are placed in the table 23 below.

Table 23 All compression result 33,9 mm x 3,2 mm pipe

33,9x3,2x200mm Experiments						
Sample	**Yield [kN]**	**Mpa**	**Max Force [kN]**	**Max Stress [Mpa]**	**Pb video [kN]**	**Pb video [kN] End rotation**
nr1	122,00	395,30	144,16	467,11	135,84	144,16
nr2	118,45	383,81	144,72	468,91	137,88	144,72
nr3	117,25	379,91	147,03	476,40	138,06	147,03
nr4	120,48	390,37	144,35	467,71	137,78	144,35
nr5	120,30	389,79	143,79	465,91	130,29	143,79
Average	119,70	387,83	144,81	469,21	135,97	144,81

33,9x3,2x250mm Experiments						
Sample	**Yield [kN]**	**Mpa**	**Max Force [kN]**	**Max Stress [Mpa]**	**Pb video [kN]**	**Pb video [kN] End rotation**
nr1	112,35	364,03	137,04	444,04	127,06	137,04
nr2	122,24	396,07	135,84	440,14	122,25	135,84
nr3	120,85	391,57	138,89	450,03	132,97	138,89
nr4	116,97	379,01	137,14	444,34	127,98	137,14
nr5	117,80	381,69	137,14	444,34	126,87	137,14
Average	118,04	382,47	137,21	444,58	127,42	137,21

33,9x3,2x300mm Experiments						
Sample	**Yield [kN]**	**Mpa**	**Max Force [kN]**	**Max Stress [Mpa]**	**Pb video [kN]**	**Pb video [kN] End rotation**
nr1	117,89	381,98	131,59	426,36	127,43	131,59
nr2	112,35	364,03	131,49	426,06	121,59	131,49
nr3	111,98	362,83	130,85	423,96	126,96	130,85
nr4	114,95	372,45	129,74	420,36	122,15	129,74
nr5	117,34	380,20	129,83	420,66	125,48	129,83
Average	114,90	372,30	130,70	423,48	124,72	130,70

33,9x3,2x500mm Experiments						
Sample	**Yield [kN]**	**Mpa**	**Max Force [kN]**	**Max Stress [Mpa]**	**Pb video [kN]**	**Pb video [kN] End rotation**
nr1	115,00	372,61	123,82	401,19	115,15	123,82
nr2	114,00	369,37	124,47	403,28	115,56	124,47
nr3	111,00	359,65	123,63	400,59	118,36	123,63
Average	113,33	367,21	123,97	401,69	116,36	123,97

33,9x3,2x750mm Experiments						
Sample	**Yield [kN]**	**Mpa**	**Max Force [kN]**	**Max Stress [Mpa]**	**Pb video [kN]**	**Pb video [kN] End rotation**
nr1	106,33	344,52	120,12	389,20	97,37	120,12
nr2	107,44	348,12	118,45	383,81	99,13	118,45
nr3	104,76	339,44	122,25	396,09	95,06	122,25
Average	106,18	344,03	120,27	389,70	97,18	120,27

33,9mmx3,2 Averages						
Sample	**Yield [kN]**	**Mpa**	**Max Force [kN]**	**Max Stress [Mpa]**	**Pb video [kN]**	**Pb video [kN] End rotation**
Total ave	114,43	370,77	131,39	425,73	120,33	131,39

4.2.3 48,5 mm x 3,9 mm tubing compression test

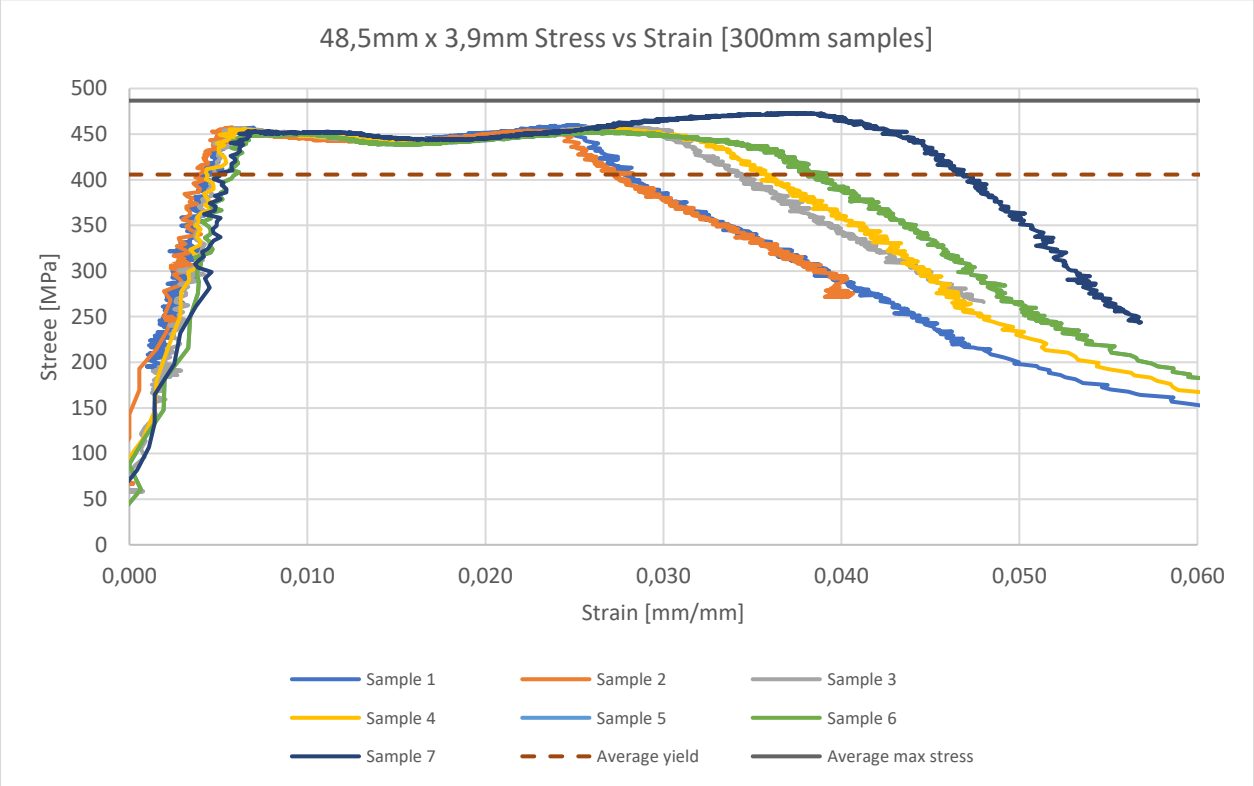

Figure 65, 48,5 mm x 3,9 mm Stress-Strain with unsupported length of 384 mm

Stress – strain graph above in figure 65, and comparison of the longest vs the smallest unsupported lengths is shown in figure 65 below. Here we also see strain hardening effect on the smallest unsupported lengths.

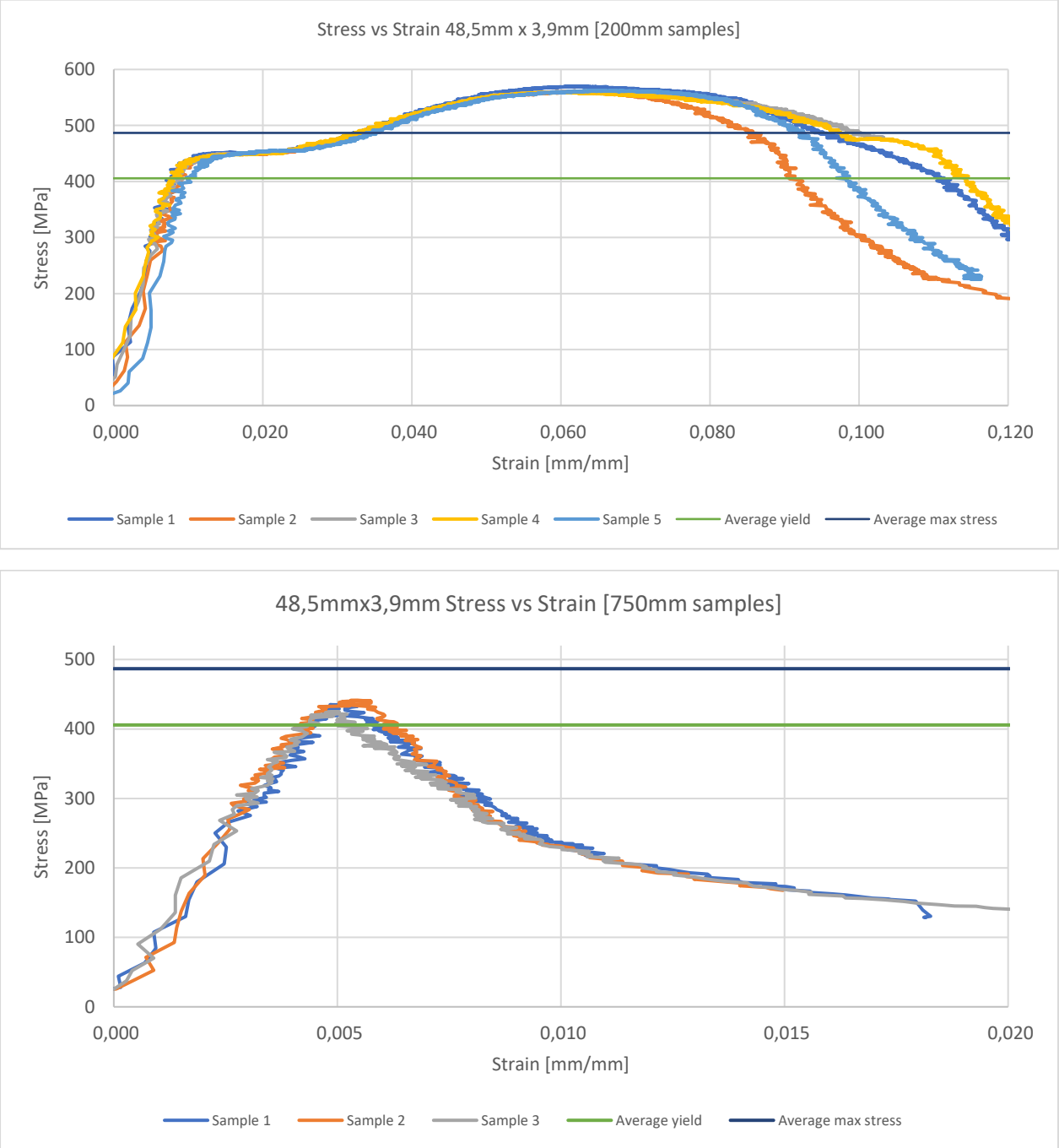

Figure 66, 48,5 mm x 3,9 mm graphs comparison for smallest to longest unsupported lengths

Figure 67 Capture from video; 48,5 mm x 3,9 mm graph comparison of smallest to longest unsupported lengths

Results of all the lengths are provided in the graph below, where we see that the buckling loads are greater than the theoretically.

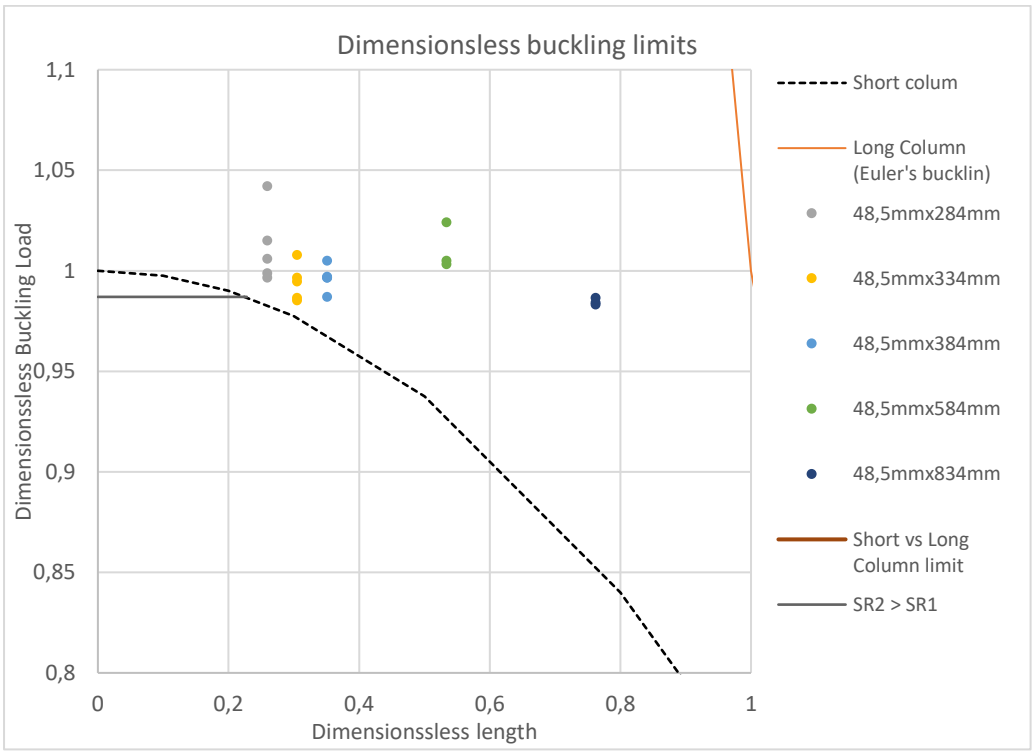

Figure 68, 48,5 mm x 3,9 mm Dimensionless buckling load vs length

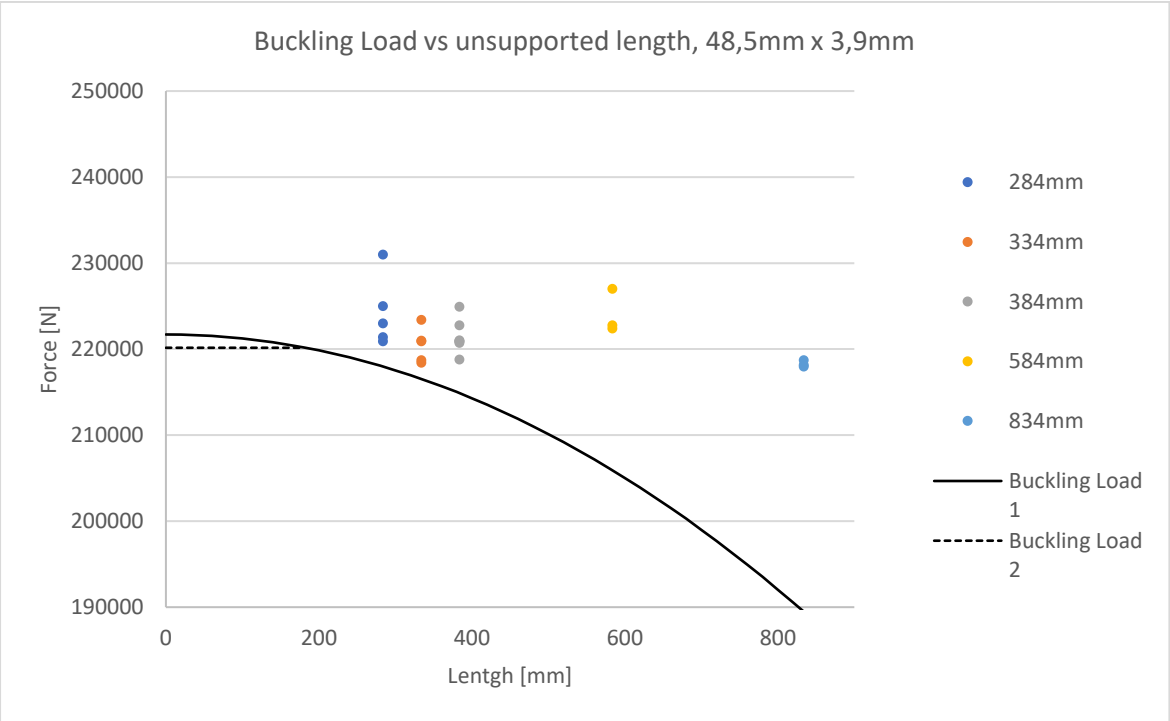

Figure 69, 48,5 mm x 3,9 mm Buckling Load vs Unsupported lengths

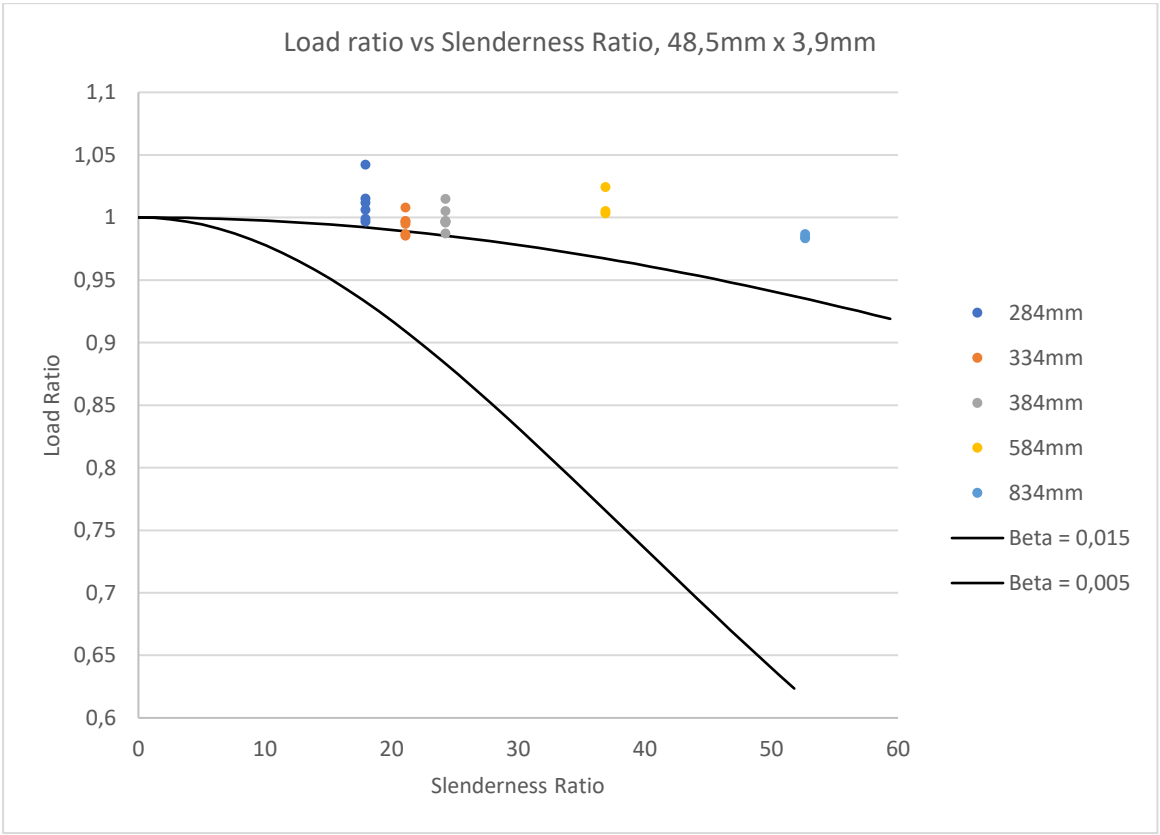

Figure 70 Load ratio vs Slenderness ratio 48,5 mm x 3,9 mm

Table 24 All compression result 48,5 mm x 3,9 mm pipe

48,5x3,9x200mm Experiments						
Sample	**Yield [kN]**	**Mpa**	**Max Force [kN]**	**Max Stress [Mpa]**	**Pb video [kN]**	**Pb video [kN] End rotation**
nr1	221,39	405,14	311,55	570,14	289,73	311,55
nr2	223,00	408,09	305,82	559,64	286,04	305,82
nr3	220,92	404,28	307,30	562,35	287,41	307,30
nr4	231,00	422,73	308,41	564,38	292,77	308,41
nr5	225,00	411,75	307,30	562,35	275,11	307,30
Average	224,26	410,40	308,07	563,77	286,21	308,07

48,5x3,9x250mm Experiments						
Sample	**Yield [kN]**	**Mpa**	**Max Force [kN]**	**Max Stress [Mpa]**	**Pb video [kN]**	**Pb video [kN] End rotation**
nr1	221,00	404,430	295,83	541,37	277,61	295,83
nr2	220,92	404,283	285,19	521,90	244,97	285,19
nr3	223,40	408,822	291,39	533,24	245,61	291,39
nr4	218,40	399,672	285,47	522,41	245,89	285,47
nr5	218,70	400,22	285,19	521,90	243,58	285,19
Average	220,48	403,49	288,61	528,16	251,53	288,61

48,5x3,9x300mm Experiments						
Sample	**Yield [kN]**	**Mpa**	**Max Force [kN]**	**Max Stress [Mpa]**	**Pb video [kN]**	**Pb video [kN] End rotation**
nr1	220,91	404,26	251,35	459,96		
nr2	218,79	400,39	249,87	457,26		
nr3	221,01	404,46	250,79	458,95		
nr4	222,77	407,67	249,68	456,92	no video	no video
nr5	220,92	404,29	247,37	452,69		
nr6	224,92	411,61	261,98	479,43		
nr7	220,74	403,94	258,56	473,16		
Average	221,44	405,23	252,80	462,62	0	0

48,5x3,9x500mm Experiments						
Sample	**Yield [kN]**	**Mpa**	**Max Force [kN]**	**Max Stress [Mpa]**	**Pb video [kN]**	**Pb video [kN] End rotation**
nr1	227,00	415,41	242,65	444,06	240,25	242,65
nr2	222,77	407,67	244,23	446,93	239,05	244,23
nr3	222,40	406,99	243,49	445,58	243,31	243,49
Average	224,06	410,02	243,46	445,52	722,60	243,46

48,5x3,9x750mm Experiments						
Sample	**Yield [kN]**	**Mpa**	**Max Force [kN]**	**Max Stress [Mpa]**	**Pb video [kN]**	**Pb video [kN] End rotation**
nr1	218,14	399,20	237,66	434,92	230,63	237,66
nr2	217,96	398,87	241,17	441,35	240,16	241,17
nr3	218,70	400,22	232,02	424,59	229,89	232,02
Average	218,27	399,43	236,95	433,62	233,56	236,95

48,5mmx3,9mm Averages						
Sample	**Yield [kN]**	**Mpa**	**Max Force [kN]**	**Max Stress [Mpa]**	**Pb video [kN]**	**Pb video [kN] End rotation**
Total averag	221,70	405,71	265,98	486,74	373,48	269,27

4.2.4 60,5 mm x 3,7 mm tubing compression test

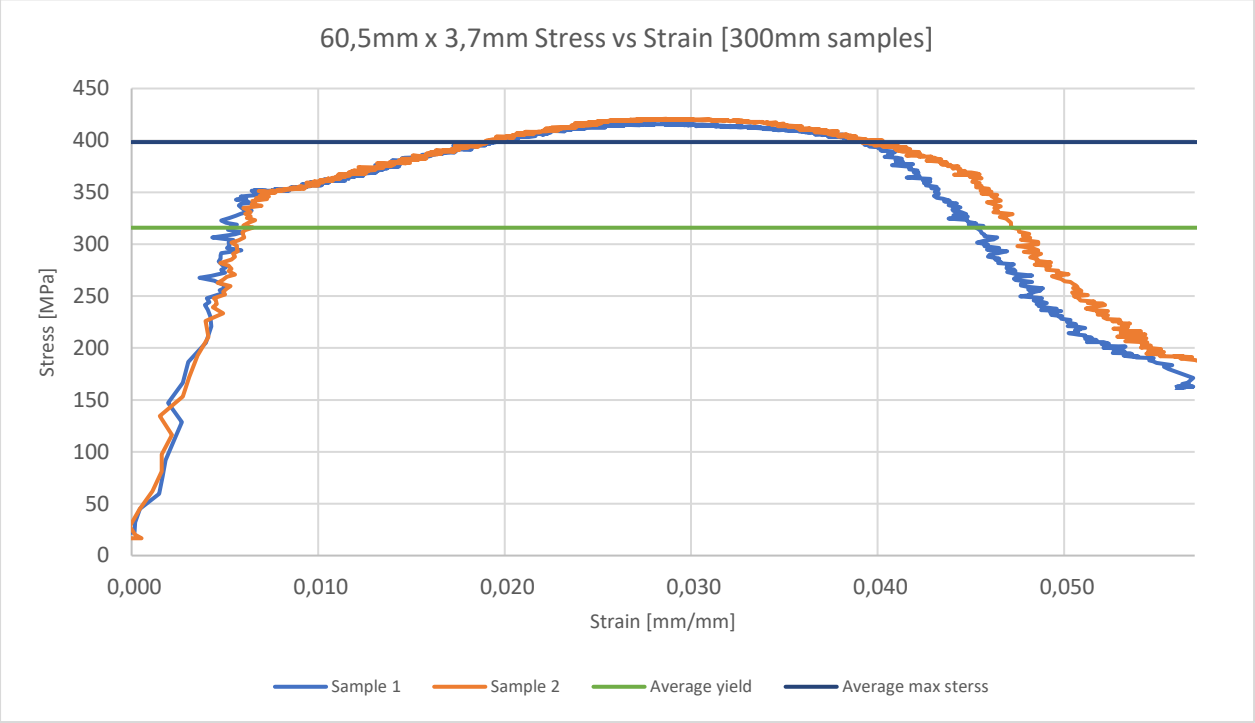

Figure 71, 60,5 mm x 3,7 mm Stress-Strain with unsupported length of 384 mm

During some of these compressive test, the smallest unsupported pipes did not bend. Deformation is shown in the picture below for specimen nr 1 from 200 mm pipe with. This deformation of the pipe is only present for this pipe size. This is deformed in a wavy deformation that is defined as short column.

Figure 72 Deformation of tubing during compression testing

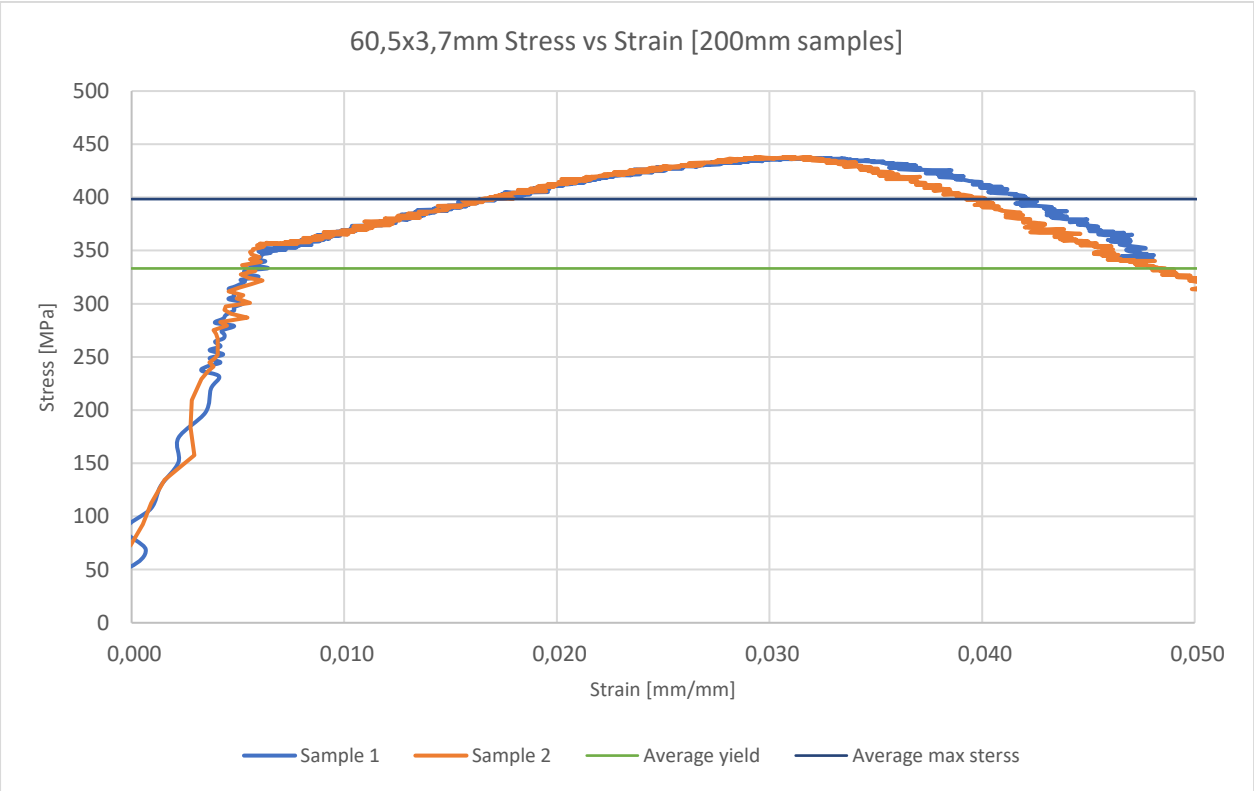

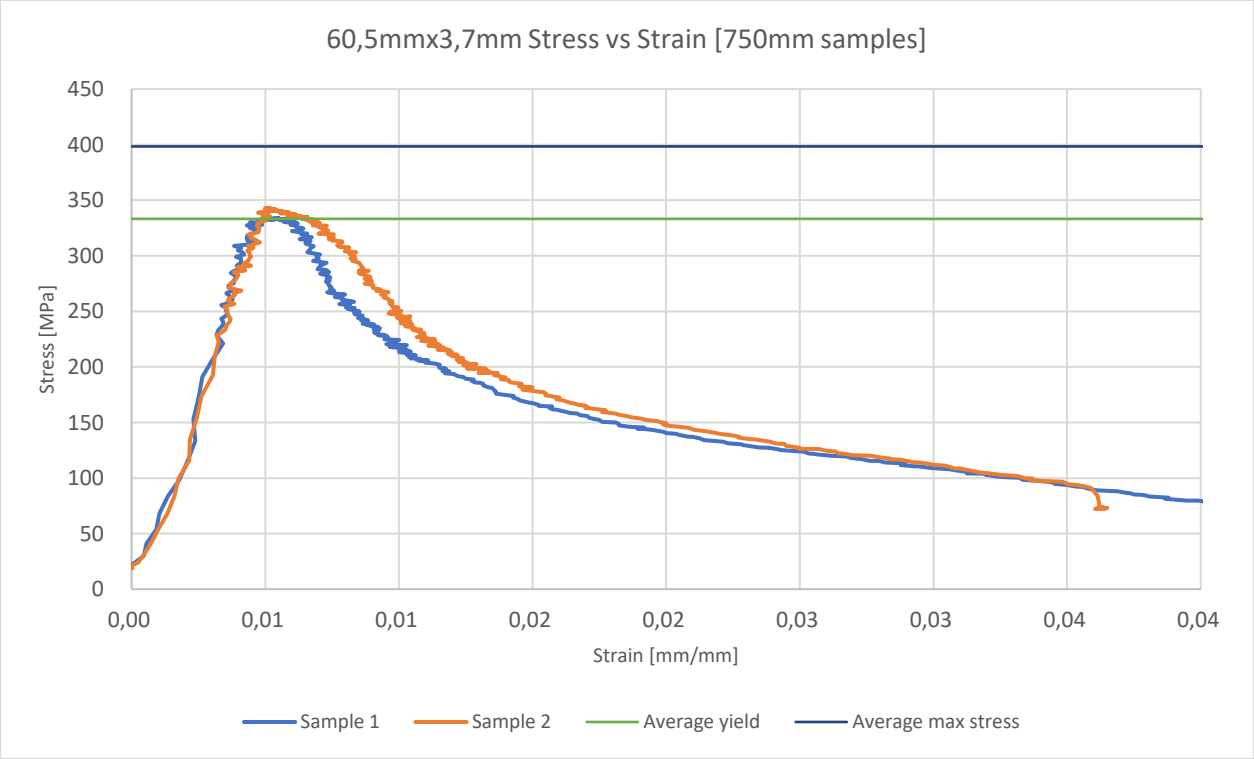

Figure 73, 60,5 mm x 3,7 mm graphs comparison for smallest to longest unsupported lengths

Figure 74 Capture from video; 60,5 mm x 3,7 mm graph comparison of smallest to longest unsupported lengths

In the graph below, all the results are shown in the same graph. Strain hardening may affect the bending results due to plastic deformation.

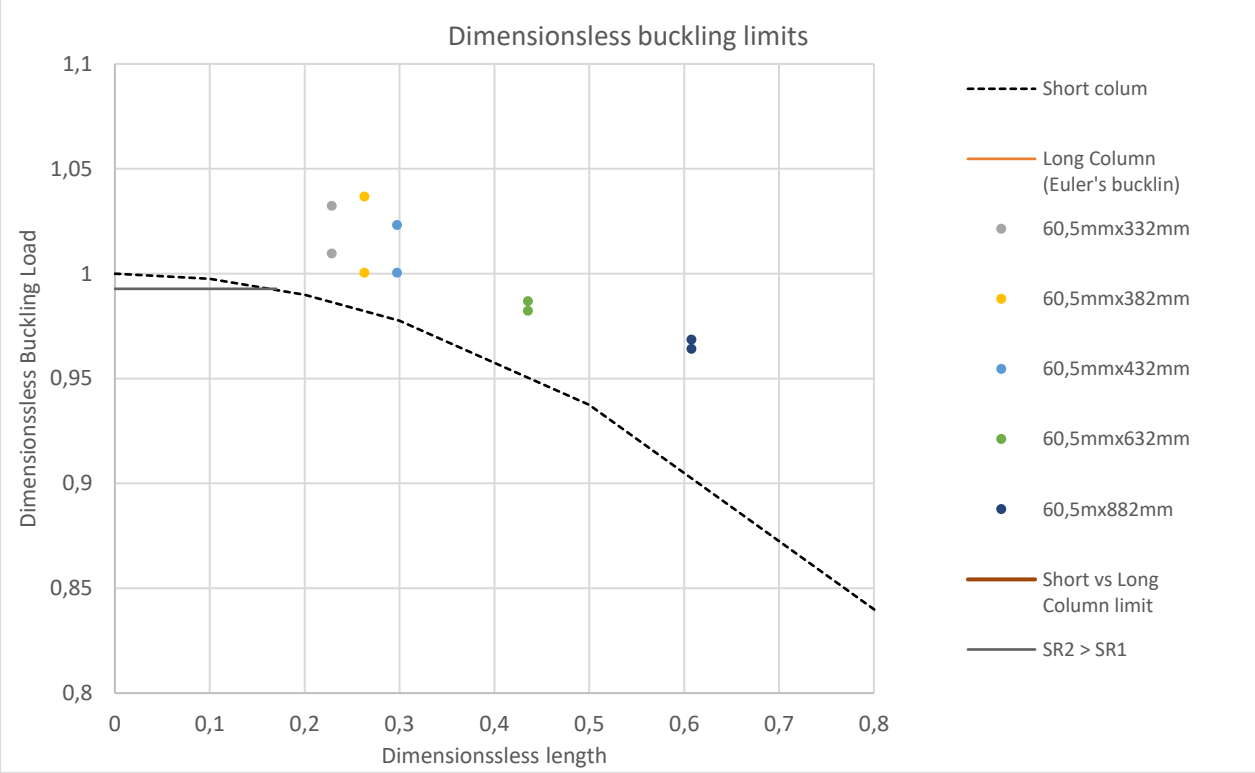

Figure 75, 60,5 mm x 3,7 mm Dimensionless buckling load vs length

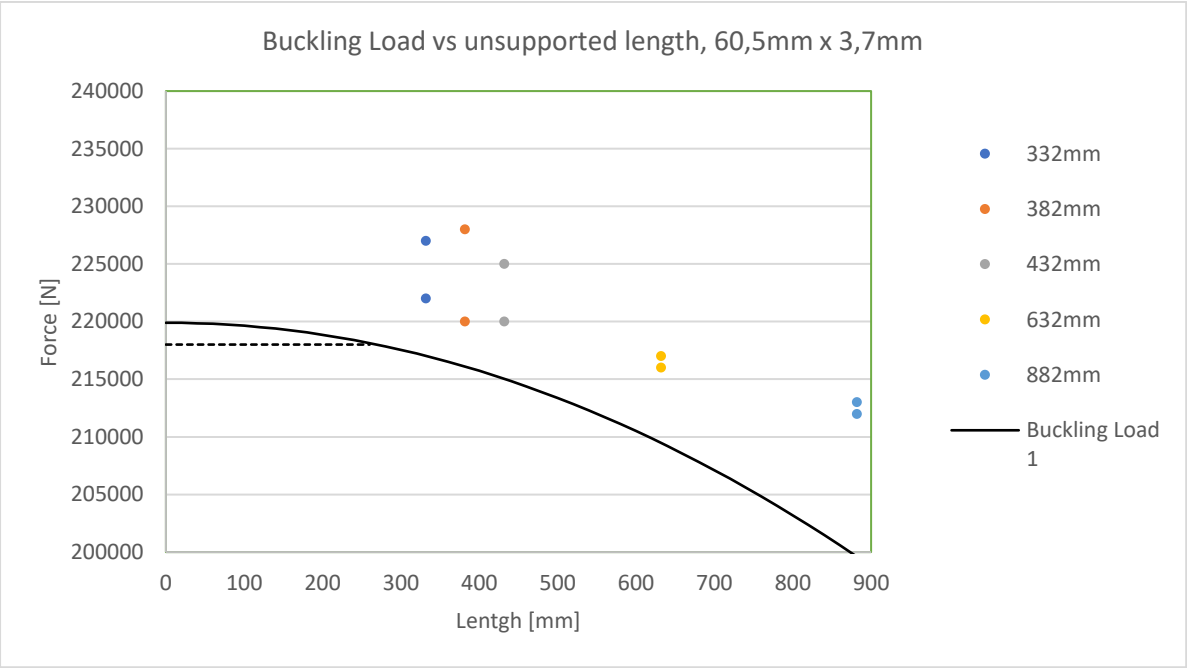

Figure 76, 60,5 mm x 3,7 mm Buckling Load vs Unsupported lengths

Buckling load 1 equals to the use of slenderness ration 1, and buckling load 2 equals to the use of slenderness ratio 2 in the figure 75 above.

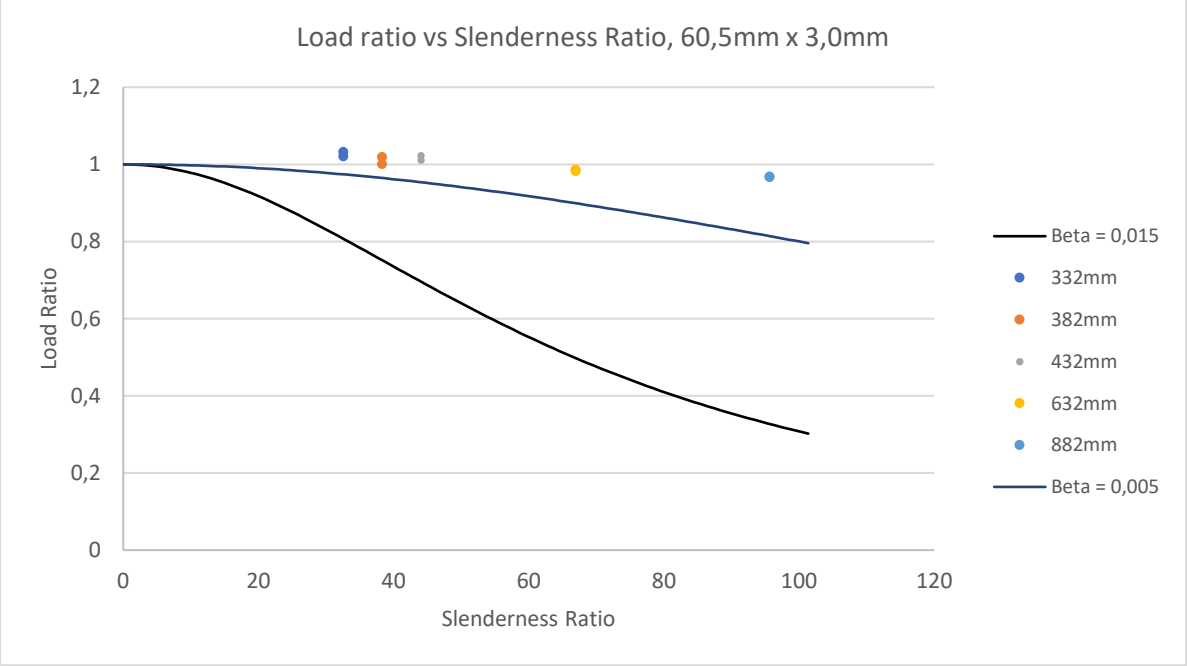

Figure 77 Load ratio vs Slenderness ratio 60,5 mm x 3,7 mm

Table 25 All compression result 60,5 mm x 3,7 mm pipe

60,5x3,7x200mm Experiments						
Sample	**Yield [kN]**	**Mpa**	**Max Force [kN]**	**Max Stress [Mpa]**	**Pb video [kN]**	**Pb video [kN] End rotation**
nr1	222,00	336,24	288,43	436,86	No bending	No rotation
nr2	227,00	343,82	289,17	437,98	No bending	No rotation
Average	224,50	340,03	288,80	437,42	0	0

60,5x3,7x250mm Experiments						
Sample	**Yield [kN]**	**Mpa**	**Max Force [kN]**	**Max Stress [Mpa]**	**Pb video [kN]**	**Pb video [kN] End rotation**
nr1	228	345,33	295,83	448,06	266,328	295,83
nr2	220	333,21	283,81	429,86	No bending	No rotation
Average	224	339,27	289,82	438,96	133,16	289,82

60,5x3,7x300mm Experiments						
Sample	**Yield [kN]**	**Mpa**	**Max Force [kN]**	**Max Stress [Mpa]**	**Pb video [kN]**	**Pb video [kN] End rotation**
nr1	220,00	333,21	275,11	416,69	265,13	275,11
nr2	225,00	340,79	277,89	420,89	266,33	277,89
Average	222,50	337,00	276,50	418,79	265,73	276,50

60,5x3,7x500mm Experiments						
Sample	**Yield [kN]**	**Mpa**	**Max Force [kN]**	**Max Stress [Mpa]**	**Pb video [kN]**	**Pb video [kN] End rotation**
nr1	216,00	327,16	234,98	355,90	227,03	234,98
nr2	217,00	328,67	238,31	360,94	227,58	238,31
Average	216,50	327,91	236,64	358,42	227,30	236,64

60,5x3,7x750mm Experiments						
Sample	**Yield [kN]**	**Mpa**	**Max Force [kN]**	**Max Stress [Mpa]**	**Pb video [kN]**	**Pb video [kN] End rotation**
nr1	212,00	321,10	220,46	333,91	214,34	220,46
nr2	213,00	322,61	226,56	343,15	213,80	226,56
Average	212,50	321,85	223,51	338,53	214,07	223,51

60,5mmx3,7mm Averages						
Sample	**Yield [kN]**	**Mpa**	**Max Force [kN]**	**Max Stress [Mpa]**	**Pb video [kN]**	**Pb video [kN] End rotation**
Total average	220,00	333,21	263,05	398,42	168,05	263,05

4.2.5 89,1 mm x 3,0 mm tubing compression test

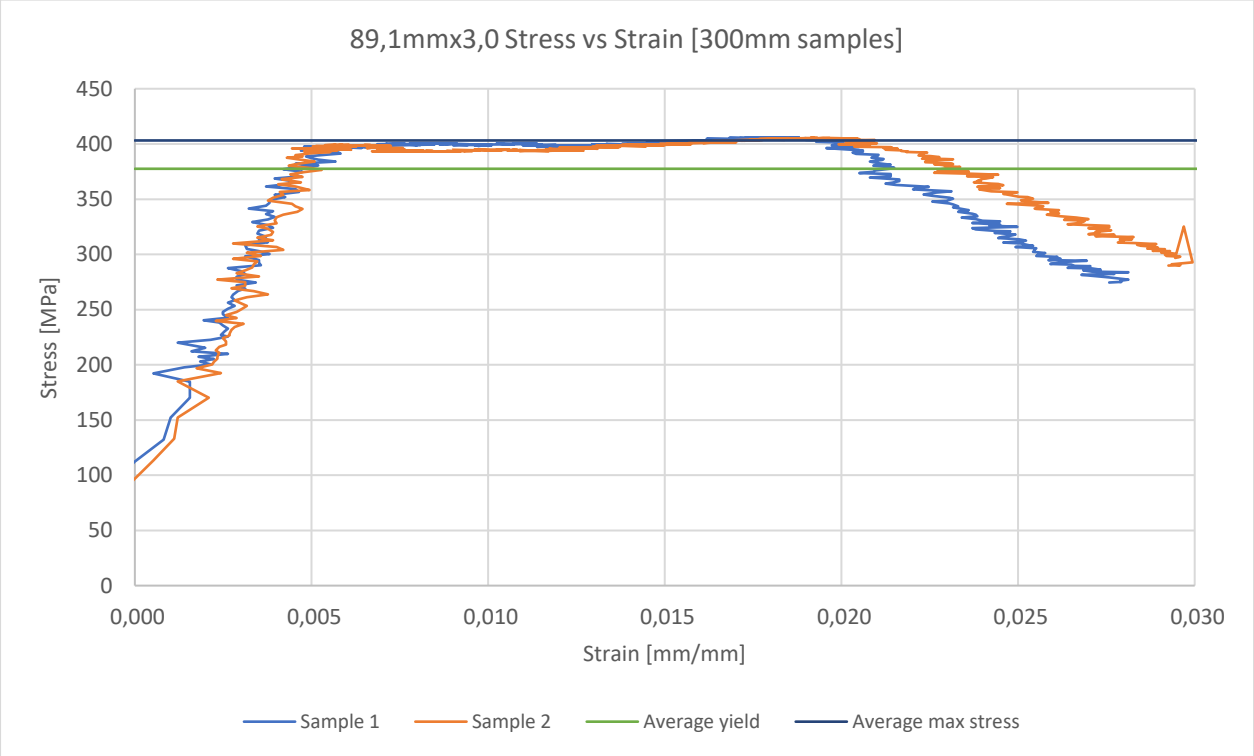

Figure 78, 89,1 mm x 3,0 mm Stress-Strain with unsupported length of 384 mm

Same as the other results, the comparison of the longest and shortest unsupported lengths are shown in the graph above. In table 26 below, all the results are present from the 89,1mm x 3,0 mm pipes for all lengths.

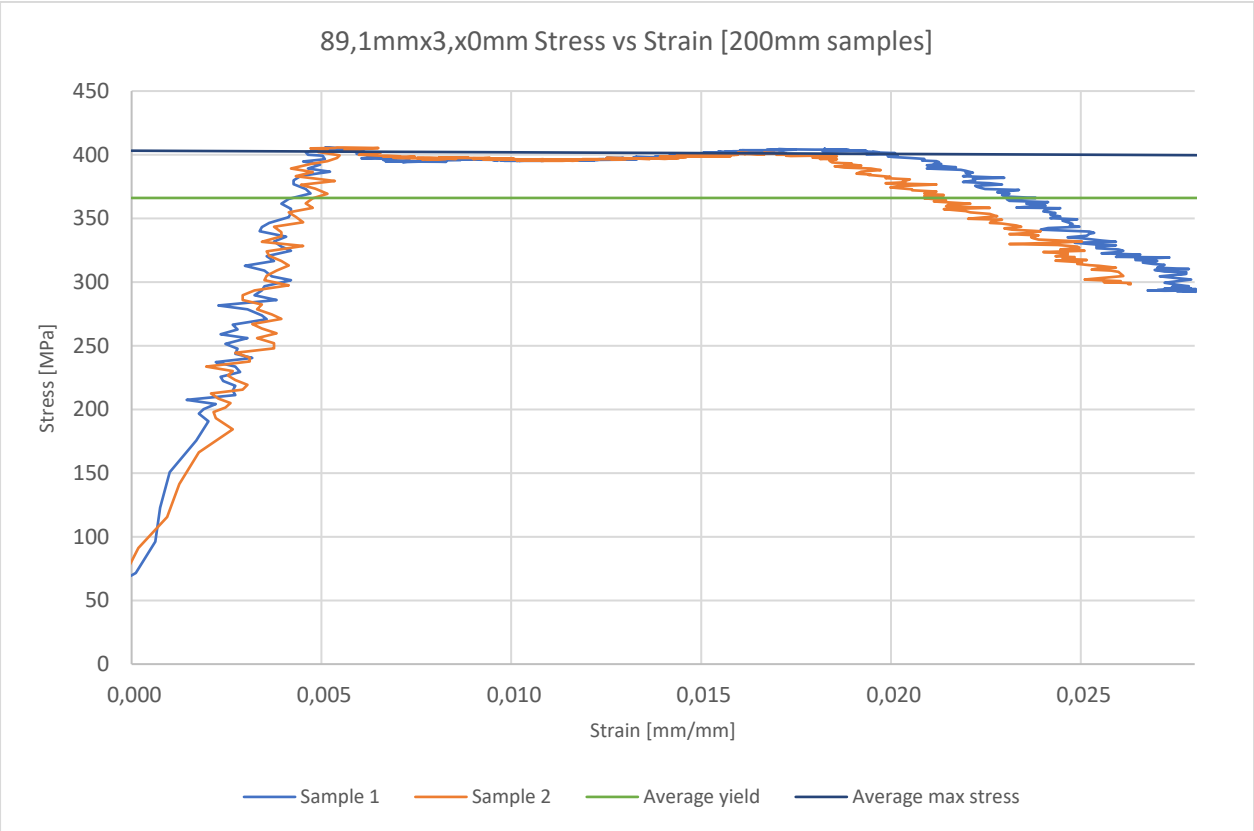

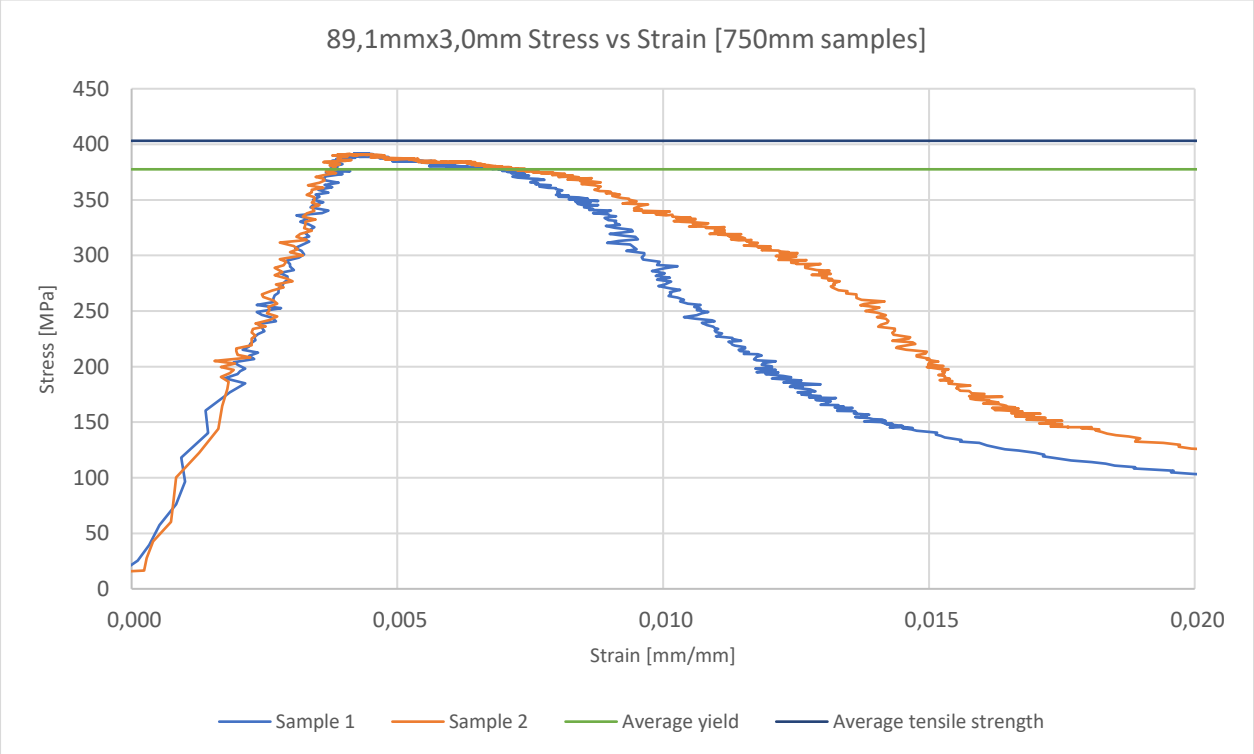

Figure 79, 89,1 mm x 3,0 mm graphs comparison for smallest to longest unsupported lengths

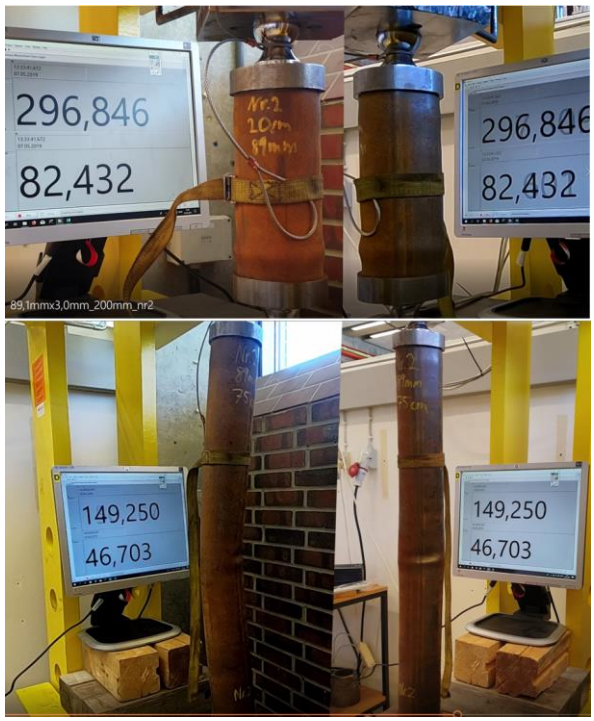

Figure 80 Capture from video; 89,1 mm x 3,0 mm graph comparison of smallest to longest unsupported lengths

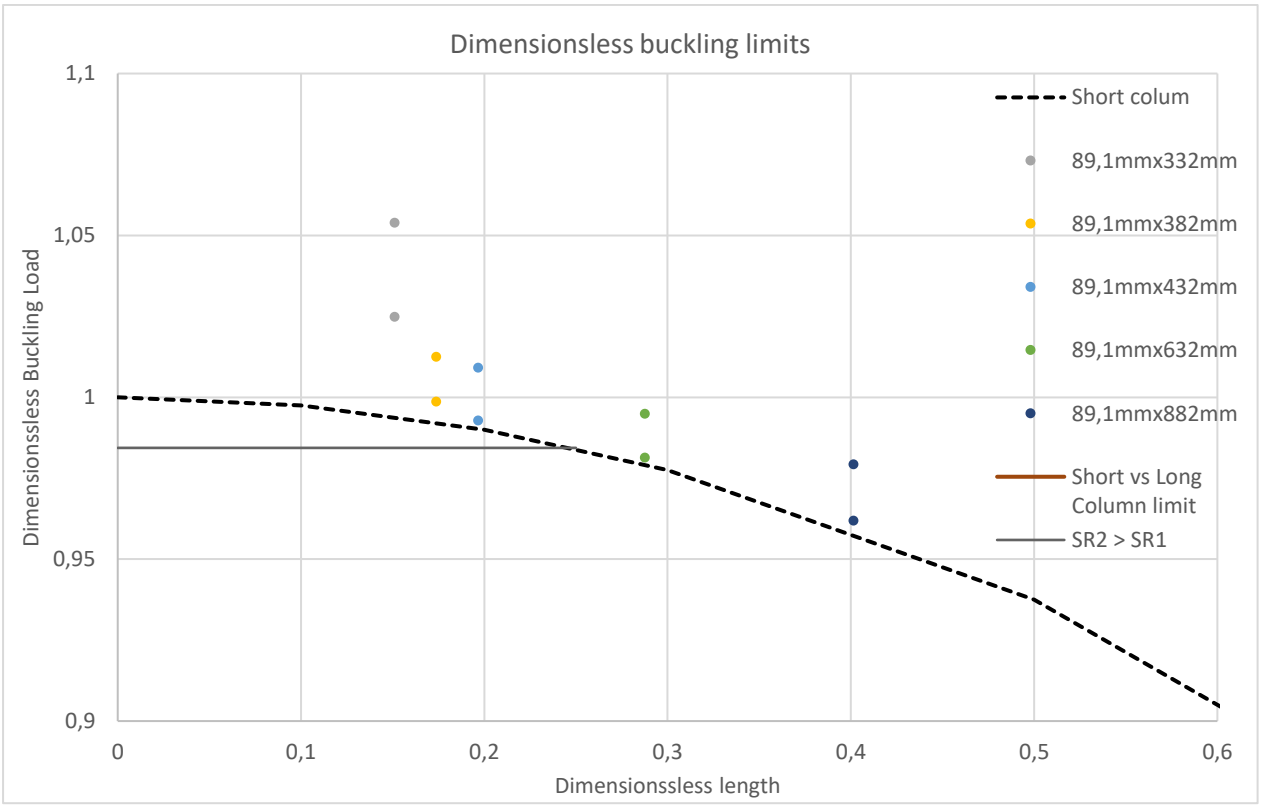

Figure 81, 89,1 mm x 3,0 mm Dimensionless buckling load vs length

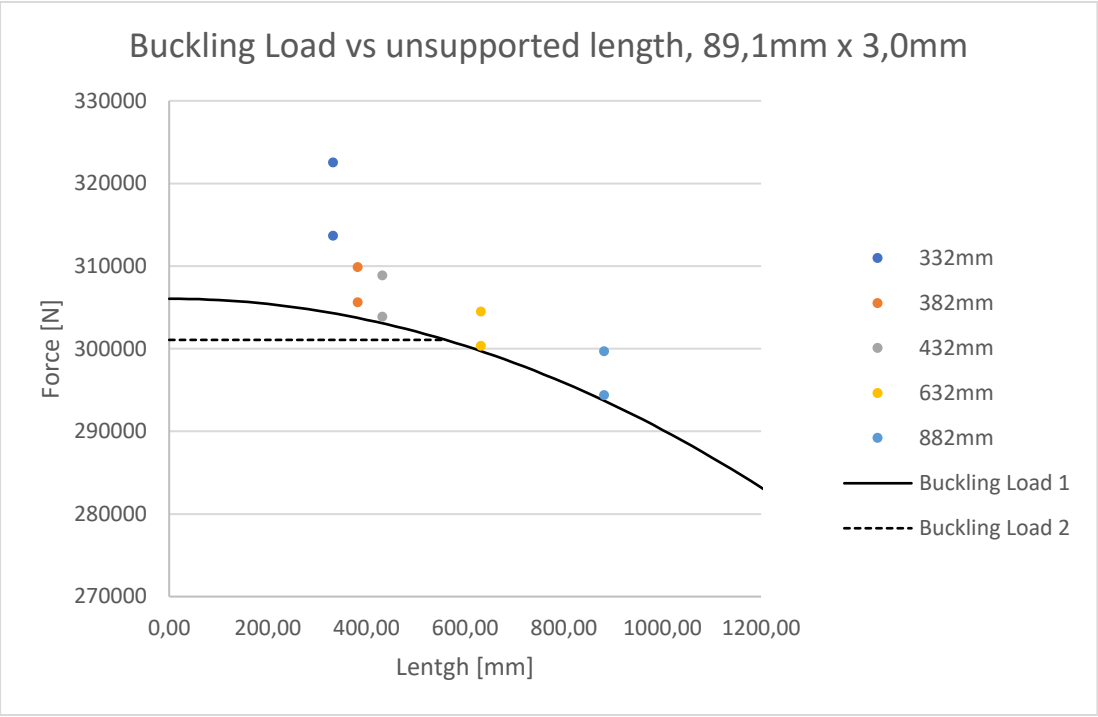

Figure 82, 89,1 mm x 3,0 mm Buckling Load vs Unsupported lengths

With the largest pipe diameter used in these experiments, we can see that the critical theoretical buckling loads are getting more accurate to the experimental results. However, we can see that it is still not crossing over the line where we use slenderness ratio 2 shown as buckling load 2 in the figure 82.

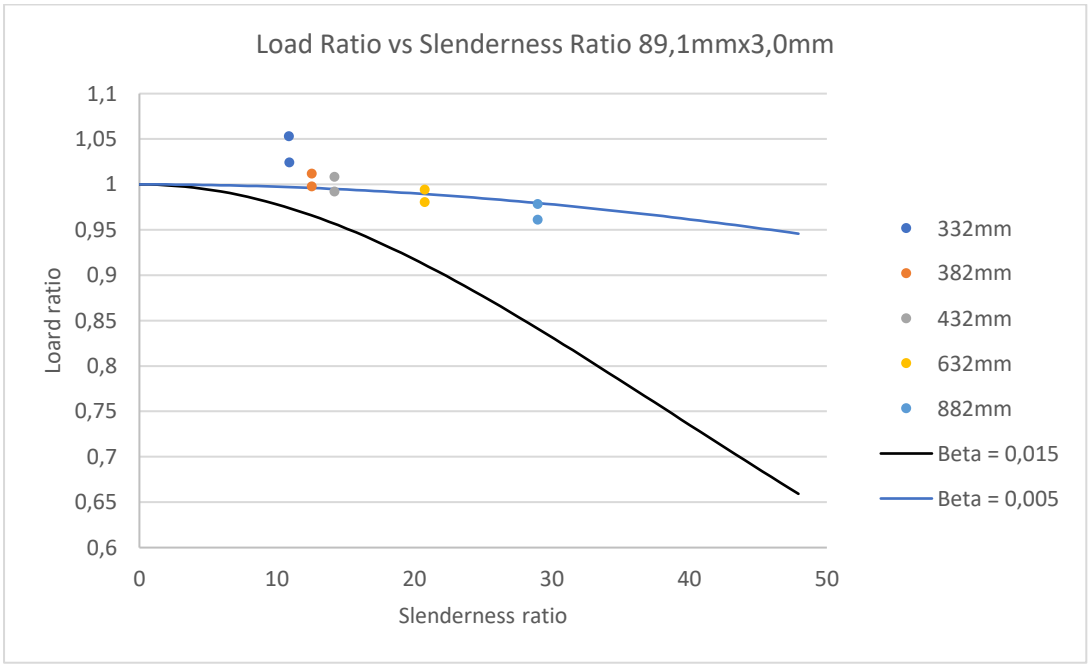

Figure 83 Load ratio vs Slenderness ratio 89,1 mm x 3,0 mm

Table 26 All compression result 89,1 mm x 3,0 mm pipe

89,1x3,0x200mm Experiments						
Sample	**Yield [kN]**	**Mpa**	**Max Force [kN]**	**Max Stress [Mpa]**	**Pb video [kN]**	**Pb video [kN] End rotation**
nr1	313,67	386,54	329,12	405,59	No bending	No rotation
nr2	322,55	397,49	329,21	405,70	No bending	No rotation
Average	318,11	392,01	329,17	405,64	0	0

89,1x3,0x250mm Experiments						
Sample	**Yield [kN]**	**Mpa**	**Max Force [kN]**	**Max Stress [Mpa]**	**Pb video [kN]**	**Pb video [kN] End rotation**
nr1	305,63	376,64	326,62	402,51	No bending	No rotation
nr2	309,88	381,87	326,07	401,82	No bending	No rotation
Average	307,76	379,25	326,35	402,17	0	0

89,1x3,0x300mm Experiments						
Sample	**Yield [kN]**	**Mpa**	**Max Force [kN]**	**Max Stress [Mpa]**	**Pb video [kN]**	**Pb video [kN] End rotation**
nr1	308,86	380,62	329,31	405,81	No bending	No rotation
nr2	303,86	374,45	329,31	405,81	No bending	No rotation
Average	306,36	377,54	329,31	405,81	0	0

89,1x3,0x500mm Experiments						
Sample	**Yield [kN]**	**Mpa**	**Max Force [kN]**	**Max Stress [Mpa]**	**Pb video [kN]**	**Pb video [kN] End rotation**
nr1	304,50	375,24	327,55	403,65	317,839	327,55
nr2	300,36	370,14	327,92	404,10	318,04	327,92
Average	302,43	372,69	327,73	403,88	317,94	327,73

89,1x3,0x750mm Experiments						
Sample	**Yield [kN]**	**Mpa**	**Max Force [kN]**	**Max Stress [Mpa]**	**Pb video [kN]**	**Pb video [kN] End rotation**
nr1	294,40	362,80	323,48	398,63	317,562	323,48
nr2	299,71	369,34	323,02	398,06	314,972	323,02
Average	297,06	366,07	323,25	398,35	316,267	323,25

89,1mmx3,0mm Averages						
Sample	**Yield [kN]**	**Mpa**	**Max Force [kN]**	**Max Stress [Mpa]**	**Pb video [kN]**	**Pb video [kN] End rotation**
Total average	306,34	377,51	327,16	403,17	317,10	325,49

5. Discussion and conclusion

Seen from the results from the Enerpac compression test, we have a great consistency that indicates that the data given in the experiments are reliable. Several pipes with same length and dimension was tested to confirm the reliability. Several assumptions to conduct these experiments was made and are listed below.

- Tubing used in these experiments is material homogeneous.
- No damage to the pipes before testing.
- The tubing thickness (cross-section) is uniform throughout the tubing length.
- The transducer calibrated on the Enerpac in the beginning of the semester's experiment lasted throughout the experimental tests.
- No vibrational impact from the compression machine.
- The welded seam was uniform throughout the pipe, not creating any weak points.
- Tensile test preparation and welding was as accurate as possible, and imperfection was neglected.

Table 27 Nominal tubing values

Actual size [mm]	Nominal OD [Inches]	t [inches]
27,3mm x 2,8 mm	3/4"	0,1102
33,9 mm x 3,2 mm	1"	0,1259
48,5 mm x 3,9 mm	1 1/2"	0,1535
60,5 mm x 3,7 mm	2 3/8"	0,1456
89,1 mm x 3,0 mm	3 1/2"	0,1181

During these experiments, the real unsupported lengths was easy to calculate and measure, but in real operation, the real unsupported lengths may be difficult to calculate. Example during CT injection, there is uncertainty of the location of the upper support due to wear and chain/stripper alignment, (K. Newman & Aasen, 1998).
In the table above, we can see the real nominal values of the pipes. The OD and nominal size do not show the same on small pipe sizes (Franklin & Abel, October, 1988). However, as we can see from table 6, the tubing in this study have some smaller wall thickness on the biggest pipes, while the smallest pipes have more or less the same wall thickness.

Results gained from the tensile test machine could also be discussed. The new method to determine the Young's elasticity modulus used in this research for pipes larger than 34 mm has not been validated experimentally. Therefore, the accuracy of the modulus gained from the three largest pipe sizes can be discussed. Some errors could occur while experimenting using this method, such as the welding may have changed the pipe's properties due to heat, damage or the bushing not being welded as linear as possible to the pipe. So, when the Instron grips the bushing, the pipe may be slightly bent, affecting the results. Also, imperfections in the cut outs will affect the results. However, the elasticity modulus gathered from the Instron experiments are used in calculations of the column slenderness and buckling loads. Based on theoretically elasticity modulus of steel, which is around 200 GPa, the result's gained from Instron varies a bit as we can see in the table below for comparison but are within the range we have from the two smallest pipe sizes that was tested according to the ISO 6892-1 2016.

Table 28 Comparison of Instron, Enerpac and Datasheet values

COMPARISON - All values are average of all experiments performed					
Data	**ENERPAC**				
Pipe	**27,3x2,8mm**	**33,9x3,2mm**	**48,5x3,9mm**	**60,5x3,9mm**	**89,1x3,0mm**
Fy [kN]	77,19	114,03	221,70	219,90	306,34
Fmax [kN]	88,21	131,39	265,98	263,05	327,16
SigmaY [MPa]	358,18	369,46	405,71	333,06	377,51
SigmaMax [MPa]	409,30	425,73	486,74	398,42	403,17
Data	**INSTRON**				
Pipe	**27,3x2,8mm**	**33,9x3,2mm**	**48,5x3,9mm**	**60,5x3,9mm**	**89,1x3,0mm**
Fy [kN]	76,91	115,27	201,80	208,57	274,60
Fmax [kN]	86,12	131,77	264,21	237,95	158,48
SigmaY [MPa]	356,85	373,50	369,30	315,90	338,40
SigmaMax [MPa]	399,60	426,97	483,50	360,40	195,30
E-modulus [GPa]	172,85	170,13	196,30	175,50	198,65
Data	**Datasheet**				
Pipe	**27,3x2,8mm**	**33,9x3,2mm**	**48,5x3,9mm**	**60,5x3,9mm**	**89,1x3,0mm**
Fy [kN]	69,40	Not available	142,90	148,63	246,27
Fmax [kN]	89,01		177,46	203,83	280,60
SigmaY [MPa]	322,00		463,00	272,00	373,00
SigmaMax [MPa]	413,00		575,00	373,00	425,00

From table 28 we can see the results from Instron tensile test and Enerpac compression test. For the two smallest pipe sizes, we can see that the results are very similar. These Instron tensile test was conducted according to ISO standard, and therefore the results are as good and comparable to the compression tests. We can see the similarity from both of the two smallest pipes. With the background from these two smallest pipes results comparison, conclusion was made to use the Enerpac compression test results of yield load in the further calculations. This due to the great consistency and compared results from the two smallest pipes done according to the standard.

The table below shows the results from Instron tensile test and in comparison the calculated elasticity modulus from the Enerpac. As seen, the values are varying, and are not comparable to the Instron values. The Instron elasticity values are more reliable than the Enerpac elasticity calculations from stress and strain.

Table 29 Elasticity comparison from the two experiments

Young's modulus from experiment stress/strain		
27,3 mm x 2,8 mm	**Experiment [GPa]**	**Instron [GPa]**
200	51,60	172,90
250	83,80	
300	85,50	
500	15,64	
750	179,60	
33,9mm x 3,2 mm		
200	52,50	170,10
250	64,80	
300	72,00	
500	110,96	
750	126,90	
48,5 mm x 3,9 mm		
200	43,70	196,30
250	51,80	
300	66,60	
500	94,50	
750	88,10	
60,5 mm x 3,7 mm		
200	45,70	175,50
250	47,70	
300	52,20	
500	65,90	
750	67,90	
89,1 mm x 3,0 mm		
200	69,70	198,65
250	82,40	
300	66,80	
500	78,50	
750	104,29	

Some of the reason the Enerpac stress-strain results are not comparable to Instron elasticity modulus may have to do with how the test were conducted. The tensile test was performed based on the ISO standard and the calculation was done accordingly to find the young's elasticity modulus. Other impact may have been the speed the compression is pushing down. This can vary depending on the loads pushing against the piston. Looking at the length vs sample in the graph below, the speed of the compression looks linear and stable. However, when using Instron to measure the elasticity, the ISO standard is used, where the speed of extension is preset before testing. This is not an option Enerpac has, and that may influence the results seen in the table above.

Another impact is that the while using tensile strength, the tubing is only being stressed in one dimension (axial), while during compression, the tubing can move freely in any direction, as well the impact of end restrains may impact the direction and create strain-hardening affecting the elasticity modulus. The figure below shows the length compressed as well as the force acing on the tubing.

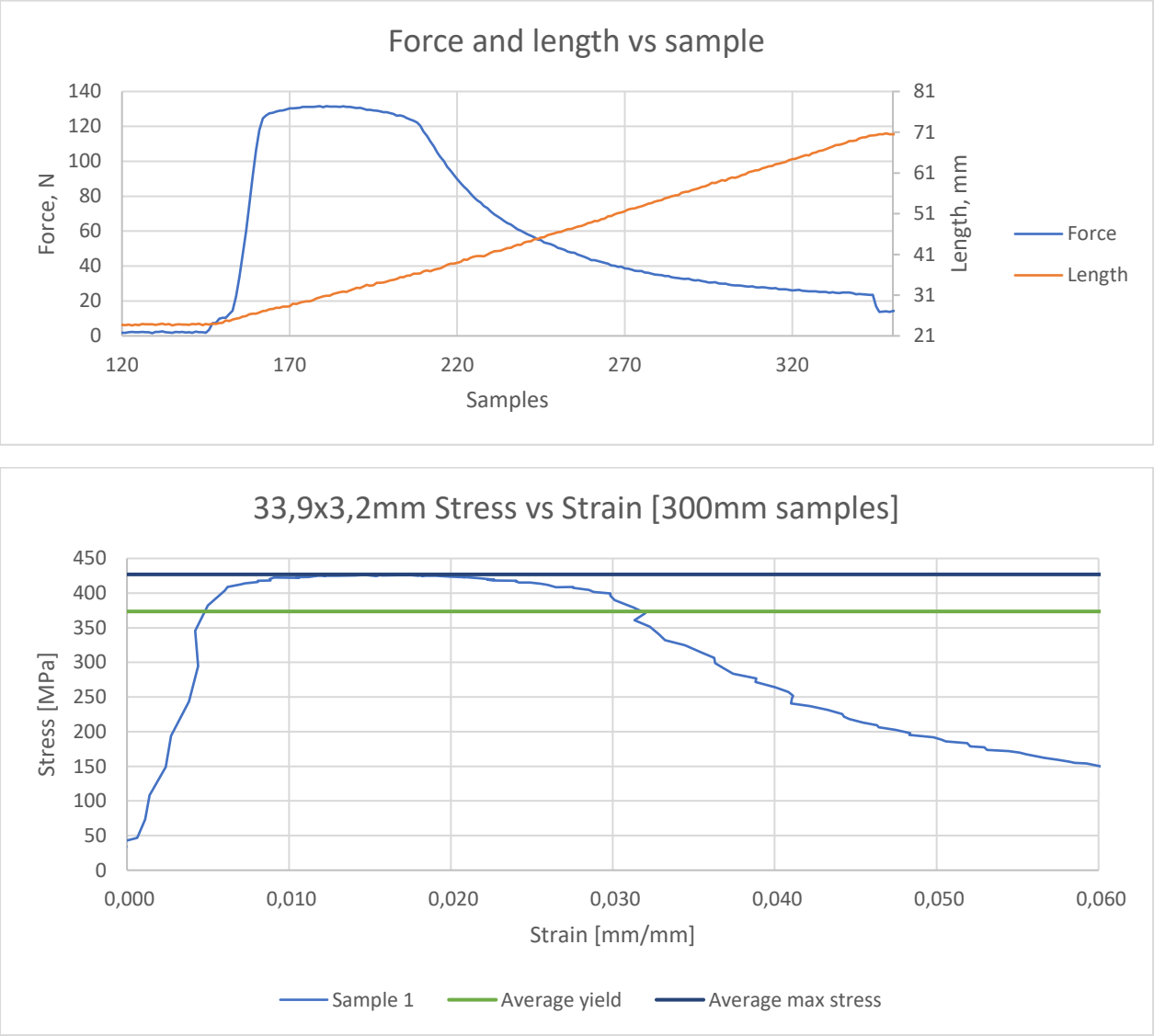

Figure 84 Force and length compressed and Stress-Strain for 33,9 mm x 3,2 mm, 334 mm

However, based on the data gathered from the two smallest pipes (27,3 and 33,9 mm), which was performed with the use of ISO standard and pipes not modified, the results from both the datasheet, tensile test and compression test are compared. The results gathered from the Enerpac looked very reliable and consistent. Therefore, the decision to use the results of yield loads from these experiments was concluded to use on all pipe sizes. Therefore, the yield load used for the three biggest pipes are assumed to be

accurate. From table 28, we can see the correlation between the yield load from the Enerpac, and the yield load generated from the tensile experiments, for the two smallest pipe sizes.

To summarize the results, let's look back at the theory being used today. There are two methods to determine the slenderness ratio. The largest of the two slenderness ratio must be used to determine the critical buckling force for unsupported buckling, and both must be calculated, (Skinner, 2019).

The unsupported lengths, normally between the top constraining device and the lower device, (length depends on if there is use of telescoping guide or not and are in some cases hard to measure), should be calibrated for their end constrains. Here we use the value k, as listed in the table in chapter 6.1.6 in table 1, to calibrate the effective length. This value is important factor when calculating compressive forces acting on the pipe.

In these experiments the value of k = 1,0 was used. This is due to both ends constrains being circular and are free to buckle in any direction. However, this value may be less, due to friction in the connection when compressed. In addition, the effect of the bushing placed 30 mm inside the pipe to connect the end constrain, may also act as a very small tubing guide, restraining the buckling. If the actual k value is somewhere less than 1, that may affect the results of the experiments.

Below graph in figure 85 is the dimensionless buckling loads and lengths. All experiments from each pipe and lengths are present as the different colored points. The yellow limit is the limit between long column (Euler's buckling) and short/intermediate column theoretical critical buckling loads (from steel-structure). In the graph, only the slenderness ratio 1 is present as the theoretical critical buckling load (dotted line) in the short and intermediate column.

None of the experimental buckling loads was below the theoretical critical buckling loads where the slenderness ratio 1 is used.

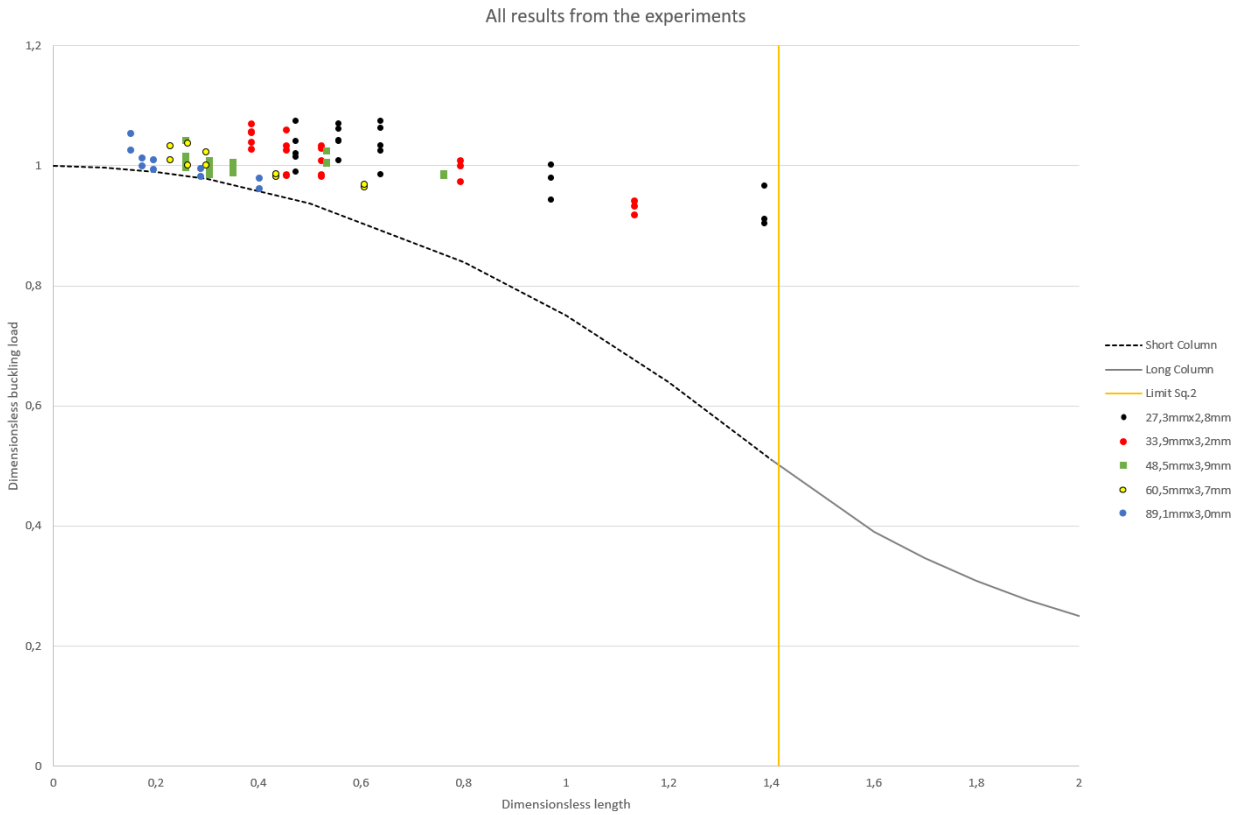

Figure 85 Dimensionless buckling loads vs dimensionless length for all experiments

During compression test of 89,1 mm x 3,0 mm, short column length failure occurred. This made the pipe compress, without bending, in a wavy shape. This pipe has very thin walled compared to the other pipes tested in this research. We can see from table that the OD/t ratio is as high as 29,7. This may be the where the slenderness ratio 2 is intended to be used, and in the oil and gas tubular sizes, may not have as high OD/t value (thin walled). From Baker engineering handbook (Baker, 1995), we have similar tubular size as the one used in these experiments (Table 6), 88,9 mm x 5,49 mm, giving a OD/t value of 16,2, which is much lower than 29,7. So this phenomena may not be realistic in real tubing size critical buckling failure.

Figure 86, 89,1 mm x 3,9 mm, 332 mm unsupported length, short column compression failure

In the table below, we can see all the different slenderness ratios compared to slenderness ratio 2 (to the right) for all pipes. As we can see, we have three pipe sizes for 89,1 mm x 3,0 mm that has greater slenderness ratio 2, 332 mm, 382 mm and 432 mm.

Table 30 All slenderness ratio results from experiments

27,3x2,8mm pipe dimension						
Slenderness Ratio						
Pipe length [mm]	**284**	**334**	**384**	**584**	**834**	**SR2**
1	32,57	38,31	44,04	66,98	95,66	**8,84**

33,9x3,2mm pipe dimensions						
Slenderness Ratio						
Pipe length [mm]	**284**	**334**	**384**	**584**	**834**	SR2
1	26,02	30,61	35,19	53,51	76,42	**10,55**

48,5mmx3,9mm pipe dimensions						
Slenderness Ratio						
Pipe length [mm]	**284**	**334**	**384**	**584**	**834**	**SR2**
1	17,94	21,10	24,26	36,90	52,69	**11,53**

60,5mmx3,7mmmm pipe dimensions						
Slenderness Ratio						
Pipe length [mm]	**332**	**382**	**432**	**632**	**882**	**SR2**
1	16,50	18,98	21,47	31,40	43,83	**13,38**

89,1mmx3,0mm pipe Dimensions						
Slenderness Ratio						
Pipe length [mm]	**332**	**382**	**432**	**632**	**882**	**SR2**
1	10,90	12,54	14,18	20,75	28,96	**18,40**

Looking at the dimensionless buckling load vs length and buckling load vs length for these sizes in graph below. We clearly see that the slenderness ratio for these three pipes is greater than the slenderness ratio 2 used for critical buckling load calculations. In the two graphs below, we can take a look at the three smallest length, dark blue, red and gray colored dots.

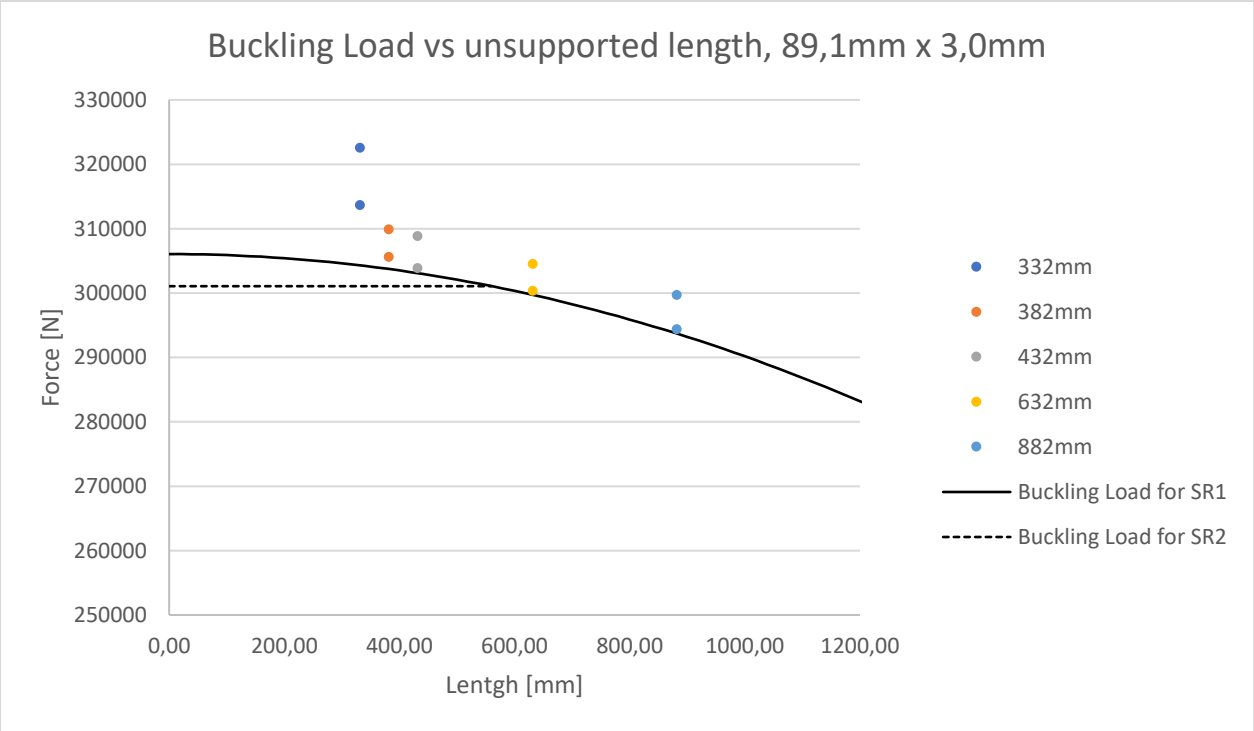

Figure 87 Buckling load vs unsupported length 89,1 mm x 3,0 mm

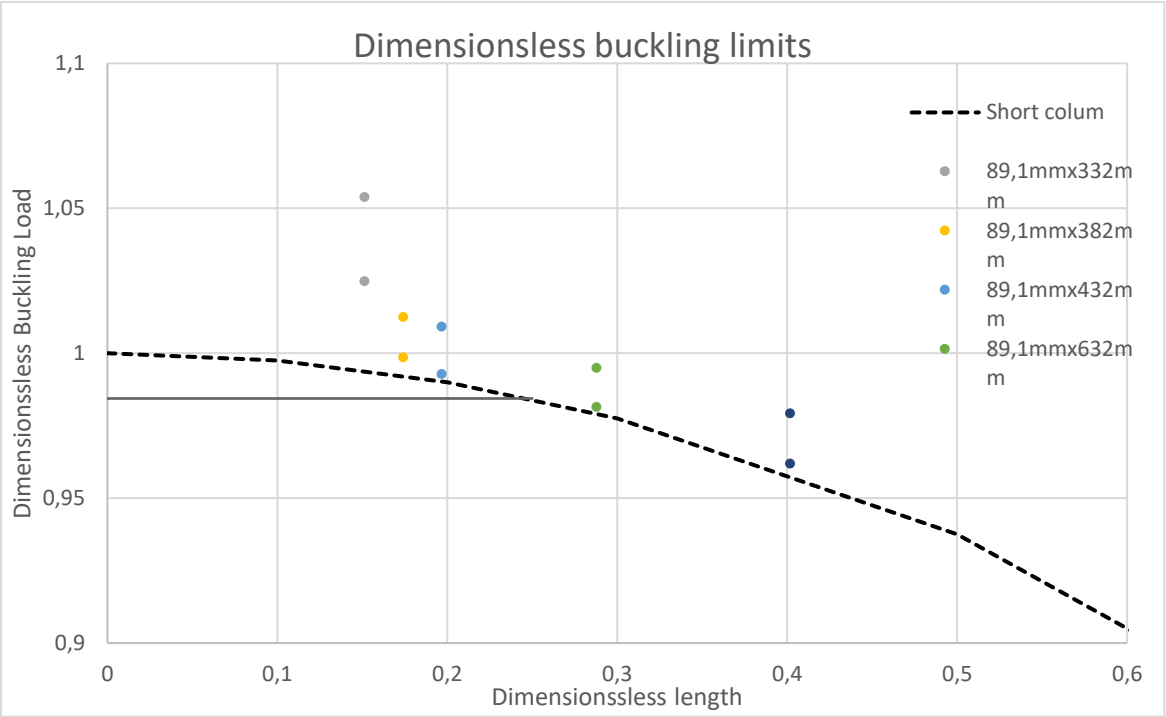

Figure 88 Dimensionless buckling 89,1 mm x 3,0 mm

We can see that the short columns is showing buckling loads higher than the theoretically critically buckling load using both slenderness ratio 1 and 2. The oil and gas business today is recommended to use the highest slenderness ratio of 1 and 2 (Skinner, 2019). From these experiments we can see that the use of slenderness ratio 1 will give the most correct theoretically value of the critically buckling compared to using the slenderness ratio 2. Both formulas are listed below.

$$SR_1 = \frac{kL}{r_g}$$

$$SR_2 = \left(4.8 + \frac{R}{255t}\right)\sqrt{\frac{R}{t}}$$

In the industry recommended practice for Canadian oil and gas industry report we can find an example of recommended snubbing calculations. The use of Johnson's equation to calculate the short column buckling is used (DACC, 2015). However, the use of slenderness ratio 2 is not present in this recommendation.

The results gained from this research indicate that the use of slenderness ratio 2 (SR2), may not apply to the oil and gas business. The results indicate that the need for further investigation and clarification should be performed to conduct more accurate calculations of critical buckling loads for safer live well intervention operations.

6. Reference

Aadnøy, B. S. (2010). *Modern Well Design*.

Aasen, J., & Skaugen, E. (2002). *Pipe Buckling At Surface In Underbalanced Drilling*. Paper presented at the IADC/SPE Asia Pacific Drilling Technology, Jakarta, Indonesia. https://doi.org/10.2118/77241-MS

Baker, B. (1995). *Bakers Oil Tools; Technical Information for Completions, Workovers and Fishin*.

Crumpton, H. (2018). *Well Control for Completions and Interventions*.

DACC, I. (2015). Snubbing Operations - An Industry Recommended Practice (IRP) for Canadian Oil and Gas Industry. *Drilling and Completion Committee (DACC), 15 - 2015*.

Franklin, R. S., & Abel, L. W. (October, 1988). Safer snubbing depends on proper pre-job calculations. *World Oil, 85 - 91*.

Mitchell, R. F. (2012). *Buckling of Tubing inside Casing*. Paper presented at the IADC/SPE Drilling Conference and Exhibition, San Diego, California, USA. https://doi.org/10.2118/150613-MS

Newman, K., & Aasen, J. (1998). *Catastrophic Buckling of Coiled Tubing in the Injector*. Paper presented at the SPE/ICoTA Coiled Tubing Roundtable, Houston, Texas. https://doi.org/10.2118/46007-MS

Newman, K. R., Overstreet, C. C., & Beynet, P. (2006). *Dynamic FEA Buckling Model for Snubbing*. Paper presented at the SPE/ICoTA Coiled Tubing Conference & Exhibition, The Woodlands, Texas, USA. https://doi.org/10.2118/99749-MS

Salmon, C. G., Johnson, J. E., & Malhas, F. A. (2009). *Steel structures Design and Behavior, Emphasizing Load and Resistance Factor Design*.

Skinner, L. (2019). *Hydraulic rig technology and operations*(First edition. ed.).

Thomeer, H. V., & Newman, K. R. (1991). *Safe Coiled-Tubing Operations*. Paper presented at the SPE Health, Safety and Environment in Oil and Gas Exploration and Production Conference, The Hague, Netherlands. https://doi.org/10.2118/23266-MS

Xin, L., Yanfei, C., Tong, Z., & Jing, Z. (2009). *Ultimate Bending Capacity of Steel Pipes Considering Strain Hardening Effect*. Paper presented at the The Nineteenth International Offshore and Polar Engineering Conference, Osaka, Japan. https://doi.org/

Zheng, A. S., & Adnan, S. (2004). *Predicting Coiled-Tubing Failure Below Injector*. Paper presented at the SPE/ICoTA Coiled Tubing Conference and Exhibition, Houston, Texas. https://doi.org/10.2118/89518-MS

Appendix A – Results Enerpac and Instron

Pipes	E-Modulus [Mpa=N/mm^2]	Area [mm^2]	Sigma Yield [N/mm^2]	I [mm^4]	OD [mm]	ID [mm]	t [mm]	K	Radius of gyration, r	R	Cc
27,3X2,8mm	172850	215,51	358,18	16381,43	27,3	21,7	2,8	1	8,72	9,45	97,60
33,9X3,2mm	170133	308,63	369,46	36755,14	33,9	27,5	3,2	1	10,91	15,35	95,34
48,5X3,9mm	196300	546,45	405,71	136910,65	48,5	40,7	3,9	1	15,83	22,30	97,73
60,5X3,7mm	175500	660,24	333,06	267390,25	60,5	53,1	3,7	1	20,12	28,40	101,99
89,1X3,0mm	198650	811,47	377,51	752865,73	89,1	83,1	3,0	1	30,46	43,05	101,97

27,3x2,8mm pipe dimension						
Slenderness Ratio						
Pipe length [mm]	**284**	**334**	**384**	**584**	**834**	**SR2**
1	32,57	38,31	44,04	66,98	95,66	**8,84**

33,9x3,2mm pipe dimensions						
Slenderness Ratio						
Pipe length [mm]	**284**	**334**	**384**	**584**	**834**	SR2
1	26,02	30,61	35,19	53,51	76,42	**10,55**

48,5mmx3,9mm pipe dimensions						
Slenderness Ratio						
Pipe length [mm]	**284**	**334**	**384**	**584**	**834**	**SR2**
1	17,94	21,10	24,26	36,90	52,69	**11,53**

60,5mmx3,7mmmm pipe dimensions						
Slenderness Ratio						
Pipe length [mm]	**332**	**382**	**432**	**632**	**882**	**SR2**
1	16,50	18,98	21,47	31,40	43,83	**13,38**

89,1mmx3,0mm pipe dimensions						
Slenderness Ratio						
Pipe length [mm]	**332**	**382**	**432**	**632**	**882**	**SR2**
1	10,90	12,54	14,18	20,75	28,96	**18,40**

Slenderness ratio 1 = Slenderness ratio 2					
Pipe OD x t	**27,3 x 2,8**	**33,9 x 3,2**	**48,5 x 3,9**	**60,5 x 3,7**	**89,1 x 3,0**
Length [mm]	77,09	115,17	182,52	269,3	560,33

27,3mm x 2,8 mm pipe

27,3x2,8x200mm experiments						
Sample	**Yield [kN]**	**Mpa**	**Max Force [kN]**	**Max Stress [Mpa]**	**Pb video [kN]**	**Pb video [kN] End rotation**
nr1	77,67	360,40	98,02	454,81		98,02
nr2	78,87	365,98	101,25	469,83	89,4	101,25
nr3	80,35	372,85	101,07	468,97	89,97	101,07
nr4	78,32	363,40	99,68	462,53	78,319	99,68
nr5	76,47	354,83	98,02	454,81	76,469	98,02
Average	78,34	363,49	99,61	462,19	83,54	99,61

27,3x2,8x250mm experiments						
Sample	**Yield [kN]**	**Mpa**	**Max Force [kN]**	**Max Stress [Mpa]**	**Pb video [kN]**	**Pb video [kN] End rotation**
nr1	82,67	383,57	92,38	428,63	82,665	92,38
nr2	80,55	373,77	91,82	426,06	80,353	91,82
nr3	77,95	361,69	91,27	423,48	77,949	91,27
nr4	81,93	380,14	92,65	429,92	81,926	92,65
nr5	80,45	373,28	92,84	430,78	85,07	92,84
Average	80,71	374,49	92,19	427,77	81,5926	92,19

27,3x2,8x300mm Experiments						
Sample	**Yield [kN]**	**Mpa**	**Max Force [kN]**	**Max Stress [Mpa]**	**Pb video [kN]**	**Pb video [kN] End rotation**
nr1	82,94	384,86	87,75	407,18	82,943	87,75
nr2	76,10	353,11	89,05	413,18	83,775	89,05
nr3	79,80	370,27	88,31	409,75	82,11	88,31
nr4	82,11	381,00	87,47	405,89	79,798	87,47
nr5	79,15	367,27	88,77	411,90	84,885	88,77
Average	80,02	371,30	88,27	409,58	82,7022	88,27

27,3x2,8x500mm Experiments						
Sample	**Yield [kN]**	**Mpa**	**Max Force [kN]**	**Max Stress [Mpa]**	**Pb video [kN]**	**Pb video [kN] End rotation**
nr1	72,90	338,26	82,57	383,15	72,995	82,57
nr2	75,63	350,93	82,30	381,86	66,851	82,30
nr3	77,39	359,10	85,07	394,73	60,378	85,07
Average	75,31	349,43	83,31	386,58	66,74	83,31

27,3x2,8x750mm Experiments						
Sample	**Yield [kN]**	**Mpa**	**Max Force [kN]**	**Max Stress [Mpa]**	**Pb video [kN]**	**Pb video [kN] End rotation**
nr1	70,36	326,48	79,34	368,13	55,29	79,34
nr2	69,81	323,92	75,17	348,82	55,38	75,17
nr3	74,61	346,20	78,50	364,26	52,80	78,50
Average	71,59	332,20	77,67	360,40	54,49	77,67

27,3mmx2,8xmm Averages						
Sample	**Yield [kN]**	**Mpa**	**Max Force [kN]**	**Max Stress [Mpa]**	**Pb video [kN]**	**Pb video [kN] End rotation**
Total average	77,19	358,18	88,21	409,30	73,81	88,21

200 mm graphs = 284 mm unsupported length

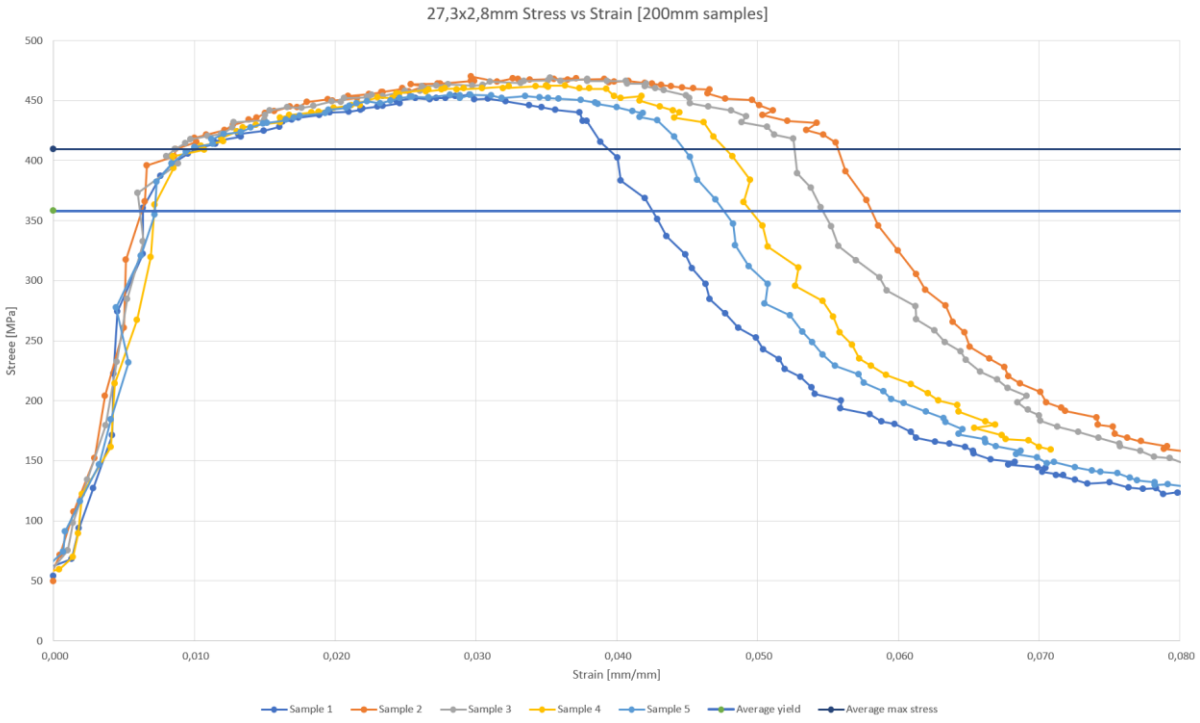

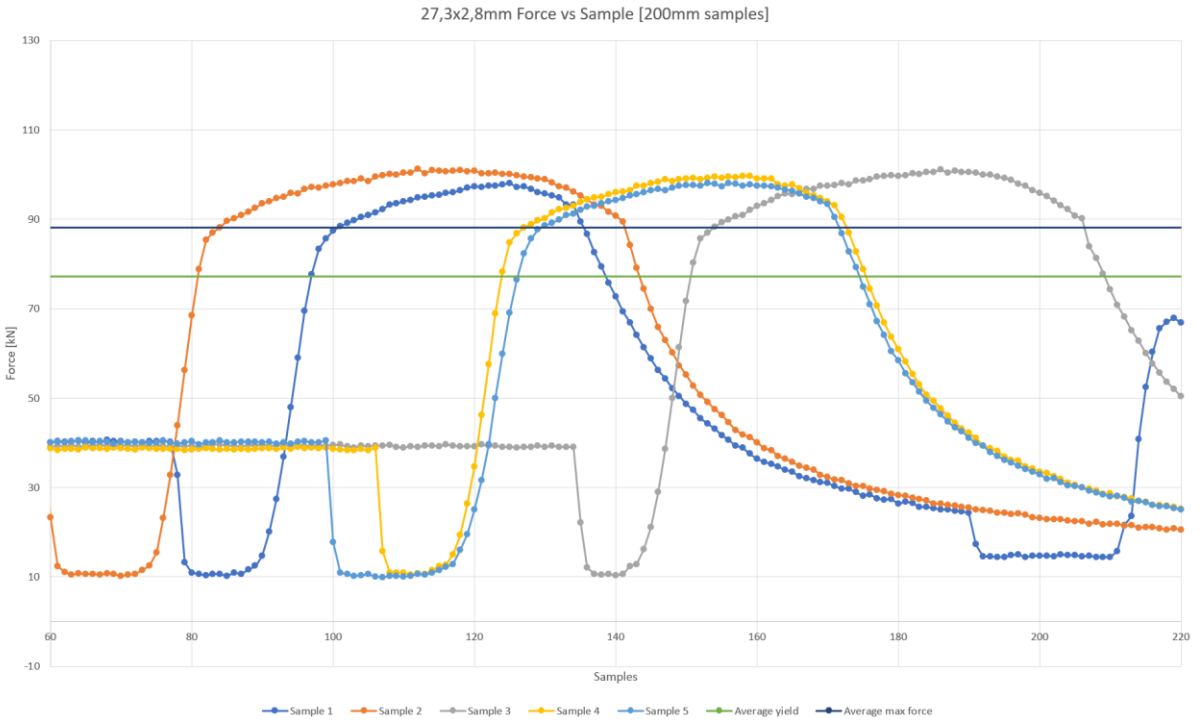

250 mm graphs = 334 mm unsupported length

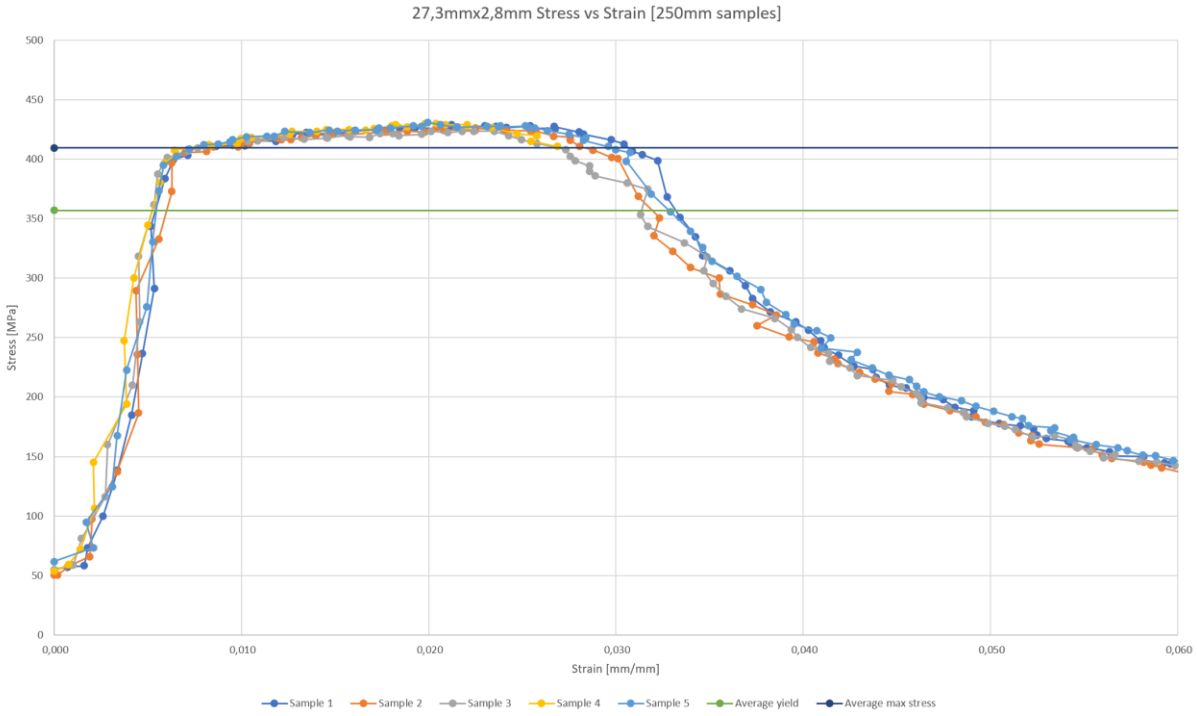

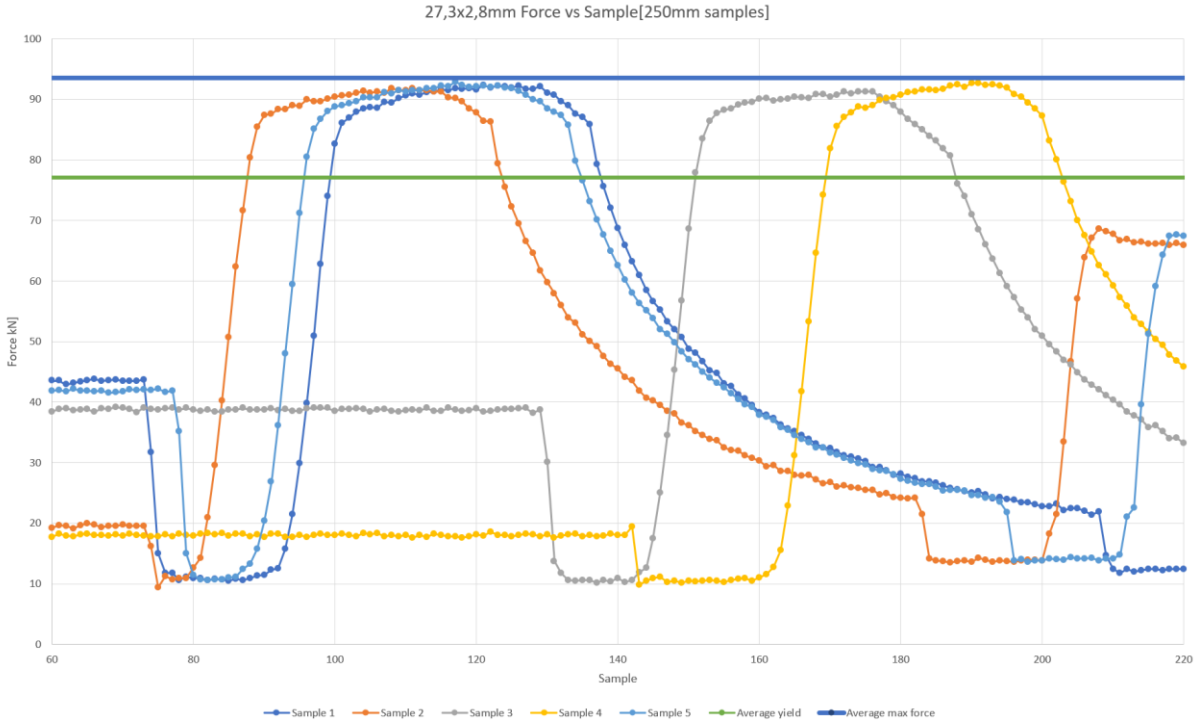

300 mm = 384 mm unsupported length

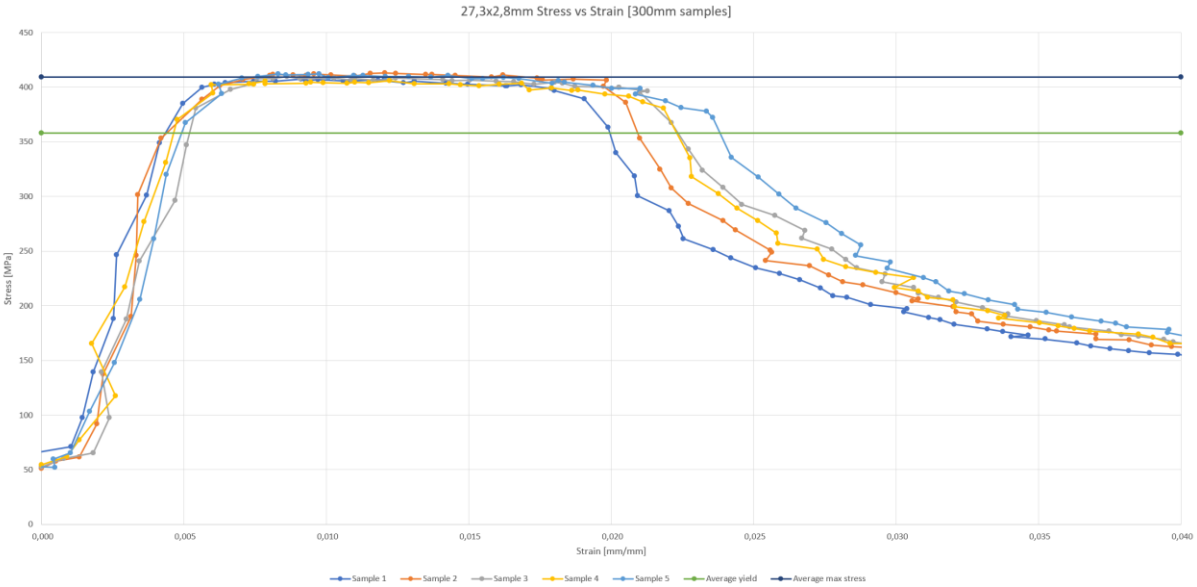

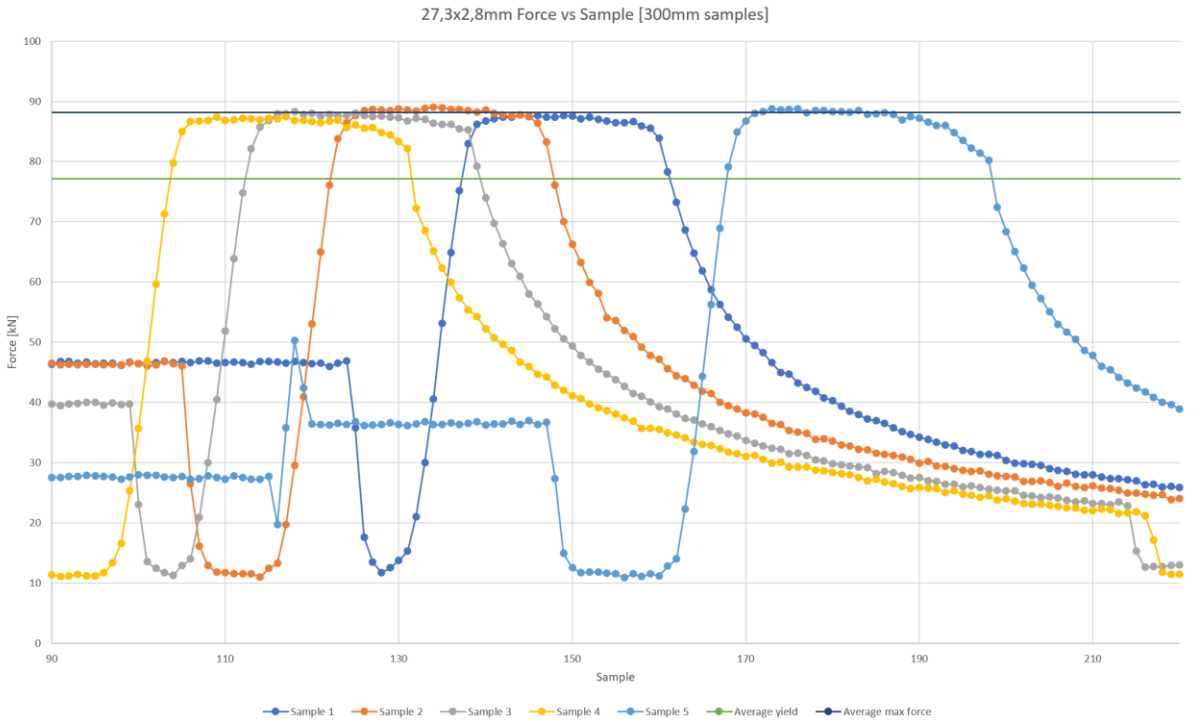

500 mm graphs = 584 mm unsupported length

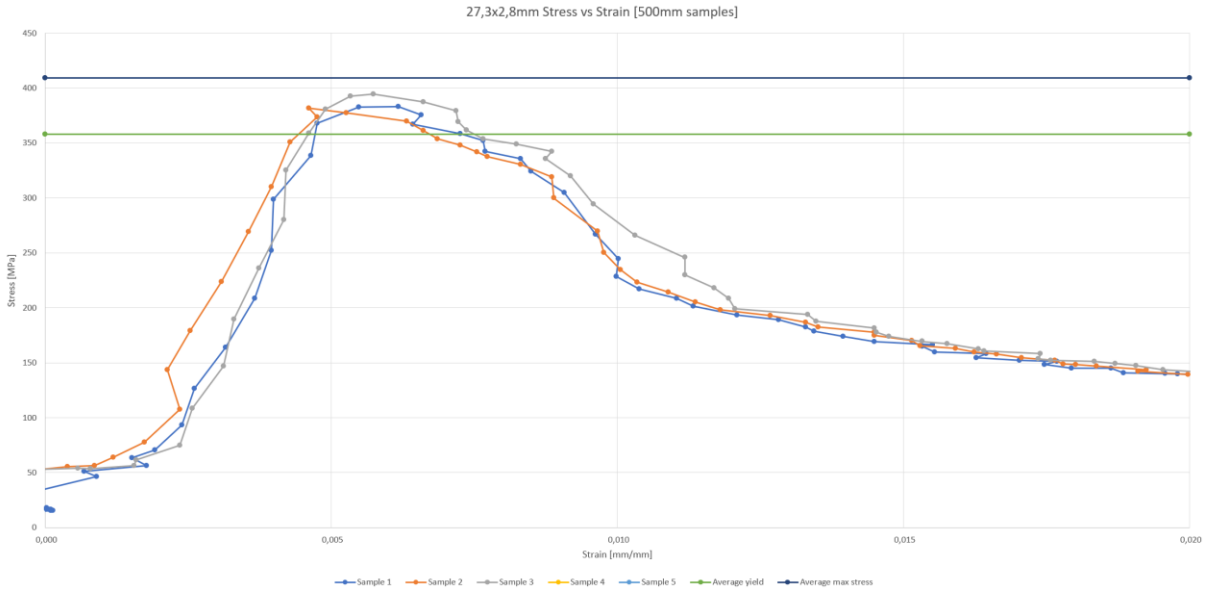

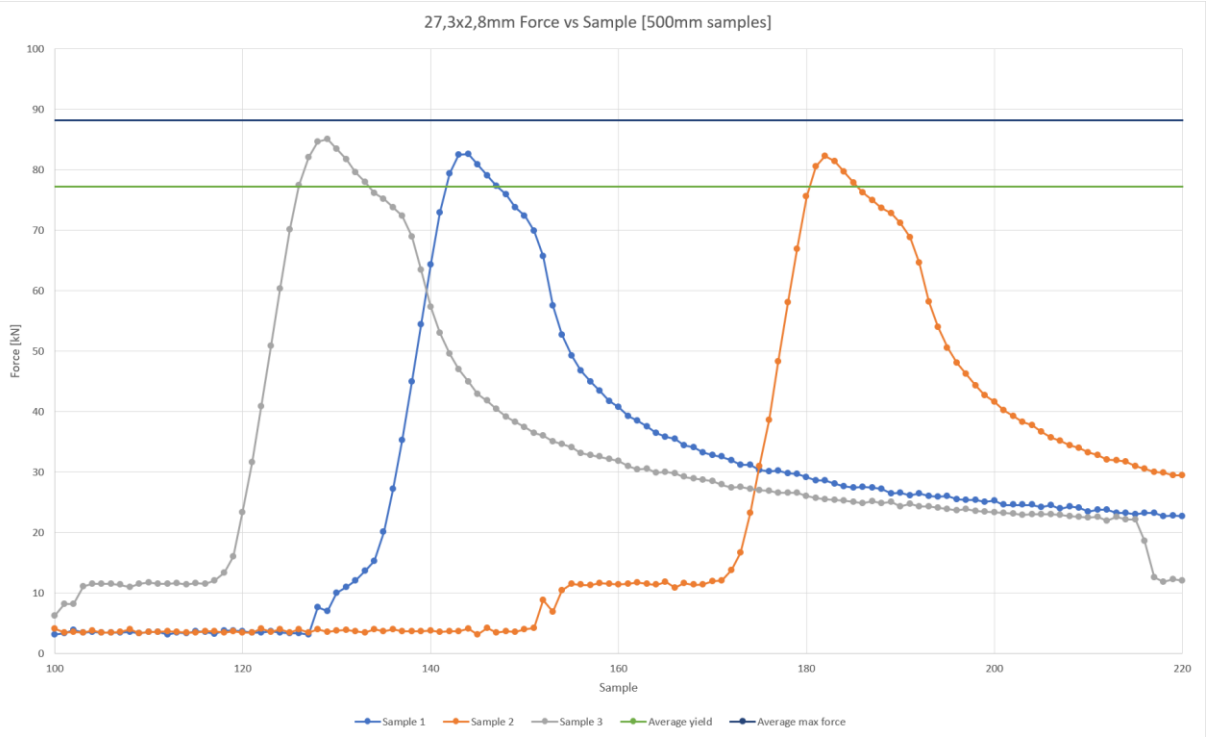

750 mm graphs = 834 mm unsupported length

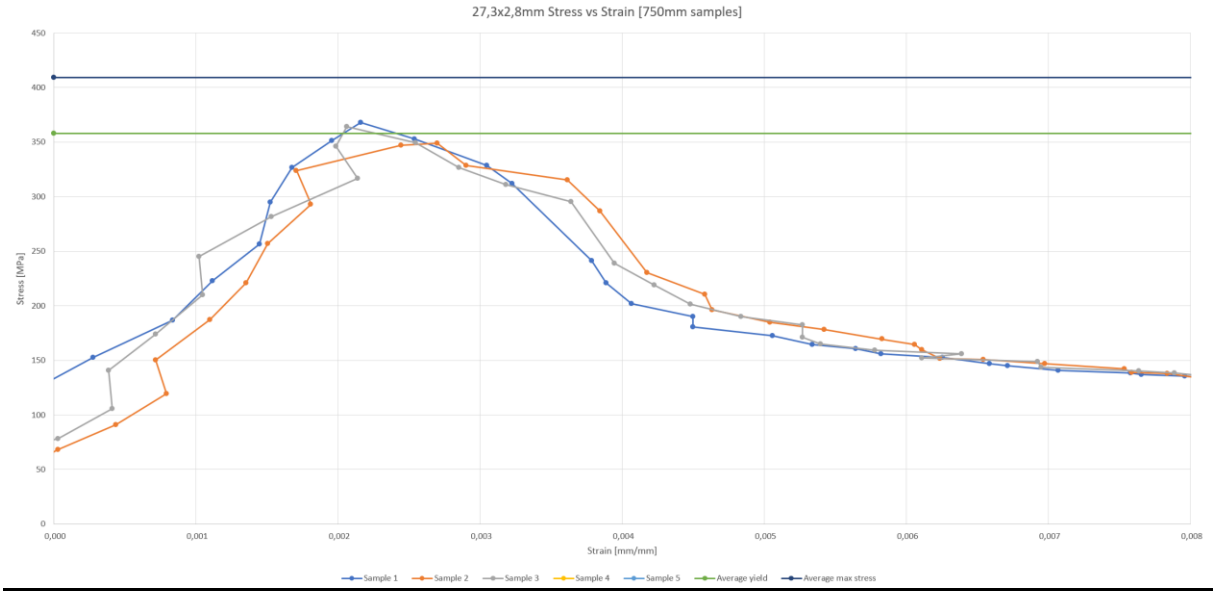

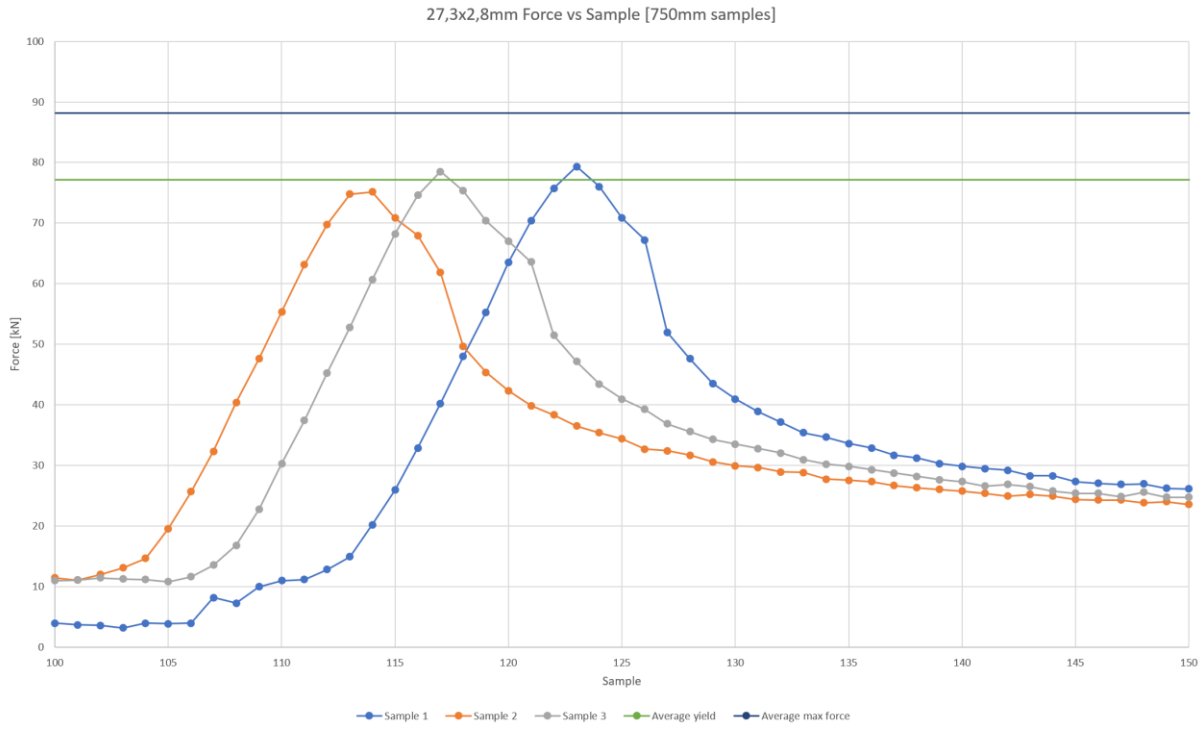

SR1 = SR2 = 77,09 mm unsupported length

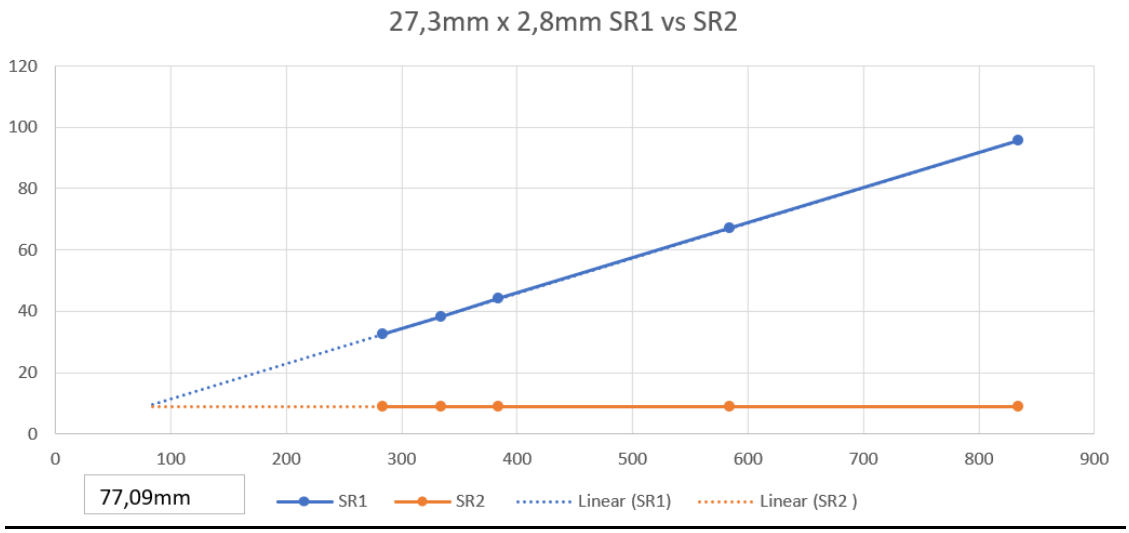

Dimensionsless buckling

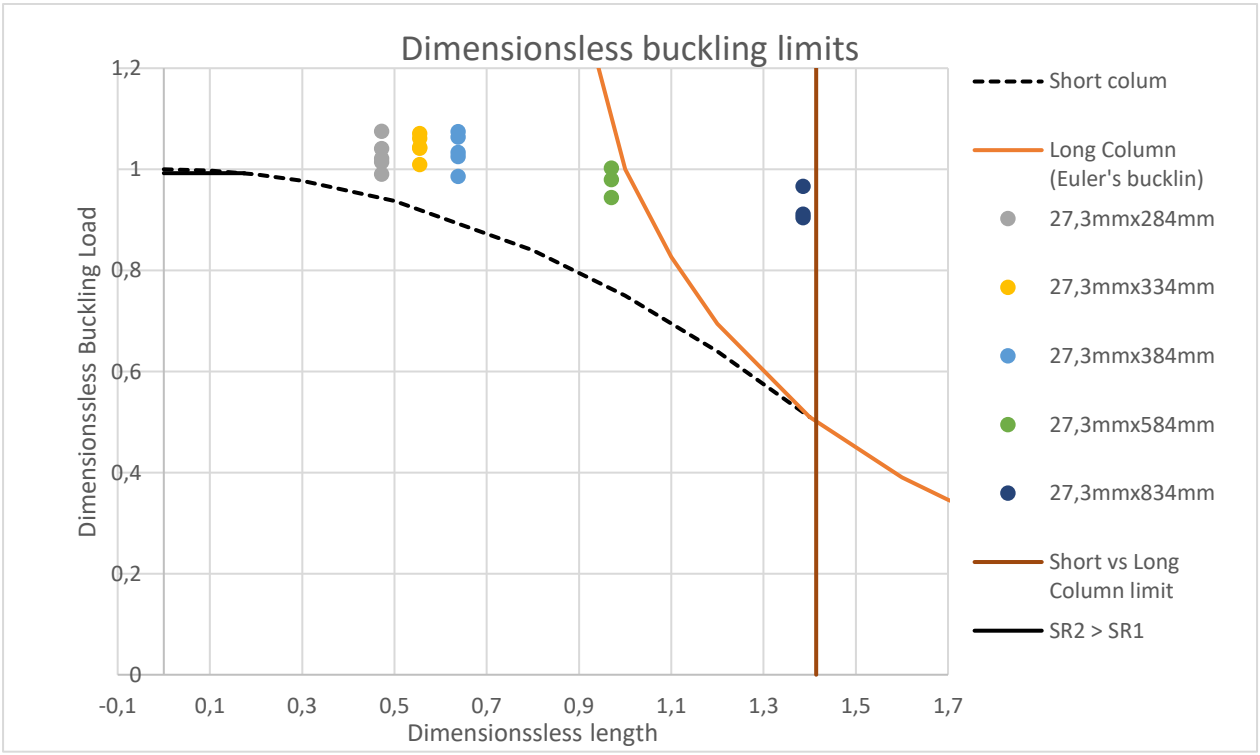

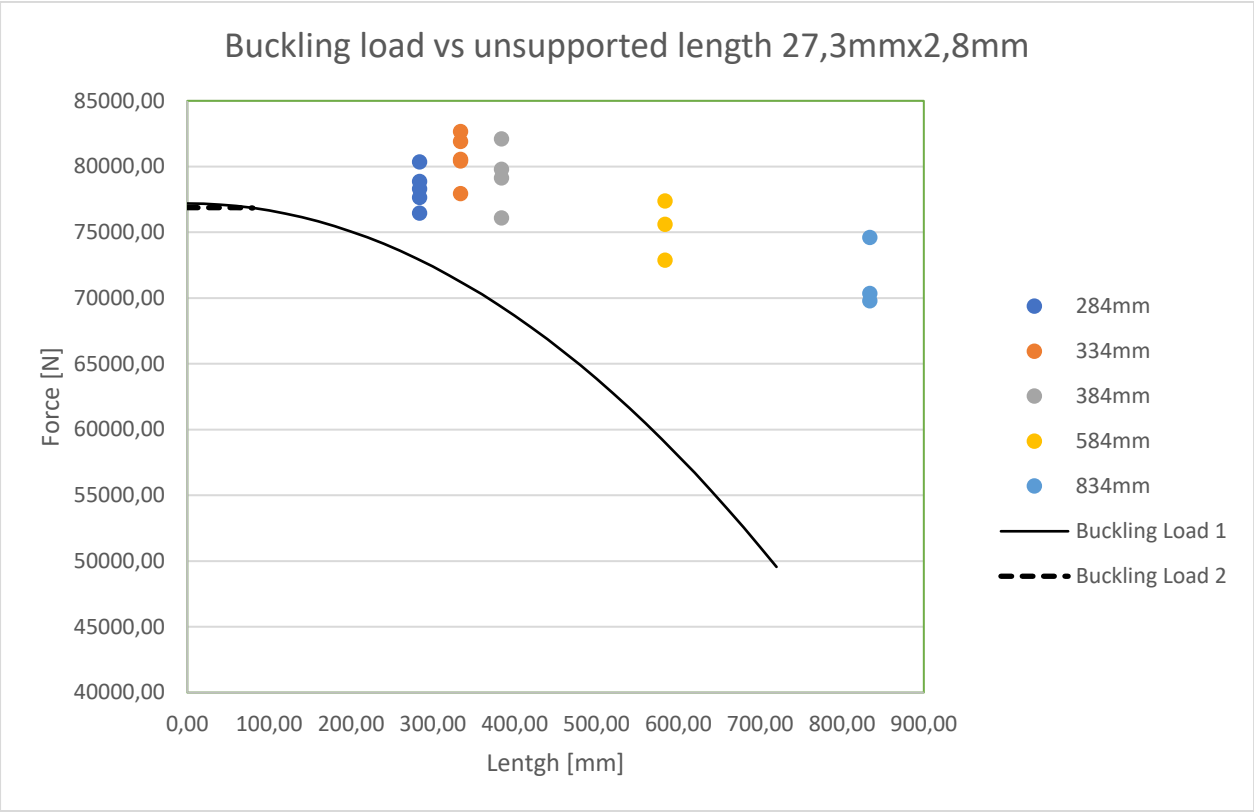
Buckling load vs unsupported length 27,3mmx2,8mm
85000,00
80000,00
75000,00
70000,00
65000,00
60000,00
55000,00
50000,00
45000,00
40000,00
Force [N]
0,00
100,00
200,00
300,00
400,00
500,00
600,00
700,00
800,00
900,00
Lentgh [mm]
284mm
334mm
384mm
584mm
834mm
Buckling Load 1
Buckling Load 2

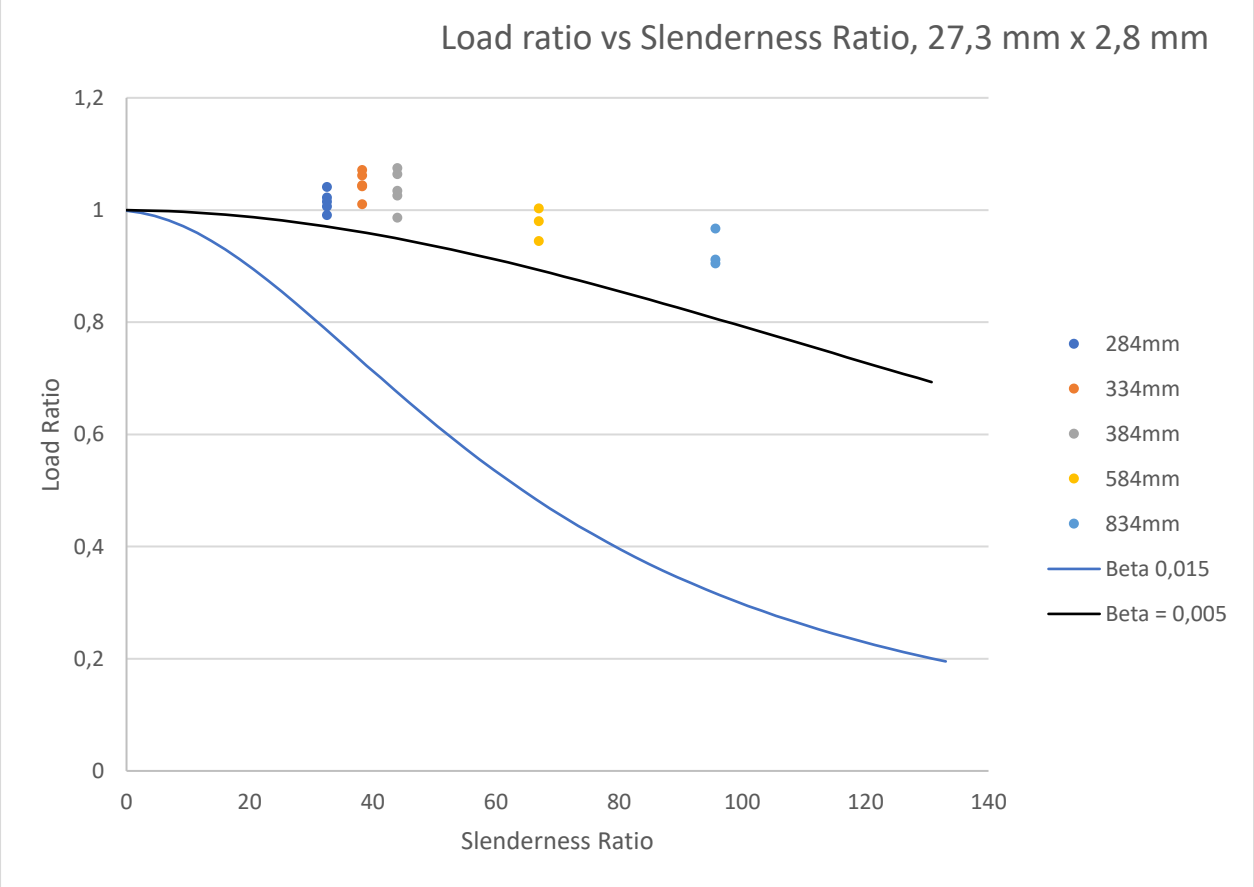
Load ratio vs Slenderness Ratio, 27,3 mm x 2,8 mm
1,2
1
0,8
0,6
0,4
0,2
0
Load Ratio
0
20
40
60
80
100
120
140
Slenderness Ratio
284mm
334mm
384mm
584mm
834mm
Beta 0,015
Beta = 0,005

33,9 mm x 3,2 mm

33,9x3,2x200mm Experiments						
Sample	**Yield [kN]**	**Mpa**	**Max Force [kN]**	**Max Stress [Mpa]**	**Pb video [kN]**	**Pb video [kN] End rotation**
nr1	122,00	395,30	144,16	467,11	135,84	144,16
nr2	118,45	383,81	144,72	468,91	137,88	144,72
nr3	117,25	379,91	147,03	476,40	138,06	147,03
nr4	120,48	390,37	144,35	467,71	137,78	144,35
nr5	120,30	389,79	143,79	465,91	130,29	143,79
Average	119,70	387,83	144,81	469,21	135,97	144,81

33,9x3,2x250mm Experiments						
Sample	**Yield [kN]**	**Mpa**	**Max Force [kN]**	**Max Stress [Mpa]**	**Pb video [kN]**	**Pb video [kN] End rotation**
nr1	112,35	364,03	137,04	444,04	127,06	137,04
nr2	122,24	396,07	135,84	440,14	122,25	135,84
nr3	120,85	391,57	138,89	450,03	132,97	138,89
nr4	116,97	379,01	137,14	444,34	127,98	137,14
nr5	117,80	381,69	137,14	444,34	126,87	137,14
Average	118,04	382,47	137,21	444,58	127,42	137,21

33,9x3,2x300mm Experiments						
Sample	**Yield [kN]**	**Mpa**	**Max Force [kN]**	**Max Stress [Mpa]**	**Pb video [kN]**	**Pb video [kN] End rotation**
nr1	117,89	381,98	131,59	426,36	127,43	131,59
nr2	112,35	364,03	131,49	426,06	121,59	131,49
nr3	111,98	362,83	130,85	423,96	126,96	130,85
nr4	114,95	372,45	129,74	420,36	122,15	129,74
nr5	117,34	380,20	129,83	420,66	125,48	129,83
Average	114,90	372,30	130,70	423,48	124,72	130,70

33,9x3,2x500mm Experiments						
Sample	**Yield [kN]**	**Mpa**	**Max Force [kN]**	**Max Stress [Mpa]**	**Pb video [kN]**	**Pb video [kN] End rotation**
nr1	115,00	372,61	123,82	401,19	115,15	123,82
nr2	114,00	369,37	124,47	403,28	115,56	124,47
nr3	111,00	359,65	123,63	400,59	118,36	123,63
Average	113,33	367,21	123,97	401,69	116,36	123,97

33,9x3,2x750mm Experiments						
Sample	**Yield [kN]**	**Mpa**	**Max Force [kN]**	**Max Stress [Mpa]**	**Pb video [kN]**	**Pb video [kN] End rotation**
nr1	106,33	344,52	120,12	389,20	97,37	120,12
nr2	107,44	348,12	118,45	383,81	99,13	118,45
nr3	104,76	339,44	122,25	396,09	95,06	122,25
Average	106,18	344,03	120,27	389,70	97,18	120,27

33,9mmx3,2 Averages						
Sample	**Yield [kN]**	**Mpa**	**Max Force [kN]**	**Max Stress [Mpa]**	**Pb video [kN]**	**Pb video [kN] End rotation**
Total ave	114,43	370,77	131,39	425,73	120,33	131,39

200 mm graphs = 284 mm unsupported length

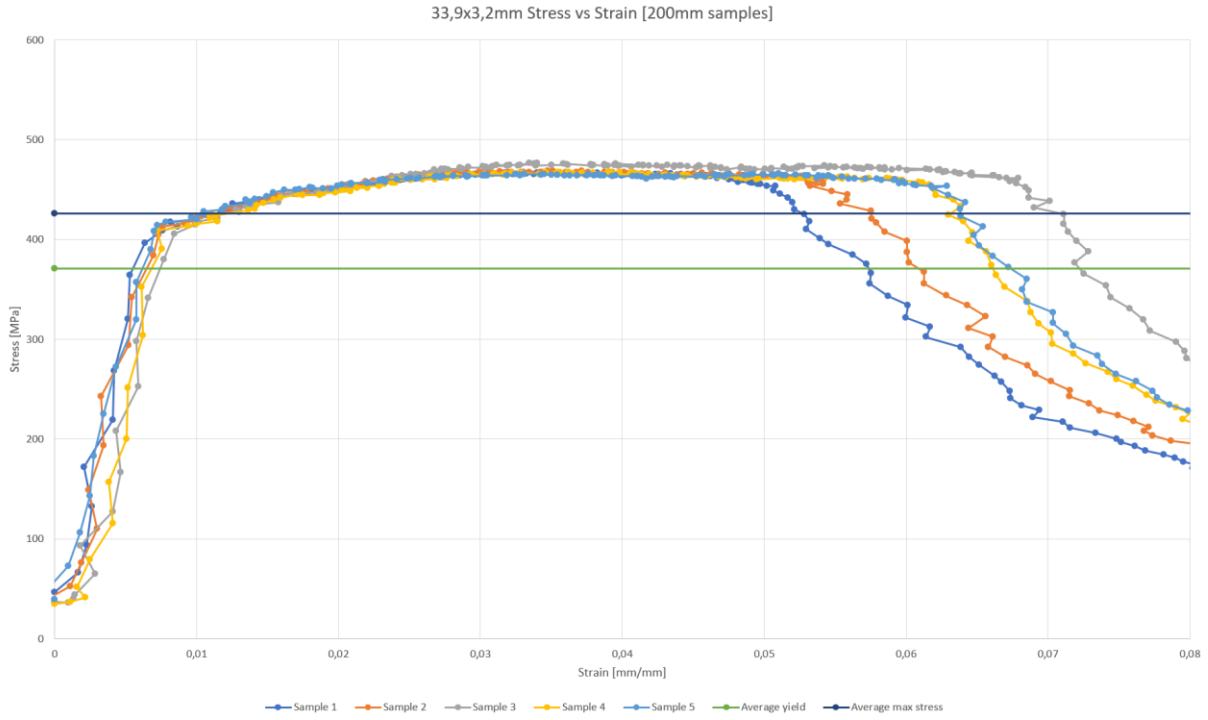

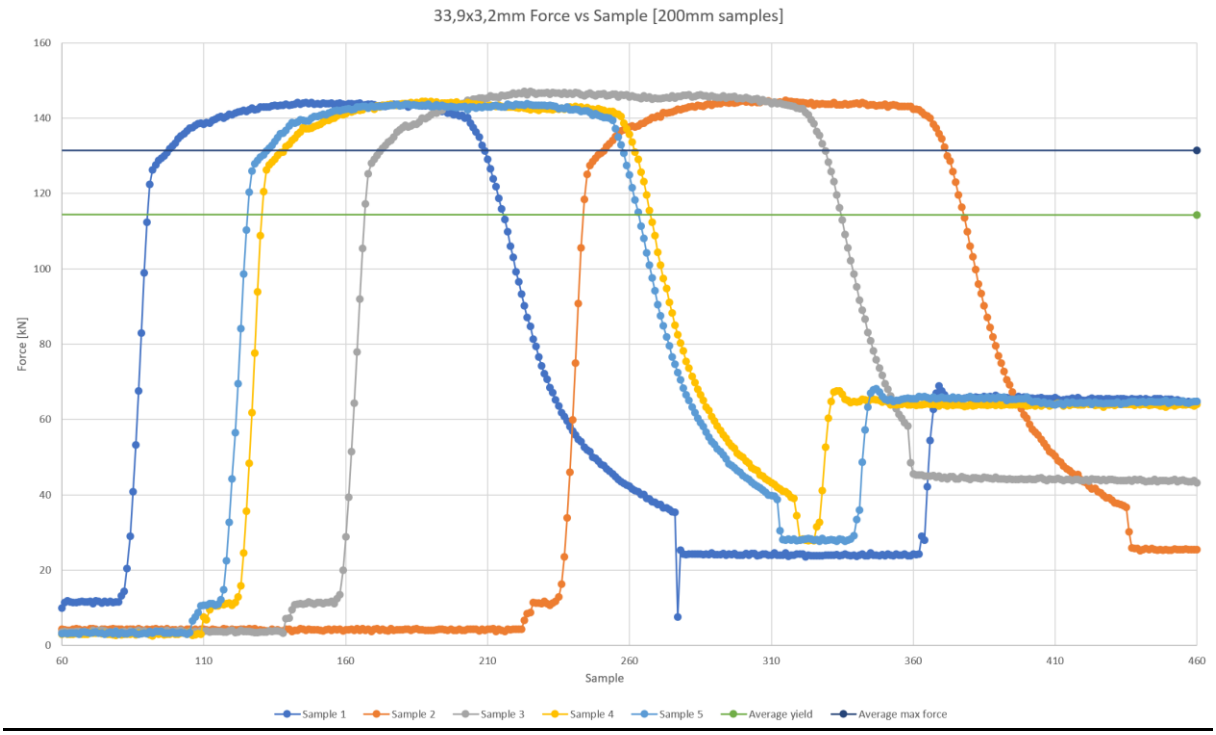

250 mm graphs = 334 mm unsupported length

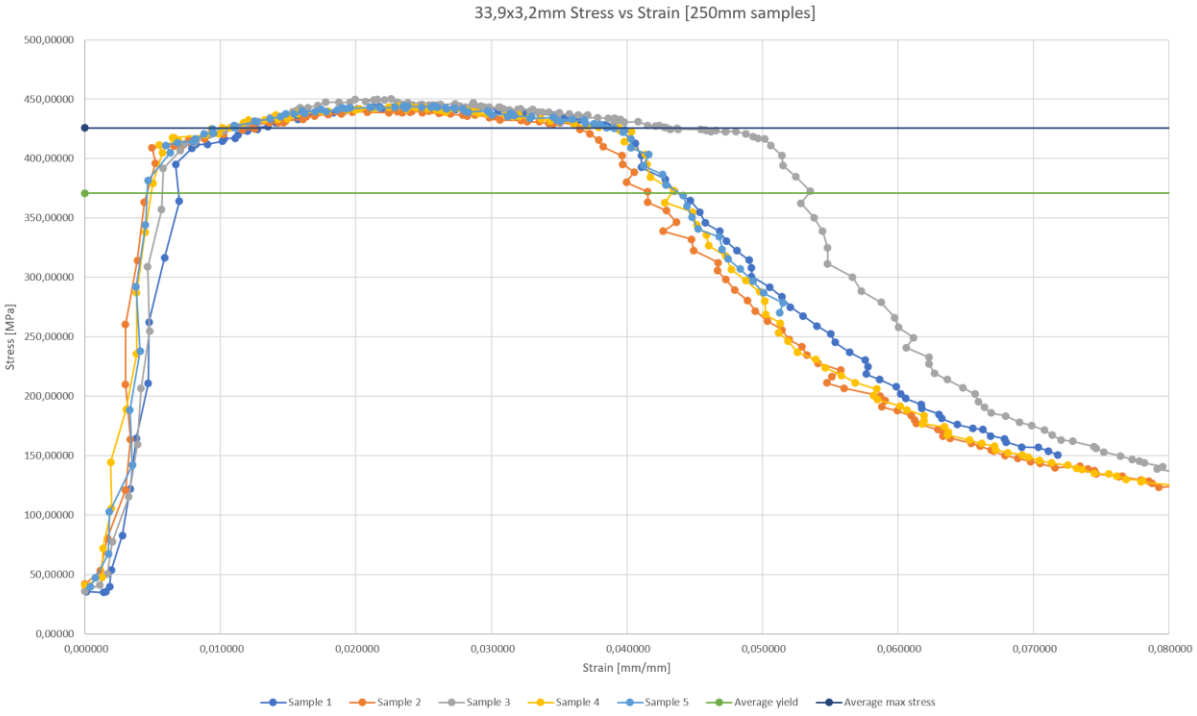

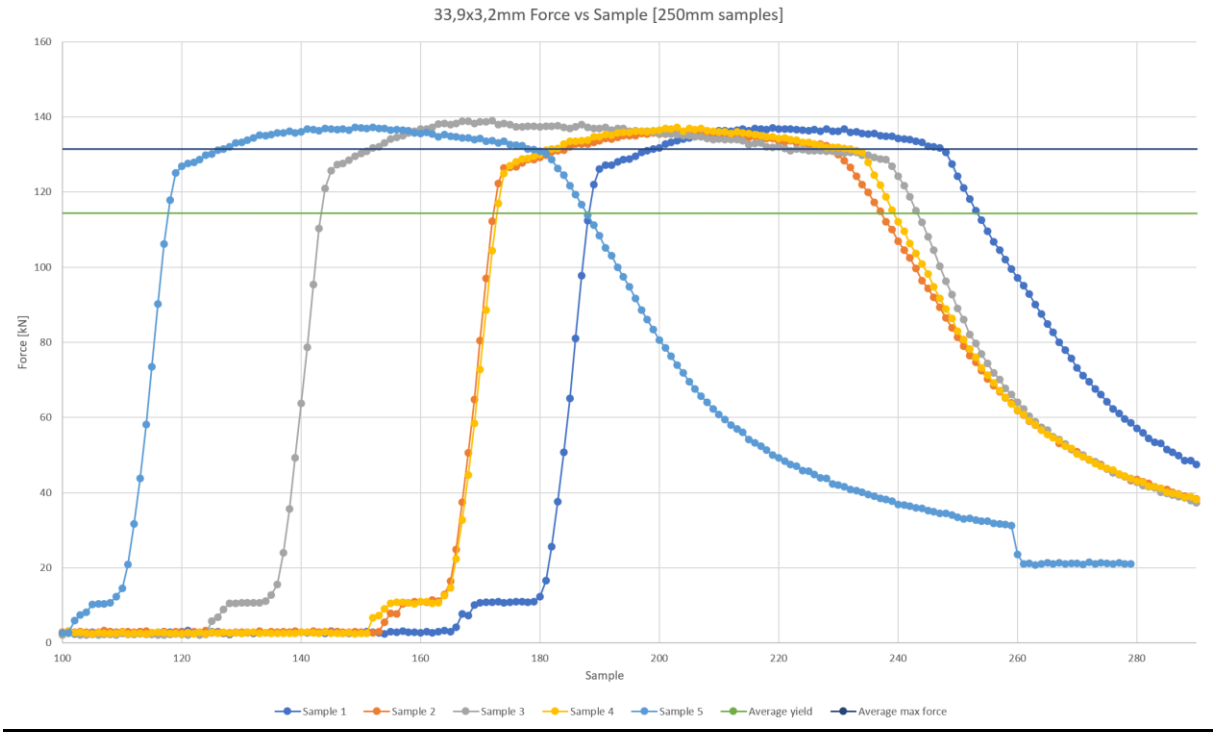

300 mm graphs = 384 mm unsupported length

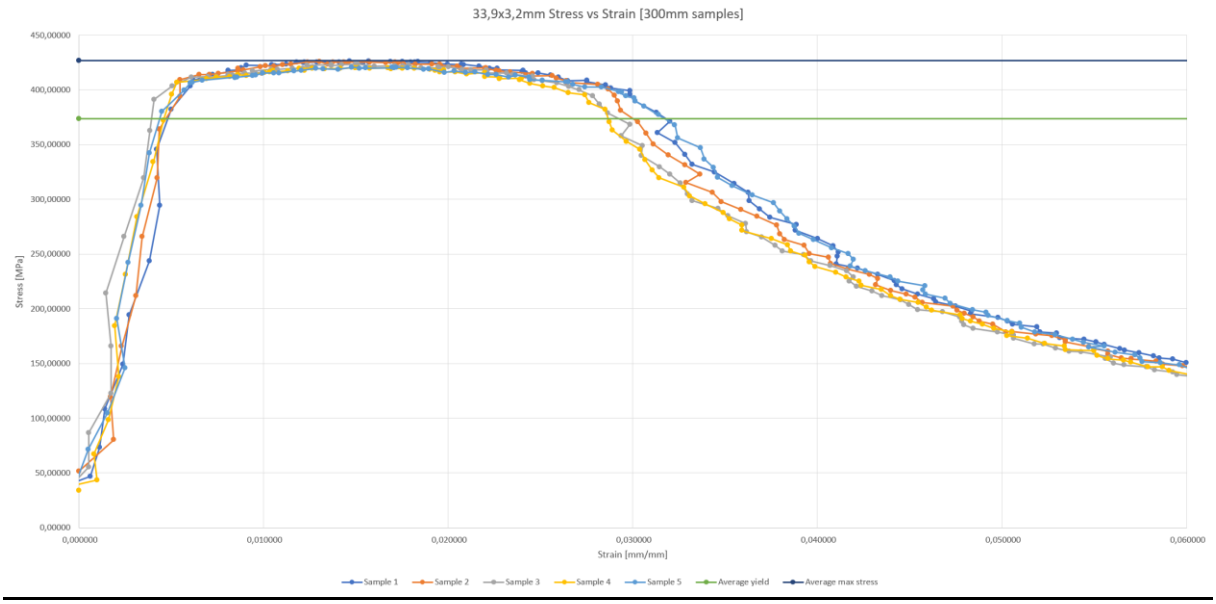

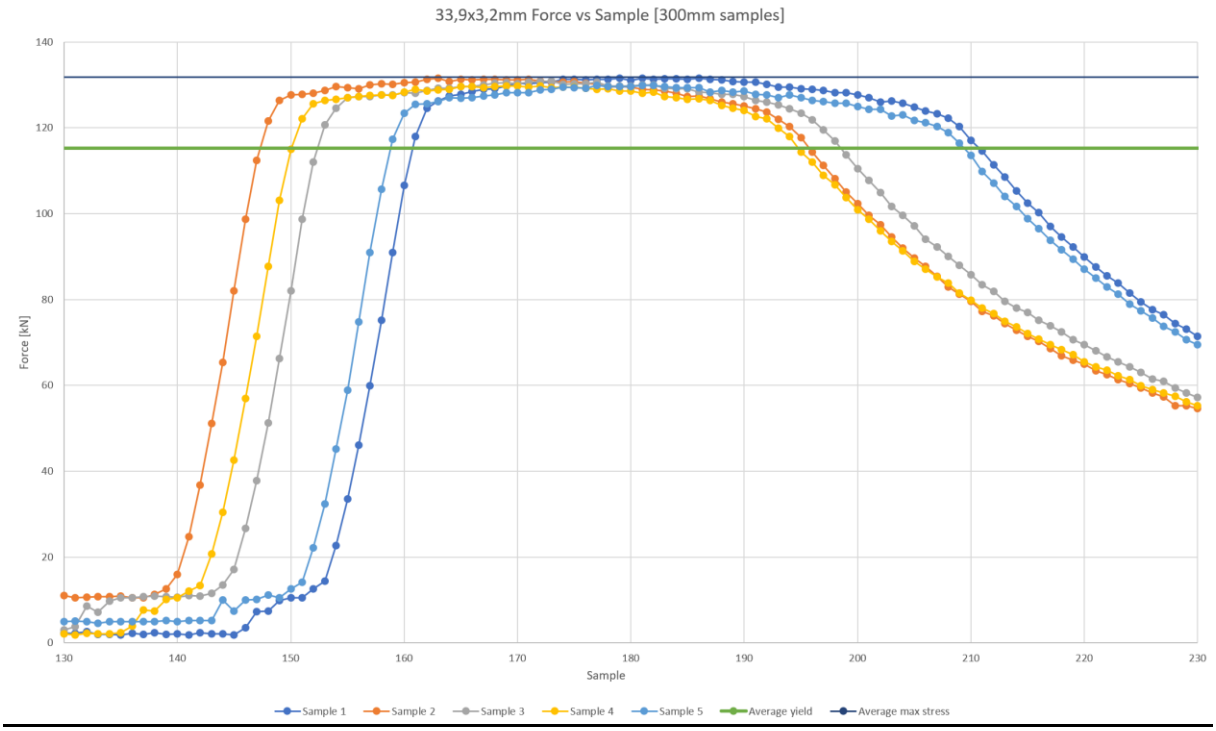

500 mm graphs = 584 mm unsupported length

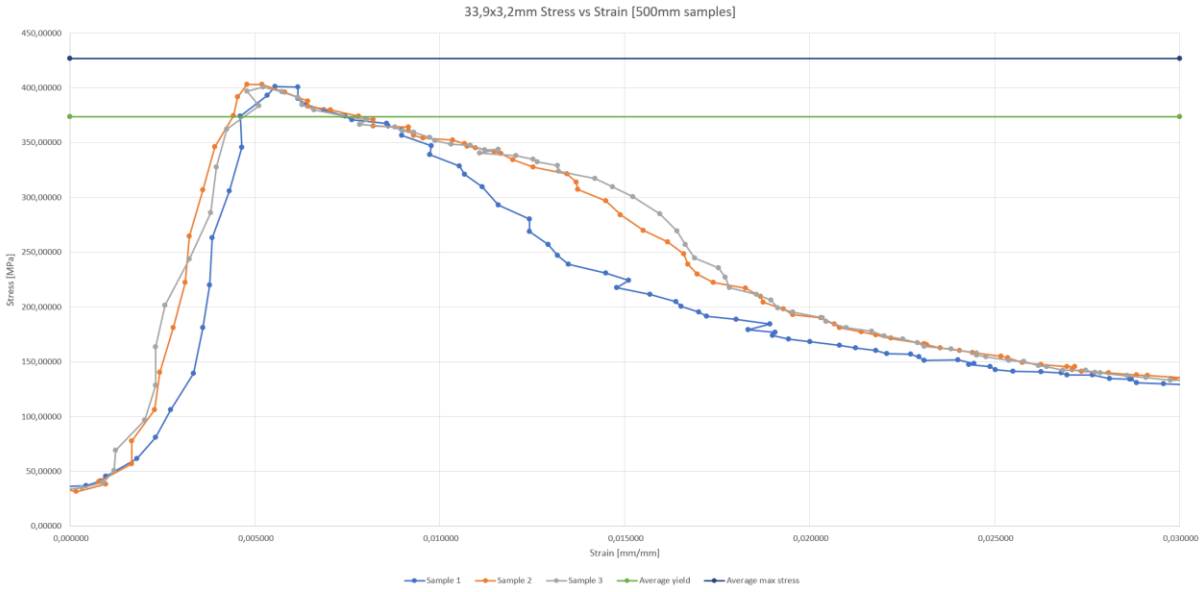

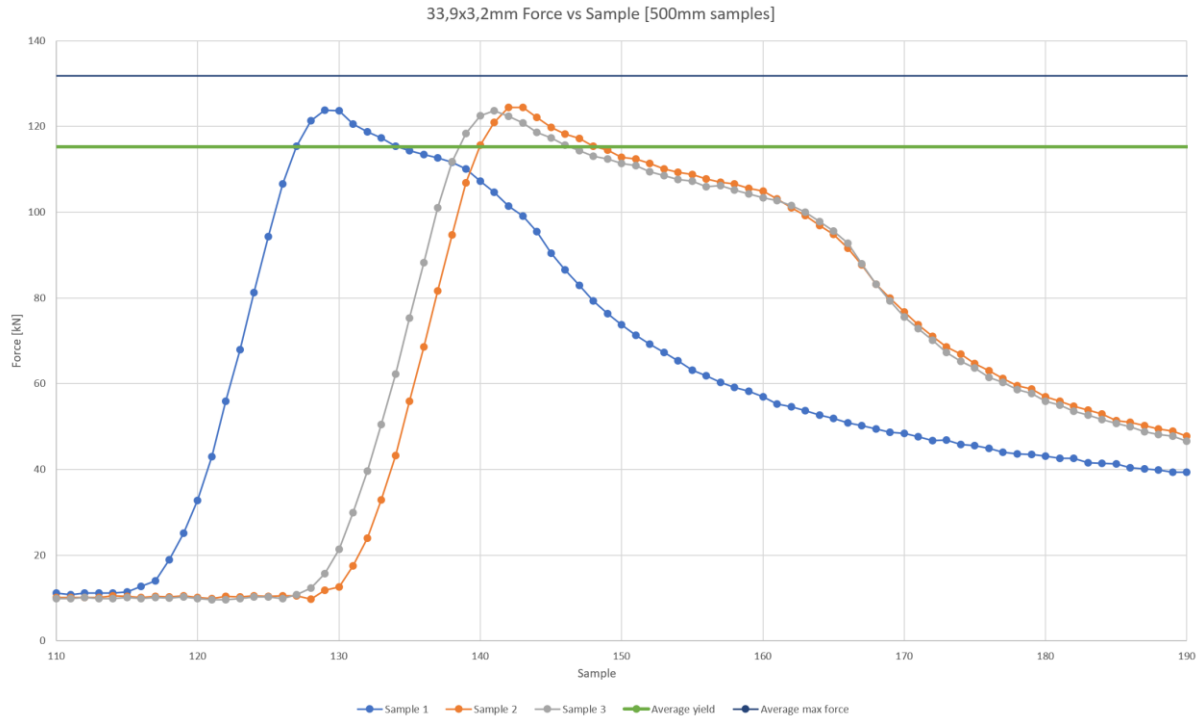

750 mm graphs = 834 mm unsupported length

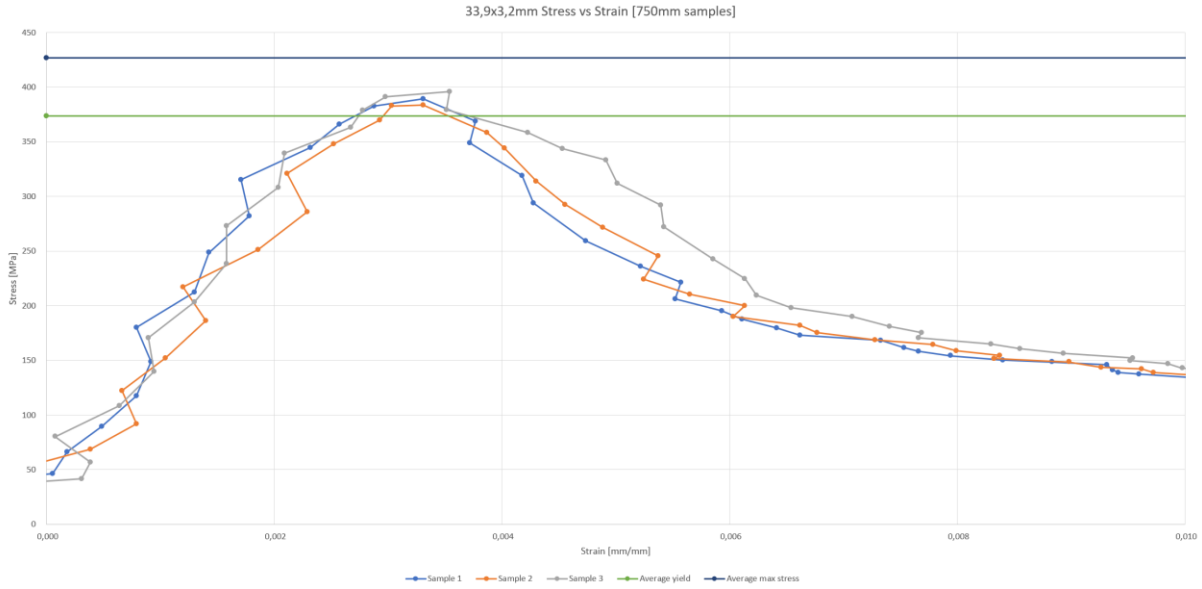

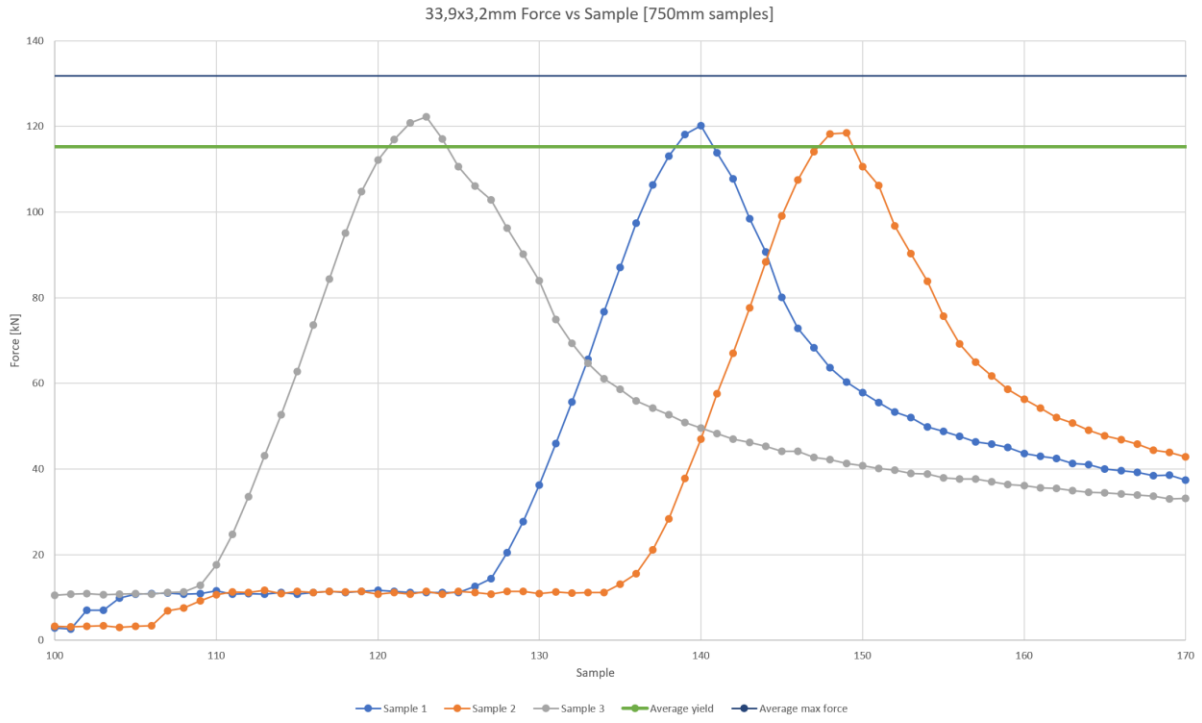

SR1 = SR2 = 115,2 mm unsupported length

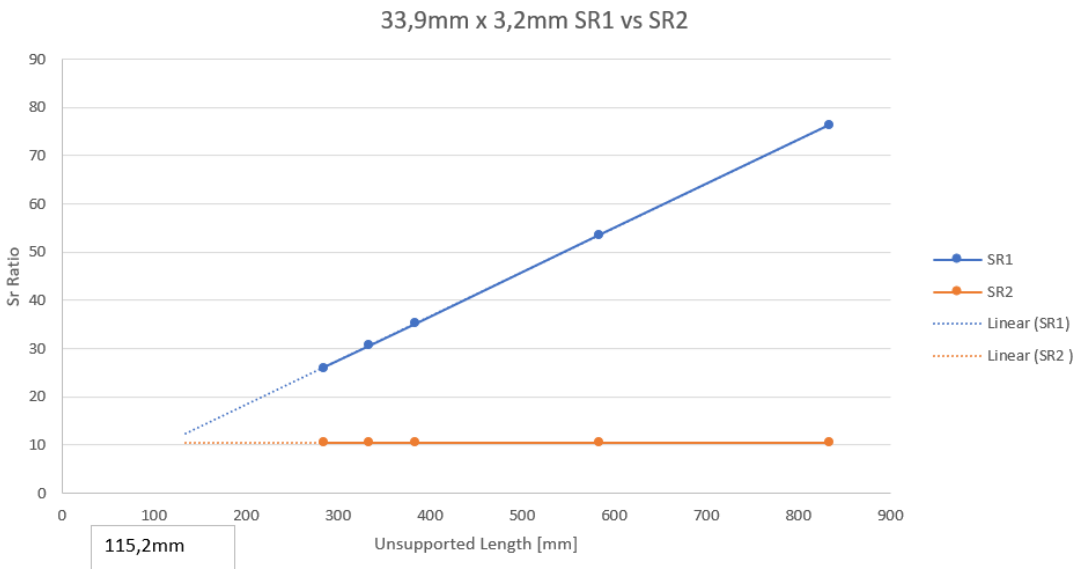

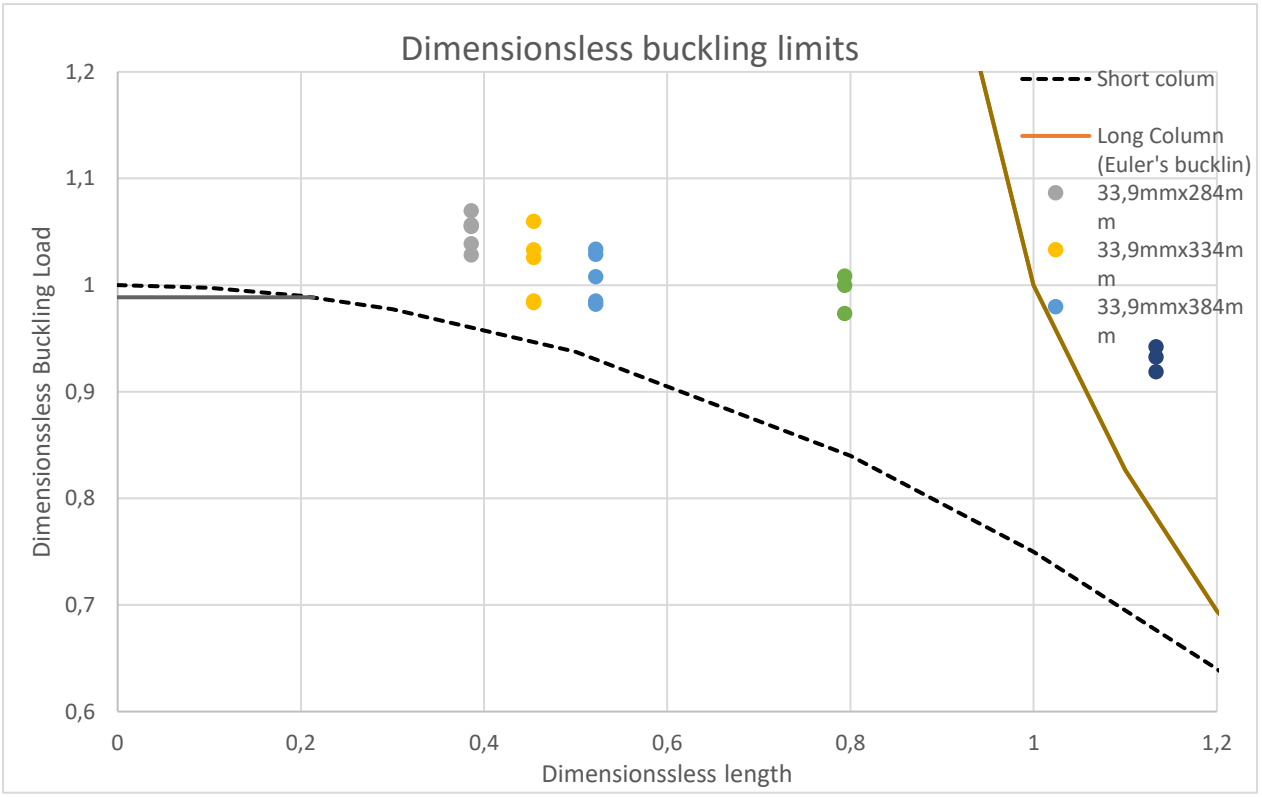

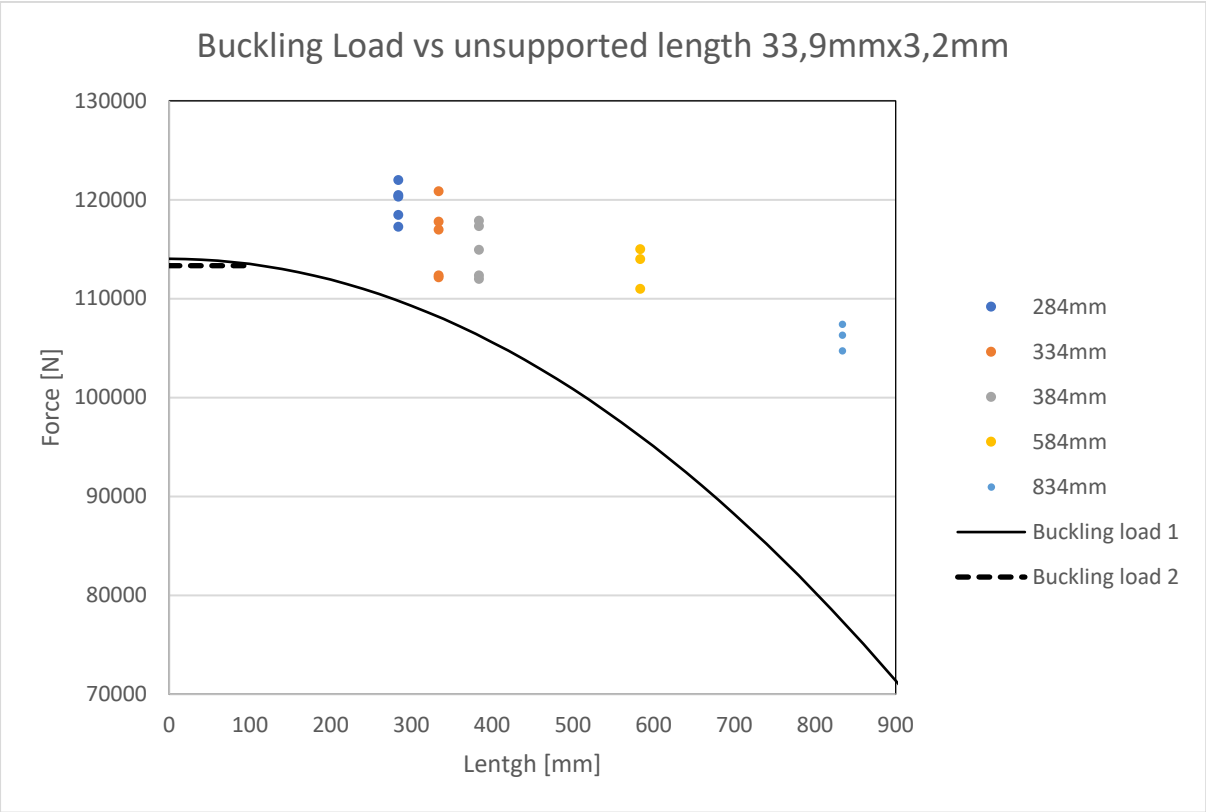
Buckling Load vs unsupported length 33,9mmx3,2mm
130000
120000
110000
100000
90000
80000
70000
Force [N]
0
100
200
300
400
500
600
700
800
900
Lentgh [mm]
284mm
334mm
384mm
584mm
834mm
Buckling load 1
Buckling load 2

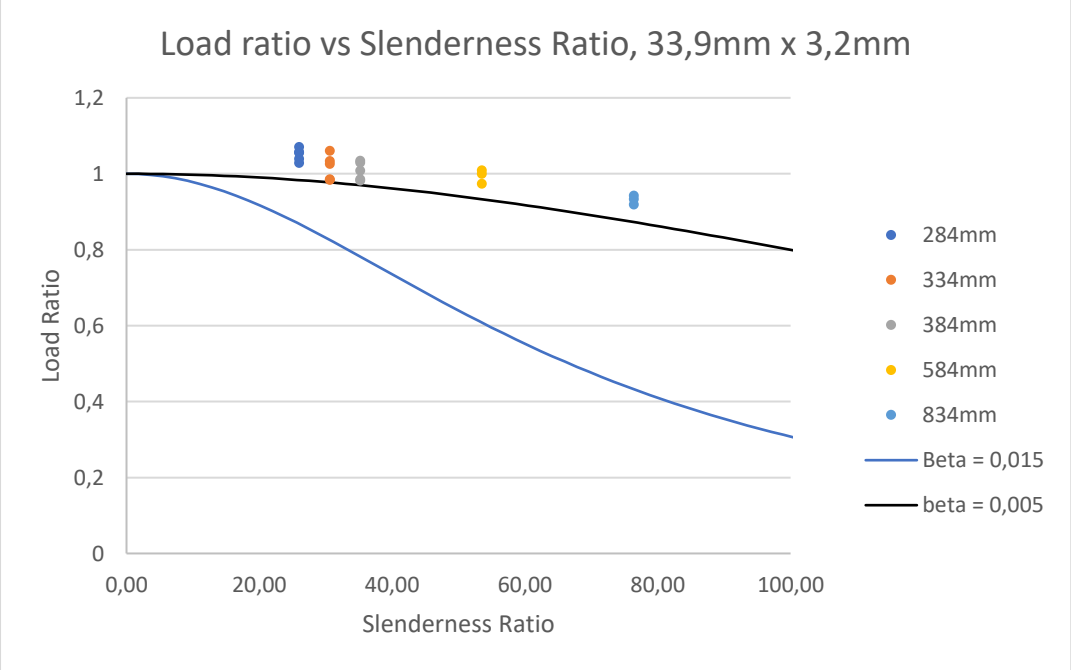
Load ratio vs Slenderness Ratio, 33,9mm x 3,2mm
1,2
1
0,8
0,6
0,4
0,2
0
Load Ratio
0,00
20,00
40,00
60,00
80,00
100,00
Slenderness Ratio
284mm
334mm
384mm
584mm
834mm
Beta = 0,015
beta = 0,005

48,5 mm x 3,9 mm results

48,5x3,9x200mm Experiments						
Sample	**Yield [kN]**	**Mpa**	**Max Force [kN]**	**Max Stress [Mpa]**	**Pb video [kN]**	**Pb video [kN] End rotation**
nr1	221,39	405,14	311,55	570,14	289,725	311,55
nr2	223,00	408,09	305,82	559,64	286,044	305,82
nr3	220,92	404,28	307,30	562,35	287,413	307,30
nr4	231,00	422,73	308,41	564,38	292,772	308,41
nr5	225,00	411,75	307,30	562,35	275,114	307,30
Average	224,26	410,40	308,07	563,77	286,2136	308,07

48,5x3,9x250mm Experiments						
Sample	**Yield [kN]**	**Mpa**	**Max Force [kN]**	**Max Stress [Mpa]**	**Pb video [kN]**	**Pb video [kN] End rotation**
nr1	221,00	404,4296	295,83	541,3683663	277,611	295,83
nr2	220,92	404,2832	285,19	521,8971855	244,966	285,19
nr3	223,40	408,8216	291,39	533,2431743	245,613	291,39
nr4	218,40	399,6716	285,47	522,409585	245,89	285,47
nr5	218,70	400,2206	285,19	521,8971855	243,579	285,19
Average	220,484	403,4853	288,614	528,1630993	251,5318	288,614

48,5x3,9x300mm Experiments						
Sample	**Yield [kN]**	**Mpa**	**Max Force [kN]**	**Max Stress [Mpa]**	**Pb video [kN]**	**Pb video [kN] End rotation**
nr1	220,91	404,26	251,35	459,96		
nr2	218,79	400,39	249,87	457,26		
nr3	221,01	404,46	250,79	458,95		
nr4	222,77	407,67	249,68	456,92	no video	no video
nr5	220,92	404,29	247,37	452,69		
nr6	224,92	411,61	261,98	479,43		
nr7	220,74	403,94	258,56	473,16		
Average	221,44	405,23	252,80	462,62	0	0

48,5x3,9x500mm Experiments						
Sample	**Yield [kN]**	**Mpa**	**Max Force [kN]**	**Max Stress [Mpa]**	**Pb video [kN]**	**Pb video [kN] End rotation**
nr1	227,00	415,41	242,65	444,06	240,249	242,65
nr2	222,77	407,67	244,23	446,93	239,047	244,23
nr3	222,40	406,99	243,49	445,58	243,308	243,49
Average	224,06	410,02	243,46	445,52	722,604	243,46

48,5x3,9x750mm Experiments						
Sample	**Yield [kN]**	**Mpa**	**Max Force [kN]**	**Max Stress [Mpa]**	**Pb video [kN]**	**Pb video [kN] End rotation**
nr1	218,14	399,20	237,66	434,92	230,631	237,66
nr2	217,96	398,87	241,17	441,35	240,157	241,17
nr3	218,70	400,22	232,02	424,59	229,892	232,02
Average	218,27	399,43	236,95	433,62	233,56	236,95

48,5mmx3,9mm Averages						
Sample	**Yield [kN]**	**Mpa**	**Max Force [kN]**	**Max Stress [Mpa]**	**Pb video [kN]**	**Pb video [kN] End rotation**
Total averag	221,7014	405,7132	265,9786593	486,7404666	373,47735	269,273332

200 mm graph = 284 mm unsupported buckling

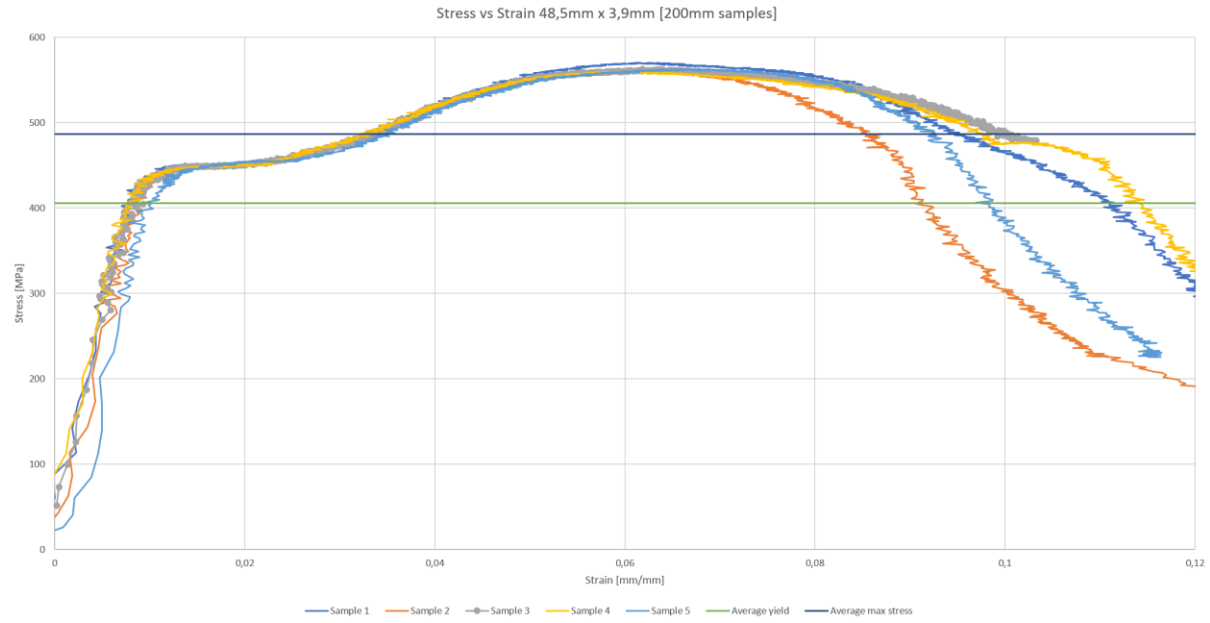

250 mm graph = 334 mm unsupported buckling

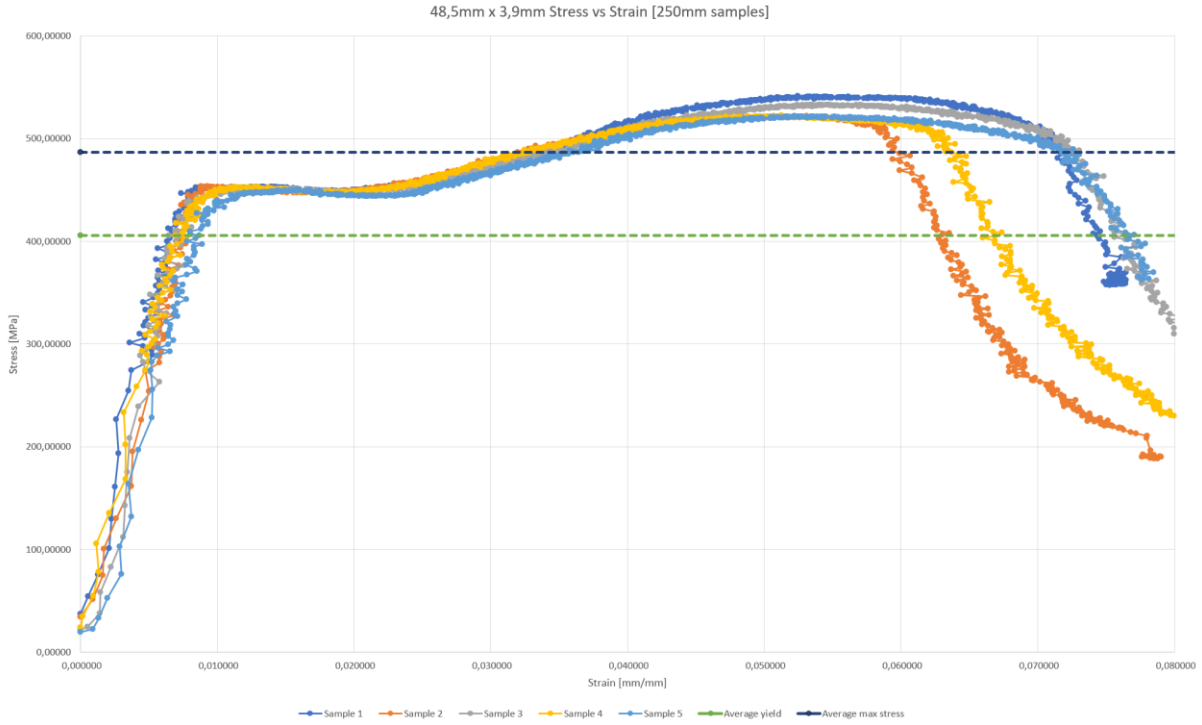

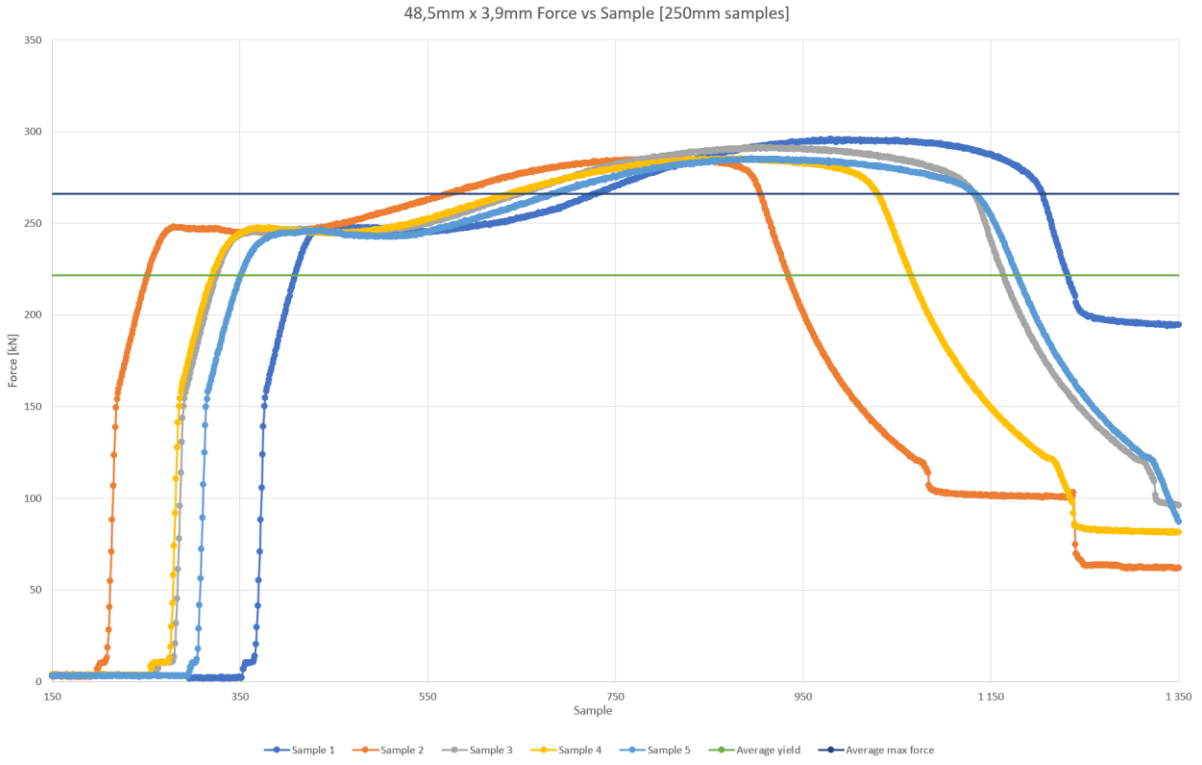

300 mm graph = 384 mm unsupported buckling

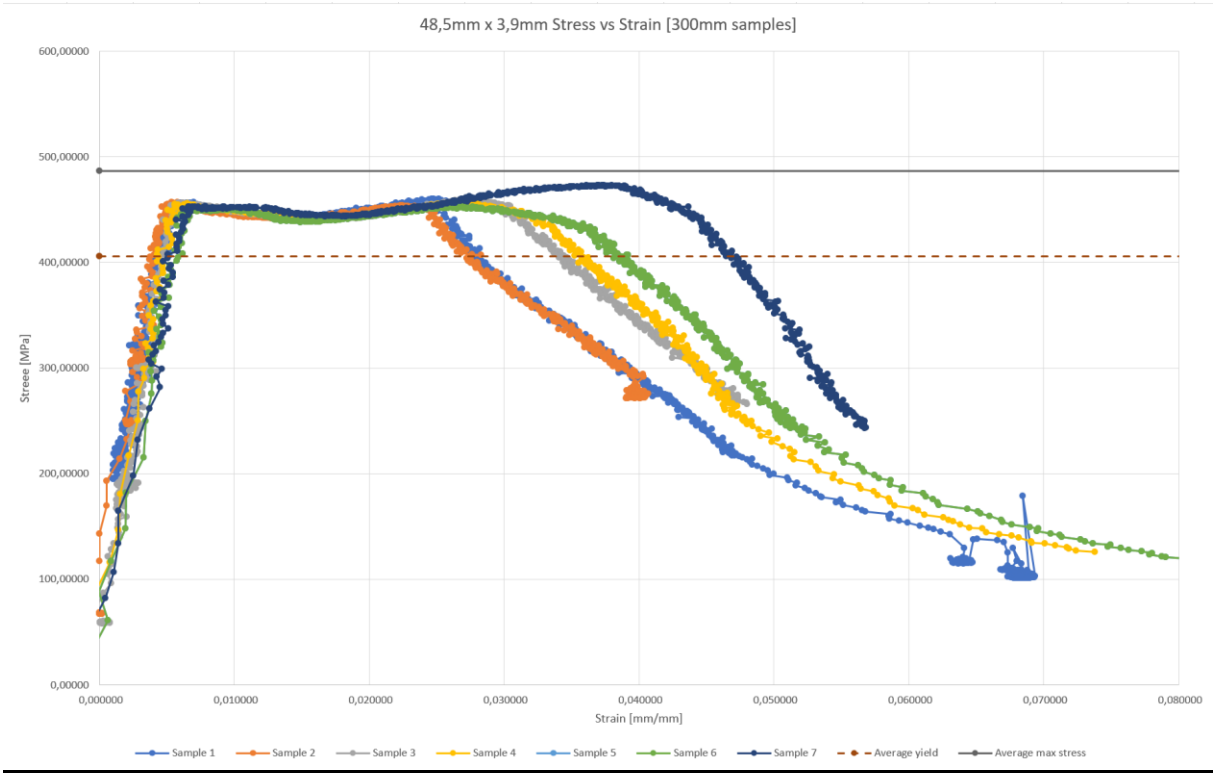

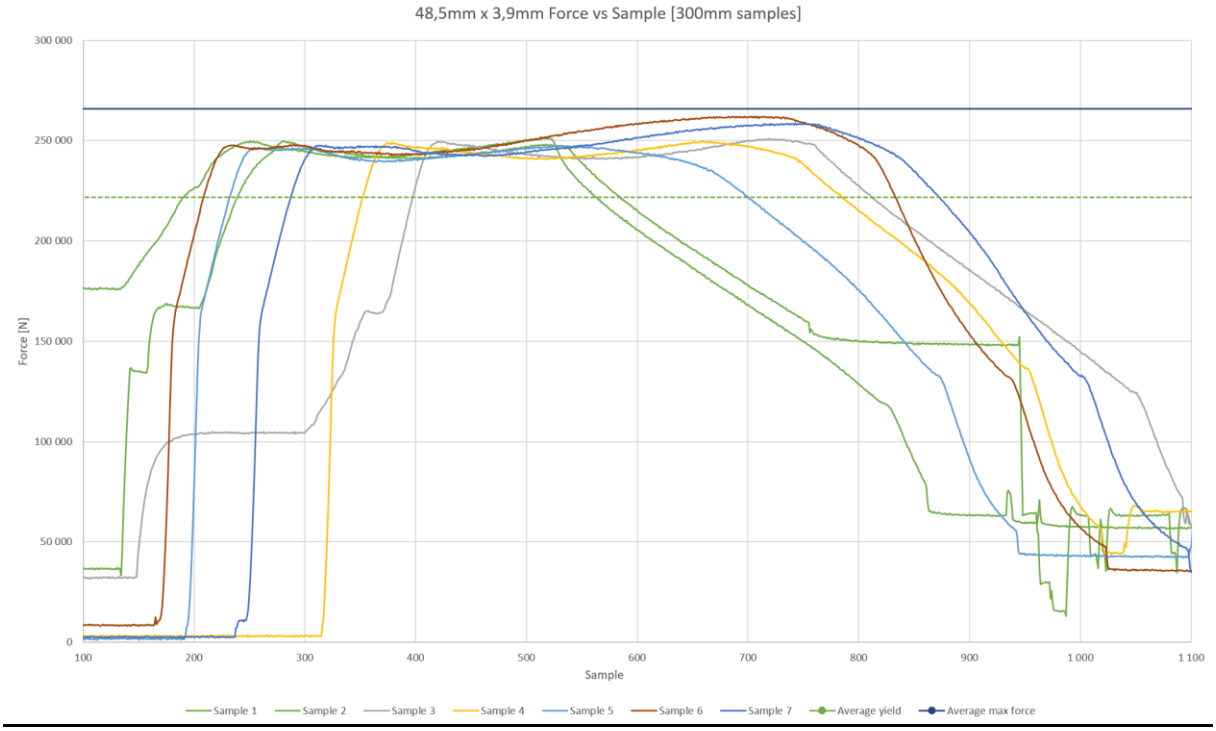

500 mm graph = 584 mm unsupported buckling

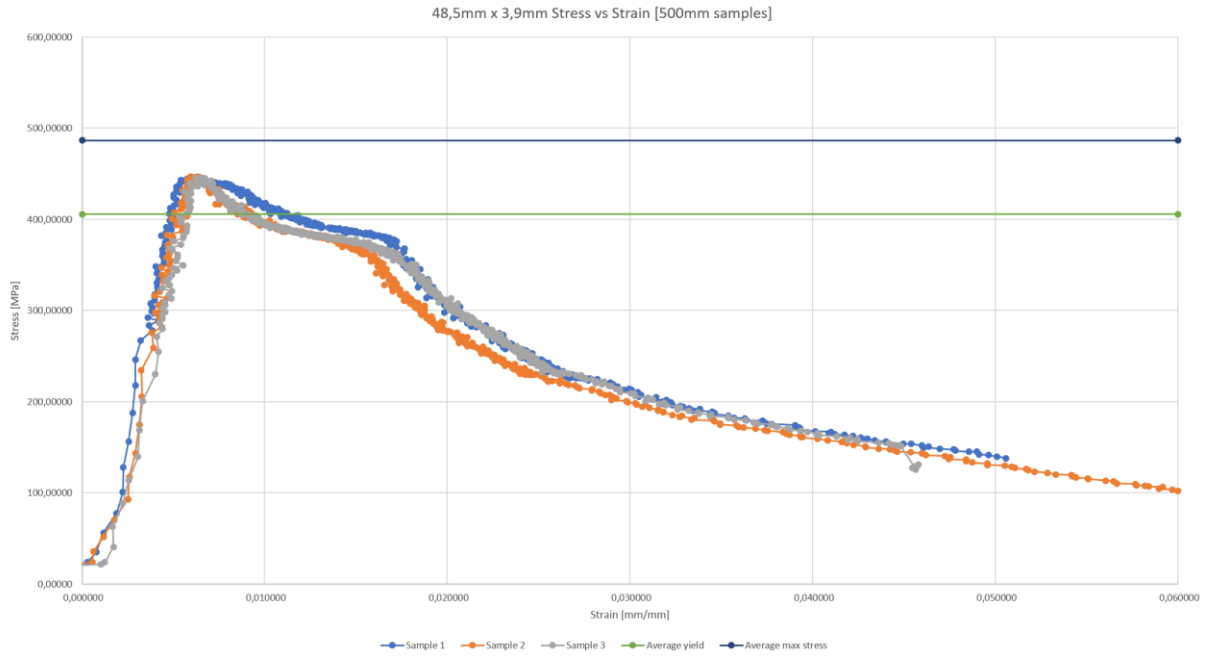

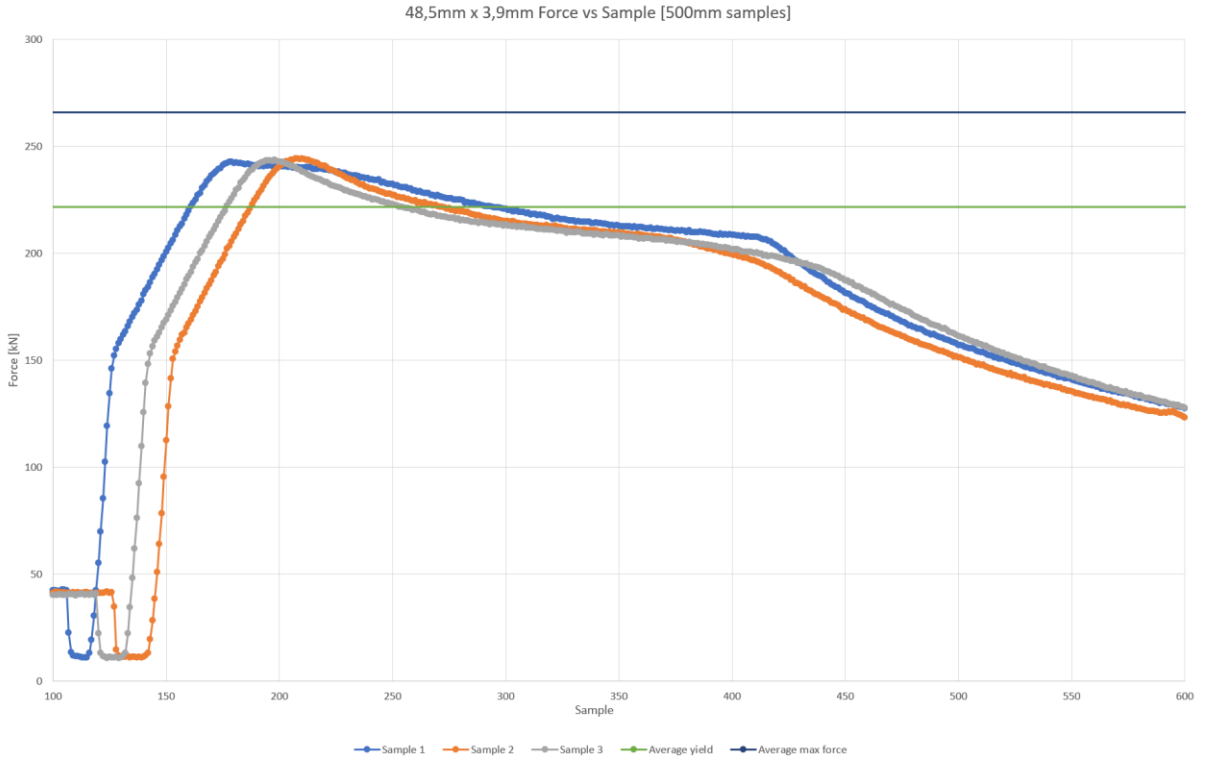

750 mm graph = 834 mm unsupported buckling

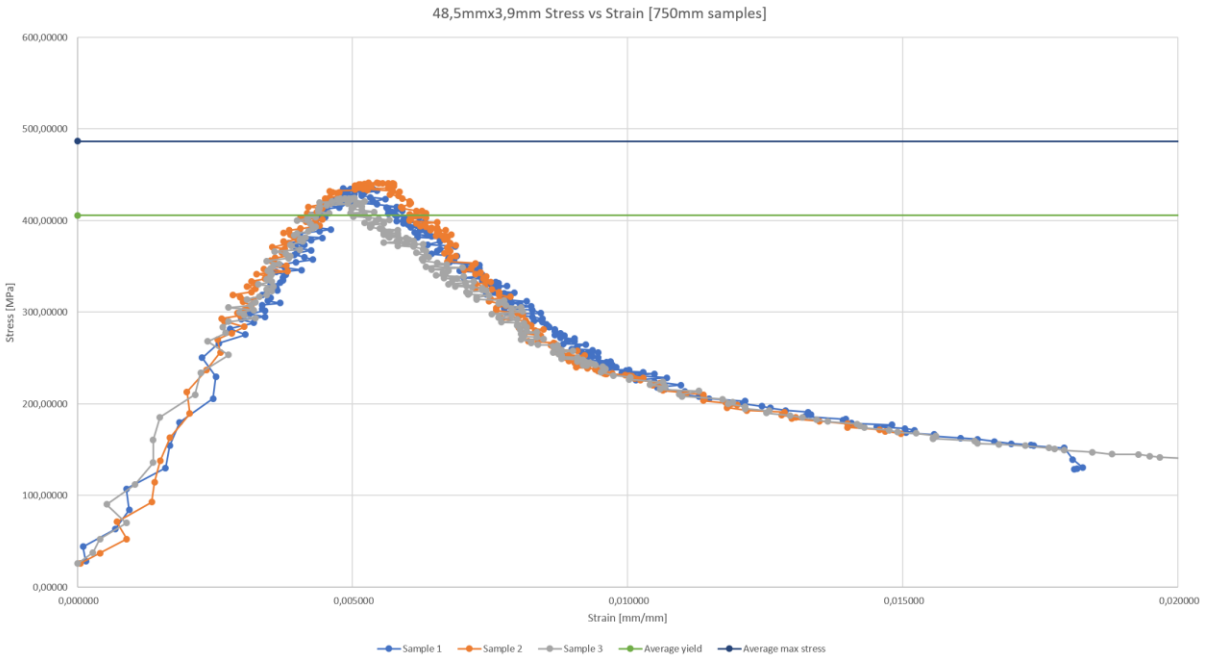

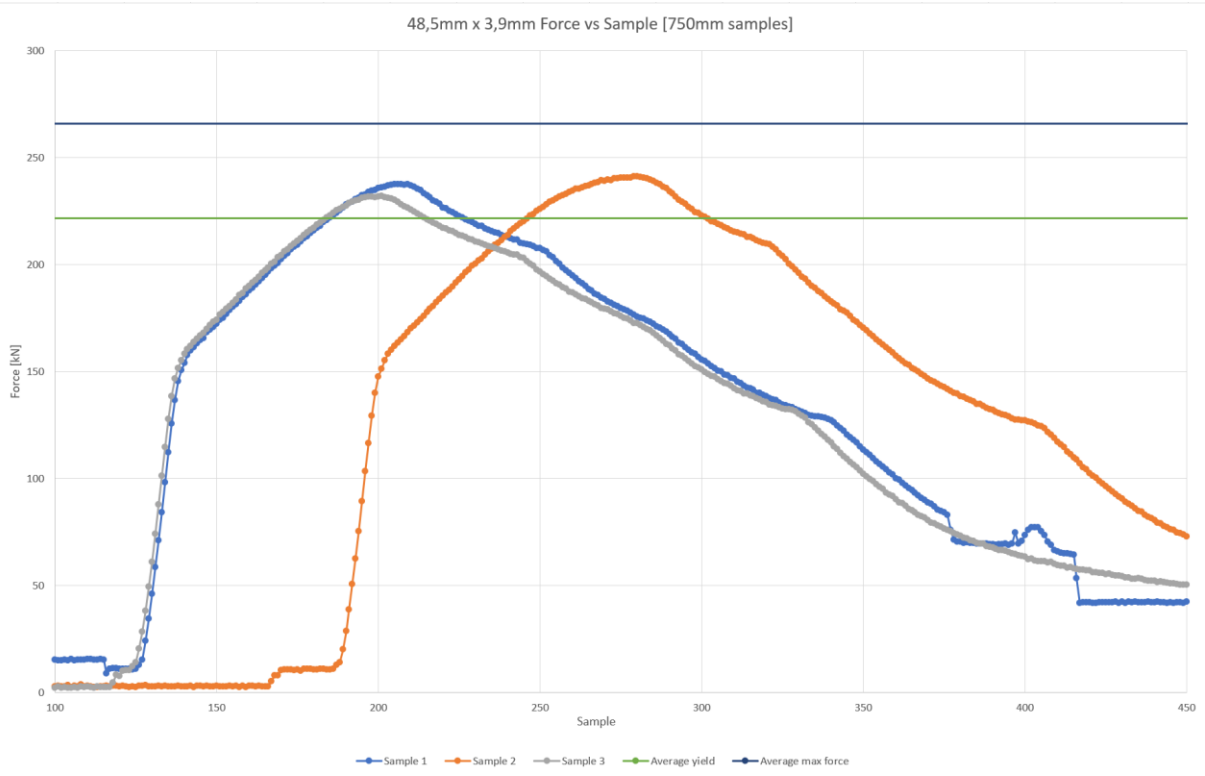

SR1 = SR2 = 182,5 mm unsupported length

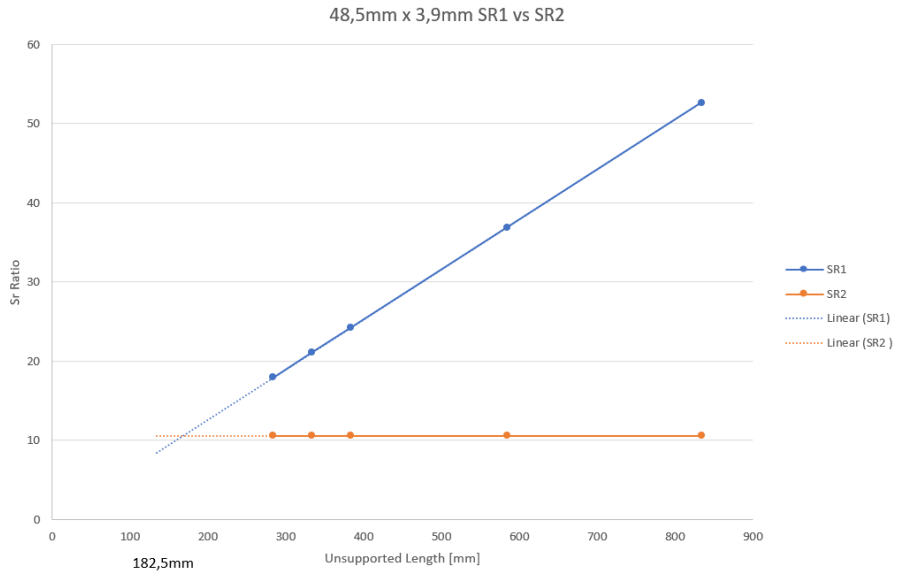

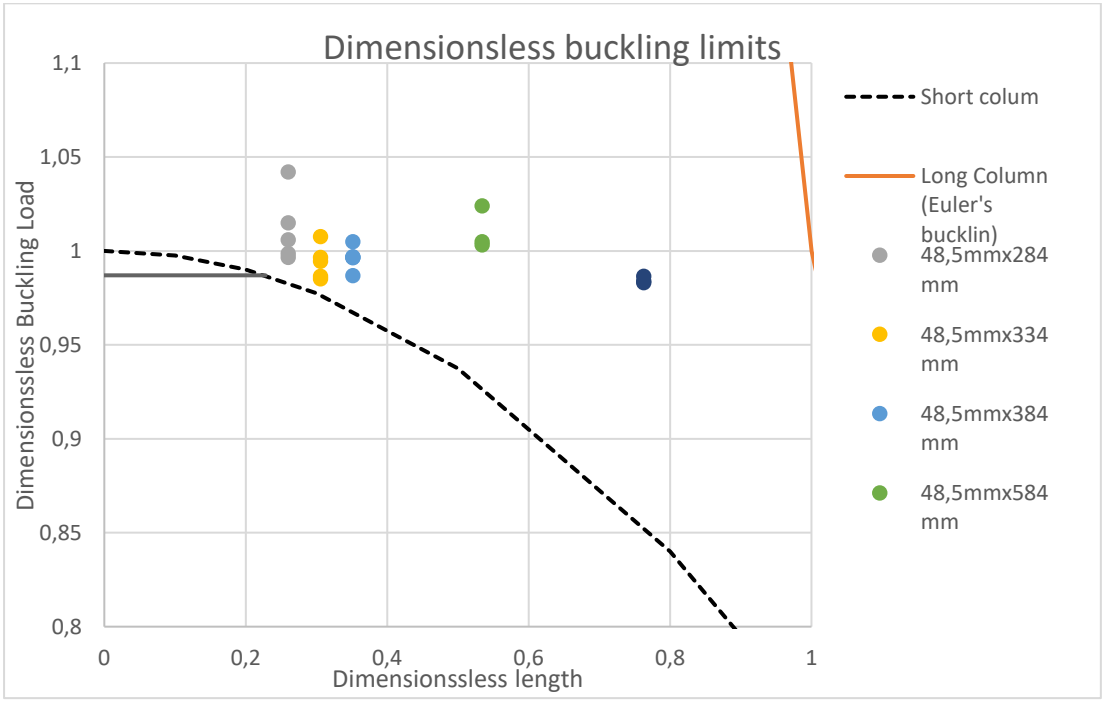

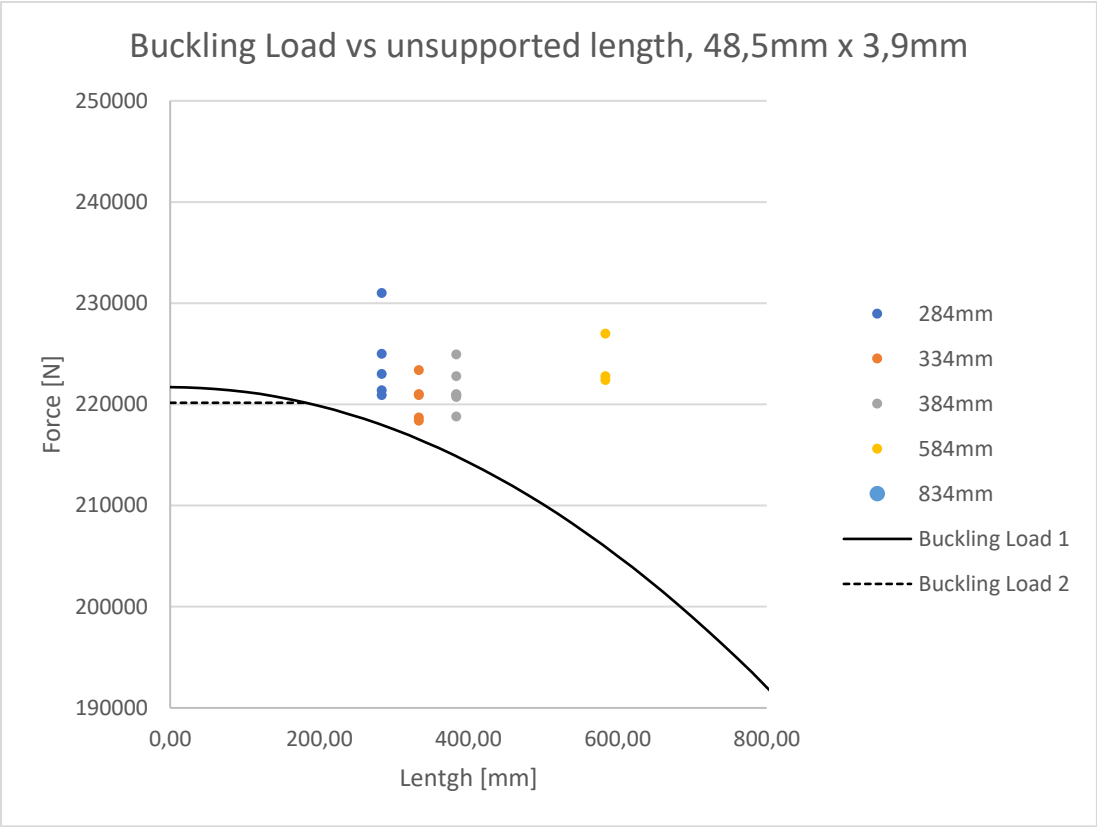
Buckling Load vs unsupported length, 48,5mm x 3,9mm
250000
240000
230000
220000
210000
200000
190000
Force [N]
0,00
200,00
400,00
600,00
800,00
Lentgh [mm]
284mm
334mm
384mm
584mm
834mm
Buckling Load 1
Buckling Load 2

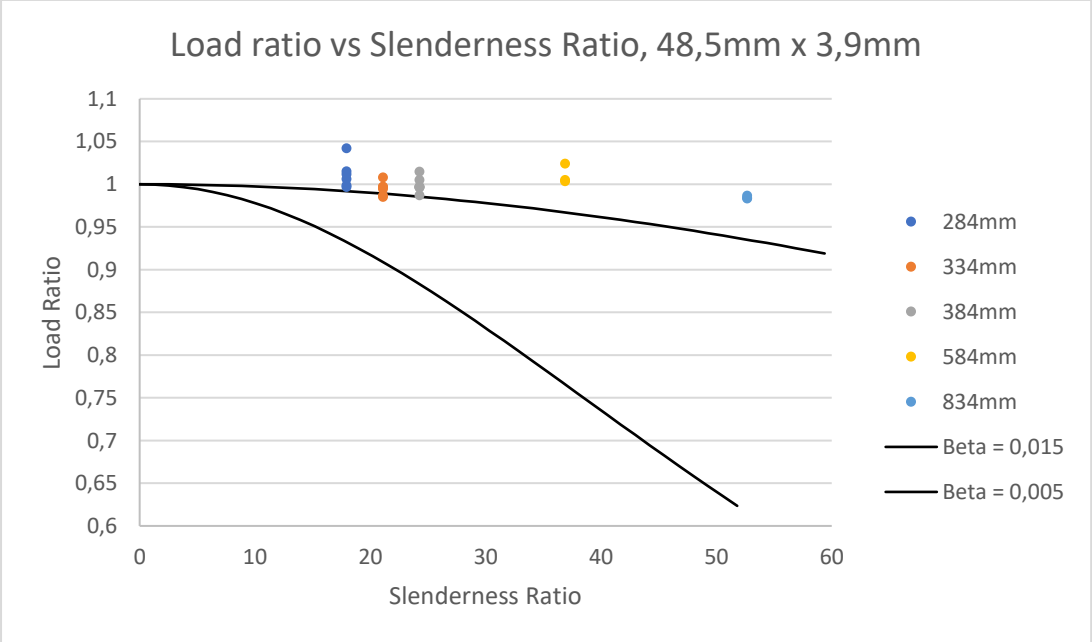
Load ratio vs Slenderness Ratio, 48,5mm x 3,9mm
1,1
1,05
1
0,95
0,9
0,85
0,8
0,75
0,7
0,65
0,6
Load Ratio
0
10
20
30
40
50
60
Slenderness Ratio
284mm
334mm
384mm
584mm
834mm
Beta = 0,015
Beta = 0,005

60,5 mm x 3,7 mm results

60,5x3,7x200mm Experiments						
Sample	**Yield [kN]**	**Mpa**	**Max Force [kN]**	**Max Stress [Mpa]**	**Pb video [kN]**	**Pb video [kN] End rotation**
nr1	222,00	336,24	288,43	436,86	No bending	No rotation
nr2	227,00	343,82	289,17	437,98	No bending	No rotation
Average	224,50	340,03	288,80	437,42	0	0

60,5x3,7x250mm Experiments						
Sample	**Yield [kN]**	**Mpa**	**Max Force [kN]**	**Max Stress [Mpa]**	**Pb video [kN]**	**Pb video [kN] End rotation**
nr1	228	345,33	295,83	448,06	266,328	295,83
nr2	220	333,21	283,81	429,86	No bending	No rotation
Average	224	339,27	289,82	438,96	133,164	289,82

60,5x3,7x300mm Experiments						
Sample	**Yield [kN]**	**Mpa**	**Max Force [kN]**	**Max Stress [Mpa]**	**Pb video [kN]**	**Pb video [kN] End rotation**
nr1	220,00	333,21	275,11	416,69	265,126	275,11
nr2	225,00	340,79	277,89	420,89	266,328	277,89
Average	222,50	337,00	276,50	418,79	265,727	276,50

60,5x3,7x500mm Experiments						
Sample	**Yield [kN]**	**Mpa**	**Max Force [kN]**	**Max Stress [Mpa]**	**Pb video [kN]**	**Pb video [kN] End rotation**
nr1	216,00	327,16	234,98	355,90	227,025	234,98
nr2	217,00	328,67	238,31	360,94	227,58	238,31
Average	216,50	327,91	236,64	358,42	227,30	236,64

60,5x3,7x750mm Experiments						
Sample	**Yield [kN]**	**Mpa**	**Max Force [kN]**	**Max Stress [Mpa]**	**Pb video [kN]**	**Pb video [kN] End rotation**
nr1	212,00	321,10	220,46	333,91	214,335	220,46
nr2	213,00	322,61	226,56	343,15	213,8	226,56
Average	212,50	321,85	223,51	338,53	214,06	223,51

60,5mmx3,7mm Averages						
Sample	**Yield [kN]**	**Mpa**	**Max Force [kN]**	**Max Stress [Mpa]**	**Pb video [kN]**	**Pb video [kN] End rotation**
Total average	220,00	333,21	263,05	398,42	168,05	263,05

200 mm graph = 332 mm unsupported length

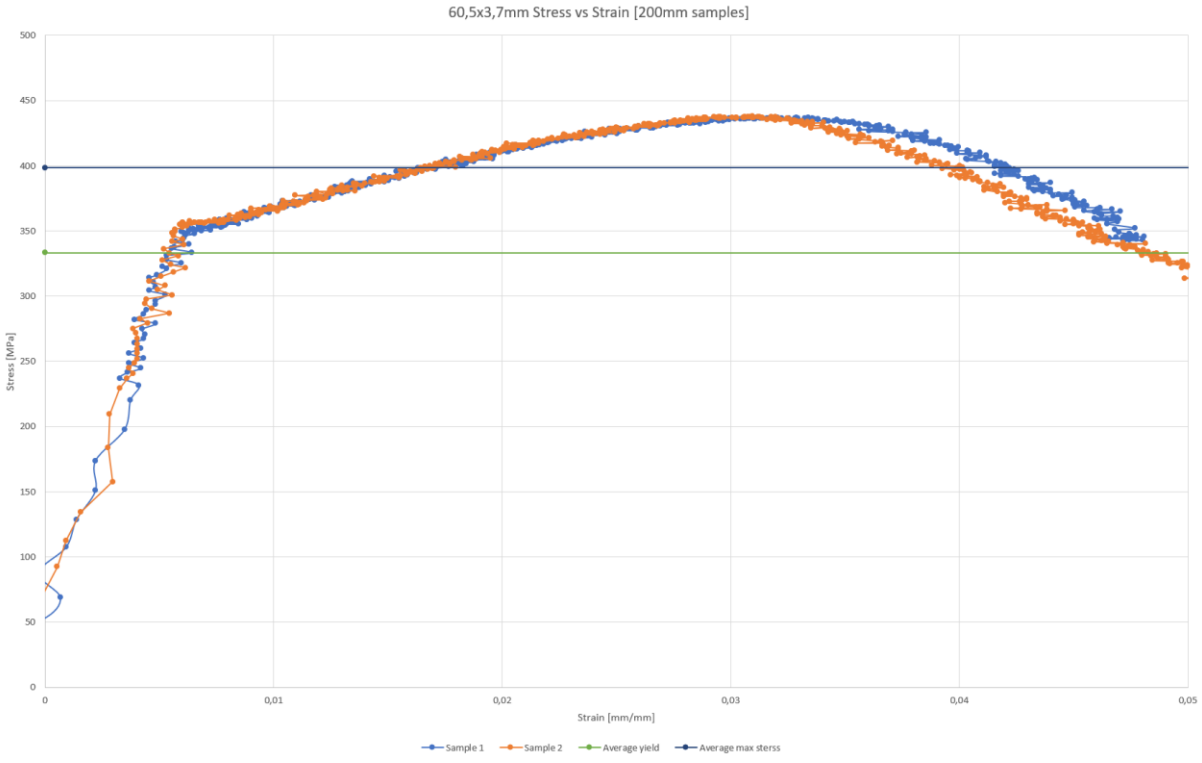

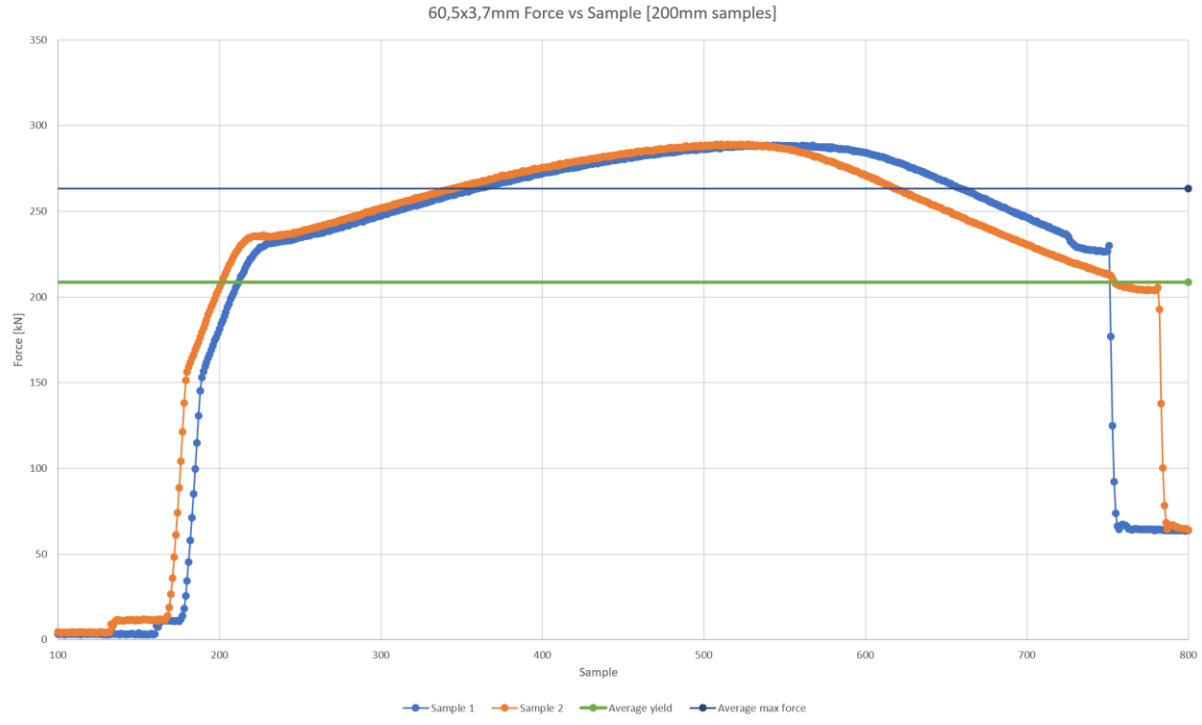

250 mm graph = 382 mm unsupported length

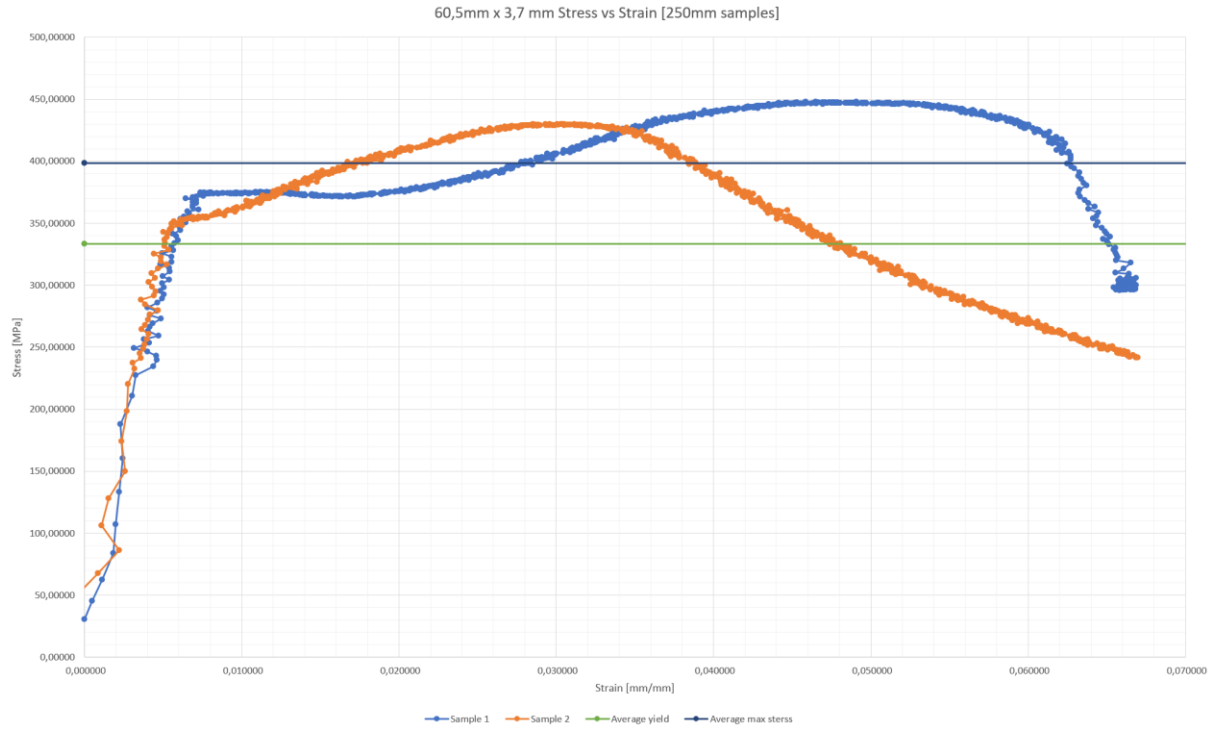

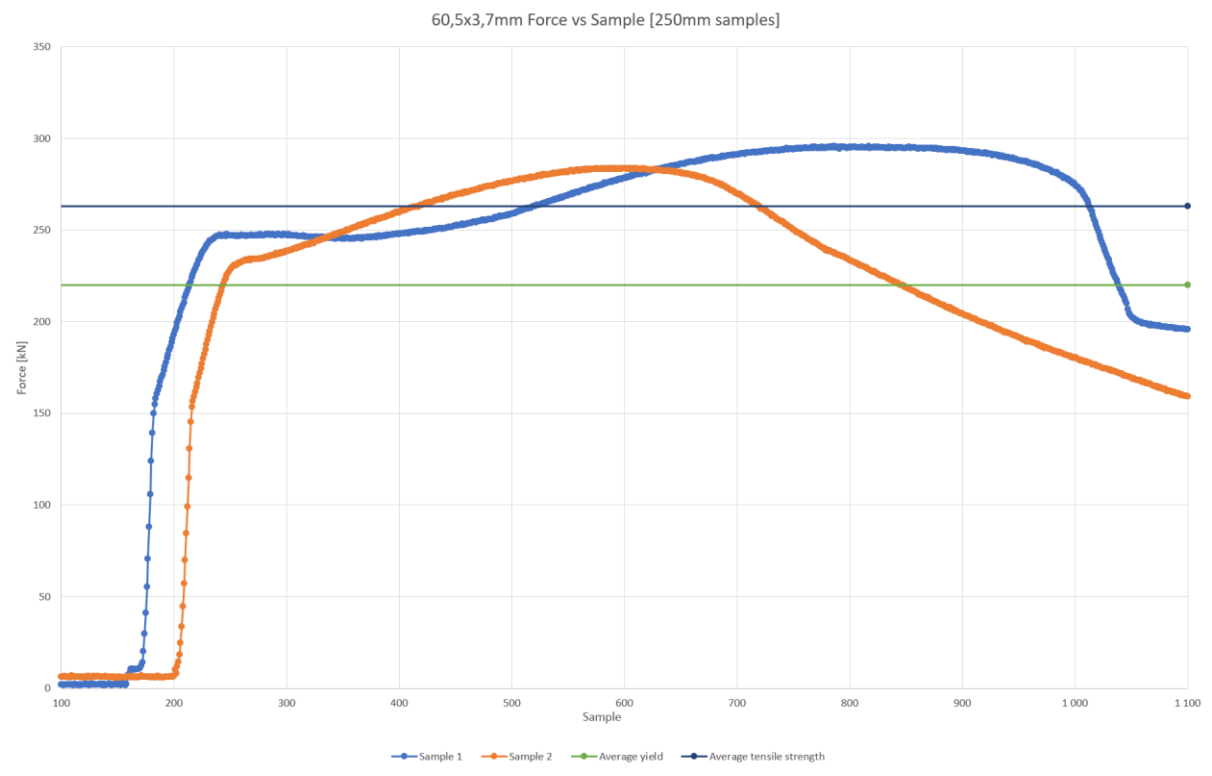

300 mm graph = 432 mm unsupported length

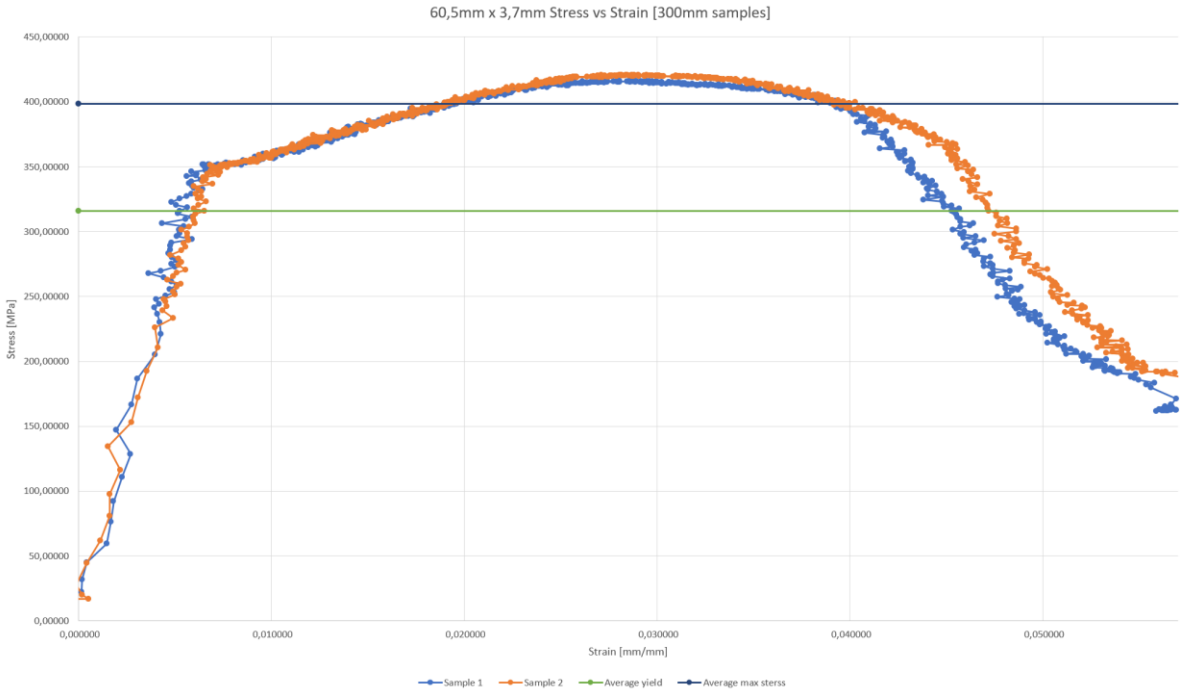

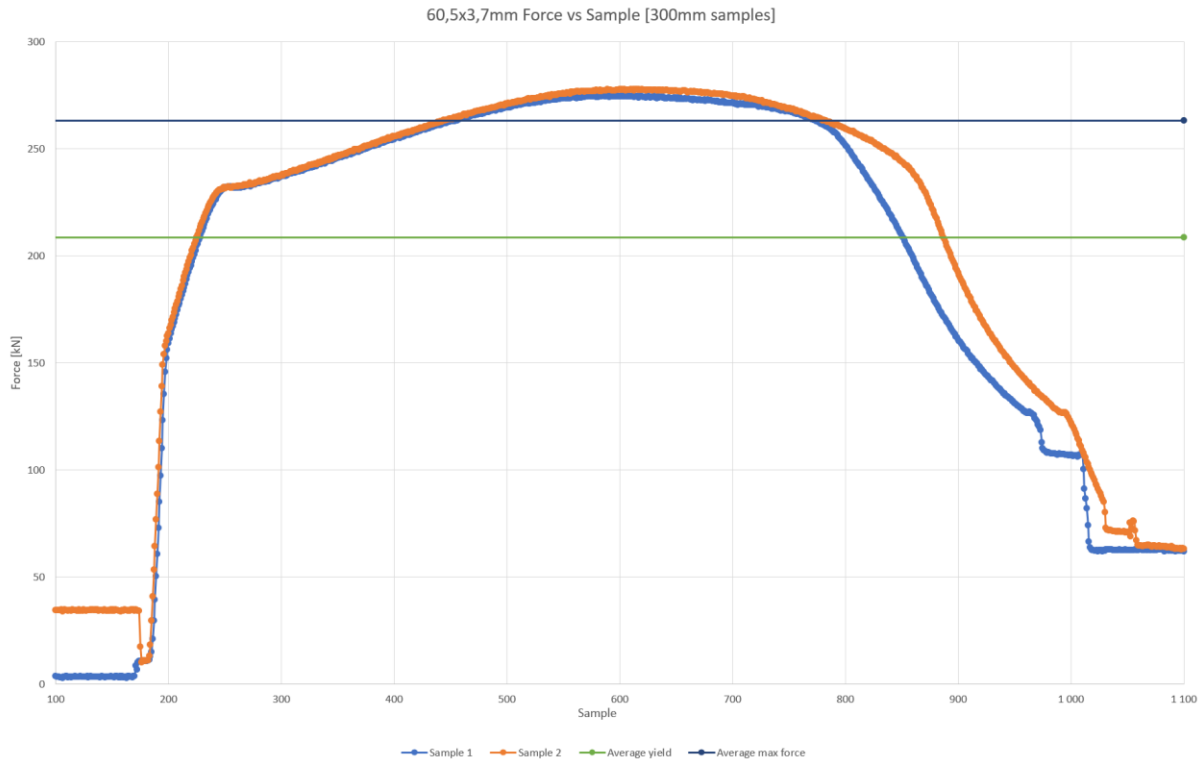

500 mm graph = 632 mm unsupported length

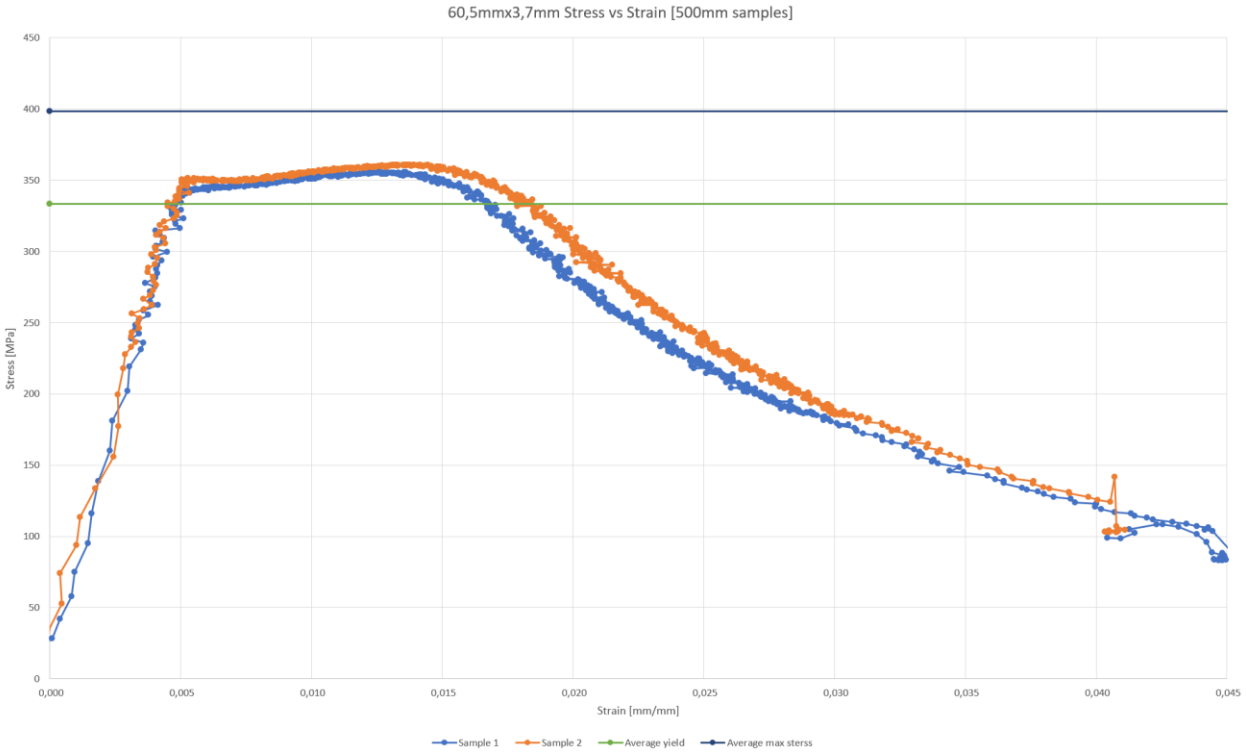

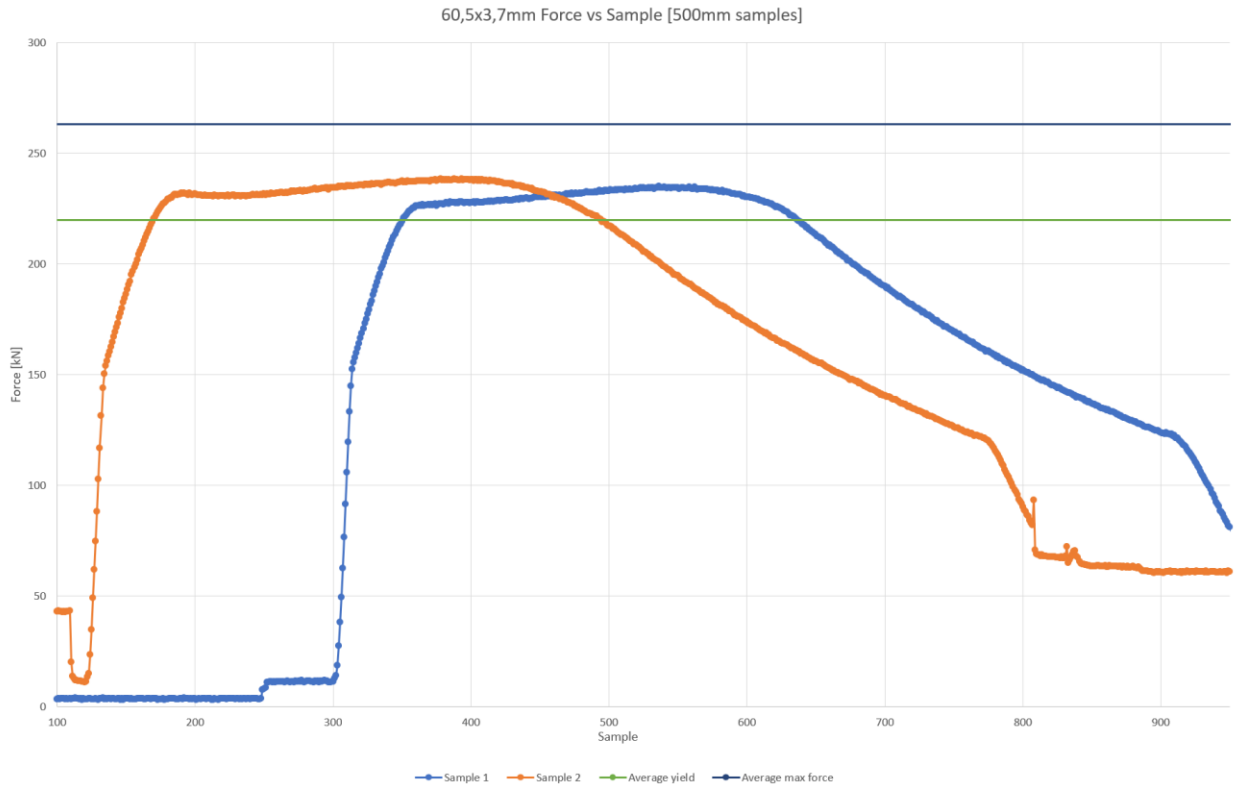

750 mm graph = 882 mm unsupported length

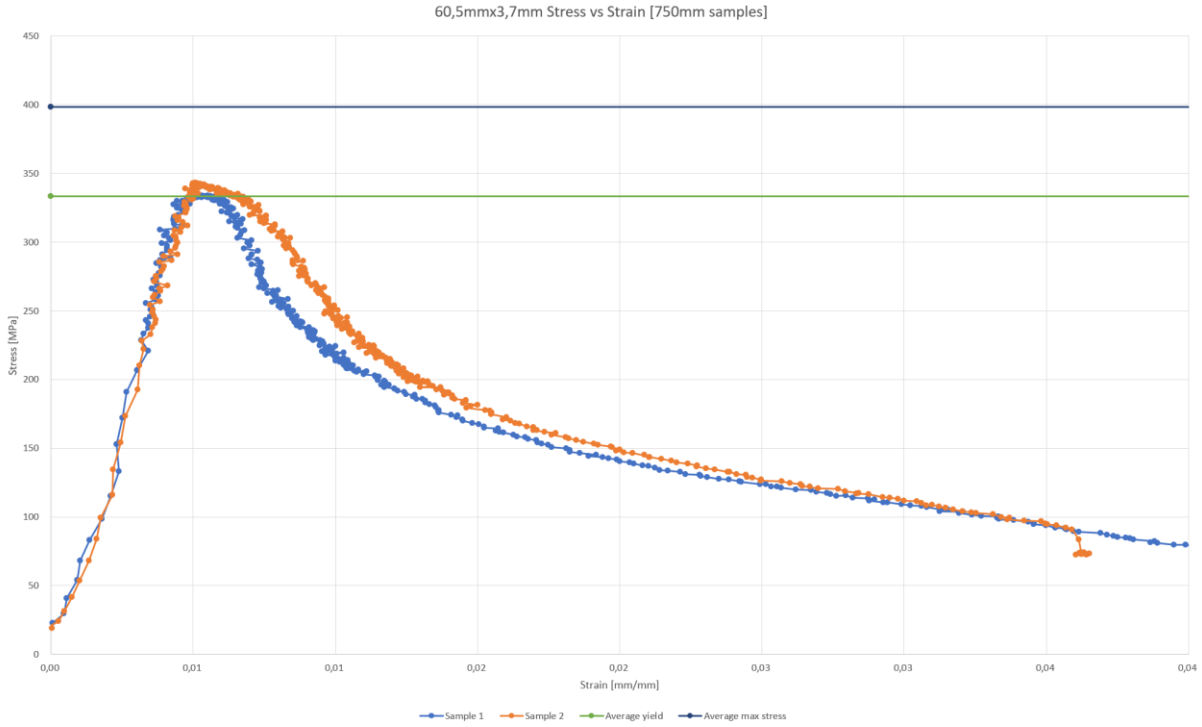

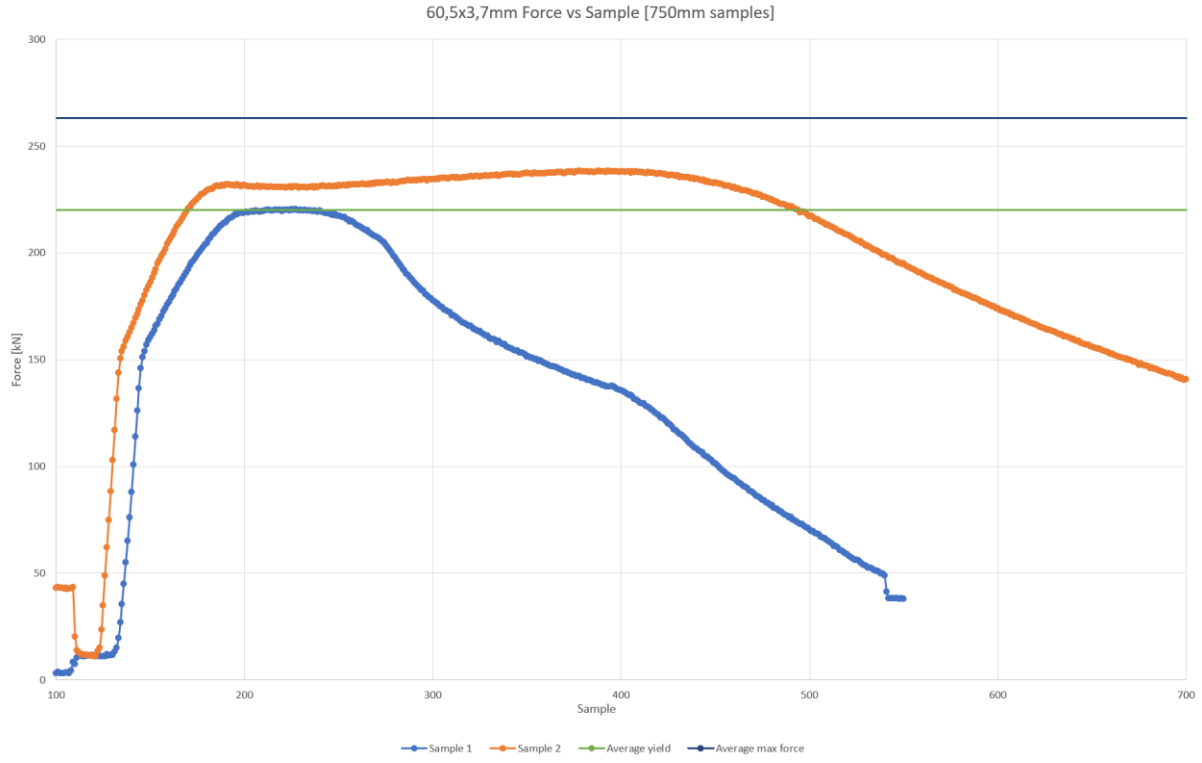

SR1 = SR2 = 269,3 mm unsupported length

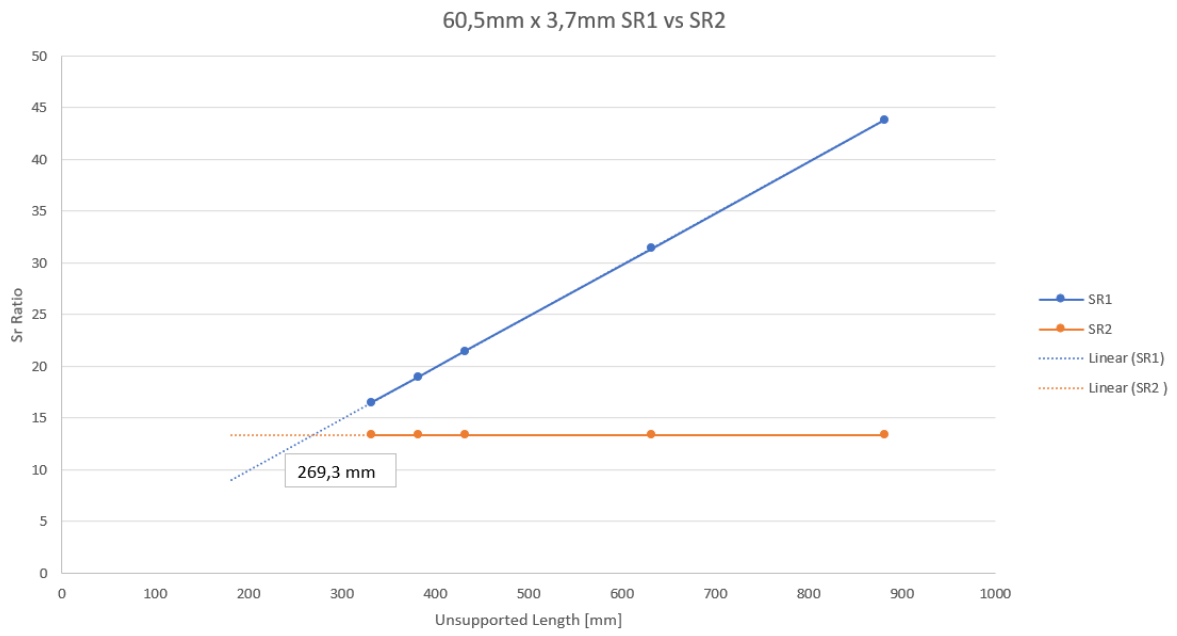

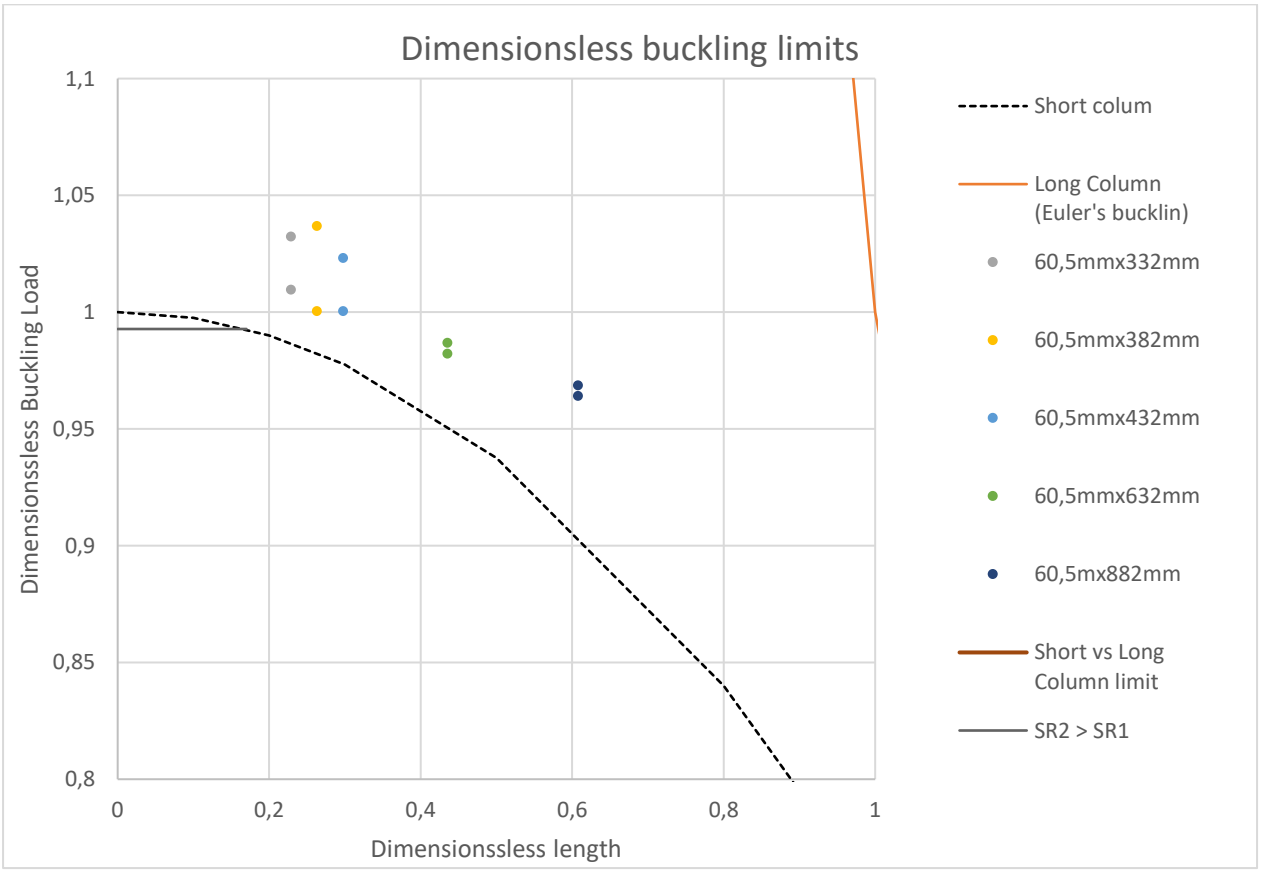

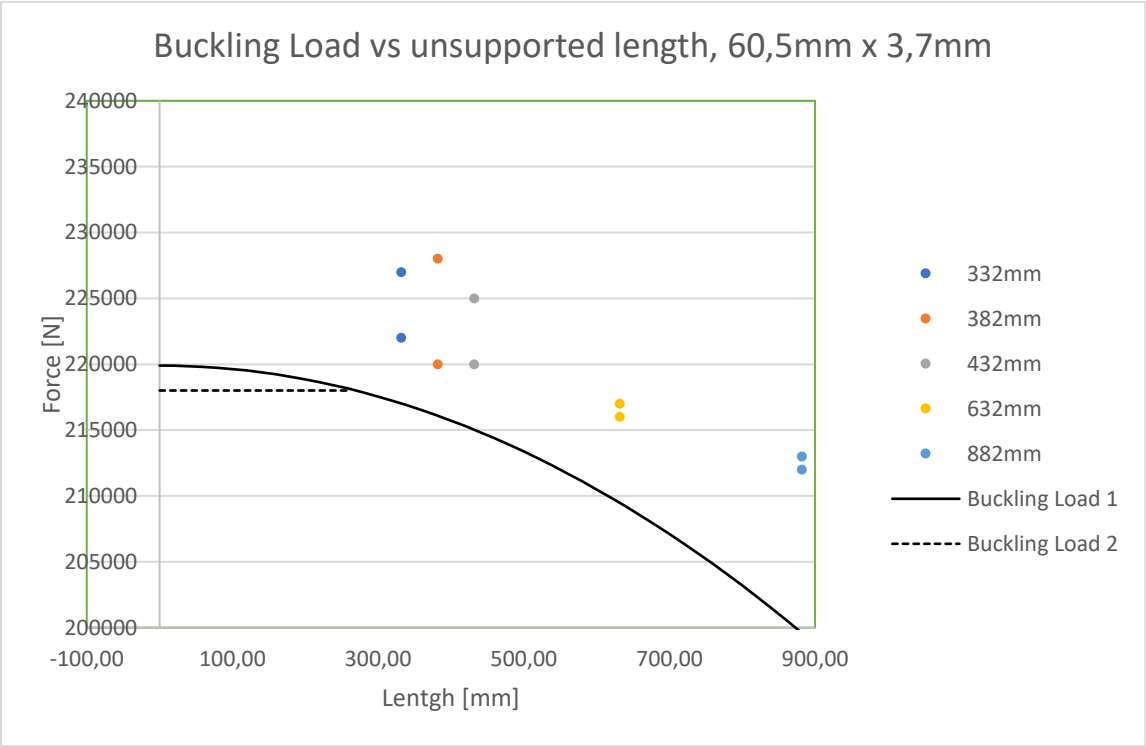
Buckling Load vs unsupported length, 60,5mm x 3,7mm
240000
235000
230000
225000
220000
215000
210000
205000
200000
Force [N]
-100,00
100,00
300,00
500,00
700,00
900,00
Lentgh [mm]
332mm
382mm
432mm
632mm
882mm
Buckling Load 1
Buckling Load 2

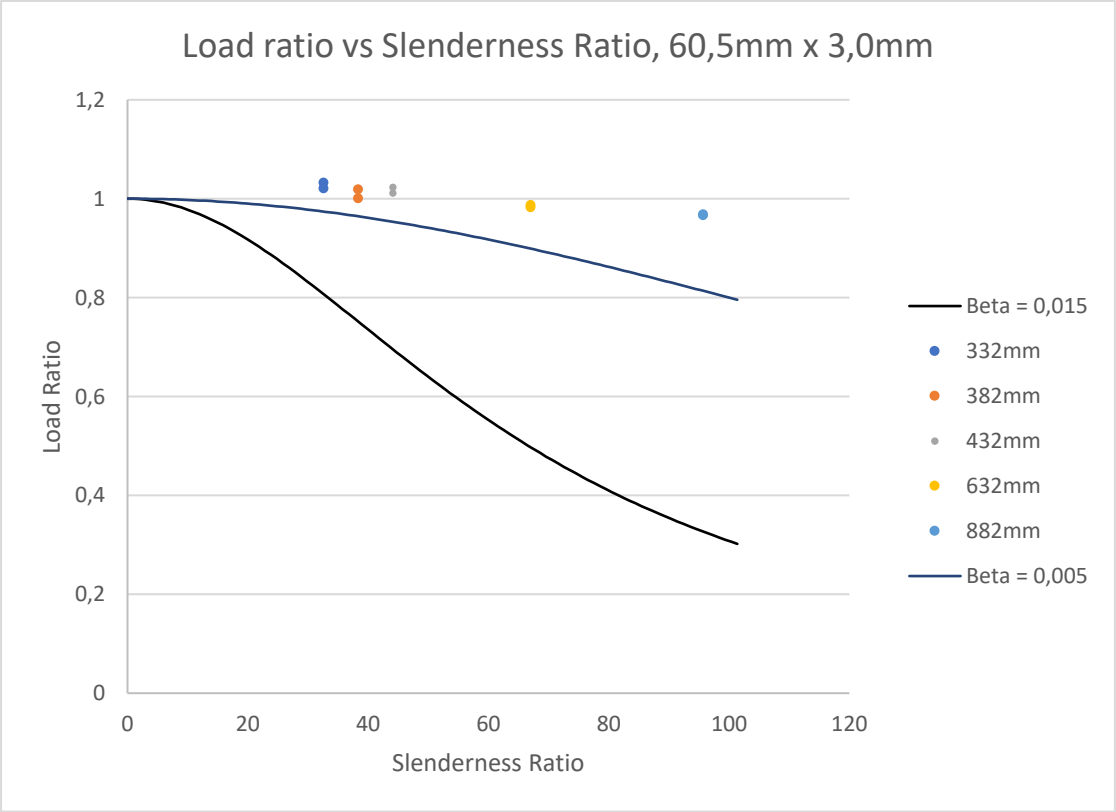
Load ratio vs Slenderness Ratio, 60,5mm x 3,0mm
1,2
1
0,8
0,6
0,4
0,2
0
Load Ratio
0
20
40
60
80
100
120
Slenderness Ratio
Beta = 0,015
332mm
382mm
432mm
632mm
882mm
Beta = 0,005

89,1 mm x 3,0 mm results

89,1x3,0x200mm Experiments						
Sample	**Yield [kN]**	**Mpa**	**Max Force [kN]**	**Max Stress [Mpa]**	**Pb video [kN]**	**Pb video [kN] End rotation**
nr1	313,67	386,54	329,12	405,59	No bending	No rotation
nr2	322,55	397,49	329,21	405,70	No bending	No rotation
Average	318,11	392,01	329,17	405,64	0	0

89,1x3,0x250mm Experiments						
Sample	**Yield [kN]**	**Mpa**	**Max Force [kN]**	**Max Stress [Mpa]**	**Pb video [kN]**	**Pb video [kN] End rotation**
nr1	305,63	376,64	326,62	402,51	No bending	No rotation
nr2	309,88	381,87	326,07	401,82	No bending	No rotation
Average	307,76	379,25	326,35	402,17	0	0

89,1x3,0x300mm Experiments						
Sample	**Yield [kN]**	**Mpa**	**Max Force [kN]**	**Max Stress [Mpa]**	**Pb video [kN]**	**Pb video [kN] End rotation**
nr1	308,86	380,62	329,31	405,81	No bending	No rotation
nr2	303,86	374,45	329,31	405,81	No bending	No rotation
Average	306,36	377,54	329,31	405,81	0	0

89,1x3,0x500mm Experiments						
Sample	**Yield [kN]**	**Mpa**	**Max Force [kN]**	**Max Stress [Mpa]**	**Pb video [kN]**	**Pb video [kN] End rotation**
nr1	304,50	375,24	327,55	403,65	317,839	327,55
nr2	300,36	370,14	327,92	404,10	318,04	327,92
Average	302,43	372,69	327,73	403,88	317,94	327,73

89,1x3,0x750mm Experiments						
Sample	**Yield [kN]**	**Mpa**	**Max Force [kN]**	**Max Stress [Mpa]**	**Pb video [kN]**	**Pb video [kN] End rotation**
nr1	294,40	362,80	323,48	398,63	317,562	323,48
nr2	299,71	369,34	323,02	398,06	314,972	323,02
Average	297,06	366,07	323,25	398,35	316,267	323,25

89,1mmx3,0mm Averages						
Sample	**Yield [kN]**	**Mpa**	**Max Force [kN]**	**Max Stress [Mpa]**	**Pb video [kN]**	**Pb video [kN] End rotation**
Total average	306,34	377,51	327,16	403,17	317,10	327,16

200 mm graph = 332 mm unsupported length

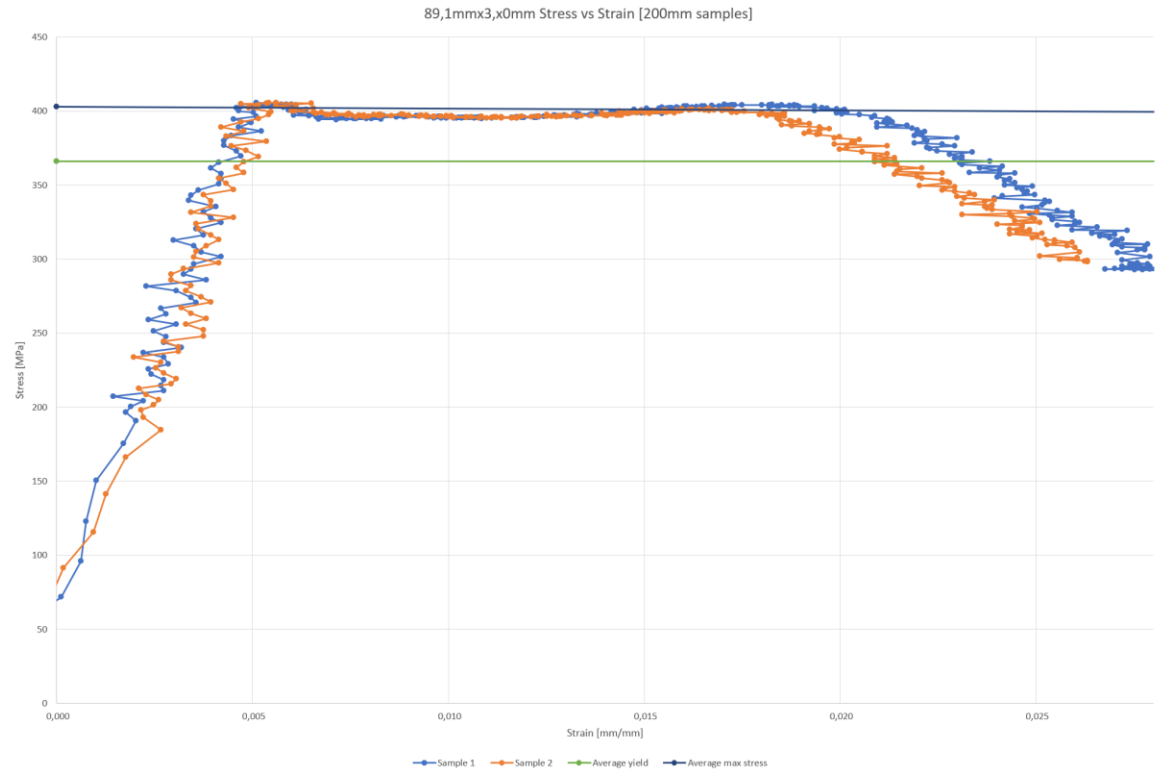

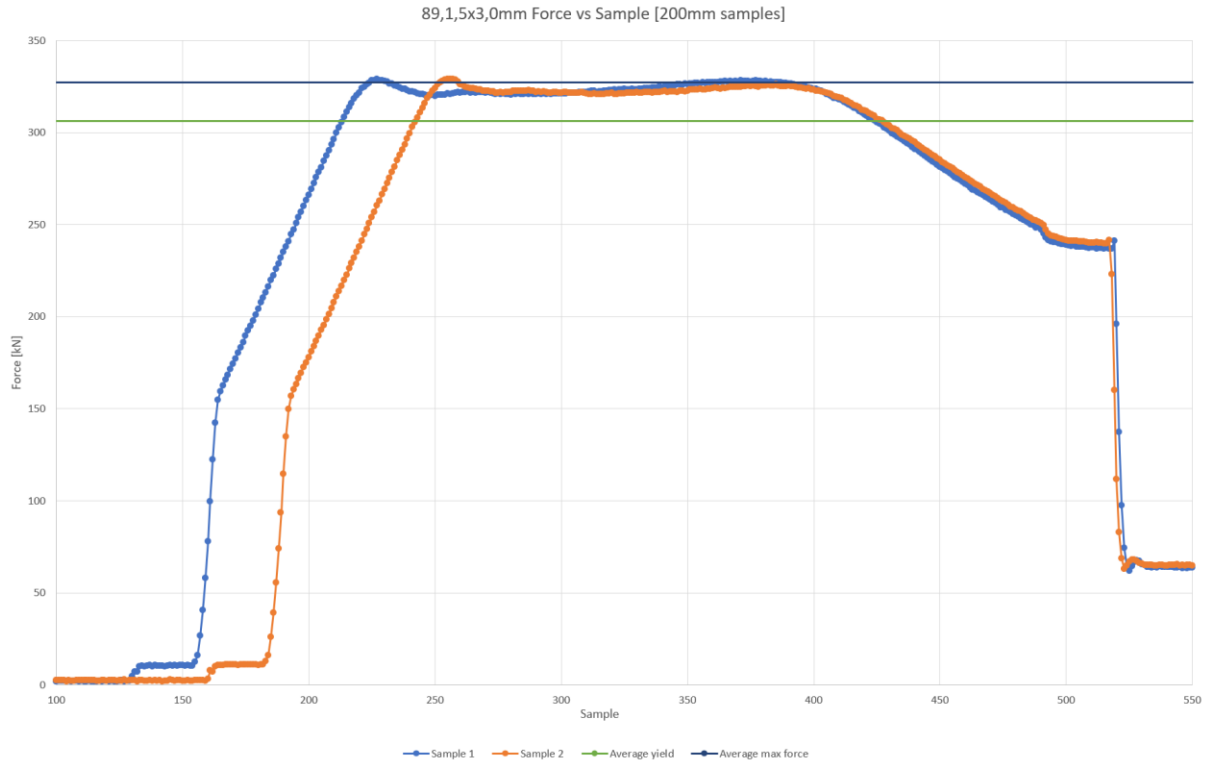

250 mm graph = 382 mm unsupported length

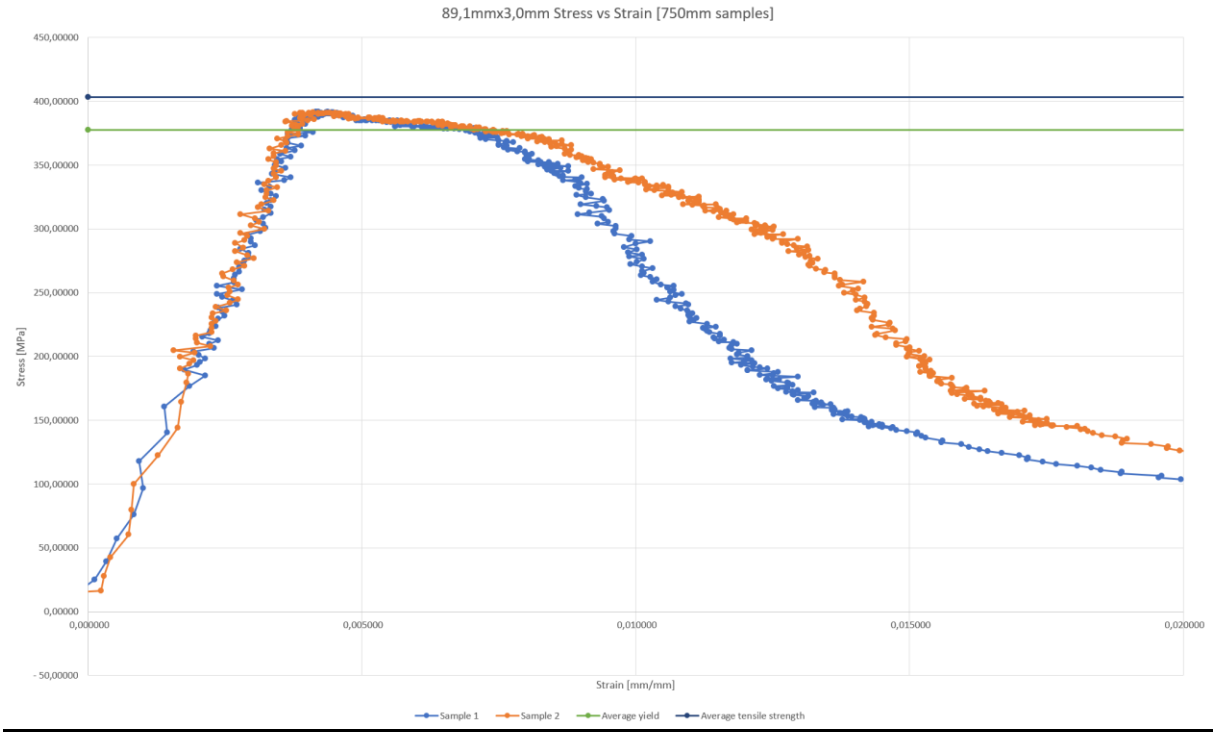

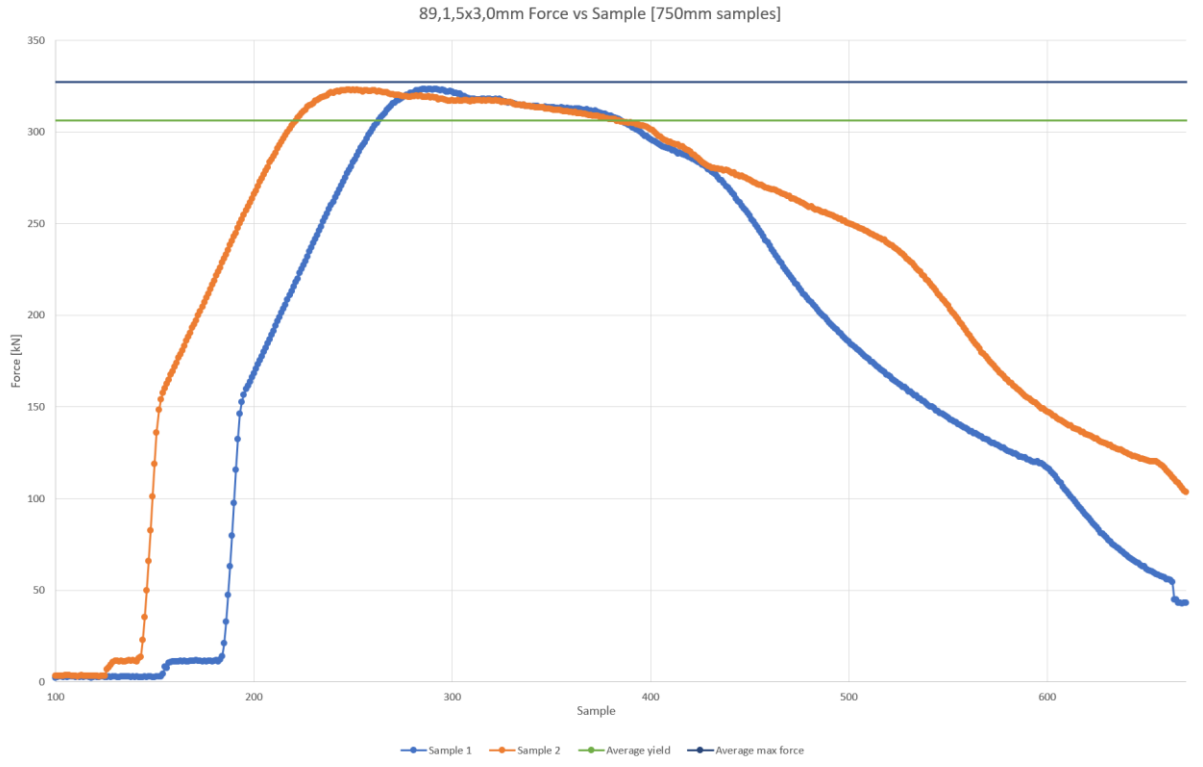

300 mm graph = 432 mm unsupported length

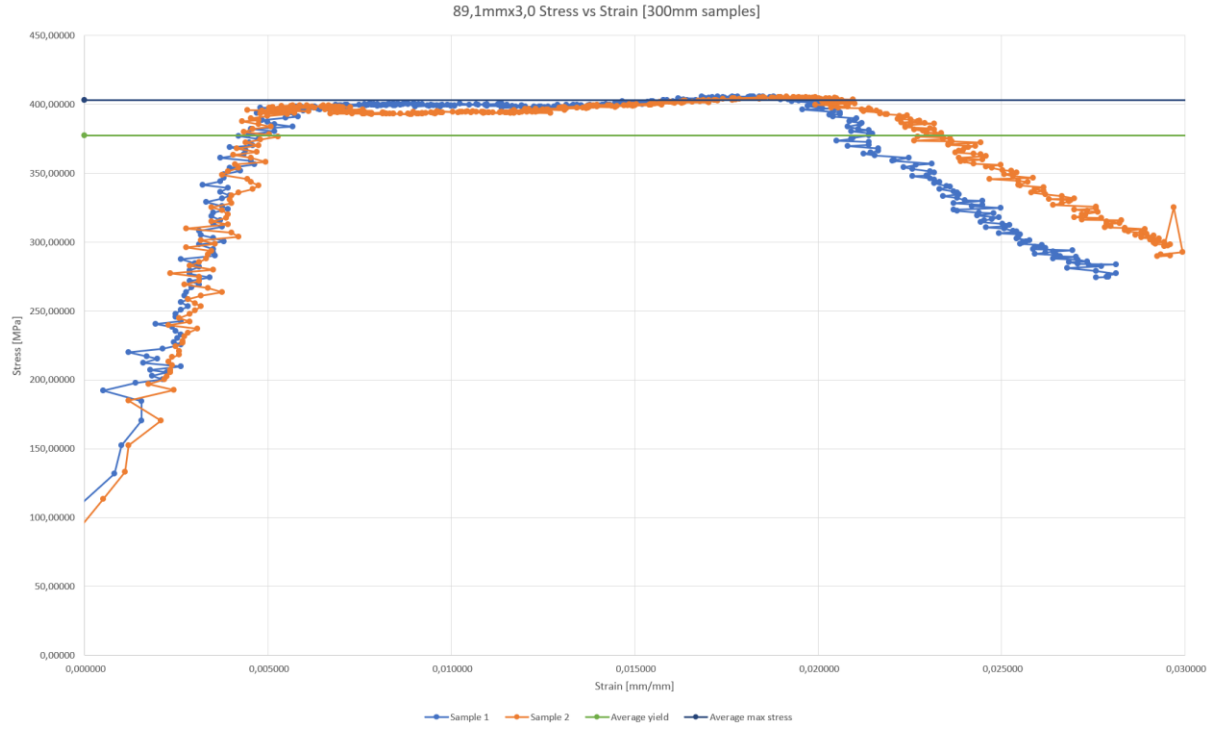

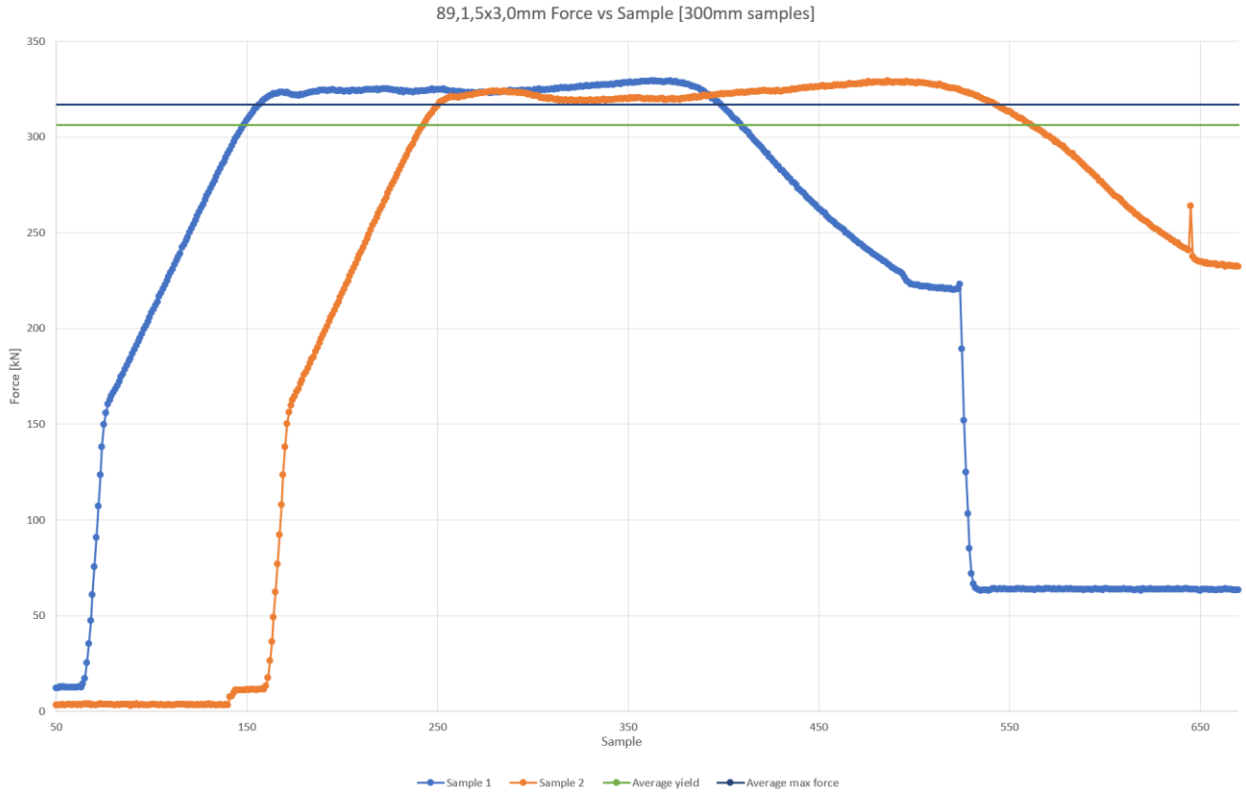

500 mm graph = 632 mm unsupported length

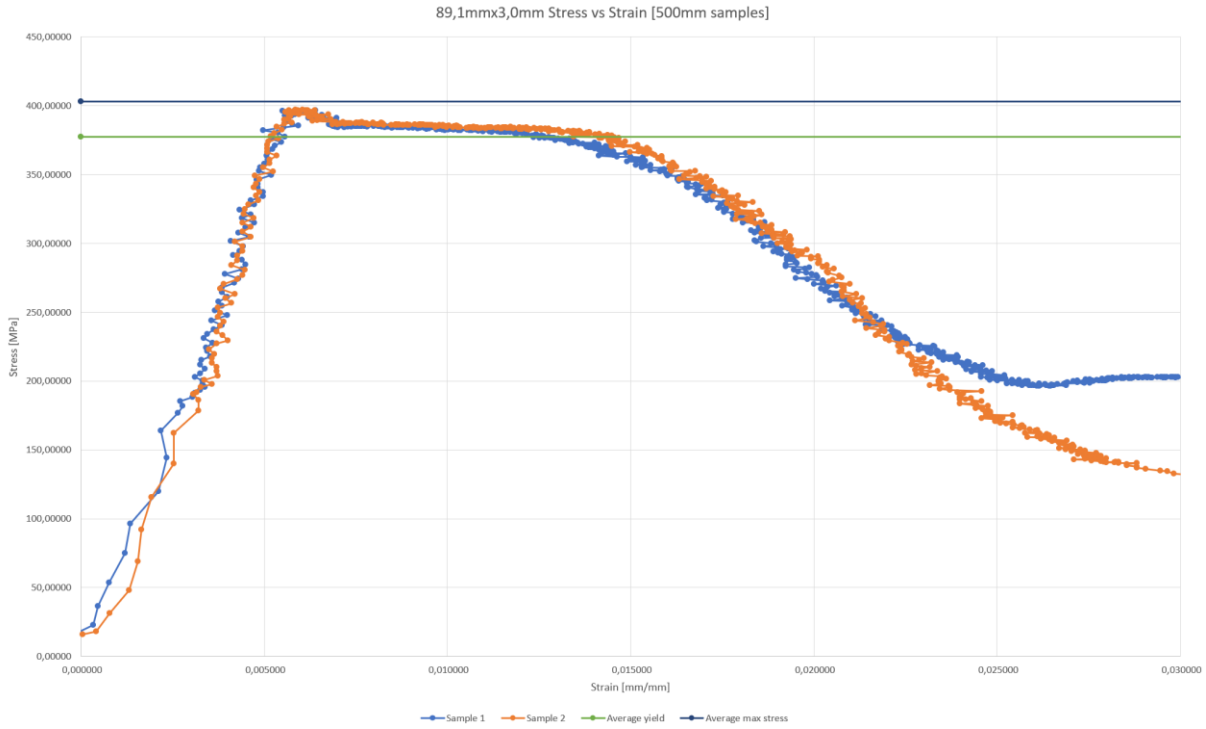

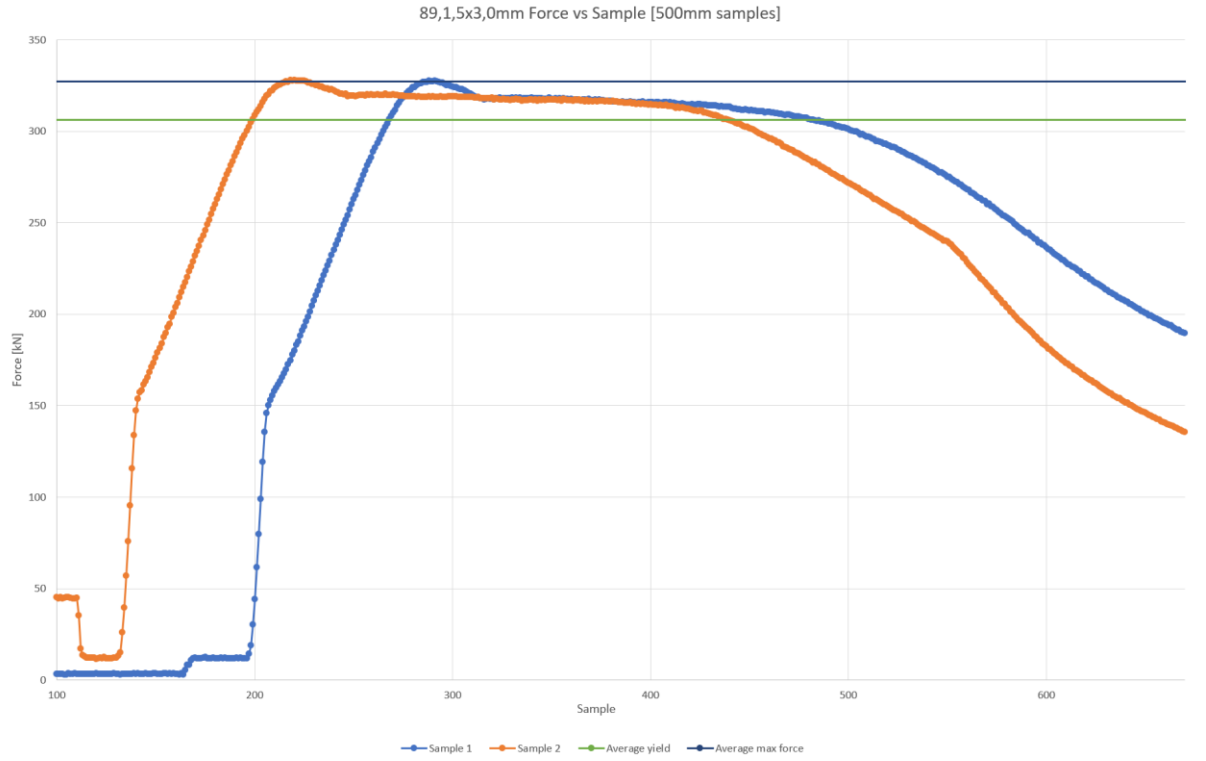

750 mm graph = 882 mm unsupported length

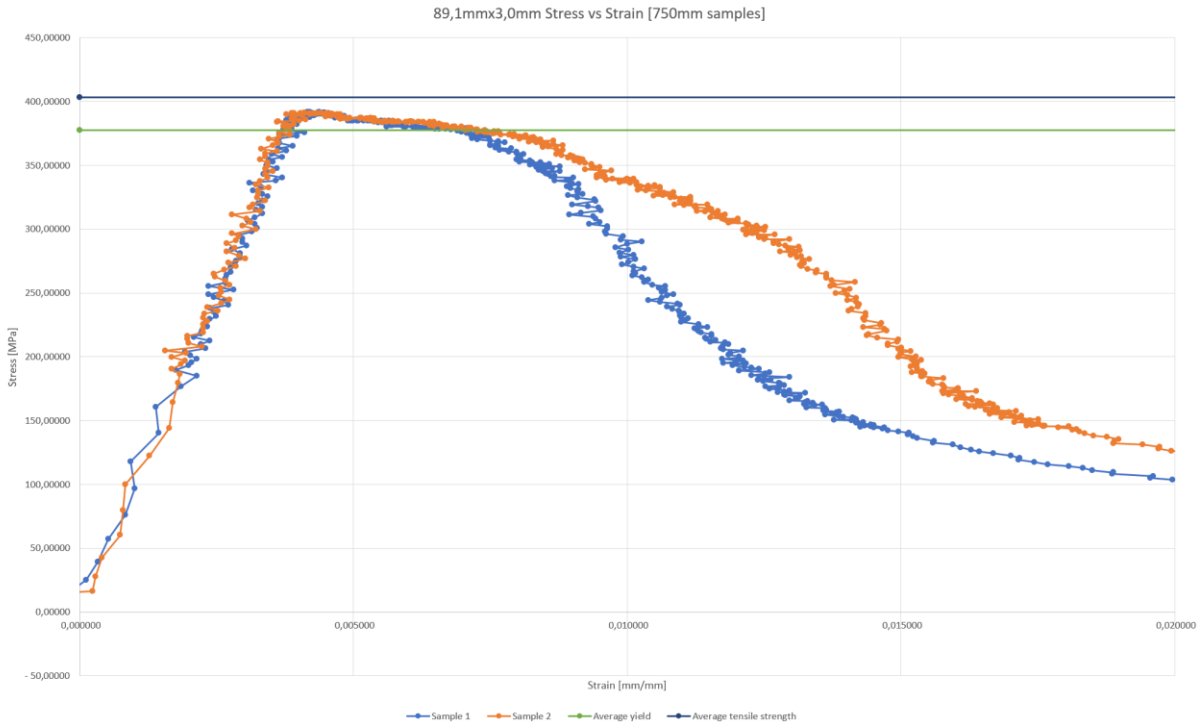

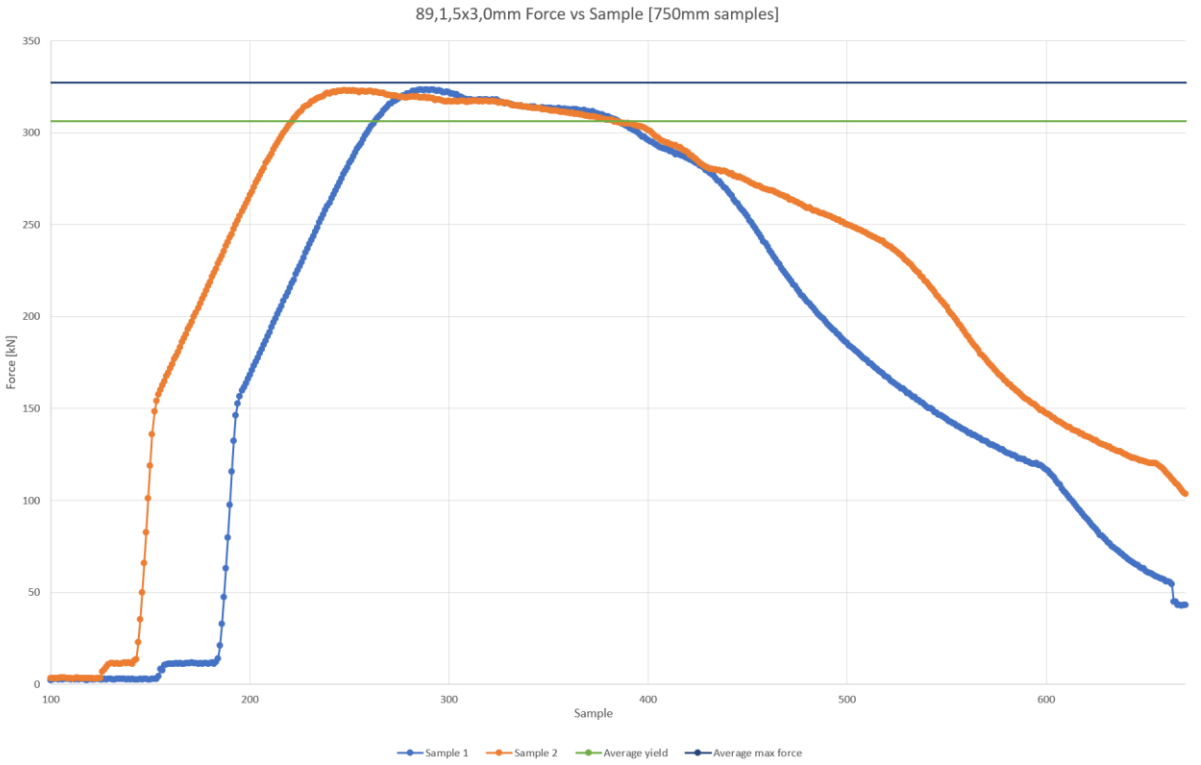

SR1 = SR2 = 560,3 mm unsupported length

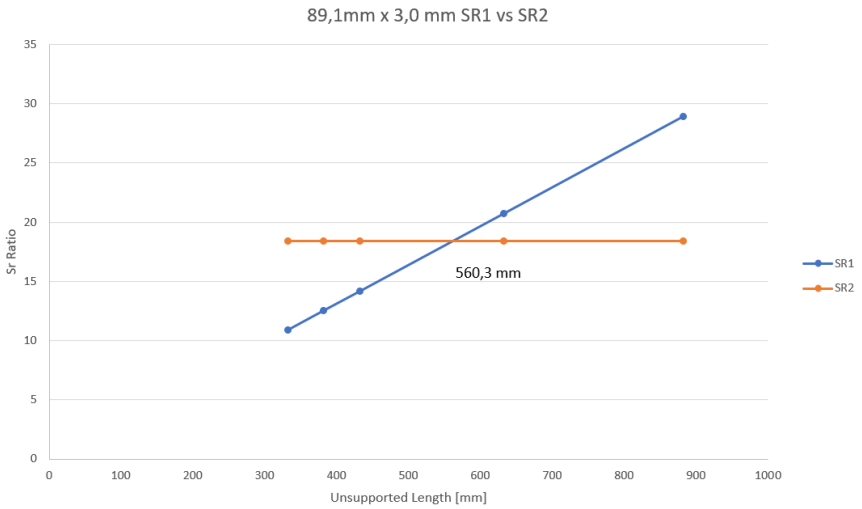

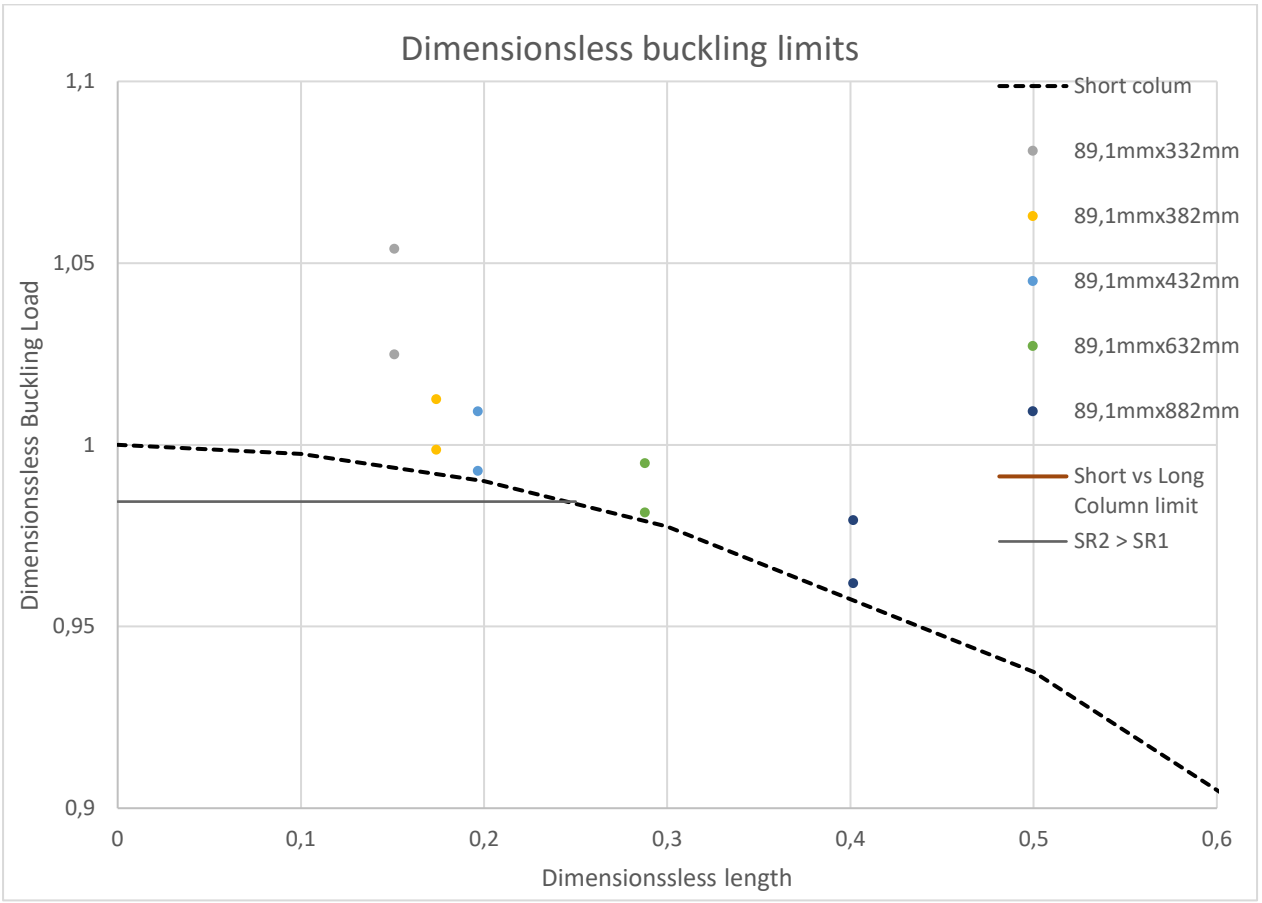

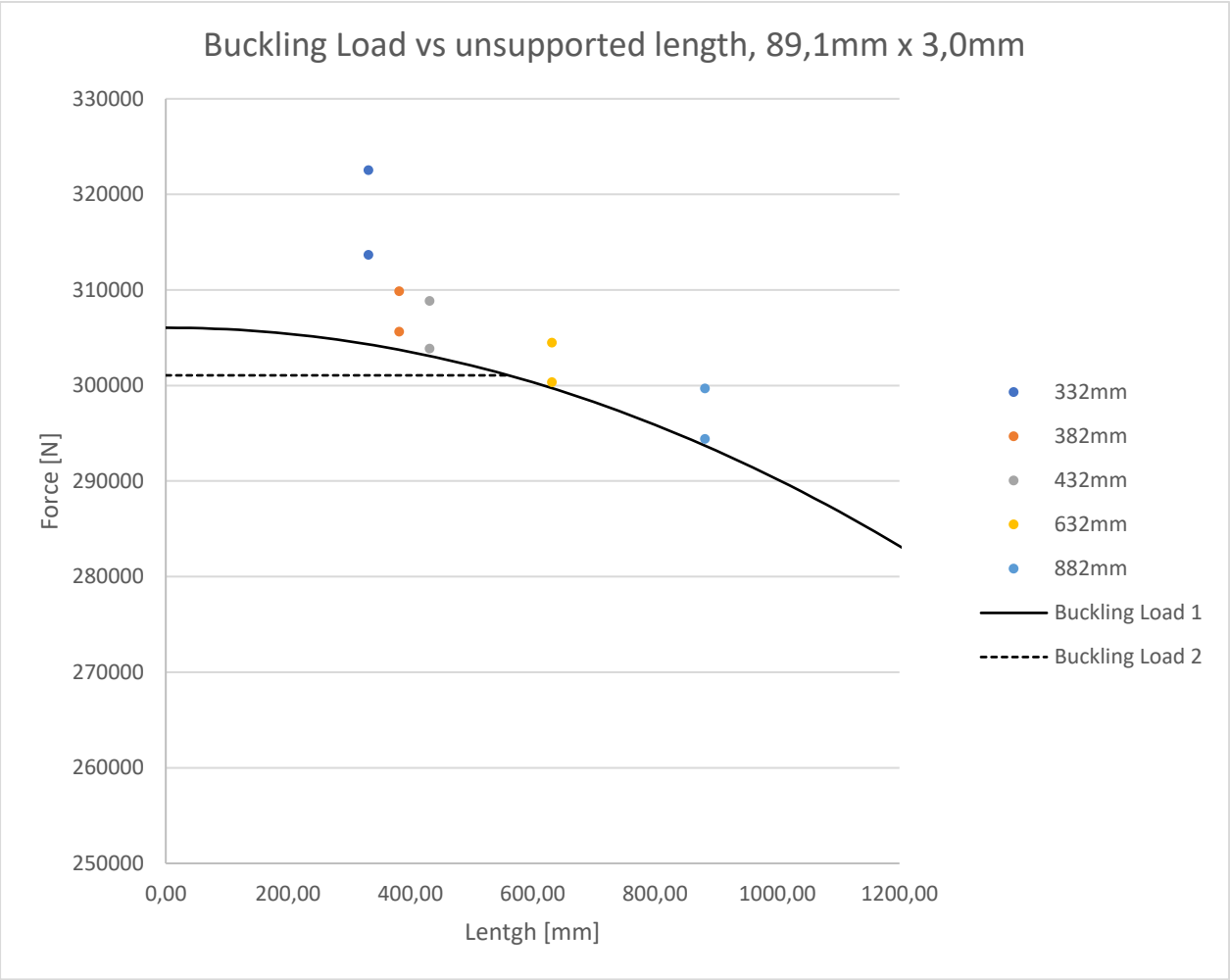
Buckling Load vs unsupported length, 89,1mm x 3,0mm
330000
320000
310000
300000
290000
280000
270000
260000
250000
Force [N]
0,00
200,00
400,00
600,00
800,00
1000,00
1200,00
Lentgh [mm]
332mm
382mm
432mm
632mm
882mm
Buckling Load 1
Buckling Load 2

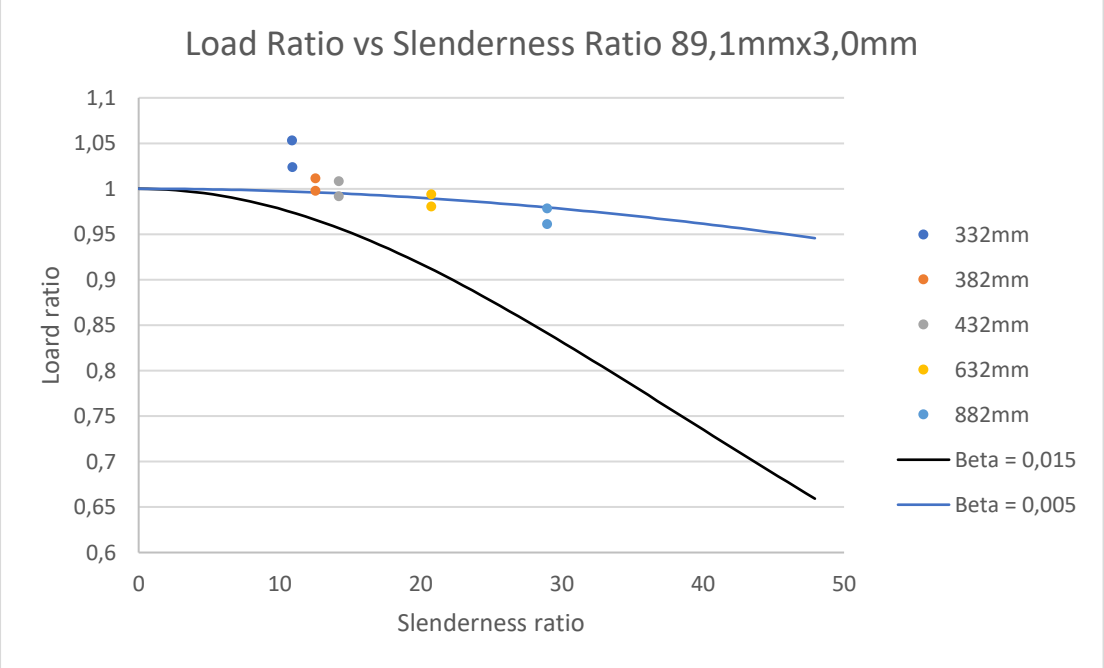
Load Ratio vs Slenderness Ratio 89,1mmx3,0mm
1,1
1,05
1
0,95
0,9
0,85
0,8
0,75
0,7
0,65
0,6
Loard ratio
0
10
20
30
40
50
Slenderness ratio
332mm
382mm
432mm
632mm
882mm
Beta = 0,015
Beta = 0,005

All experimental results in same dimensionless graph.

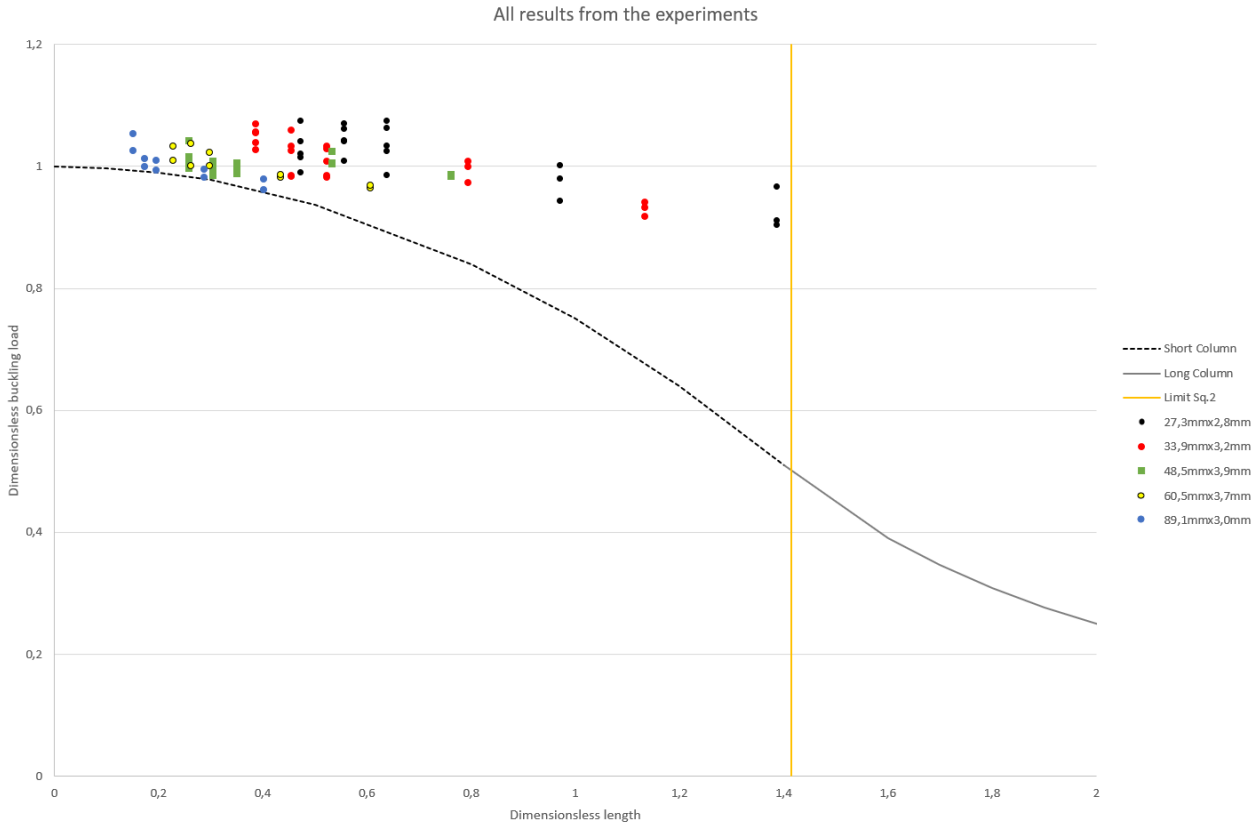

All experimental buckling force vs unsupported lengths collected together

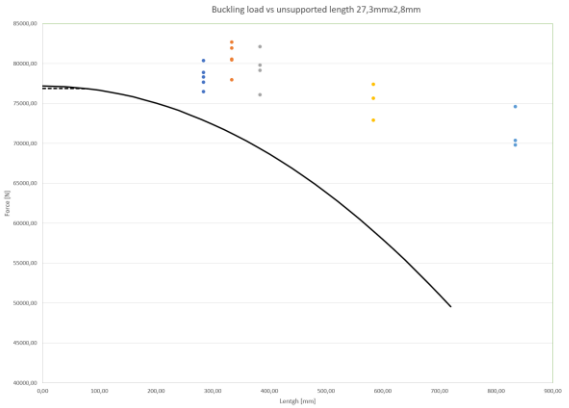

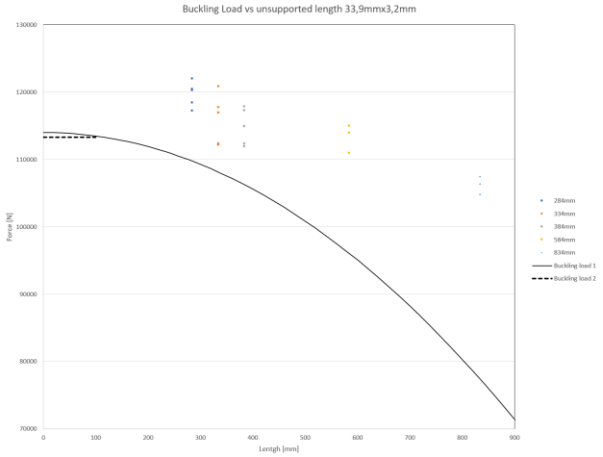

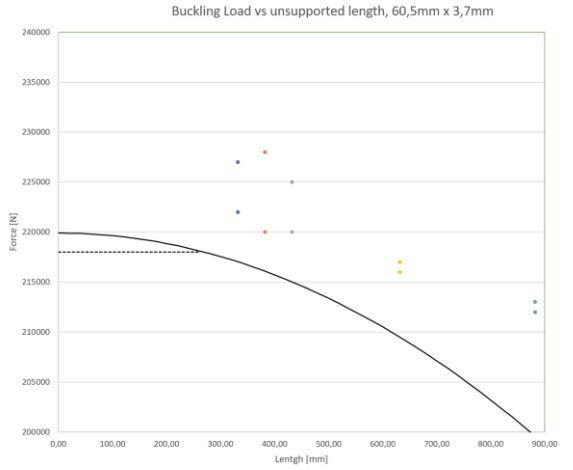

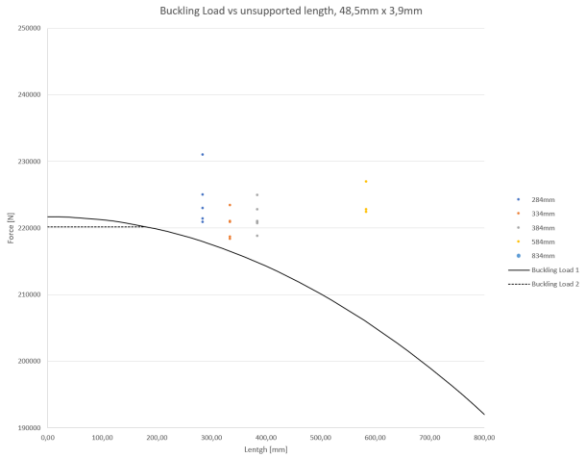

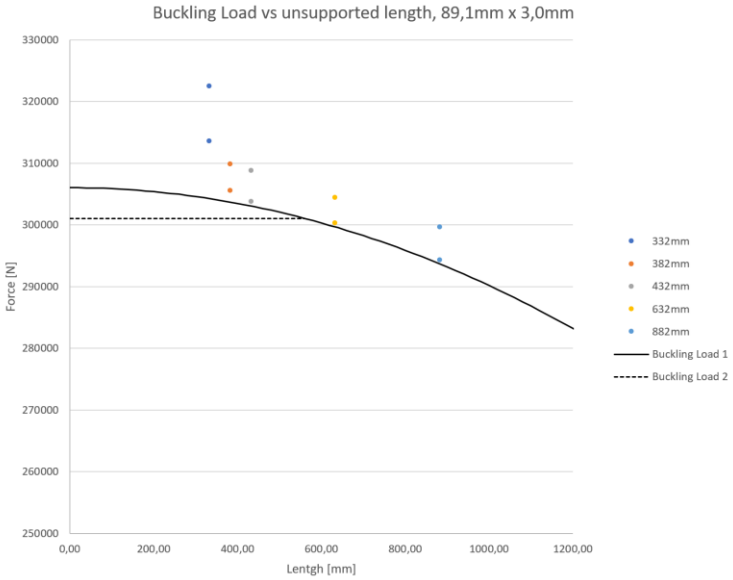

All load ratio vs slenderness ratio collected together, Beta = 0,005

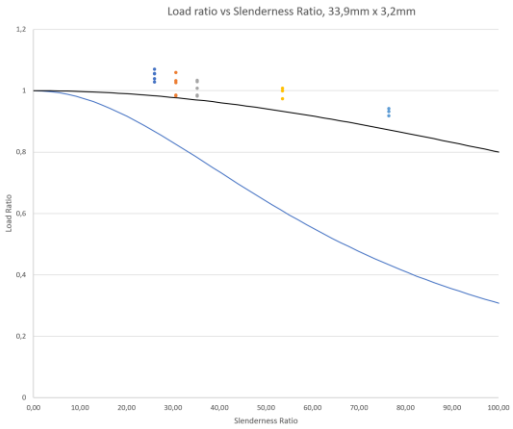

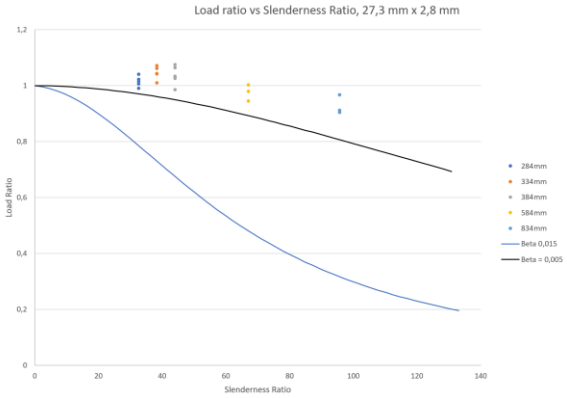

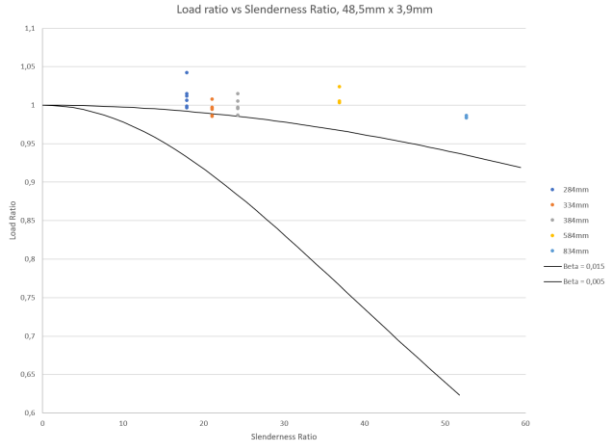

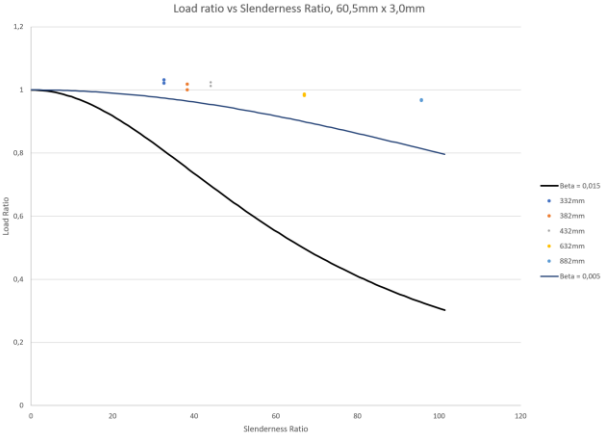

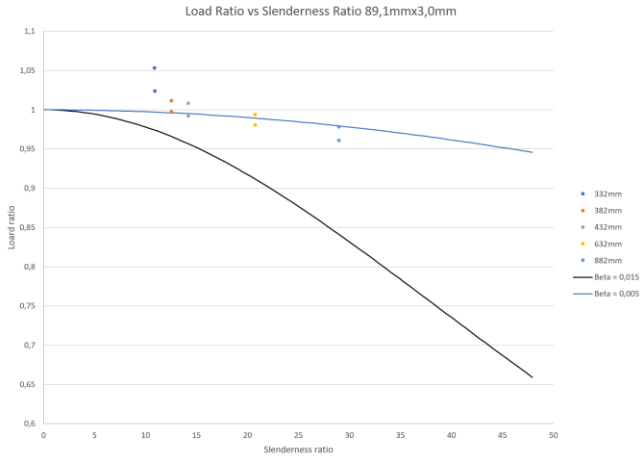

Appendix B – Procedure on how to operate the Enerpac Machine

Procedure On How To Operate The ENERPAC Machine

Before start:

- Make sure the area is ready and tidy, nothing to stumble across.
- Check the hoses, piston and the area around the machine for any oil leaks.
- Check the oil level in the machine and make sure it don't need refill.

Please clear the area around the machine of any unwanted personnel before the operation starts.

Put "TESTING ONGOING" label on the outer door and close it so no unwanted personnel can enter.

Test preparation

- Plug in the power supply to the Enerpac.
- Make sure that the computer and resistor is turned on and that Labview is running on the computer.
- Mark all test objects with number and pipe size.
- Attach the pipe to the pipe holding tools, and strap the pipe with straps.
- Turn the pressure load screw all the way out, (anti-clockwise).
- Start the Enerpac machine.
- Check that the piston is moving up and down with the controller, and familiar yourself with the buttons.
- If you need to preset the pressure, place a test block between the piston and the base. Place all personnel in the safe area . Apply the desired pressure. Then lock the pressure screw in place so it will stop at the preset pressure.

Test Procedure

- Place the pipe underneath the piston with the pipe holding tool while operating the down button to apply pressure to fasten the pipe.
- Start the “Run” recording button in the Labview program to record the pressure loads.
- Start the video recorder (if needed).
- **Make sure all personnel is placed in the safety zone.**
- Start the compressions by holding the “down” button.
- Use the pressure load crew to apply more pressure, if needed.
- When desired pressure have been obtained, and pipe compressed, press the “up” button.
- Turn off the machine and remove the pipe.
- Save the file created in Labview and name as desired.
- Now repeat the procedure for all prepared tests.
- When all test are completed, move the piston all the way up and turn off the machine.
- Unplug the two power supplies to the Enerpac machine.

After test is completed

- Remove and store all pipes/tools that have been used and place it in the right area.
- Remove the label “TESTING ONGOING” from the door.
- Download the datafile from the Labview, using an external hard drive.

Clean the area after yourself when you are finished.

Appendix C – Picture collage

Picture collage of some preparation that was done.

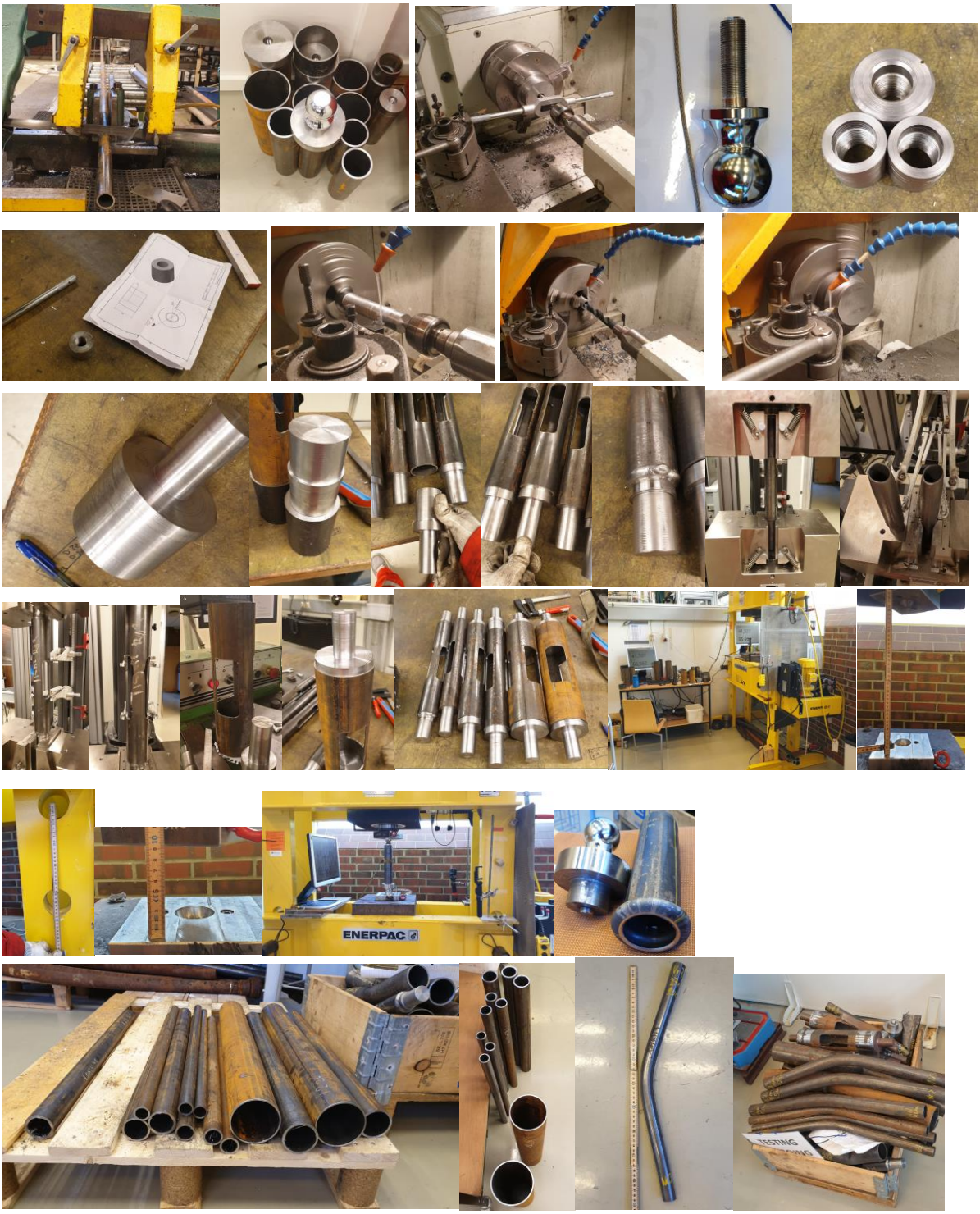

Method

1. Name the task that the analyses applies to

2. Describe the revant subtasks

3. Appraise the subtasks in accordance (whatever that may lead to an undesirable incident(s))

   - Physical conditions such as lifting, unilateral movement, electrical hazards etc.
   - Chemical conditions such as toxicity, possible allergy risk, possible harmful for the environment etc.
   - Other conditions such as noise, temperatur, workplace design, emissions etc.

4. Describe the measures that have been taken or needs to be taken that these tasks should be under control

   Specify what kind of training is required and what protective equipment to be used.
   Note: Protective devices shall be given priority over personal protection.

NOTE: Number the subtasks – what can cause an undesirable incident, and possible preventive measures - so that it becomes clear which ones who belong together, see the form example below.

SAFE JOB ANALYSIS (SJA)

Department/Unit: TN / IEP
Participants: Joakim Haram Svensson and Sivert Bakken Drangeid
Task: Compressive testing pipes using the Enerpac machine
Date: 18.01.2019 updated 04.02.2019
Signature:

Subtasks	**What can cause an undesirable incident(s)**	**Possible preventive measures** (including training and protective equipement)
Cutting of pipe with the use of automatic watercooled bandsaw	Sharp objects - Cut fingers Get smal objects on eye Get stuck in machin Loud noise Dropped objects Risk of entrapment	Safety Shoes Safety goggles Protective gloves Ear protection Protective coat
Lifting heavy pipes	Transport of pipes Dropped objects Risk of entrapment Spinal injury Muscle damage Sharp edges	Safety Shoes Safety goggles Protective gloves Correct lifting technique Protective coat

Attache pipe to the Enerpac Machine while operating the hight.	Risk of entrapment Dropped objects Flying objects Damaged equipment while attaching pipe	Protective gloves Safety goggles Protective coat Safety shoes Hold the pipe with a suitable tool to avoid injury to fingers Strap pipe to ensure no flying objects or place the shield in front of the machine
Starting the compression test	Loud noise Dropped objects Flying objects Risk of entrapment Hydraulic leakage	Safety shoes Ear protection Safety goggles Protective coat Protective gloves Strap pipe to ensure no flying objects All personnel must stand in safe sector Make sure the area is closed and marked with "TESTING ONGOING"
Remove bended pipe after the test while operating the machine	Dropped objects Damaged equipment	Protective gloves Safety goggles Safety shoes Protective coat All personnel must stand in safe sector untill the machine is turned off Turn off machine before removing pipe

Appendix E – Instron Software BlueHill 3 procedure

INSTRON250kN tensile test machine

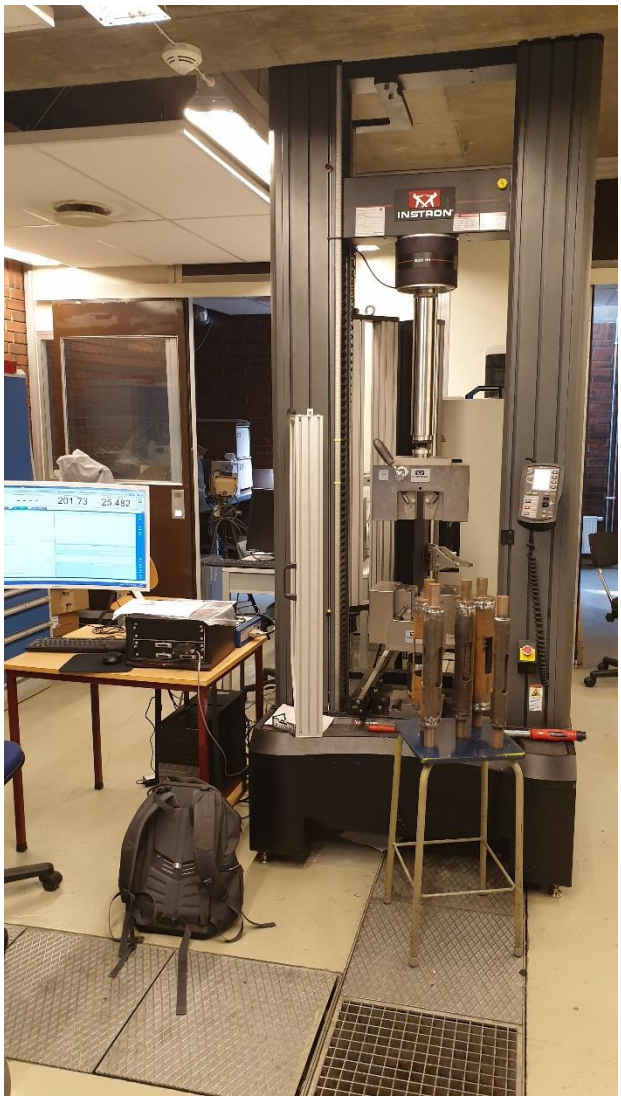

Intstron tensile test machine was connected to the software Bluehill 3.

This document is a basic instruction with pictures on how to use and operate the tensile test software pictures. The Bluehill 3 software helps you make methods designed for what mechanical properties the test specimen you want to test have and what results you want in the report. During test in this experimental study, ISO standard NS-EN ISO 7892-1 2016 was used.

Procedure

Click the program BlueHill 3 icon found on the desktop on the computer connected to INSTRON. In picture below, it's on the top right corner.

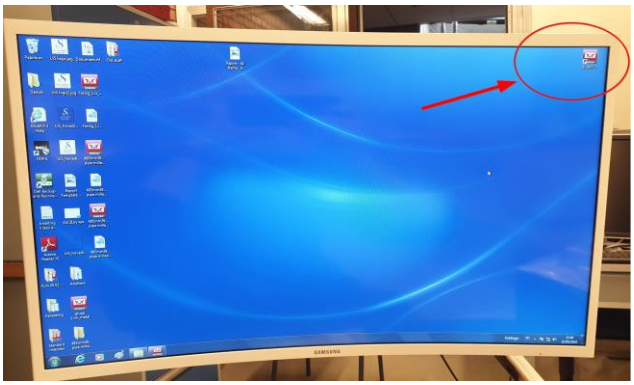

In the software, you now have three different options, “Test”, “Method” and “Analyses”.

Test

Test is where you enter when you want to test a new specimen and already know or have a method on the computer you want to use. Press the test button

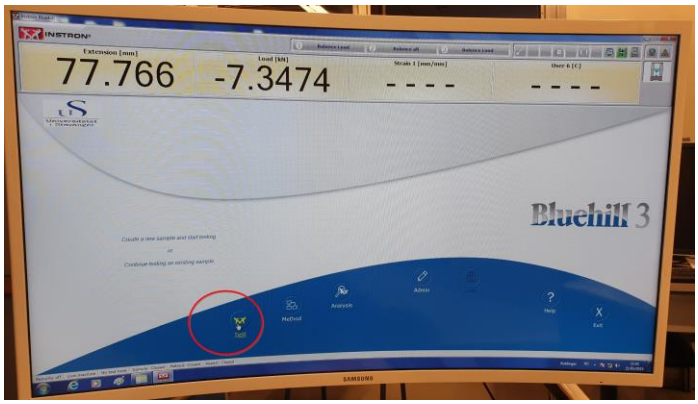

Now you can see the method’s already been made and used before. These can be found in picture below in the window marked 1. In the window marked 2, you can see what the method consists of. Here you can see what material used, the ramp rates and what’s calculated in the result tables. Under brows in mark 3 in the picture below, you can choose the location of a method and open it from the folder structure. If you don’t find a method that suits your test, you can go back and create your own under “Method”.

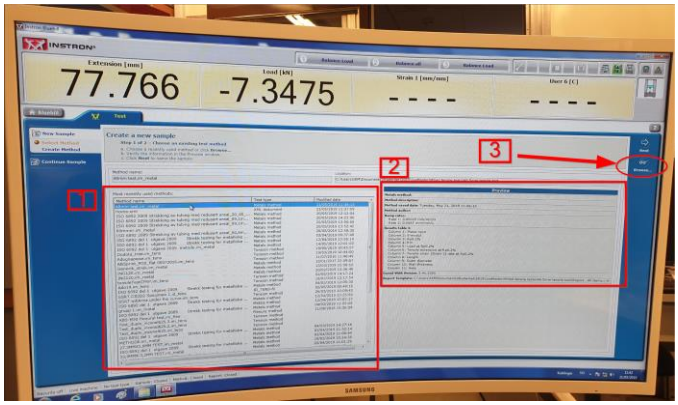

Press next when you have chosen the method, then write the name of the file you are creating and press next. Now you have opened the method and are ready to enter specimen data. Choose what calculations needed, and the layout of the display. On the top of the display, you can now press method to edit the method and change the report generated after test is finished. Picture below shows example om tubular specimen properties and the default values. In the drop-down menu below “Geometry and default dimensions”, you can choose different specimen properties.

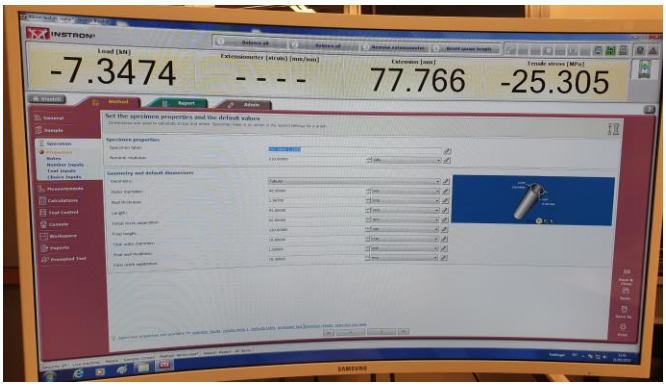

Further down the menu to the left, you can add measurements, calculations, workspace display and export of raw files method’s. Go through all the setup listed to the right.

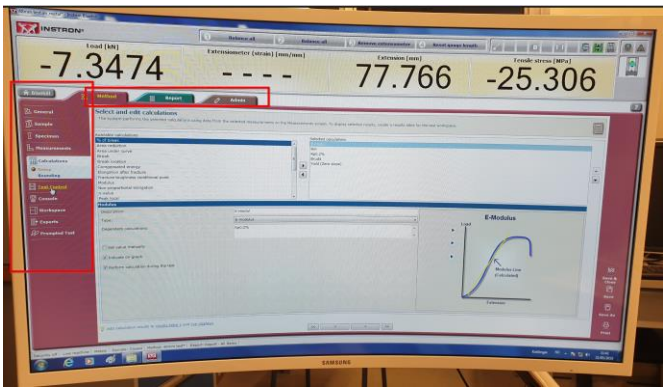

The picture below shows an example of a layout used. This is the display showed when running the test.

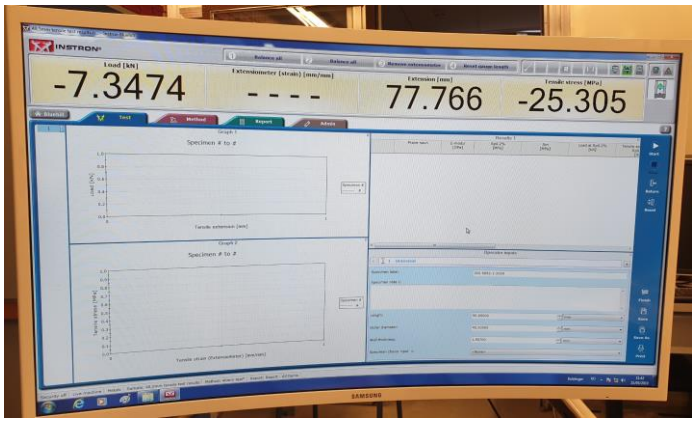

When everything is ready and set up inside the INSTRON machine, followed by the instructions of the ISO standard used (if using), then press “Start” button to start the test.

The extension meter needs to be set at its correct position. In the picture below, you can see how to edit the distance between the attachment points of the extension meter. Press move to move it up and down depending on your input in the target carriage position. Several adjustments is needed to get the spacing and placement desired. When the target is achieved, press “close arms” to calibrate the program to the new setpoint.

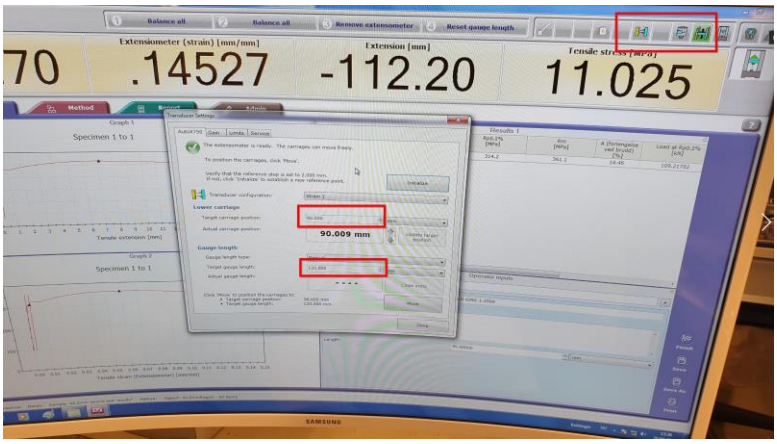

Method
Under method, you can create your own method, use standard methods already made and saved on the computer or edit already made method. See ISO 6892-1 2016 for example of method for steel tests.

Analysis
In the analysis, you can analyze previous test’s, change the method used, edit specimen input data and edit the report. Re-calculations can be performed If specimen in-data needs to be edited.

Appendix F - Reports from Instron tensile test BlueHill 3 software

27,3mm x 2,8 mm tensile test result

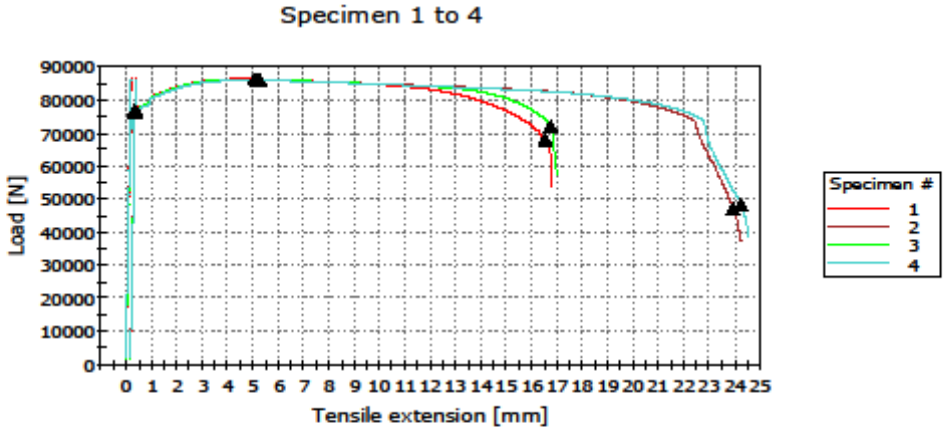

	Prøve navn	E-modul [GPa]	Rp0.2% [MPa]	Rm [MPa]
1	ISO 6892-1:2009	166.9	357.2	400.5
2	ISO 6892-1:2009	173.2	357.4	399.7
3	ISO 6892-1:2009	178.4	357.7	400.2
4	ISO 6892-1:2009	172.9	355.1	398.8

	A (forlengelse ved brudd) [%]	Wall thickness [mm]	Outer diameter [mm]
1	18.15	2.80000	27.30000
2	26.43	2.80000	27.30000
3	18.41	2.80000	27.30000
4	26.72	2.80000	27.30000

33,9 x 3,2 mm tensile test results

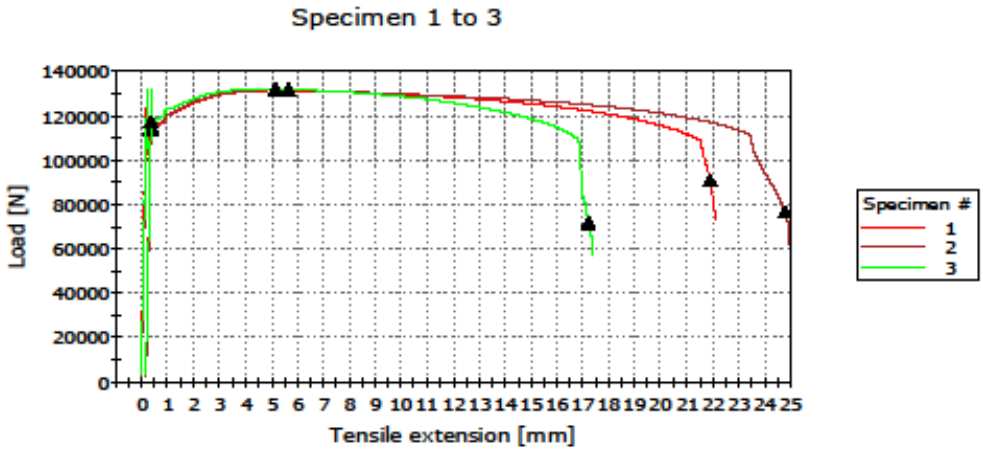

	Prøve navn	E-modul [GPa]	Rp0.2% [MPa]	Rm [MPa]
1	ISO 6892-1:2009	169.6	368.3	426.1
2	ISO 6892-1:2009	174.3	372.0	426.6
3	ISO 6892-1:2009	166.5	380.2	428.2

	A (forlengelse ved brudd) [%]	Wall thickness [mm]	Outer diameter [mm]
1	24.10	3.20000	33.90000
2	27.33	3.20000	33.90000
3	18.94	3.20000	33.90000

48,5mm x 3,2 mm tensile test results

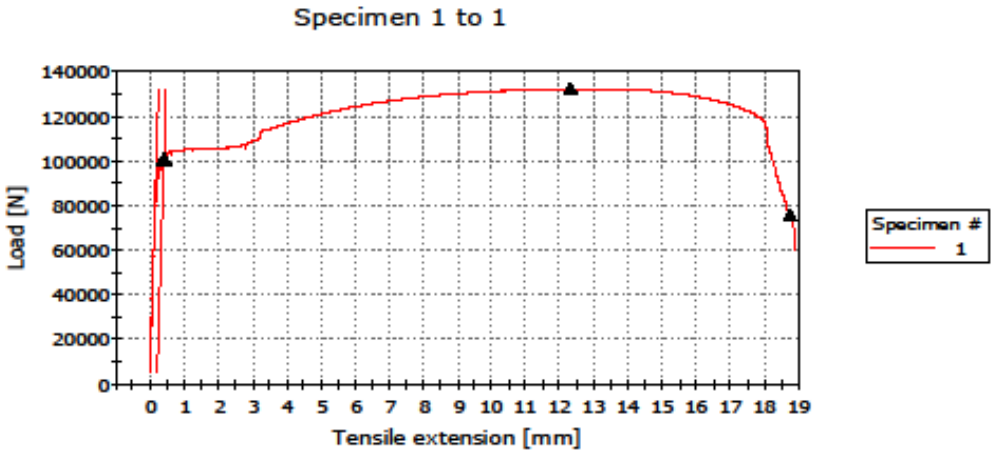

	Prøve navn	E-modul [GPa]	Rp0.2% [MPa]	Rm [MPa]
1	ISO 6892-1:2009	196.3	369.3	483.5

	A (forlengelse ved brudd) [%]	Wall thickness [mm]	Outer diameter [mm]
1	16.90	1.86800	48.50000

60,5 x 3,0 mm tensile test result nr 1

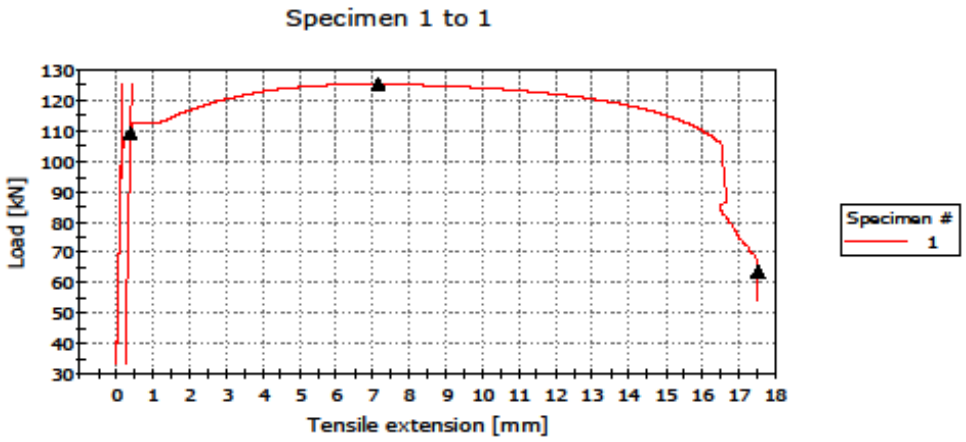

	Prøve navn	E-modul [GPa]	Rp0.2% [MPa]	Rm [MPa]
1	ISO 6892-1:2009	178.0	314.2	361.1

	A (forlengelse ved brudd) [%]	Wall thickness [mm]	Outer diameter [mm]
1	14.46	1.88780	60.50000

60,5 x 3,2 mm tensile test result nr 2

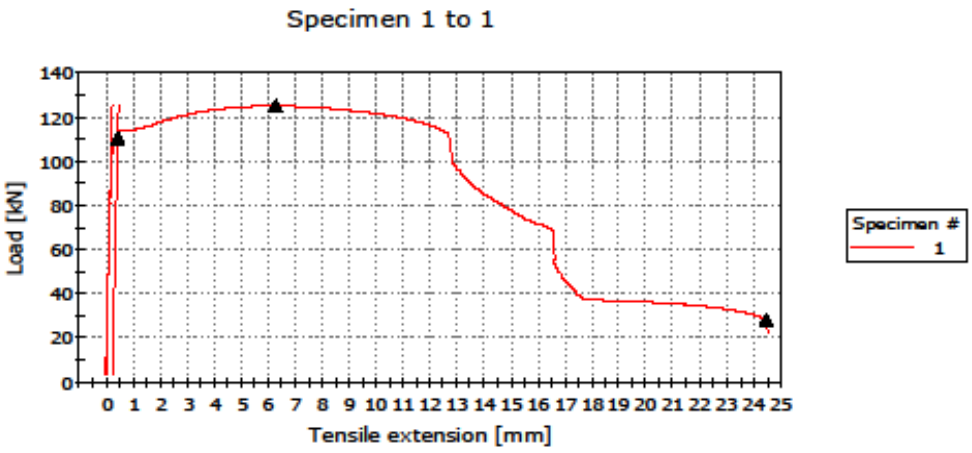

	Prøve navn	E-modul [GPa]	Rp0.2% [MPa]	Rm [MPa]
1	ISO 6892-1:2009	173.0	317.6	359.7

	A (forlengelse ved brudd) [%]	Wall thickness [mm]	Outer diameter [mm]
1	20.33	1.88780	60.50000

89,1mm x 3,0 mm tensile test results

89,1mm tensile test results.is_metal

24 May 2019

UiS IMBM sitt test laboratorium

Specimen 1 to 2

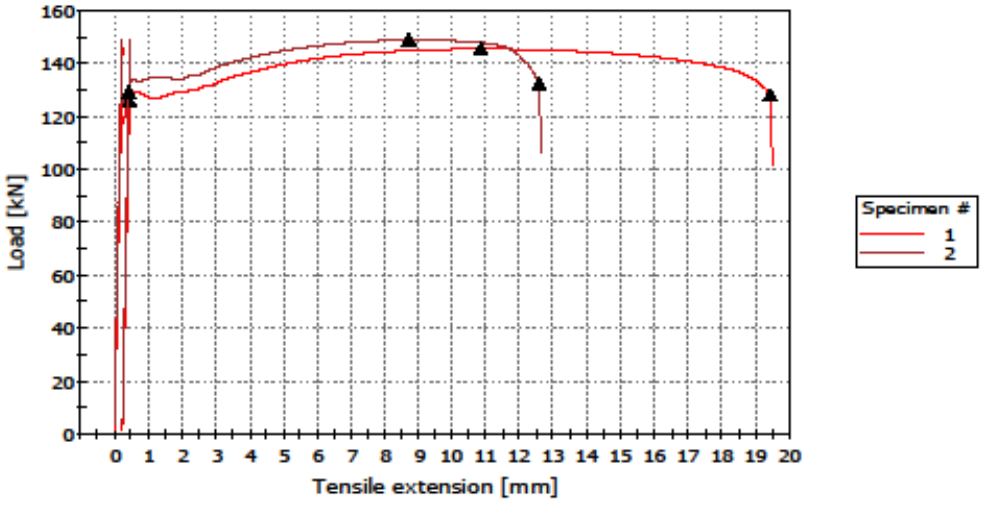

Graph 2

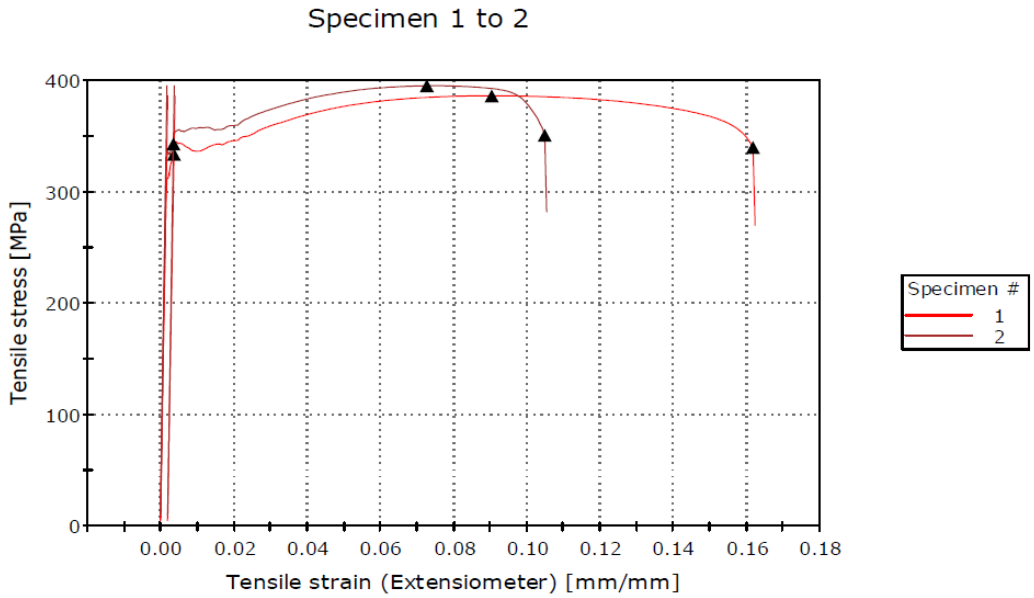

	Prøve navn	E-modul [GPa]	Rp0.2% [MPa]	Rm [MPa]	A (forlengelse ved brudd) [%]	Wall thickness [mm]	Outer diameter [mm]
1	ISO 6892-1:2009	184.7	333.8	386.1	15.97	1.36640	89.10000
2	ISO 6892-1:2009	212.6	343.0	395.1	10.31	1.36640	89.10000